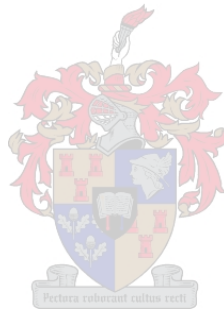# Development of a Membrane Immobilised Amidase Bioreactor System

by

Ryne Du preez

Thesis presented in partial fulfilment of the requirements for the degree of

Master of Science at the Department of
Process Engineering, Stellenbosch University

Study leader: Dr. K.G. Clarke

December 2008

Declaration

By submitting this thesis electronically, I declare that the entirety of the work contained therein is my own, original work, that I am the owner of the copyright thereof (unless to the extent explicitly otherwise stated) and that I have not previously in its entirety or in part submitted it for obtaining any qualification.

Date: 8 December 2008

Abstract

Nitriles are precursors of important amides and organic acids (e.g. acrylamide, nicotinamide, mandelic acid and acrylic acid) which are used, *inter alia*, as food additives, in plasticisers, detergents, make-up, medicine and as chemical intermediates in the production of various important polymers.

Traditionally, chemical processes are used to convert nitriles to amides and organic acids but these processes are non-specific causing various by-products to form. Chemical processes are also environmentally unfriendly and require harsh conditions. Nitrile conversions through an enzymatic route, on the other hand, have the distinct advantages of excellent chemo-, regio- and stereo selectivities, mild process conditions and reduced downstream processing costs. The enzymatic process is mediated via an initial nitrilase catalysed conversion to amide, followed by an amidase catalysed conversion to acid.

This research focused on the latter part of the enzymatic transformation of nitriles, which is the amidase catalysed biotransformation of an amide to an acid, specifically with respect to the development of a membrane immobilised amidase continuous process which has the major advantage of enzyme retention coupled with product separation. The research was conducted in three parts namely the characterisation of the free amidase, the development of the experimental bioreactor system and the quantification of the membrane immobilised amidase process.

The first part of the research, the characterisation of the free amidase, focused on characterising the free amidase in terms of optimum pH, optimum temperature, kinetic parameters (K_m and v_{max}) and functional stability. A factorial design yielded pH and temperature optima of 8.0 and 50ºC respectively and confirmed the interaction between the pH and temperature to be insignificant. Data obtained from initial rate studies established that the rate of reaction of amidase catalysed reactions can be predicted by the Michaelis-Menten model. The kinetic parameters K_m and v_{max} were determined from non-linear regression of initial rate data for lactamide as substrate as 68 mM and 1.48 mM/min respectively. From the initial rate data it could also be seen that no significant increase in the amidase reaction rate occurred above a substrate concentration of 80 mM; consequently this substrate concentration was decided on for future experiments. In order to determine the functional stability of the amidase the decrease in the amidase activity was measured over time at a pH of 8.0, temperature of 50ºC and substrate concentrations of 40 mM and 80 mM. Non-linear regression of the data obtained showed the amidase activity follows a typical one-phase exponential decay with a deactivation constant of 0.0023 min^{-1} and a half-life of 5 hours. The difference between the data obtained at the two substrate

concentrations was found to be statistically insignificant which proved the amidase functional stability was not dependent on the substrate concentration.

The second part of this research was concerned with the development of the experimental membrane bioreactor system. The membrane bioreactor consisted of an ultrafiltration ceramic capillary membrane with a molecular weight cut-off of 8 kDa in a glass shell. The amidase was to be immobilised in the pores of the ceramic membrane thereby causing the reaction to take place in the membrane wall. The reactor was therefore designed to accommodate a continuous feed of substrate to the shell side, with substrate that did not permeate the membrane being recycled. Substrate which did permeate the membrane was converted to product by the amidase in the membrane wall. The product was then collected from the permeate stream. An applied transmembrane pressure ensured the permeation of substrate through the membrane. Part of the development of the system consisted of the determination of an optimum rotation for the reactor in which dead volume was minimised. Computational fluid dynamic modeling of the reactor was used to determine the velocity profiles in the reactor for three different reactor orientations (13.4º, 30º and 90º) and two different feed entry points (top and bottom) at a flow rate of 200 mL/min. No difference in the amount of dead volume present was found between the different reactor orientations and feed entry points. The amount of dead volume in the reactor therefore did not depend on the orientation of the reactor if the flow rate was 200 mL/min. This flow rate was used in subsequent experiments. Computational fluid dynamic modeling was also used to determine whether the assumptions of constant temperature and pressure through the reactor were accurate. These assumptions were to be made during the development of a mathematical model of the reactor. The temperature and pressure profiles at reactor orientations of 13.4º, 30º and 90º and feed entry points at the top or bottom all showed a constant temperature and pressure was maintained through the reactor. Measurement of the inlet and outlet temperatures and pressures during reactor operation validated these results.

The development of the system also consisted of the characterisation of the membrane. The permeability of pure water, phosphate buffer with pH 8.0 and a 80 mM lactamide-buffer solution was determined by measuring the permeate flux of each solution at different transmembrane pressures. The slope of a plot of flux against transmembrane pressure for each solution gave the permeabilities as 68.16 L/m^2.h.bar, 43.66 L/m^2.h.bar and 42.33 L/m^2.h.bar respectively. The pure water or buffer permeability was measured before and after experiments to ensure that membrane fouling, which would result in a decrease in the membrane permeability, did not occur. The plot of flux against transmembrane pressure for the 80 mM lactamide-buffer solution, which was a typical feed during experiments, was used to determine the critical flux of the membrane. The critical flux of 88.48 L/m^2.h.bar

occurred at a transmembrane pressure of 2.2 bar. To prevent permanent fouling of the membrane all experiments were conducted at a transmembrane pressure of 0.5 bar which is well below 2.2 bar.

The third and final part of this research was the quantification of the membrane immobilised amidase process. Quantification of the process included evaluation of the effectiveness of the immobilisation method, the development of a mathematical model that could predict the performance of the reactor, validation of the model by means of experiments and using the model to predict the effect of amidase activity, amidase functional stability, permeate flux, amount of immobilised enzyme protein and substrate concentration on the performance of the reactor.

The effectiveness of the immobilisation method was evaluated by looking at the amount of amidase that could be immobilised, the physical retention of the amidase in the membrane during operation and the effect of immobilisation of the amidase activity and functional stability. Three experimental runs, with the initial immobilisation feed containing enzyme protein concentrations of 0.0184 mg/L, 0.021 mg/L and 1.07 mg/L respectively, were conducted.

An increase in the enzyme protein concentration of the initial immobilisation feed resulted in more enzyme protein being immobilised (6, 6.38 and 20.09 mg for the three experiments respectively). However, an exponential decrease in the percentage of enzyme protein in the feed being immobilised was observed. 38.7%, 30.4% and 4.7% of the initial enzyme protein in the immobilisation feed was immobilised in the three experiments respectively. This suggests that an increase in the enzyme protein concentration in the immobilisaion feed results in an increase in the competition for pores between the enzyme protein molecules.

The physical retention of enzyme protein was evaluated by measuring the concentration of enzyme protein in the permeate and retentate streams at intervals of approximately 1 hour during operation of the three experiments. The three experiments lasted 3 hours, 20.5 hours and 21 hours respectively. No enzyme protein losses occurred during any of the experiments which indicated that the membrane effectively retained the enzyme protein.

The immobilised amidase activities were 7, 9 and 36 times lower than the free amidase activities for the three experiments respectively. These results indicated that higher enzyme protein concentrations in the initial immobilisation feed not only resulted in a lower percentage of enzyme protein being immobilised but was also responsible for lower immobilised amidase activity. The increased competition for pores between molecules at higher enzyme protein concentrations could be the reason for the lower amidase activities.

However, the effect of the immobilisation procedure on the amidase activity could not be determined accurately since mass transfer effects in the reactor were significant. In order to determine the effect of the immobilisation procedure on the amidase activity, the reactor should be operated in a reaction limited regime instead of a mass transfer limited regime.

The functional stability of the immobilised amidase was determined by measuring the product concentration in the permeate stream over time and relating it to amidase specific activity. Non-linear regression of the data showed that the functional stability was improved on immobilisation with a decrease in the deactivation constant from 0.0023min^{-1} to 0.0016min^{-1} and an increase in the half-life from 5 to 9.4 hours.

A mathematical model that could predict the performance of the reactor was developed from first principles. The instability of the amidase dictated an unsteady state CSTR model. Differential mass balances were derived from first principles and the reaction rate equation incorporated enzyme deactivation into the Michaelis-Menten model. The performance of the reactor was evaluated in terms of the instantaneous conversion and instantaneous productivity due to the process being operated at unsteady state and the cumulative amount of product produced over time was used to quantify the feasibility of the process. An ordinary differential equation solver package (Polymath) was used to solve the model equations simultaneously.

Model validation was done by comparing the instantaneous conversion and instantaneous productivity achieved in two experimental runs with that predicted by the model. Two different sets of conditions were used in order to test the validity of the model over a range of values. The first run was operated at a permeate flux of 0.0005 L/min, substrate concentration of 80 mM and 6.38 mg of immobilised amidase with an initial amidase activity of 1.4 U/mg and the second run was operated at a permeate flux of 0.0001 L/min, substrate concentration of 40 mM and 20.09 mg of immobilised amidase with an initial amidase activity of 0.357 U/mg. The model predictions fitted the experimental data exceptionally well with correlation coefficients of 95.4% and 80% for the two experiments respectively.

Model predictions were then used to evaluate the effect of amidase functional stability, amidase activity, permeate flux, amount of immobilised enzyme protein and substrate concentration on the reactor performance. Evaluation of the effect of each specific parameter was carried out by changing the value of the parameter in the model while keeping all other parameters constant.

Both the actual activity and functional stability of the immobilised amidase was low with activities in the range 0.01 U/mg to 0.18 U/mg and a half-life of 9.4 hours. For the process to be economically feasible both should be improved considerably. The model showed that

an increase in the amidase specific activity had a greater effect on the maximum instantaneous conversion and productivity than an increase in the amidase stability. At a specific activity of 2 U/mg an increase in the half-life of the amidase from 1.8 hours to 115.5 hours only increased the maximum instantaneous conversion from approximately 17% to 25% and the maximum instantaneous productivity from approximately 0.6 to 0.85 mmol/L.min. At a half-life of 115.5 hours the maximum instantaneous conversion and productivity was increased from 1% to 25% and 1 to 0.85 mmol/L.min respectively for an increase in amidase specific activity from 0.05 U/mg to 2 U/mg. From a process improvement perspective both the activity and functional stability of the amidase should be improved with the emphasis on the activity.

Permeate fluxes below 0.001 L/min were found to have a significant effect on the reactor performance. An increase in the permeate flux from 0.00001 L/min to 0.001 L/min, which corresponded to an decrease in the residence time from 1186 minutes to 11.9 minutes, resulted in a sharp decrease in the instantaneous conversion and increase in the instantaneous productivity. For permeate fluxes above 0.001 L/min, however, no significant change in the instantaneous conversion or productivity was seen since the residence times were all so low that the substrate essentially passed through the membrane without being converted. These results indicated the existence of a threshold flux in a bioreactor system. For optimisation purposes the determination of the threshold flux of a particular system is very important since working at fluxes above the critical flux would yield no improvement in either the instantaneous conversion or productivity. This particular system should be operated at permeate fluxes below 0.001 L/min.

An increase in the amount of enzyme protein immobilised resulted in a linear increase in both the instantaneous conversion and instantaneous productivity. This trend, however, is the result of a significant limitation in the model. No correlation to account for the increase in mass transfer resistance, which usually occurs with an increase in the amount of immobilised enzyme protein, has been inserted into the model. An optimum amount of immobilised enzyme protein, above which a decrease in the instantaneous conversion and productivity would be observed, should exist. Future work should therefore include the development of an empirical model to predict the effect of the amount of immobilised enzyme protein on the mass transfer resistance in the reactor. This correlation can then be integrated into the reaction rate equation in the model to predict the effect of increased amounts of immobilised enzyme protein on the instantaneous conversion and instantaneous productivity.

An increase in the substrate concentration used in the reactor resulted in a decrease in the instantaneous conversion and an increase in the instantaneous productivity. For substrate

concentrations below 50 mM the low amidase reaction rates resulted in a significant decrease in the instantaneous productivity whereas substrate concentrations above 70 mM resulted in low instantaneous conversions. These results indicated that an optimum substrate concentration range exists in bioreactor systems. For optimisation purposes the determination of this range is very important. For this bioreactor system the optimum substrate concentration range is 50 mM to 70 mM.

In this research the free amidase was successfully characterised and an efficient membrane bioreactor system was designed. The immobilisation method also proved to be effective. The low functional stability of the amidase necessitated the development of an unsteady state CSTR model from first principles. The model predictions formed the technological platform on which the optimisation of the reactor performance was based. A sensitivity analysis predicted improved reactor performance under the following conditions:

- The activity and functional stability of the amidase should be improved.

- The system should be operated below the threshold permeate flux of 0.001 L/min.

- The system should operate in a substrate range of 50 mM to 70 mM.

Abstract (Afrikaans)

Nitriele is voorgangers van belangrike amiedes en organiese sure (soos bv. akrielamied, nikotienamied, mandeliek suur en akriel suur) wat onder andere gebruik word in kosse, plastiekmiddels, skoonmaakmiddels, grimering, medisyne en as chemiese tussenprodukte in die vervaardiging van verskeie belangrike polimere.

In die verlede is chemiese prosesse meesal gebruik om nitriele om te skakel na amiede en organiese sure, maar verskeie byprodukte is gevorm omdat die prosesse nie spesifiek is nie. Chemiese prosesse is ook nie omgewingsvriendelik nie en benodig dikwels baie hoë drukke of temperature. Nitriel omskakelings deur middel van ensieme, aan die ander kant, het voordele soos uitstekende chemo-, regio- en stereo selektiwiteit, laer temperature en drukke as proseskondisies en die prosessering van die produk is goedkoper. Die omskakeling van nitriele deur ensieme geskied via 'n nitrilase gekataliseerde omskakeling van die nitriele na amiede wat gevolg word deur 'n amidase gekataliseerde omskakeling van die amiede na sure.

Hierdie navorsing het gefokus op die tweede stap in the ensiematiese omskakeling van nitriele – die omskakeling van 'n amied na 'n suur met amidase as die biokatalis. Die spesifieke fokus was om 'n kontinue proses te ontwikkel waar die amidase in 'n membraan geimmobiliseer is. Die voordeel van hierdie tipe proses is dat die membraan die ensiem in die reaktor hou en tergelyketyd ook die produk van die substraat skei. Die navorsing was in drie dele gedoen naamlik: die karakterisering van die vry amidase, die ontwikkeling van die experimentele membraan bioreaktor sisteem en die kwantifisering van die membraan geimmobiliseerde amidase proses.

In die eerste deel van die navorsing, die karakterisering van die vry amidase, is die amidase gekarakteriseer in terme van optimum pH, optimum temperatuur, kinetiese parameters (K_m and v_{max}) en funksionele stabiliteit. Faktoriaal eksperimente het 'n optimum pH en temperatuur van onderskeidelik 8.0 en 50ºC gelewer en het bewys dat die interaksie tussen die pH en temperatuur weglaatbaar is. Data wat uit studies van die aanvanklike reaksietempo van die amidase verkry is het bevestig dat die reaksietempo voorspel kan word met die Michaelis-Menten model. Die kinetiese parameters K_m en v_{max} was bereken as onderskeidelik 68 mM en 1.48 mM/min vir laktamied deur die nie-liniêre regressie van die data van die aanvanklike reaksietempo studies. Die data van die aanvanklike reaksietempo studies het ook getoon dat daar geen beduidende toename in die amidase se reaksietempo is vir substraatkonsentrasies bo 80 mM nie, dus was hierdie konsentrasie in verdere eksperimente gebruik. Die funksionele stabiliteit van die amidase was bepaal deur die afname in die amidase se aktiwiteit oor tyd te meet by 'n pH van 8.0, temperatuur

van 50ºC en substraatkonsentrasies van 80 mM. Nie-linieêre regressie van die stabiliteit data het getoon dat die amidase aktiwiteit 'n tipisie eenfase ekponensiële afname oor tyd het met 'n deaktiverings konstante van 0.0023 min^{-1} en 'n half-leeftyd van 5 hours. Daar is bepaal dat die verskil tussen die data wat verkry is by die twee verskillende substraatkonsentrasies statisties onbelangrik is wat bewys het dat die amidase se funktionele stabiliteit nie afhanklik is van die substraatkonsentrasie nie.

Die tweede deel van die navorsing was gemoeid met die ontwikkeling van die eksperimentele membraan bioreaktor sisteem. Die bioreaktor het bestaan 'n ultrafiltrasie, kappilêre keramiek membraan, met 'n molekulêre afsnypunt van 8 kDa, wat binne-in 'n glas omhulsel geplaas is. Die amidase sou in die wand porieë van die membraan geimmobiliseer word wat sou veroorsaak het dat die ensiematiese reaksie dus in die wand van die membraan plaasvind. Die reaktor was dus ontwerp om 'n kontinue voer van substraat na die glasomhulsel te kan hanteer. Substraat wat nie deur die wand van die membraan geforseer is nie is gehersirkuleer. Substraat wat wel deur die want van die membraaan geforseer is, is deur die amidase in die membraanwand omgeskakel na produk toe. Die produk was dan gekollekteer in die vorm van die filtraatstroom. 'n Aangewende trans-membraan druk het verseker dat die substraat deur die membraan forseer word. Deel van die ontwikkeling van die sisteem was om die optimum oriëntasie van die reaktor (wat die dooie volume in die reaktor minimeer) te bepaal. Berekeningsvloeidinamika modellering van die reaktor was gebruik om the snelheidsprofiele in die reaktor vir drie verskillende reaktor oriëntasies (13.4º, 30º and 90º) en twee verskillende voerpunte (bo en onder) by 'n vloeitempo van 200 mL/min te bepaal. Die hoeveelheid dooie volume in die reaktor was onveranderd in al die simulasies wat dus beteken dat die oriëntasie van die reaktor geen invloed op die dooie volume in die reaktor het by 'n vloeitempo van 200 mL/min nie. Hierdie vloeitempo was vir alle eksperimente gebruik. Berekeninigsvloeidinamika modellering was ook gebruik om die bepaal of die aannames van konstante temperatuur en druk deur die reaktor akkuraat is. Hierdie aannames was nodig vir die ontwikkeling van 'n wiskundige model van die reaktor. Vir reaktor oriëntasies van 13.4º, 30º en 90º en voerpunte aan die bo- en onderkant van die reaktor het die temperatuur en druk profiele konstant gebly deur die reaktor. Die inlaat en uitlaat temperature en drukke wat gemeet is tydens eksperimente het hierdie resultate gevalideer.

Die volgende stap in die ontwikkeling van die sisteem was om die membraan te karakteriseer. Die deurlaatbaarheid van water, fosfaat buffer (pH 8.0) en 'n 80 mM laktamied-buffer oplossing was bepaal deur die filtraattempo van elke oplossing by verskillende trans-membraan drukke te meet. Die helling van die grafiek van filtraattempo teen trans-membraan druk vir elke oplossing, is die deurlaatbaarheid. Water, fosfaat buffer

en die laktamied-buffer oplossing het deulaatbaarhede van onderskeidelik 68.16 L/m^2.h.bar, 43.66 L/m^2.h.bar en 42.33 L/m^2.h.bar getoon. Die water of buffer deurlaatbaarheid is voor en na elke eksperiment bepaal om te verseker dat die membraan nie vuil geraak het nie. Die grafiek van filtraattempo teen die trans-membraan druk vir die 80 mM laktamied-buffer oplossing was gebruik om die kritiese filtraattempo te bepaal. Die kritiese filtraattempo van 88.48 L/m^2.h.bar het by 'n trans-membraan druk van 2.2 bar plaasgevind. Om permanente beskadiging deur aanpaksels op die membraan te voorkom is die druk van alle eksperimente ver onder 2.2 bar gehou (tipies 0.5 bar).

Die derde, en laaste, deel van die navorsing het gefokus op die kwantifisering van die membraan geimmobiliseerde amidase proses. Kwantifisering van die proses het die volgende ingesluit: evaluasie van die effektiwiteit van die immobilisasie metode, die ontwikkeling van 'n wiskundige model om die reaktor te beskryf, validasie van die model deur middel van eksperimente en die gebruik van die model om die effek van amidase aktiwiteit, amidase funksionele stabiliteit, filtraattempo, hoeveelheid geimmobiliseerde ensiem protein en substraat konsentrasie op die reaktor uitlaat te voorspel.

Die effektiwiteit van die immobilisasie metode was geevalueer deur te kyk na die hoeveelheid amidase wat geimmobiliseer is, die fisiese retensie van die amidase in die membraan deur die loop van die eksperimente en die effek van immobilisasie op die amidase aktiwiteit en funksionele stabiliteit. Drie eksperimentele lopies, met ensiem protein konsentrasies van onderskeidelik 0.0184 mg/L, 0.021 mg/L and 1.07 mg/L in die immobilisasie voer, is uitgevoer.

'n Toename in die ensiem protein konsentrasie in die immobilisasie voer het veroorsaak dat meer ensiem protein geimmobiliseer word (6, 6.38 and 20.09 mg for the three experiments respectively) maar dat die persentasie van die ensiem protein in die voer wat geimmobiliseer word ekspnensieël afneem. In die drie eksperimente is 38.7%, 30.4% and 4.7% van die ensiem protein in die immobilisasie voer onderskeidelik geimmobiliseer. Dit lei tot die gevolgtrekking dat 'n toename in die ensiem protein konsentrasie in die immobilisasie voer 'n toename in die kompetisie tussen die ensiem molekules vir membraan porieë tot gevolg het.

Die fisiese retensie van die ensiem protein was geevalueer deur die konsentrasie van ensiem protein in die filtraat en die hersirkulasie stroom in intervalle van 1 uur te meet tydens die drie eksperimente. Die drie eksperimente het onderskeidelik 3 ure, 20.5 ure en 21 ure geduur en geen ensiem protein is tydens enige eksperiment uit die membraan verloor nie. Dit dui daarop dat die membraan die ensiem protein effektief kan terughou.

Die geimmobiliseerde amidase aktiwiteite was 7, 9 en 36 keer lae as die van die vry amidase vir die drie eksperimente onderskeidelik. Die resultate dui daarop dat hoër ensiem protein konsentrasies in die immobilisasie voer nie net verantwoordelik is vir laer persentasies geimmobiliseerde ensiem protein nie, maar ook vir laer geimmobiliseerde amidase aktiwiteite. Die toename in die kompetisie tussen die ensiem protein molekules vir die membraan porieë by hoër ensiem protein konsentrasies kan die rede wees vir die laer aktiwiteite. Die effek van die immobilisasie prosedure op die amidase aktiwiteit kon egter nie akkuraat bepaal word nie omdat massaoordrag limitasies in die reaktor beduidend was. Om die effek van die immobilisasie prosedure op die amidase aktiwiteit te bepaal sal die reaktor in 'n reaksie-beperkte omgewing in plaas van 'n massordrag-beperkte omgewing bestuur moet word.

Die funksionele stabiliteit van die geimmobiliseerde amidase was bepaal deur die produk konsentrasie in the filtraat stroom oor tyd te meet en dit dan om te skakel na amidase spesifieke aktiwiteit. Nie-linieêre regressie van die data het gewys dat die funksionele stabiliteit van die amidase toegeneem het met immobilisasie met 'n toename in die deaktiverings konstante van 0.0023min^{-1} tot 0.0016min^{-1} en 'n toename in die half-leeftyd van 5 to 9.4 ure.

'n Wiskunde model was vanaf eerste beginsels ontwikkel om die lewering van die reaktor te voorspel. Die onstabiliteit van die amidase het bepaal dat 'n CSTR model wat nie by ewewig is nie gebruik moet word. Differensiële massa balanse was vanaf eerste beginsels afgelei en die reaksietempo vergelyking het 'n term vir ensiem deaktivering in die Michaelis-Menten vergelyking geinkorporeer. Die lewering van die reaktor was geevalueer in terme van onmiddellike omskakeling, onmiddellike produktiwiteit en die kumulatiewe hoeveelheid produk wat gevorm het oor tyd. Die pakket, Polymath, was gebruik om al die gewone differensiaalvergelykings gelyktydig op te los.

Die model was gevalideer deur die onmiddellike omskakeling en onmiddellike produktiwiteit wat in twee eksperimentele lopies behaal is te vergelyk met dit wat deur die model voorspel is vir daardie spesifieke kondisies. In die eerste eksperiment is 'n filtraattempo van 0.0005 L/min, substraatkonsentrasie van 80 mM en 6.38 mg geimmobiliseerde ensiem protein met 'n aktiwiteit van 1.4 U/mg gebruik. Die tweede eksperiment was gedoen met 'n filtraattempo van 0.0001 L/min, substraatkonsentrasie van 40 mM en 20.09 mg geimmobiliseerde ensiem protein met 'n aktiwiteit van 0.357 U/mg. Die model voorspellings het baie goed met die eksperimentele waardes vergelyk en korrelasie koeffisiënte van onderskeidelik 95.4% en 80% is vir die twee eksperimente verkry.

Die wiskundige model is gebruik om voorspellings te maak aangaande die effek van die amidase funksionele stabiliteit, amidase aktiwiteit, filtraattempo, hoeveelheid

geimmobiliseerde ensiem protein en substraatkonsentrasie op die lewering van die reaktor. Evaluasie van die effek van elke spesifieke parameter was gedoen deur slegs die waarde van daardie parameter te verander en alle ander parameters konstant te hou.

Beide die werklike aktiwiteit en funksionele stabiliteit van die geimmobiliseerde amidase was laag met aktiwiteite in die interval 0.01 U/mg tot 0.18 U/mg en 'n half-leeftyd van 9.4 ure. Vir die proses om ekonomies te wees sal beide die aktiwiteit en stabiliteit van die amidase moet verbeter. Die model het getoon dat 'n toename in die amidase se spesifieke aktiwiteit 'n groter effek op die maksimum onmiddellike omskakeling en produktiwiteit sal he as 'n toename in die amidase stabiliteit. By 'n spesifieke aktiwiteit van 2 U/mg het 'n toename van 1.8 ure tot 115.5 ure in die half-leeftyd van die amidase 'n toename van slegs 17% tot 25% en 0.6 tot 0.85 mmol/L.min in die maksimum onmiddellike omskakeling en produktiwiteit onderskeidelik veroorsaak. By 'n half-leeftyd van 115.5 ure het 'n toename in die amidase spesifieke aktiwiteit van 0.05 U/mg tot 2 U/mg vir 'n toename van 1% tot 25% en 0.1 tot 0.85 mmol/L.min vir die maksimum onmiddellike omskakeling en produktiwiteit onderskeidelik gesorg. Vanaf 'n prosesverbeterings oogpunt sal beide die aktiwiteit en stabiliteit van die amidase moet verbeter met die klem op die aktiwiteit.

Filtraatvloeitempo's onder 0.001 L/min het 'n beduidende invloed op die reaktor lewering gehad. 'n Toename in die filtraattempo vanaf 0.00001 L/min tot 0.001 L/min, wat ooreenstem met 'n afname in die residensietyd van 1186 minute to 11.9 minute, het die onmiddellike omskakeling skerp laat daal en die onmiddellike produktiwiteit skerp laat styg. Vir filtraatvloeitempo's bo 0.001 L/min was daar egter geen beduidende verandering in die onmiddellike omskakeling of produktiwiteit nie omdat die residensietye almal so kort is dat die substraat eintlik net deur die membraan vloei sonder om omgeskakel te word. Hierdie resultate dui die bestaan van 'n drumpel waarde vir die filtraatvloeitempo in 'n bioreaktor sisteem aan. Vir optimiserings doeleindes is dit belangrik om die waarde van die drumpel filtraatvloeitempo te bereken want as daar bo daardie waarde gewerk word hou dit geen voordeel vir die omskakeling of die produktiwiteit in nie. Hierdie spesifieke sisteem se filtraatvloeitempo moet onder 0.001 L/min gehou word.

'n Toename in die hoeveelheid ensiem protein wat geimmobiliseer word het 'n liniêre toename in beide die onmiddellike omskakeling en onmiddellike produktiwiteit veroorsaak. Hierdie patroon is egter die resultaat van 'n beduidende beperking van die model. Geen korrelasie om die massaoordrag weerstand, wat gewoonlik toeneem met 'n toename in die hoeveelheid geimmobiliseerde ensiem protein, was in die model ingewerk nie. 'n Optimum hoeveelheid geimmobiliseerde ensiem protein is veronderstel om te bestaan. As die ensiem protein hierdie waarde oorskry is die onmiddellike omskakeling en produktiwiteit veronderstel om af te neem. Toekomstige werk sal dus die ontwikkeling van 'n empiriese

korrelasie, wat die effek van die hoeveelheid geimmobiliseerde ensiem protein op die massaoordrag weerstand uitdruk, moet insluit. Die korrelasie kan dan in die reaksietempo vergelyking geintegreer word sodat die model gebruik kan word om voorspellings aangaande die effek van die hoeveelheid geimmobiliseerde ensiem protein op die onmiddellike omskakeling en produktiwiteit te maak.

'n Toename in die substraatkonsentrasie in die reaktor het 'n afname in die onmiddellike omskakeling en 'n toename in die onmiddellike produktiwiteit veroorsaak. 'n Beduidende afname in die onmiddellike produktiwiteit is gesien by substraatkonsentrasies onder 50 mM as gevolg van die lae reaksie tempo's van die amidase. Bo substraatkonsentrasies van 70 mM was lae onmiddellike omskakelings weer gekry. Die resultate dui daarop dat 'n optimum konsentrasie interval in bioreaktro sisteme bestaan. Vir optimisasie doeleindes is die bepaling van hierdie interval baie belangrik. Vir hierdie bioreaktor is die optimum substraatkonsentrasie interval 50 mM tot 70 mM.

In hierdie navorsing was die vry amidase suksesvol gekarakteriseer en 'n effektiewe membraan bioreaktor sisteem was ontwerp. Die immobilisasie metode was ook effectief. Die lae funksionele stabiliteit van die amidase het die ontwikkeling van 'n wiskundige CSTR model wat nie by ewewig is nie, genoodsaak. Die model voorspellings het die tegnologiese platform gevorm waarop die optimisasie van die reaktor lewering gebasseer was. 'n Sensitiwiteitsanalise het verbeterde reaktor lewering voorspel mits die volgende kondisies gehandhaaf word:

- Die aktiwiteit en funksionele stabiliteit van die amidase moet verbeter word.

- Die sisteem moet onder die drumpel filtraatvloeitempo van 0.001 L/min gehou word.

- 'n Substraatkonsentrasie tussen 50 mM tot 70 mM moet in die reaktor gehandhaaf word.

Acknowledgements

I would like to thank the following persons for their invaluable support during the completion of my thesis:

My husband, Rudolph, for his help during the construction of my experimental set-up, his presence during late-night experiments and his valuable ideas regarding some aspects of the project.

My parents, Schalk and Dorette, for their continuous prayers, love and motivational messages at the right times

My siblings, Elsje, Daniël and Z.W for encouragement and an outlet for when I needed to show someone the interesting graphs obtained during the research.

My supervisor, Dr. Clarke, for her invaluable input, patience, time and interesting discussions during meetings. The presence of the "goue draadjie" (golden thread) in the thesis structure can also be attributed to her since it is one of the first and most important lessons she taught me.

My co-supervisor, Prof. Burton, for her input from a biochemistry perspective and also for supplying me with the amidase.

Johan Bezuidenhout for drawing my reactor in *Gambit* and teaching me how to use *Fluent*.

Prof. Aldrich for his valuable discussions regarding statistical analysis and model validation.

Prof. Cowan for supplying the amidase required for the project.

All my friends, for their friendship during the last 6 years in Stellenbosch. In particular I would like to thank Francis, Elinda, Johan, Philip and Pieter for their support and interesting discussions during coffee breaks and braai's.

Lynette Bresler, Juliana Steyl, Enid Thom and Sherry-Lynn Moses for all their administrative help and interesting conversations.

Ruan Havenstein for the Visual Basic program that allowed the integration of curves.

Last, but definitely not the least, I would like to thank my Father in heaven for giving me the ability and perseverance to complete this thesis.

Table of Contents

List of Figures

List of Tables

Nomenclature

$a0_{free}$	Specific activity of free amidase (U/mg)
$a0_{imm}$	Specific activity of immobilised amidase (U/mg)
Ca	Concentration of lactic acid in the permeate stream (mM)
Ca_0	Concentration of lactic acid at time zero of the reaction (mM)
c_{enzyme}	Concentration of enzyme protein in a given solution (mg/L)
C_i	Concentration of enzyme protein in the initial immobilisation feed (mg/L)
C_p	Concentration of enzyme protein in the collective permeate (mg/L)
C_r	Concentration of enzyme protein in the collective retentate (mg/L)
Cs	Concentration of lactamide in the reactor (mM)
Cs_0	Concentration of lactamide at time zero of the reaction (mM)
D_A	Diffusivity coefficient of the substrate solution through the membrane (m^2/s)
D_{eff}	Effective diffusivity of the solution through the membrane (m^2/s)
e_a	Amount of active enzyme at a specific time during reaction (mg)
e_{a0}	Amount of active enzyme at the start of the reaction (mg)
F_p	Instantaneous productivity of the reactor (mmol/L.min)
J	Permeate flux (L/h/m^2)
k_2	Dissociation of enzyme-substrate complex (mmol/L.mg)
k_{cat}	Enzyme catalytic constant (mM/min.mg)
k_d	Enzyme deactivation constant (min^{-1} or h^{-1})
K_m	Amidase Michaelis constant (mM)

L	Membrane wall thickness (m)
l	Membrane thickness (L)
L_p	Membrane permeability (L/h/m^2/bar)
M	Molecular weight of solvent (water) (g/mol)
m_{enzyme}	Amount of enzyme protein in a solution (mg)
$m_{enzyme,imm}$	Amount of immobilised enzyme protein (mg)
$m_{enzyme,permeate\&retentate}$	Amount of enzyme protein in the permeate and retentate washings (mg)
$m_{enzyme,res.feed}$	Amount of enzyme protein remaining in the immobilisation feed after immobilisation (mg)
R^2	Regression coefficient (-)
r_d	Enzyme deactivation rate (mg/min)
s	Substrate concentration (mM)
t	Time (minutes or hours)
T	Temperature (K or ºC)
t_h	Enzyme half-life (min^{-1} or h^{-1})
U	Units of enzyme specific activity (µmol/min.mg$_{enzyme}$)
V	Volume of a solution (L)
V_i	Volume of the initial immobilisation feed (L)
V_m	Molar volume of solute (lactamide) at boiling point (m^3/kmol)
$V_{membrane}$	Membrane volume (L)
X	Conversion or instantaneous conversion (%)

Greek letters

η	Effectiveness factor (-)
$v_{\max}$	Maximum rate of reaction (mM/min)
v_p	Permeate flux or permeate velocity (L/min or mL/min)
v_r	Rate of reaction (mM/min)
σ	Membrane constriction factor (-)
τ	Residence time in membrane (min or h)
τ_t	Membrane pore tortuosity (-)
Φ	Thiele modulus (-)
φ_p	Membrane porosity (-)

Glossary of terms, abbreviations and acronyms

ABS	Absorbance (nm)
BASF	Baden Aniline and Soda Factory
BSA	Bovine serum albumin (protein)
CFD	Computational fluid dynamics
CSTR	Continuous stirred tank reactor
DTT	Dithiothreitol (reducing agent)
EDTA	Ethylene diamine tetra-acetic acid (metal chelating agent)
HIV	Human immunodeficiency virus
MBR	Membrane bioreactor
mM	mmol/L
MW	Molecular weight
MWCO	Molecular weight cut-off

NAC	N-acetylcysteine (reducing agent)
NHase	Nitrile hydratase (enzyme)
ODE	Ordinary differential equation
P	Pressure gauge
PP	Peristaltic pump
S	Sample point
SS	Sum of squares
TMP	Transmembrane pressure

1 <u>Introduction</u>

1.1 <u>Rationale</u>

In nature nitrile compounds occur in plants and can be found as intermediates in microbial metabolism. Nitriles are formed as products in the petrochemical industry and are extensively used as pesticides, solvents, extractants, recrystalising agents, chiral synthons, feedstocks, intermediates in organic synthesis and as the precursors of amides and organic acids [Kobayashi & Shimizu, 2000; Graham *et al.*, 2000; Banerjee *et al.*, 2002; Wang, 2005]. Some of the well-known products obtained by chemical or enzymatic hydrolysis of nitriles are mandelic acid, acrylic acid [Martinkova and Mylerova, 2003], metacrylic acid [Nagasawa and Yamada, 1995], acrylamide and nicotinamide [Banerjee *et al.*, 2002].

The wide distribution of nitriles as potential pollutants in the environment (through industrial waste water and residual agricultural chemicals) has also led to an increased demand for new and more efficient processes for their conversion or degradation [Graham *et al.*, 2000].

Increasing attention is being paid to the biotransformation of nitriles, with microbial cells or isolated enzymes as biocatalysts, as opposed to chemical conversions owing to the following reasons:

- Biotransformation processes are environmentally friendly processes since no chemical additives are required [Giorno *et al.*, 2000].

- Biotransformations can proceed at mild conditions of pH, temperature and pressure.

- The formation of by-products in biotransformations can be significantly reduced due to the selective nature of enzymes [D'Souza, 1999; Giorno *et al.*, 2000].

- In some cases biocatalysts show higher reaction rates and greater stereospecificity than chemical catalysts [Giorno *et al.*, 2000].

- Biocatalysts can be regio-, chemo- and enantioselective [Thomas *et al.*, 2002].

- Biotransformations, in some cases, show higher product yields than chemical conversions [Martinkova and Mylerova, 2003].

Biocatalysts are used to catalyse biotransformations of specific reactants and can be either whole cells or isolated enzymes. The following guidelines can be used to determine whether whole cells or isolated enzymes should be used in a specific situation:

- If the enzyme that is to be used is from plant or animal origin, isolation and purification are usually unavoidable since tissue is not suitable for biocatalysis.

- If several enzymes are used in sequence in a process, whole cells may provide a multipurpose catalyst [Tramper, 1996; D'Souza, 1999].

- When co-factors are required, whole cell catalysts are preferred since the regeneration of co-factors in metabolically active cells is generally easier and less expensive than the *in vitro* regeneration procedure [Schmidt *et al.*, 2001].

- If the formation of by-products is undesirable and no co-factors are required, isolated enzymes should be used [Setti, 1997].

- If the downstream processing cost constitutes a large part of the overall process cost a cell-free system would be better since it would eliminate many of the separation steps which would lead to a significant reduction in the process cost.

Other factors such as the cost of isolated enzymes, the purity of the product and the yield also play a role when determining whether whole cells or isolated enzymes would be the best option [Setti, 1997; Tramper, 1996].

Isolated enzymes are frequently used to act as biocatalysts in cell-free systems due to their specificity which leads to reduced by-product formation [Giorno *et al.*, 2000; Boshoff *et al.*, 1998; Wenten & Widiasa, 2002]. However, isolated enzymes, especially intracellular enzymes, are very expensive and must therefore be retained to allow for reuse. Enzymes can be retained by immobilisation on a matrix through various chemical or physical techniques [Kragl *et al.*, 1999]. The immobilisation of enzymes has a number of advantages:

- It allows reuse of the enzymes which reduces the cost of the process. If expensive enzymes are not retained the process can easily become unfeasible [Tischer and Kasche, 1999].

- Immobilisation has been found to increase the thermal and pH stability of some enzymes, making them less prone to deactivate in changing environments [Makhongela, 2005; Ye *et al.*, 2006; Tramper, 1996].

- Higher volumetric activities can be realised with respect to free enzymes [D'Souza, 1999].

- Due to less enzyme leakages from reactors, product purity is improved and the waste generated by the process is reduced [Giorno and Drioli, 2000].

In order to design an efficient continuous process (which uses immobilised enzymes as biocatalysts), each step in the process must be optimised for the particular enzyme used. This includes choosing an effective immobilisation method which retains the enzyme physically, retains the enzyme activity and improves the enzyme functional stability as well as optimisation of the process conditions.

It is unfortunate that the most effective immobilisation techniques used to retain the enzyme frequently result in deactivation of the enzyme, whereas milder immobilisation techniques (which do not affect the enzyme activity to a great extent) may not effectively retain the enzyme in a continuous system. In order to determine the most effective immobilisation or retention method, a compromise may have to be reached between the activity and the physical retention of the enzyme.

The optimisation of conditions for the bioconversion and the most appropriate immobilisation method are equally crucial to the success of the industrial process. Usually the optimum conditions for bioconversion are the conditions at which the functional stability and activity of the enzyme are at an optimum (for example with regard to pH and temperature). In systems where two enzymes are used for the conversion, the dual system's efficiency needs to be considered to compensate for possible different conversion rates. The best way to optimise the process in such a case would be to separate the component reactions into two steps and to optimise each step for the enzyme involved.

1.2 **Scope of the project**

The three major classes of nitrile degrading enzymes are nitrilases, nitrile hydratases (NHases) and amidases [Banerjee *et al.*, 2002]. The degradation of nitriles can occur through two different enzymatic pathways. Nitrilase can hydrolyse nitriles directly to their corresponding acids and ammonia or NHase can hydrolyse nitriles to their corresponding amides which are then converted by amidase to the acids and ammonia [Kobayashi and Shimizu, 2000; Yildirim, 2005]. The broad research project is focused on the development and optimisation of a process in which nitriles are converted by the latter enzymatic pathway. The model system that was chosen for the project is the conversion of lactonitrile, via lactamide as the intermediate, to lactic acid and ammonia (Figure 1.1).
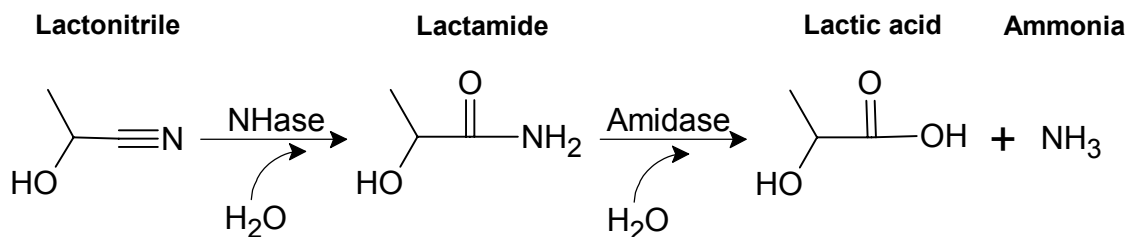
Figure 1.1: Enzymatic biotransformation of nitriles to carboxylic acids and ammonia

This particular research project focused on the development and optimisation of the second step in biotransformation of lactonitrile, which is the biotransformation of lactamide to lactic acid and ammonia with amidase as the biocatalyst (Figure 1.1).

The aims of this project were to:

- Characterise the free amidase in terms of optimum pH, temperature, functional stability and kinetic parameters for lactamide as substrate.

- Develop an experimental membrane bioreactor (MBR) system. This step included using computational fluid dynamic modeling to determine whether an optimum reactor orientation existed for which dead volume would be minimised and whether the assumptions of constant temperature and pressure through the reactor (which was to be used in the development of the mathematical model of the reactor) were valid. The membrane was also characterised in terms of permeability and critical flux.

- Quantify the membrane immobilised amidase process. The first step in the quantification of the process was to evaluate the effectiveness of the immobilisation method. A mathematical model of the reactor was then developed from first principles. The model was statistically validated with the results of two experiments whereafter it was used to predict the effect of amidase activity, amidase functional stability, permeate flux, amount of enzyme protein immobilised and substrate concentration on the reactor performance.

2 <u>Literature review</u>

2.1 <u>Nitrile degrading enzymes</u>

Nitrilase, nitrile hydratase and amidase are collectively called nitrile degrading enzymes. A large number of mesophilic nitrile degrading enzymes have been isolated and characterised. These enzymes have temperature and pH optima in the range 25ºC - 55ºC and 7.0 – 9.0 respectively and are relatively unstable at temperatures exceeding 50ºC [O'Reilly and Turner, 2003; Banerjee *et al.*, 2002; Martinkova and Mylerova, 2003]. This has been given as the reason why the application of biotransformations on industrial scale is very rarely seen.

The possibility of employing more stable enzymes at temperatures exceeding 50ºC has led to a search for thermophilic nitrile degrading enzymes [Cowan *et al.*, 1998]. Characterisation of these enzymes has shown them to have temperature optima of 65ºC [Almatawah *et al.*, 1999; Gavagan *et al.*, 1999]. This means that processes with these enzymes can be operated at higher temperatures. Higher temperatures will lead to higher reaction rates which in turn will lead to an increase in the productivity of the process.

2.1.1 <u>Nitrilase</u>

Nitrilase was the first nitrile-degrading enzyme to be discovered approximately 43 years ago [Banerjee *et al.*, 2002] and is found in plant cells, mammalian cells [Fournand and Arnaud, 2001], fungi and bacteria [O'Reilly and Turner, 2003]. Nitrilases are inducible enzymes which catalyse the conversion of nitriles to their corresponding carboxylic acids and ammonia in a single step [Yildirim, 2005].

Microbial nitrilases are differentiated into three different categories based on their substrate specificity. The first catagory is known to hydrolyse aromatic and heterocyclic nitriles to their corresponding acids and ammonia whereas the second and third catagories preferentially hydrolyse either arylacetonitriles or aliphatic nitriles [Banerjee *et al.*, 2002].

Nitrilases from mesophilic bacterial species such as *Arthrobacter*, *Alcaligenes*, *Norcadia*, *Comamonas*, *Klebsiella*, *Rhodococcus* [Almatawah *et al.*, 1999] and *Acinetobacter* [Pereira *et al.*, 1998] have been isolated and characterised. Thermostable nitrilases found in *Acidovorax ficilis* and *Bacillus pallidus* have been characterised.

A well-known application of nitrilases in industry is the production of *R*-mandelic acid from a racemic mixture of mandelonitrile. This process is used by BASF in Germany [Schmid *et al.*, 2001].

2.1.2 <u>Nitrile hydratase</u>

Nitrile hydratases (NHases) have been studied mainly in bacteria [Brady *et al.*, 2004]. These enzymes are responsible for the conversion of nitriles to their corresponding amides [Kobayashi and Shimizu, 1998] and are key enzymes in the bi-enzymatic pathway for conversion of nitriles to acids [Banerjee *et al.*, 2002].

NHases are metalloenzymes and are classified into two groups on the basis of the metal ion present: cobalt NHases and ferric NHases. The metal ion plays a catalytic role in nitrile hydration and is also required for the folding of the enzyme. Owing to the presence of the catalytic metal center, the specific activity of NHases has been found to be much higher than that of nitrilases although both enzymes attack nitriles [Kobayashi and Shimizu, 1998; Banerjee *et al.*, 2002].

Mesophilic NHases have been studied in various organisms including the following: *Rhodococcus* sp. N 771 (Fe) [Yamada and Kobayashi, 1996], *Rhodococcus* sp. YH3-3 (Co) [Kato *et al.*, 1999], *Rhodococcus rhodochrous* J1 (Co) [Okada *et al.*, 1997] and *Agrobacterium tumefaciens* d3 (Fe) [Bauer *et al.*, 1994]. *Pseudonocardia thermophila* JCM3095 (Co) [Yamaki *et al.*, 1997] and *Bacillus* sp. RAPc8 (Fe) [Pereira *et al.*, 1998] are some of the thermophilic bacteria containing thermostable NHase that have been characterised.

Some applications of NHases include the production of acrylamide and nicotinamide on industrial scale [Thomas *et al.*, 2002].

2.1.3 <u>Amidase</u>

Most of the characterised amidases have been found in bacteria but yeasts, fungi, plants and animal cells containing amidases have also been found [Fournand and Arnaud, 2001]. Amidases are responsible for the hydrolysis of amides to carboxylic acids and ammonia and are sometimes used in conjunction with NHase in a bi-enzymatic pathway to convert nitriles to carboxylic acids via an amide intermediate [Yildirim, 2005].

It is generally thought that amidases (with the exception of those from *Stenotropomonas maltophilia* and *Corynebacterium* sp. C5) have sulfhydryl groups which are essential for catalysis [Kotlova *et al.*, 1999].

Amidases are classified as those hydrolysing short-chain aliphatic amides and those hydrolysing mid-chain aliphatic amides and are known for their stereoselectivity [Fournand and Arnaud, 2001; Banerjee *et al.*, 2002].

Mesophilic amidases have been studied in *Arthrobacter* sp. J1, *Klebsiella pneumoniae* NCTR1, *and Pseudomonas chlororaphis* B23 [Banerjee *et al.*, 2002]. *Ochrobactrum anthropi* SV3 [Komeda and Asano, 2000] and various *Rhodococcus* species [Banerjee *et al.*, 2002]. Only a few thermostable amidases have been found and characterised. These include the amidase from *Pseudonocardia thermophila* [Egorova *et al.*, 2004] and from *Giobacillus pallidus* RAPc8 [Pereira *et al.*, 1998].

Lonza uses a stereospecific amidase to resolve *(R,S)*-Piperazine-2-carboxylic acid to form *(S)*-Piperazine-2-carboxylic acid which is used in compounds such as Crixivan (a HIV protease inhibitor) and BASF and Mitsubishi Rayon uses amidases for the production of *(R)*-mandelic acid and its derivatives [Breuer *et al.*, 2004; Schmid *et al.*, 2001].

2.2 <u>Enzyme kinetics</u>

Enzymes are protein catalysts which speed up the rate of chemical reactions without being chemically changed in the process. An enzyme temporarily binds to a substrate molecule with the effect that it lowers the activation energy required to convert the substrate to product. The rate at which an enzyme works (its catalytic activity) can be influenced by temperature, pH, substrate concentration, the presence of inhibitors, the presence of oxidsing or reducing agents, fluid forces, chemical agents or irradiation [Bailey and Ollis, 1986; http://users.rcn.com].

During enzyme-catalysed reactions the enzyme also loses some of its activity over time. This process is called enzyme deactivation. The rate at which enzyme deactivation occurs is dependent on the reaction conditions (e.g. pH, temperature, presence of denaturants) and the structure of the specific enzyme [Bailey and Ollis, 1986].

In this section the effect of temperature, pH, substrate concentration, oxidising or reducing agents and metal chelating agents on the activity of an enzyme and the model for irreversible enzyme deactivation will be discussed.

2.2.1 <u>Effect of temperature on enzyme activity</u>

Substrate can only be converted to product if the enzyme collides with and then binds to the substrate at the active site. The temperature of a system is directly related to the kinetic energy of the molecules in the system. An increase in the temperature will therefore mean

an increase in the kinetic energy of the system. This will result in a higher number of substrate-enzyme collisions. The rate of reaction will therefore increase with an increase in temperature.

An increase in temperature will also cause an increase in the internal energy of the molecules in the system. Some of this internal energy may be converted to chemical potential energy. If the chemical potential energy rises enough some of the weak hydrogen bonds (which are responsible for determining the three dimensional shape of the protein) may be broken. The result is the denaturation (and therefore the inactivation) of the protein. The rate of enzyme catalysis may therefore decrease if the temperature becomes too high [Bailey and Ollis, 1986; http://academic.brooklyn.cuny.edu].

The activity of enzymes typically follows a bell-shaped curve with the optimum temperature being the temperature at which the activity is at its highest.

2.2.2 Effect of pH on enzyme activity

Proteins are constructed from various amino acids. These amino acids possess basic, neutral or acidic groups in their side chains. An enzyme may therefore contain groups that are both positively and negatively charged at any pH. These ionisable groups are often part of the active site of the enzyme. For the suitable acid or base catalysis to be achievable these ionisable groups must have a particular charge. The enzyme will therefore only be active in one particular ionisation state. Depending on the pH, a large or small fraction of the total enzyme present may be active. Changes in pH may also affect the shape or charge properties of the substrate. This will prevent the substrate from binding to the active site or prevent it from being catalysed [http://academic.brooklyn.cuny.edu].

Usually the catalytic activity of the enzyme reaches a maximum at the optimum pH and then decreases as the pH is increased thereafter [Bailey and Ollis, 1986].

2.2.3 Effect of substrate concentration on enzyme activity

By increasing the substrate concentration the effective time required for an enzyme molecule to collide and bind to a substrate molecule is decreased (more substrate molecules means quicker collisions) [http://users.rcn.com]. Thus, the reaction rate will increase with an increase in substrate concentration. At a specific substrate concentration, however, the active sites of the enzyme molecules become saturated and a further increase in the substrate concentration will have very little effect on the reaction rate.

Michaelis and Menten developed the following mathematical expression for the relationship between the substrate concentration and the reaction rate of enzyme catalysed reactions:

$$v = \frac{v_{max}s}{K_m + s}$$

Equation 2.1

A reaction rate curve for a typical enzyme that follows Michaelis-Menten kinetics (without substrate inhibition) can be seen in Figure 2.1. v_{max} is the maximum reaction rate and can be seen on the graph as the asymptote to which the curve strives. K_m is the Michaelis-constant and can be expressed as the substrate concentration at which the reaction rate is half of its maximum [Bailey and Ollis, 1986].
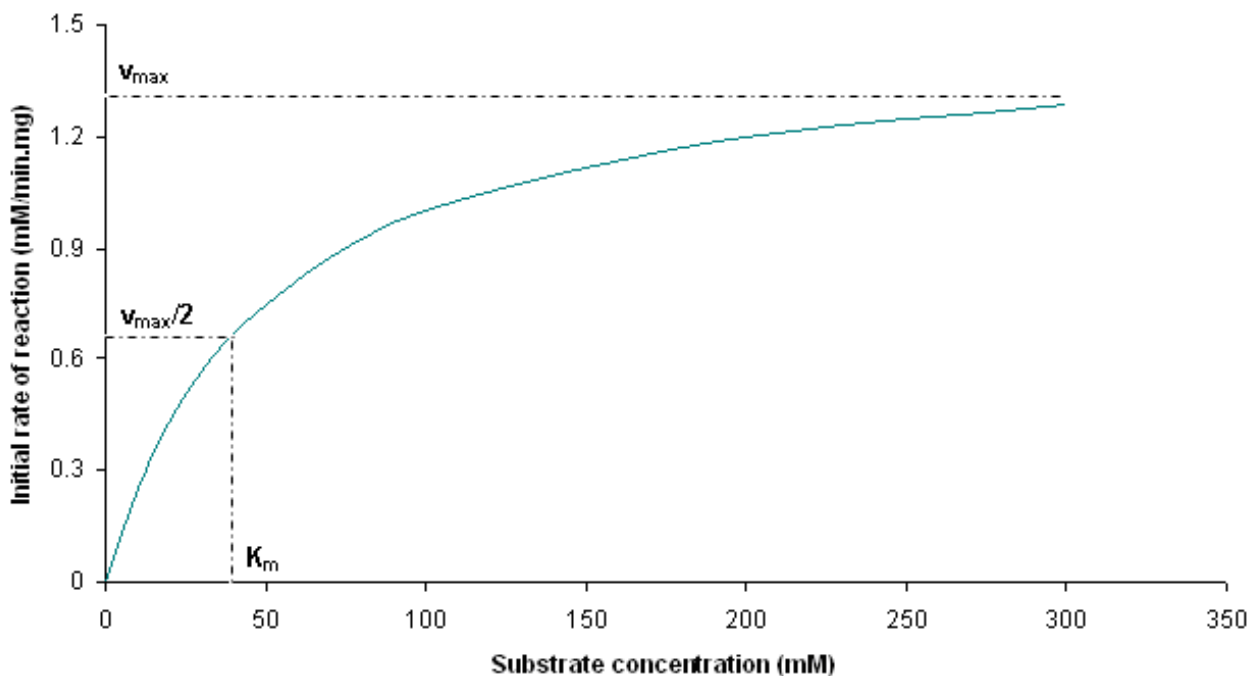
Figure 2.1: Reaction curve for a typical enzyme that follows Michaelis-Menten kinetics

K_m and v_{max} are both parameters which are characteristic of a specific enzyme-substrate combination. K_m is essentially an equilibrium constant for the formation of the enzyme-substrate complex and therefore gives an indication of the affinity of the enzyme for the substrate. A high value of K_m suggests a low affinity for the substrate since higher substrate concentrations are required to achieve the maximum reaction rate. A change in pH or temperature will have an effect on K_m.

v_{max} is the maximum reaction rate that can be obtained by the enzyme and can be used to determine the rate (k_2) at which the enzyme-substrate complex is dissociated to form the

product. v_{max} will change with a change in the initial enzyme concentration since the rate of reaction is directly proportional to the amount of enzyme present.

In some cases, however, enzymes are inhibited by the substrate. In increase in the substrate concentration above a certain threshold will then result in a significant decrease in the reaction rate. For the purpose of this literature review modeling of enzyme kinetics with the Michaelis-Menten model without substrate inhibition will be discussed.

In order to mathematically model an enzyme's kinetics with the Michaelis-Menten model (Equation 2.1) K_m and v_{max} need to be determined. The first step is to obtain data for the rate of reaction as a function of substrate concentration. Usually initial rate data are used since experimental conditions (such as enzyme and substrate concentrations) are known most accurately at the start of the reaction. The data can then be plotted in various ways to determine K_m and v_{max} [Doran, 2004]. Three of the plots generally used to determine K_m and v_{max} are the Lineweaver-Burk plot, the Hanes-Woolf plot and non-linear regression.

2.2.3.1 Lineweaver-Burk Plot

For the Lineweaver-Burk Plot the Michaelis-Menten equation is mathematically manipulated into the following form:

$$\frac{1}{v} = \frac{K_m}{v_{\max} s} + \frac{1}{v_{\max}}$$

Equation 2.2

By plotting 1/v against 1/s a straight line is obtained. v_{max} can be determined from the y-intercept of this line (which is equal to 1/v_{max}) and K_m can be determined from the slope (which is equal to K_m/v_{max}) [Doran, 2004].

The problem with this method of linearisation is that the most accurate rate values (those determined at higher substrate concentrations) will be grouped near the origin and the rate values that are the least accurate (those at lower substrate concentrations) will be far from the origin and will therefore have the strongest influence on the slope of the line [Bailey and Ollis, 1986].

2.2.3.2 Hanes-Woolf Plot

The following equation is known as the Hanes-Woolf equation:

$$\frac{s}{v} = \frac{s}{v_{max}} + \frac{K_m}{v_{max}}$$

Equation 2.3

A straight line can be obtained by plotting *s/v* against *s*. *v_{max}* can be determined from the slope of the line (which is equal to *1/v_{max}*) and *K_m* can be determined from the y-intercept (which is equal to *K_m/v_{max}*).

A disadvantage of the Hanes-Woolf Plot is that the x- and the y-coordinate are not independent of each other. Both of these coordinates are dependent on the substrate concentration. Consequently, the correlation coefficient (R^2), which is a measure of goodness of fit, is not applicable [Bas and Boyaci, 2007].

2.2.3.3 Nonlinear regression

Nonlinear regression is a method that can be used to fit data to any nonlinear equation in order to obtain values for certain parameters in the equation. For example: nonlinear regression can be used to determine *K_m* and *v_{max}* in the Michaelis-Menten equation (Equation 2.1) by fitting experimental data directly to the curve [Motulsky and Ransnas, 1987]. Nonlinear regression techniques usually give more accurate results than linear regression [Doran, 2004].

The ultimate goal of nonlinear regression is to determine values for the parameters which will minimise the residual sum of squares (SS) through iteration. The SS is the sum of the squares of the distances from the actual data points to the fitted curve.

2.2.4 **Effect of oxidising or reducing agents and metal chelating agents on enzyme activity**

Some enzymes contain essential catalytic groups, for example sulfhydryl groups, in their catalytic center. On contact with an oxidsing agent (like oxygen) these groups are oxidised and therefore lose their catalytic ability. The addition of a reducing agent will cause these groups to be reduced back to their original state, thereby restoring the catalytic activity of the enzyme [Cleland, 1963].

Trace metal ions sometimes inhibit the catalytic activity of an enzyme by binding with active groups in the catalytic center of the enzyme. If this is the case, the addition of a metal chelating agent will result in an increase in the enzyme activity since it forms chelates with the metal ions, thereby preventing it from binding to active groups in the catalytic center [http://scifun.chem.wisc.edu].

2.2.5 Enzyme deactivation and stability

In a model of irreversible enzyme deactivation it is assumed that the active enzyme undergoes irreversible transformation and becomes inactive. Generally the rate of deactivation (r_d) will be expressed to be first order in the concentration or the amount of active enzyme (e_a):

$$r_d = k_d e_a \qquad\qquad \textbf{Equation 2.4}$$

k_d is called the deactivation rate constant. If deactivation can be assumed to be the only process affecting the concentration or amount of active enzyme (for example in a closed system with no external factors having an influence) the deactivation can be described as one-phase exponential decay and r_d can be expressed as:

$$r_d = \frac{-de_a}{dt} = k_d e_a \qquad\qquad \textbf{Equation 2.5}$$

Equation 2.5 can then be integrated to obtain the following expression for the fraction of the amount or concentration of active enzyme as a function of time:

$$\frac{e_a}{e_{a0}} = e^{-k_d t} \qquad\qquad \textbf{Equation 2.6}$$

The term *half-life* is generally used to express the stability of an enzyme. The half-life of an enzyme occurs at the time at which the concentration or amount of active enzyme is 50% of what it was at the beginning of the reaction, therefore:

$$e_a = \frac{e_{a0}}{2} \qquad\qquad \textbf{Equation 2.7}$$

By substituting Equation 2.7 into Equation 2.6, taking the natural logarithms and rearranging, the following mathematical expression for half-life (t_h) can be found [Bailey and Ollis, 1986; Doran, 1995]:

$$t_h = \frac{\ln 2}{k_d} \qquad\qquad \textbf{Equation 2.8}$$

2.3 <u>Enzyme immobilisation</u>

Immobilised enzymes are defined as enzymes which are physically confined or localized in a certain defined region of space with retention of their catalytic activities and which can be used repeatedly and continuously [Kragl *et al.*, 1999].

Enzyme immobilisation is necessary because enzymes (especially intracellular enzymes) have become so expensive that some processes catalysed by these enzymes become unfeasible if the enzyme cannot be re-used continuously. Immobilisation can prevent the enzyme from being flushed away during a continuous operation and allows their reuse which therefore reduces the cost of the process.

Enzyme immobilisation is also necessary if an enzyme with a high temperature and pH stability is required in a process. Immobilisation has been found to increase the thermal and pH stability of some enzymes, making them less prone to deactivate in changing environments. This may sometimes be necessary in industrial operations were temperature and pH fluctuations in the upstream process cannot be prevented. If the enzyme is thermostable and pH stable it will not deactivate with fluctuations in temperature or pH [Makhongela, 2005; Ye *et al.*, 2006; Monsan and Combes, 1988].

Although immobilization has the advantages discussed above, there are some disadvantages associated with this procedure. The disadvantages are:

- A reactive group of the enzyme may be involved in a bonding reaction with the support or matrix and thus is not available for catalysis of the enzymatic reaction.

- The structural configuration of the immobilised enzyme may hinder the access of the substrate to the active center [Sousa *et al.*, 2001].

- Enzyme activity may decrease during and after immobilisation due to unfavourable immobilisation conditions which may cause denaturation.

- The immobilisation strategy may require a high initial investment [Makhongela, 2005].

If an enzyme is to be immobilised, it is necessary that the functional groups in the active center should not be involved in the immobilisation reaction or be affected by the reagents used. Further, the immobilisation reaction must be carried out under mild conditions so as not to damage the tertiary structure (which is maintained by weak hydrogen binding forces) of the protein [Sato & Tosa, 1999].

A method of immobilisation that is both perfect and applicable to all systems does not exist. For each different case the individual steps must be evaluated according to criteria such as enzyme activity, enzyme stability, simplicity of the method and economic feasibility [Sanchez Marcano & Tsotsis, 2002]. The general methods of immobilisation are:

- Immobilisation by adsorption.

- Immobilisation by cross-linking.

- Immobilisation by entrapment.

- Immobilisation by covalent bonding.

- Immobilisation through the use of membranes.

2.3.1   Immobilisation by adsorption

Immobilisation by adsorption is probably the simplest method of immobilisation. This method involves the non-specific physical interaction between the enzyme and the surface of the matrix (support structure) [http://www.rpi.edu/dept/chem-eng/Biotech-Environ.htm]. This interaction is due to weak electrostatic forces such as hydrogen and ionic bonding and van der Waals forces. Figure 2.2 illustrates this immobilisation technique.
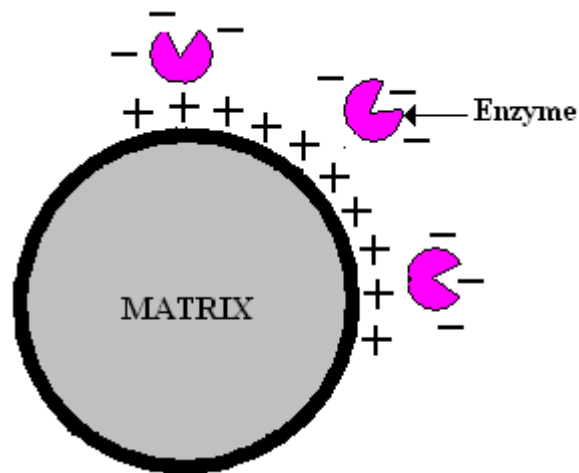
Figure 2.2: Immobilisation by adsorption

Immobilisation can be brought about by mixing a concentrated solution of enzyme with a solid matrix under suitable conditions. Afterwards the material must be washed to remove any unbound enzyme [Bickerstaff, 1997]. Support materials which are commonly used for adsorption are:

- Inorganic material including silica, alumna, porous glass and ceramics.

- Organic material which include cellulose, starch and activated carbon.

- Ion-exchange resins including amberlite, sephadex and dowex [Makhongela, 2005].

A major advantage of adsorption is that no reagents and only a minimum number of activation steps are required, with the result that the method is relatively inexpensive and can be carried out easily. This method is also less disruptive to the enzyme than chemical means of attachment.

The main disadvantage of this technique is that desorption of the enzyme easily occurs with changes in temperature, pH, ionic strength and the presence of a substrate [http://www.rpi.edu/dept/chem-eng/Biotech-Environ.htm]. Other disadvantages include non-specific binding of other proteins or substances and steric hindrance by the matrix [Makhongela, 2005].

2.3.2 Immobilisation by cross-linking

This method is based on the formation of chemical bonds between molecules. An enzyme can either be cross-linked with itself or with functional groups on a support matrix [Sato & Tosa, 1999]. This technique is illustrated in Figure 2.3.
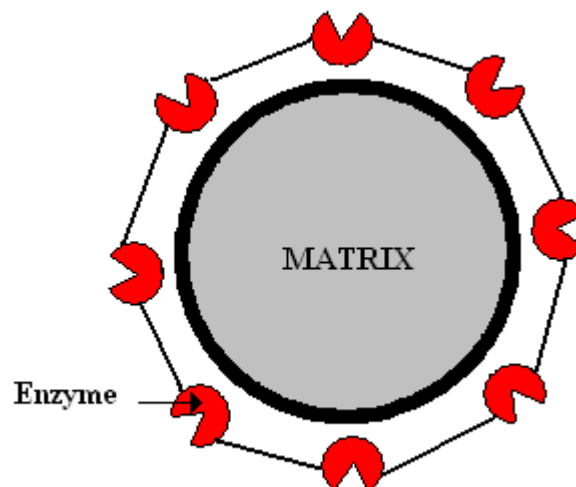
Figure 2.3: Immobilisation by cross-linking

Cross-linking can be achieved by physical or chemical methods. Physical methods use flocculating agents such as polyamines, polyethyleneimine and various phosphates to induce flocculation of the molecules. Chemical cross-linking can be achieved by using a bi-

or multifunctional reagent such as gluteraldehyde or toluene diisocyanate which induces covalent bonding of the enzyme molecules [Bickerstaff, 1997].

Cross-linking an enzyme to itself can be very expensive and inefficient since some of the enzyme molecules will have to act as matrix material, thereby lowering the activity of the enzyme [http://www.rpi.edu/dept/chem-eng/Biotech-Environ.htm]. Another disadvantage of this method is the toxicity of most of the cross-linking reagents [Makhongela, 2005].

In general this method is used in conjunction with other methods for example immobilisation by adsorption. If the enzyme is cross-linked to the support matrix after adsorption, very little desorption is likely to take place [http://www.rpi.edu/dept/chem-eng/Biotech-Environ.htm].

2.3.3 Immobilisation by entrapment

Immobilisation by entrapment is based on confining enzymes in the lattice of a polymer matrix or gel. In this method the enzyme does not bind to the matrix and, in theory, involves no disruption of the protein [Sato & Tosa, 1999]. Figure 2.4 illustrates immobilisation by entrapment.
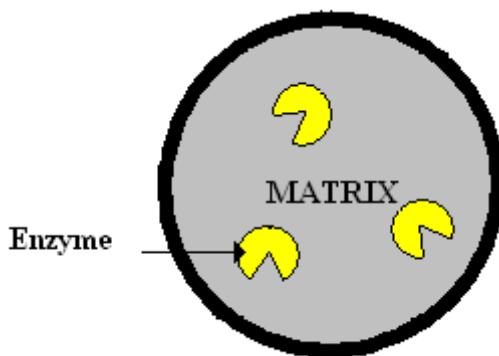
Figure 2.4: Immobilisation by entrapment in a matrix

Immobilisation by entrapment can be achieved by mixing enzyme molecules with chemical monomers (for example acrylamide monomers) that are then polymerized to form a cross-linked polymeric network (for example polyacrylamide) which traps the enzyme inside the lattice [Bickerstaff, 1997].

A major disadvantage of this method relates to free radicals which are generated during the polymerization reaction. These free radicals can affect the activity of the entrapped enzymes.

2.3.4 <u>Immobilisation by covalent bonding</u>

In this method immobilisation is achieved by the formation of covalent bonds between the enzyme and a support matrix. The covalent bond is usually formed between amino acid residues on the surface of the enzyme molecule and functional groups on the support matrix [Makhongela, 2005]. This immobilisation technique is illustrated in Figure 2.5.
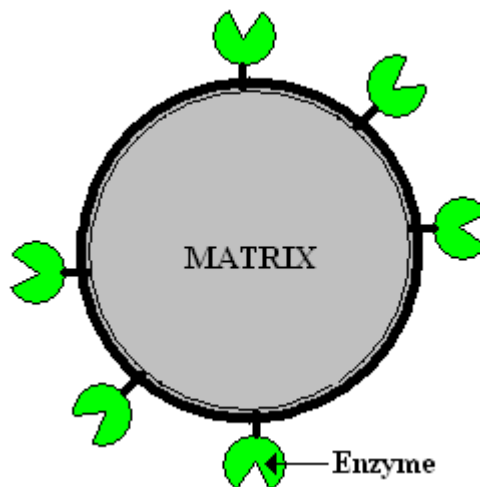
Figure 2.5: Immobilisation by covalent bonding

The functional groups of proteins which are suitable for binding under mild conditions include the following:

- The alpha amino groups of the chain and the epsilon amino groups of arginine and lysine.

- The alpha carboxyl group of the chain end and the beta and gamma carboxyl groups of glutamic and aspartic acids.

- The phenol ring of tyrosine.

- The thiol group of cysteine.

- The hydroxyl groups of threonine and serine.

- The imidazile group of histidine.

- The indole group of tryptophan [http://www.rpi.edu/dept/chem-eng/Biotech-Environ.htm].

Literature reports that the hydrophilicity of the support matrix is the most important factor for maintaining enzyme activity [Gemeiner, 1992]. Some of the support materials that are most often used include polysaccharide polymers such as cellulose, dextran, starch and agarose [Makhongela, 2005].

As with cross-linking, the major advantage of this method is the fact that very little enzyme leakage takes place [http://www.rpi.edu/dept/chem-eng/Biotech-Environ.htm]. Previous work has also proved that amidase that has been covalently bonded on Eupergit C beads, showed in increase in thermal and pH stability [Makhongela, 2005]. Its disadvantages are that the method is expensive and usually results in a loss of enzyme activity [Bailey and Ollis, 1986].

2.3.5 Immobilisation through the use of membranes

Membranes can be used in different ways to immobilise enzymes. The first membrane immobilisation method involves the immobilisation of the enzyme (through any of the techniques discussed above) on a membrane surface (which serves as the support matrix) [Sanchez Marcano & Tsotsis, 2002]. In the immobilisation techniques described above, it is usually unavoidable to modify the native enzyme or its microenvironment in order to retain it effectively. Modification of the enzyme or its microenvironment often results in a decrease in enzyme activity or selectivity [Salmon & Robertson, 1995].

Another membrane immobilisation method is to retain the enzyme in the pores of a semipermeable membrane through physical adsorption. This immobilisation technique is illustrated in Figure 2.6. In this method the enzyme is forced into the membrane pores through the porous support by applying a transmembrane pressure over the membrane. The cut-off layer of the semipermeable membrane prevents the enzyme from passing through the membrane.

Figure 2.6: Immobilisation through physical adsorption in membrane pores

Physical adsorption has no effect on the form of the native enzyme thereby reducing the probability of activity losses during immobilisation. Soluble material (such as substrate and products) can diffuse through the membrane but the macromolecular enzyme is retained. Previous research on physical adsorption has shown the following:

- Approximately 10% of the enzyme circulated through a MBR can be immobilised in the membrane pores if the pores in the cut-off layer is small enough to prevent the enzyme from passing through it [Giorno *et al.*, 2000].

- Membrane entrapment does not have a significant influence on the intrinsic kinetics (thereby leading to high retention of enzyme activity) whereas other immobilisation methods generally result in a 10 – 90% loss in activity [Salmon & Robertson, 1995; Sousa *et al.*, 2001].

Table 2.1 shows a comparison between processes using enzymes immobilised on the membrane surface and processes using enzymes entrapped in the membrane pores (retained by the membrane) [Sato & Tosa, 1999; Kragl *et al.*, 1999]:

Table 2.1: Comparison between enzymes immobilised on the membrane surface and enzymes physically entrapped in membrane pores

Enzyme fixed on a membrane	Enzyme retained in membrane pores
Used in continuous or batch process	Used in continuous or batch process
Improved enzyme stability	Lower enzyme stability
Loss of activity during immobilisation	No loss of activity during immobilisation
Immobilisation costs	No immobilisation costs
Established technology	New technology
Higher investment costs	Easy supply of new enzyme

The advantages associated with membrane immobilisation include the following:

- Efficient contact between the enzyme and the substrate which may lead to high volumetric productivity in the reactor.

- The facility of a continuous separation functions simultaneously with bioconversion.

- Lower susceptibility to process interruption.

- Decreased sterilization requirements [Belfort, 1989].

A disadvantage of membrane immobilisation is that macromolecular substrates (with high molecular weights) may not diffuse rapidly through the membrane to the enzyme making

this method only suitable for enzymes that act on low molecular weight substrates [http://www.rpi.edu/dept/chem-eng/Biotech-Environ.htm].

2.4 Quantification of immobilisation effectiveness

In this research membranes will be investigated as support matrices for physical adsorption of the amidase in the membrane pores due to the various advantages associated with it (Section 2.3.5).

In order to know how effective a membrane immobilisation strategy has been, the effectiveness of the strategy is measured by looking at how much of the free enzyme activity is retained, the functional stability of the immobilised enzyme and the physical amount of enzyme protein that is retained during the operation of the process. The immobilisation technique will be regarded as successful if the enzyme's activity has been retained and can be maintained over a longer period of time than that of the free enzyme (higher functional stability) and no, or very little, enzyme protein is lost during production of the target product.

2.4.1 Immobilised enzyme activity

When an enzyme is immobilised it is possible that it may be partially or completely deactivated. This deactivation can be caused by among others solvents, chemicals, harsh immobilisation conditions or the loss of some enzyme activity centers due to binding to the matrix. Little activity loss after immobilisation indicates a good immobilisation method [www.kochmembrane.com].

2.4.2 Immobilised enzyme functional stability

Immobilised enzyme functional stability is determined by investigating the length of time over which the substrate conversion stays constant. Various researchers have found that immobilisation tends to increase the enzyme stability [Giorno and Drioli, 2000; Carvalho *et al.*, 2000; Long *et al.*, 2005].

2.4.3 Physical amount of enzyme protein retained

The ultimate goal of immobilisation is to retain all the enzyme protein. The more enzyme protein that binds to the membrane, the better the immobilisation method [Makhongela,

2005]. In flow systems it is also desirable that the initial amount of immobilised enzyme protein is retained for as long as possible.

The amount of bound enzyme protein can be determined from a mass balance between the enzyme protein in the initial solution (C_iV_i) and the enzyme protein present in the collective permeate (C_pV_p) and retentate (C_rV_r) [Giorno *et al.*, 2000]. The amount of enzyme protein immobilised can then be determined from Equation 2.9:

Amount of bound enzyme = $C_iV_i - C_pV_p - C_rV_r$ **Equation 2.9**

2.5 Development of a membrane bioreactor

When developing a MBR some of the critical steps in the process are the selection of an appropriate membrane for the particular enzyme that has to be retained, deciding on the membrane geometry that is to be used, choosing a reactor configuration that is suitable and determining the effect of mass transfer limitations.

2.5.1 Selection of the appropriate membrane

Membranes are characterized in terms of their ability to retain molecules of a certain molecular weight (MW). The term molecular weight cut-off (MWCO) defines the size of the molecule that would be, approximately 90%, retained by a specific membrane [Cheryan, 1998; Flaschel & Wandrey, 1979]. The amidase used in this research has a MW of 35 kDa therefore an ultrafiltration membrane with a MWCO of less than 35 kDa will be required for retaining the amidase.

The support structure of ultrafiltration membranes can be either isotropic or asymmetric. The support structure of isotropic membranes is uniform in structure and typically 10 – 30 µm in thickness. Asymmetric membranes consist of a porous, spongy support structure (with a typical thickness of 50 – 500 µm) with a thin layer, about 0.5 µm in depth, which provides the MWCO. Asymmetric membranes exhibit less mass transfer resistance than isotropic membranes but are more easily damaged mechanically [Salmon & Robertson, 1995]. Figure 2.7 shows a photo of an asymmetric capillary membrane as seen under a microscope.
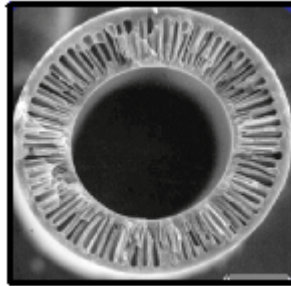
Figure 2.7: Structure of an asymmetric capillary membrane [http://www.rpi.edu/dept/chem-eng/ Biotech-Environ.htm]

The membranes that are to be used in this research must be able to withstand a temperature and pH of at least 50°C and 8.0 respectively (for experimental purposes). In addition the membranes used must be able to withstand the transmembrane pressures that are to be used and must be stable against sterilizing agents. It could also be advantageous to use hydrophilic membranes in MBRs since these types of membranes are less prone to cause deactivation of the enzymes [Flaschel & Wandrey, 1979].

In previous research on the immobilisation of different enzymes on membranes, various membrane materials proved to be successful. Some of the membrane materials used was:

- Polysulfone [Giorno *et al.*, 2000; Edwards *et al.*, 1998; Giorno and Drioli, 2000; Charcosset, 2006; Sousa *et al.*, 2001; Solomon *et al.*, 2002]. Polyethersulfone [Boshoff *et al.*, 1998; Edwards *et al.*, 1998].

- Cellulose triacetate [Giorno and Drioli, 2000].

- Ceramic membranes [Coronas and Santamaria, 1999; Magnan *et al.*, 2004; Nakajima *et al.*, 1989].

Although polymeric membranes proved to be successful in previous research, ceramic membranes were found to have a number of advantages when compared with polymeric membranes. These advantages include the following:

- Ceramic membranes exhibit a higher permeability than equivalent polymeric membranes [Lee and Cho, 2004; Grzeoekowiak-Przywecka and Slominska, 2005].

- Ceramic membranes are superior physically to polymeric membranes and can therefore be used for longer periods [Lee and Cho, 2004].

- Ceramic membranes can withstand extremes of pH (0 – 14), high temperatures (sometimes up to 350°C), abrasives and steam sterilisation [www.novasep.com].

Various authors have investigated the immobilisation of enzymes in the pores of polymeric membranes. Only a few authors, however, have done research on immobilising enzymes in the pores of ceramic membranes [Carvalho *et al.*, 2000; Giorno *et al.*, 2001; Grzeoekowiak-Przywecka and Slominska, 2005].

2.5.2 Selection of a membrane geometry

For the purpose of this research an ultrafiltration ceramic membrane was chosen since the cut-off would allow the retention of the amidase and the ceramic support would be able to withstand the operating conditions. Ultrafiltration membranes are generally manufactured in three geometries:

- Flat sheet membranes.

- Tubular membranes (hollow-fiber or capillary membranes) [Flaschel & Wandrey, 1979].

- Spiral wound membrane (this geometry may be found by wrapping alternate layers of flat sheet membrane and separator screens concentrically around a hollow core) [Kalayanpur, 1999].

Figure 2.8 shows the structures of a hollow fiber membrane and a spiral wound membrane [www.kochmembrane.com].
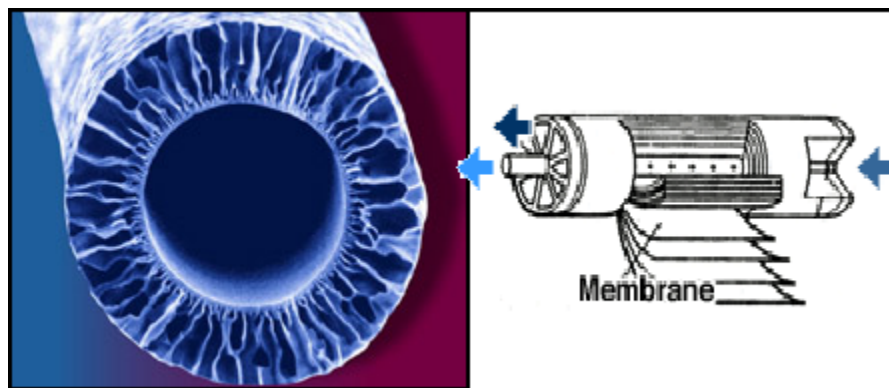
Figure 2.8: A hollow fiber membrane (left) and a spiral wound membrane (right) [www.kochmembrane.com]

The most commonly used geometry for use in MBRs is the tubular or capillary membranes due to the following reasons:

- They are less expensive and less complicated than flat sheet membranes with the same surface area.

- The contact times of reactants with the enzymes are longer than with other types of membranes due to their high surface-to-volume ratios [Salmon & Robertson, 1995; Sanchez Marcano & Tsotsis, 2002; Charcosset, 2006].

- Tangential flow along the membrane surface limits membrane fouling.

- They can be backflushed to remove solids which get lodged in the membrane pores, thereby extending the operational time between chemical cleaning cycles.

- The flow hydraulics can be controlled [http://www.kochmembrane.com].

- They are self-supporting [http://www.cheresources.com].

These advantages associated with tubular or capillary membranes made it a good choice for the reactor in this project.

2.5.3 <u>Configuration of the capillary membrane bioreactor</u>

There are currently no simple rules which can be followed to determine the best capillary MBR configuration for a specific case. Different configurations must therefore be investigated on a case-by-case basis to determine which one would give the optimum conversion and reaction rate [Giorno and Drioli, 2000]. Two important aspects that need to be considered is the mode of operation ("lumen-to-shell" or "shell-to-lumen") and the orientation of the reactor (vertical, horisontal or at an angle).

2.5.3.1 *Mode of operation*

A capillary MBR is a flow reactor in which membranes are used to separate cells or enzymes from the feed or product streams. A common characteristic, and one of the major advantages of these MBRs, is that feed streams are delivered continuously to the reactor. In the case of an enzymatic MBR the product is also removed continuously.

In most enzymatic MBRs, enzymes are entrapped without a chemical immobilisation technique. Earlier research on hollow-fiber membrane reactors used the vertebrate circulatory system as a model. In this system tissues are maintained by nutrients provided through selectively permeable capillaries. In most MBRs the cells or enzymes are therefore retained (not chemically or physically immobilised on the membrane) in the shell side of the membrane with the MWCO layer also on the shell side. Nutrients or substrates are then delivered through the lumina of the hollow-fibers. This arrangement, called the "lumen-to-shell" operating mode, has been found to be preferable because the flow pattern of the

substrate through the lumina closely approximates plug flow which is advantageous for situations where the reaction rate decreases as the substrate conversion increases. This configuration also improves mass transport through the reactor [Salmon & Robertson, 1995]. The use of this reactor configuration seems to be limited to cases where no immobilisation is used (the enzyme is just retained) or where the enzyme is immobilised on the membrane surface [Boshoff *et al.*, 1998; Salmon & Robertson, 1995].

The work of several groups [Bisset and Krieg, 2006; Edward *et al.*, 2005; Giorno *et al.*, 2000] indicates the use of a shell-and-tube reactor configuration where the substrate solution is recycled through the shell side and the permeate is collected from the lumen. This mode of operation, called the "shell-to-lumen" mode, is used when the enzyme is physically immobilised in the pores of an asymmetric capillary membrane with the selective cut-off layer on the lumen side. An applied transmembrane pressure allows the substrate to pass through the membrane and make contact with the enzyme.

The manufacturers of the membranes design the membranes for a specific operational mode. For example, KMS Hollow Fiber membranes from Romicon® are designed specifically for lumen-to-shell operation [www.kochmembrane.com] whereas the InsideCeram^{TM} and Filtanium^{TM} membranes manufactured by Tami Industries in France are specifically designed for shell-to-lumen operation [www.tami-industries.com].

The mode of operation of the MBR would therefore depend on the type of membrane that is to be used or, if a specific mode of operation is required, specific membranes would have to be used. Information regarding the mode of operation will be given with the purchase of the membrane.

2.5.3.2 Orientation of reactor

In general MBRs have been operated in a horizontal orientation [Giorno *et al.*, 2000; Boshoff *et al.*, 1998]. In order to determine if the orientation of the reactor will have a significant effect on the flow patterns, flow velocity, dead volume, pressure drop and temperature distribution in the reactor, computational fluid dynamics (CFD) can be used. CFD modeling involves the use of numerical methods to yield "discrete" solutions of the fundamental equations for flowing fluids that resemble possible analytical solutions as closely as possible.

2.5.4 Determination of the effect of mass transfer limitations

In order for a reactor to function optimally, it should operate in a reaction-limited regime rather than a diffusion-limited regime. The Thiele modulus is a parameter that is used to determine in which regime the reactor is operating and is given by the following equation:

$$\phi = L \left(\frac{v_{max}}{D_{eff} . K_m} \right)^{\frac{1}{2}}$$

Equation 2.10

Where L is the membrane thickness (meters), v_{max} is the maximum reaction velocity (mM/s), D_{eff} is the effective diffusivity of the solution through the membrane (m^2/s) and K_m is the Michaelis-Menten constant (mM) [Giorno and Drioli, 2000].

In order to determine the Thiele modulus, the effective diffusivity must be known. This parameter can be theoretically estimated with the following equation:

$$D_{eff} = \frac{D_A \varphi_p \sigma}{\tau}$$

Equation 2.11

Where D_A is the diffusion coefficient of the substrate solution (m^2/s), φ_p is the membrane porosity, σ is the constriction factor and τ is the tortuosity of the pores. The diffusion coefficient can be calculated from the following equation which describes the diffusivity of the substrate solution through the membrane:

$$D_A = \frac{1.173 \times 10^{-13} (\phi_{ass} M)^{0.5} T}{\mu V_m^{0.6}}$$

Equation 2.12

Where ϕ_{ass} is the association factor for the solvent (m^2/s), M (g/mol) is the molecular weight of the solvent, T is the temperature (K), μ is the viscosity of the solvent (mN.s/m^2) and V_m is the molar volume of the solute at its boiling point (m^3/kmol).

If the Thiele modulus is known it can be used to determine the effectiveness factor. The effectiveness factor gives a ratio between the actual reaction rate and the reaction rate that would result if mass transfer limitations were negligible. Mathematical equations relating the Thiele modulus to the effectiveness factor for specific catalyst shapes and reaction orders can be derived from first principles. The solutions of these equations are frequently used to draw plots relating the effectiveness factor to the Thiele modulus. A plot relating the effectiveness factor to the Thiele modulus for enzymes with intrinsic Michaelis-Menten kinetics that is immobilised in a porous support can be seen in Appendix V [Bailey and Ollis, 1987]. If $\phi \leq 0.3$, it leads to an effectiveness factor of approximately 1 which

indicates that the system is essentially controlled by kinetics and that mass-transfer limitations are negligible [Giorno and Drioli, 2000; Bailey and Ollis, 1987].

2.6 Modeling a membrane bioreactor

Appropriate mathematical modeling of a reactor is an excellent tool for optimisation. The two main types of models used to model MBRs are empirical models and theoretical models derived from first principles.

2.6.1 Empirical models

Empirical models are sometimes referred to as 'black box' models since it uses only inputs and outputs to develop the model. The actual mechanism in the reactor is unknown. These types of models only represent the expected performance of the specific reactor that was modeled for the range over which experimental measurements have been made [Wimpenny, 1997]. The advantage of this type of model is that if the process is too complicated to be modeled from first principles (as is the case with many industrial processes) the appropriate set of experiments can result in data that can be used to make sufficiently accurate predictions about the system.

Mountzouris *et al.* [1999] used an empirical model to describe the effects of enzyme concentration, substrate concentration and transmembrane pressure on the enzymatic depolymerisation of dextran using an endodextranase. From the model the optimum conditions for the system were determined. Lopez-Ulibarri and Hall [1997] also used an empirical model to show that retention time, substrate concentration and enzyme-to-substrate ratio are the factors which have the most significant impact on the process of starch to glucose conversion with glucoamylase in a MBR. The empirical model was transposed onto a mathematical model and was shown to be fairly accurate.

2.6.2 Mathematical models derived from first principles

Theoretical models derived from first principles are developed by taking the characteristic properties of a system under investigation and translating these properties into mathematical equations. The mathematical equations define relationships within the model (for example the relationship between the substrate concentration and conversion or the substrate concentration and the rate of reaction). The function of the model is therefore to mathematically predict the behaviour in the system as a function of the characteristic properties of the system. These types of models need to be validated with experimental results [Wimpenny, 1997].

The advantage of a theoretical model is that if the model has been validated it is possible to quickly assess the influence of numerous variables on the performance of the reactor whereas the same assessment may take much longer when it is done experimentally. The approach to theoretical modeling followed by different groups of authors is not very diverse [Bouwer *et al.*, 1997].

The Michaelis-Menten model (in conjunction with a substrate mass balance) is very often used to model the kinetics of the immobilised enzyme system [Belhocine *et al.*, 2000; Guit *et al.*, 1991; Malcata *et al.*, 1992]. Belhocine *et al.* [2000] used this model to predict the percentage conversion of haemoglobin by an industrial papain enzyme in a MBR at steady state. The model described the experimental results relatively well. By injecting a tracer into the system it was also determined that the MBR operated like an ideal continuous stirred tank reactor (CSTR).

Long *et al.* [2005] (who also used the Michaelis-Menten model to describe kinetics) studied the lipase-catalysed hydrolysis of an ibuprofen ester in a MBR and found that the application of a CSTR model to the MBR delivers good results if the recycle stream is much larger than the stream of fluid leaving the reactor. Results obtained by Carvalho *et al.* [2001] who studied ester synthesis by recombinant cutinase also proved that at high recirculation rates a MBR essentially behaves like a CSTR.

The problem with the Michaelis-Menten model is that on its own it does not describe the effect of convection and diffusion in the membrane [Bouwer *et al.*, 1997]. Some authors have used the equation for mass transport with chemical reaction across a single membrane fiber wall but only for processes at steady state. This model was developed in order to predict the substrate distribution in a hollow fiber membrane when mass transport effects are not negligible [Wenten and Widiasa, 2002].

2.6.3 **Modeling principles**

The following four general steps can be followed when theoretically modeling a system from first principles:

Step 1: Definition of the problem

This requires an assumption as to the mechanism of the system e.g. steady- or unsteady state, plug flow or mixed flow.

Step 2: Formulation of the model from first principles

For model formulation the conservation law is applied to a deferential element of space or time. Transport properties and rate equations are also introduced.

Step 3: Estimation of the parameters

Parameters (for example kinetic parameters) can be assumed or evaluated from experimental data.

Step 4: Validation of the model

The model is validated by evaluating the goodness of fit between the values predicted by model and experimental values [Konar and Oysal, 2003; Walas, 1998]. Two very important assumptions are made when a model is developed. The first assumption is that the variability in the parameter on the y-axis (residuals) is random and follows a normal distribution. It is also assumed that the parameter on the x-axis is known precisely. A second important assumption that is made is that of uniform variance (homoscedacity). It means that the standard deviation of the residuals is assumed to be the same for the whole curve [Motulsky and Christopoulos, 2003]. When a computer program is used to do nonlinear regression on data, several pages of results are usually generated [Motulsky and Ransnas, 1987]. These results must then be evaluated in order to answer the following important questions:

- Is the fitted curve a good representation of the experimental data?

- Are the best-fit values that were generated for the parameters scientifically possible?

- How certain are the best-fit parameters (what is the range of the 95% confidence interval)?

- Are there any violations of the basic assumptions [Motulsky and Christopoulos, 2003]?

After a model has been validated it can be used (instead of experiments) to predict the effects of various parameters on the system and to optimise the system.

2.7 <u>Investigation of membrane bioreactor system performance</u>

Reactor performance is generally measured in terms of the degree of conversion and productivity [Giorno *et al.* 2000]. Some of the parameters that usually have a significant impact on the reactor performance are the following:

Immobilised enzyme activity and stability

The activity and stability of immobilised enzymes have a very significant impact on the total conversion and productivity that will be achieved. Immobilised enzymes with low activity and functional stability will result in reactor systems with low conversions of substrate and consequently low productivities. If the activity is low, the reaction rate will be slow and if the stability is low the amount of active enzyme will decrease quickly which will result in even lower reaction rates.

Permeate flux

The permeate flux is directly proportional to the transmembrane pressure and inversely proportional to the residence time of substrate. The residence time in a membrane MBR with enzyme immobilised in the pores of the membrane is defined as the length of time during which the substrate solution is in contact with the immobilised enzyme. The following equation can be used to determine residence time:

$$\tau = \frac{l}{v_p}$$
                                                     Equation 2.13

Where:

l = membrane volume (liters)

v_p = velocity of permeate (liters per minute) [Giorno *et al.* 2001].

The relationship between transmembrane pressure and the permeate flux can be found from permeability studies and can be related to the residence time by using Equation 2.13. Studies done by Grzeoekowiak-Przywecka and Slominska [2005], Wenten and Widiasa [2002], Giorno *et al.* [2001] and Carvalho *et al.* [2001] showed that by decreasing the flux rate (and thereby increasing the residence time) an increase in conversion but a decrease in the productivity will be observed.

Amount of immobilised enzyme

Giorno *et al.* [2001] found that there was an amount of immobilised enzyme protein in a membrane corresponding to an optimum conversion. In their investigations the conversion of substrate increased with an increase in the amount of enzyme protein immobilised up to a point whereafter it decreased with a further increase in the amount of immobilised enzyme. The reasoning behind this phenomenon is that at higher amounts of enzyme protein a gel layer forms on the membrane surface, resulting in an increase in mass transfer resistance and therefore a decrease in reaction rate which, in turn, will lead to a decrease in conversion.

Substrate concentration

If the enzyme follows Michaelis-Menten kinetics (without substrate inhibition) the reaction rate is dependent on the substrate concentration up until a point whereafter an increase in substrate concentration will have no effect on the reaction rate (due to saturation of the enzymes' active sites). By increasing the substrate concentration above that threshold value, the mass transfer resistance may increase which will lead to a lower conversion of substrate. If, however, the enzyme follows Michaelis-Menten kinetics with substrate inhibition the reaction rate will decrease significantly if the threshold value of the substrate concentration is exceeded.

2.8 <u>Hypotheses and research objectives</u>

From this section onwards the project will be divided and discussed in three main sections. These sections are: characterisation of free amidase, development of the MBR system and quantification of the membrane immobilised amidase process. From the literature review the following hypotheses are made:

2.8.1 <u>Characterisation of free amidase</u>

1. ***The pH and temperature of the reaction mixture have a significant influence on the activity of the amidase. The interaction between the pH and the temperature, however, are insignificant. By using the experimental data showing the amidase activity at different pH's and temperatures it is possible to predict the amidase activity at a specific pH and temperature.***

    The determination of an enzyme's optimum pH and temperature is a very important step in characterising an enzyme. These experiments are frequently done with the assumption that no interaction exists between the pH and the

temperature [Kotlova *et al.*, 1999; Almatawah *et al.*, 1999; Kobayashi *et al.*, 1989; Egorova *et al.*, 2004]. The effect of the interaction between the pH and the temperature was determined by doing an analysis of variance on data obtained from factorial design experiments (in which the pH and temperature were the input variables and the specific activity of the enzyme was the response variable). A model was also developed from this data to predict the amidase activity at specific pH's and temperatures.

2.   ***The activity and the stability of the amidase can be improved by the addition of a metal chelating agent or a reducing agent.***

Some amidases are inhibited by trace elements of metal ions. Trace elements of metal ions may be present in the substrates used for reactions. By adding a metal chelating agent to the reaction, all metal ions will form chelates with the agent and will be prevented from interfering with the enzyme reaction [http://scifun.chem.wisc.edu].

Exposure to oxygen can also cause a loss in amidase activity if the enzyme contains sulfhydryl groups which are essential for catalysis since these groups can be oxidised. Should this be the case, the addition of reducing agents will cause an increase in activity because it will reduce the oxidised sulfhydryl groups (disulfides) back to sulfhydryl groups [Makhongela, 2005].

Since the amidase that was used in this research contains sulfhydryl groups in its catalytic center and was found to be inhibited by trace metals ions [Makhongela, 2005], the effect of a metal chelating agent and reducing agents on the amidase activity was evaluated.

3.   ***The rate of reaction catalysed by the amidase can be predicted using the Michaelis-Menten model.***

The kinetics of the amidase was compared with the Michaelis-Menten model to determine if the model can be used to predict the kinetic parameters (K_m and v_{max}) for the amidase. These parameters were required for the development of the mathematical model of the MBR.

2.8.2 Development of the experimental membrane bioreactor system

1. ***Constant temperature and pressure are maintained over the whole length of the MBR system, irrespective of the orientation of the MBR.***

    In order to model an enzymatic MBR it is very important to ensure that the temperature and pressure are constant throughout the system since variations could alter the enzyme activity and the permeate flux and residence time at different positions in the reactor. Computational fluid dynamics is a useful tool to predict the distribution of temperature and pressure in a reactor in order to validate the assumption of uniform temperature and pressure.

2. ***The velocity profile in the MBR is the same for all reactor orientations.***

    By using computational fluid dynamics it is possible to predict the type of flow patterns that will occur in a reactor for specific flow rates and orientations. The flow patterns are very useful in identifying stagnant zones or dead volume in the reactor. It is preferable to have no dead volume in a reactor since dead volume causes a decrease in the active membrane area. The effect of the reactor orientation on dead volume was investigated with CFD modeling in order to determine whether there is an optimal reactor orientation for which dead volume would be minimised.

3. ***External mass transfer limitations in the MBR are significant.***

    Membrane support matrices usually act as resistance against substrate diffusion. If the maximum mass transfer rate is significantly smaller than the maximum reaction rate, it is probable that a reactor is operating in the reaction-limited regime. It is important to know when a reactor is operating in the reaction-limited regime since operation in this regime will mean that the kinetic parameters and reaction rates that are measured are apparent values and not intrinsic values. Although apparent values have been used to provide adequate models of the immobilised enzyme kinetics [Wenten and Widiasa, 2002], it is not generally correct since it does not take into consideration the dependence of K_m on fluid properties and hydrodynamics [Bailey and Ollis, 1986].

2.8.3 Quantification of the membrane immobilised amidase process

1. ***The amidase can be effectively immobilised through physical adsorption in the pores of an asymmetric, ceramic capillary membrane in a MBR.***

    The average pore size of the membrane support is 3.5 µm (which is equivalent to approximately 35000 kDa). The pores are therefore 1000 times larger than the molecular weight of the amidase which is 35 kDa. Since the amidase is significantly smaller than the pores it was expected that the amidase would easily enter the pores of the membrane during the immobilisation procedure. Furthermore, since the molecular weight cut-off of the membrane (8 kDa) is significantly smaller than the molecular weight of the amidase (35 kDa), it was likely that the membrane would effectively retain the amidase when a transmembrane pressure was applied during the process.

2. ***The stability of the amidase will be increased by immobilisation.***

    Enzyme immobilisation in porous structures has often been found to increase the stability of the enzyme [Monsan and Combes, 1988] since the pores of the support structure protects the enzyme and thereby prevents its direct exposure to changes in the characteristics (for example pH, temperature and substrate concentration) of the bulk fluid [Zhang *et al.*, 2005]. It was expected that the membrane support structure would protect the amidase when immobilised and that its stability would therefore be higher than when free in solution.

3. ***The MBR can be modeled theoretically and the percentage conversion of lactamide and the reactor productivity can be predicted by using an ordinary differential equation (ODE) solver software package.***

    The four basic modeling principles (definition of the problem, formulation of the model from first principles, estimation of parameters and validation of the model) were followed to develop a theoretical model to predict the reactor performance in terms of the conversion and productivity. The influence of key system parameters (enzyme activity and stability, permeate flux, amount of enzyme protein immobilised and substrate concentration) on the reactor performance was predicted by this model. An ODE solver package was used to solve the model differential mass balance equations simultaneously.

3 Experimental materials and methodology

3.1 Materials and chemicals

The University of the Western Cape originally isolated the thermostable, unpurified amidase that was used in this project. The amidase was isolated from *Bacillus* sp. RAPc8, cloned and over-expressed in *E. coli* BL21 pNH 223 pLySs. It has a molecular weight of approximately 35 kDa. The University of Cape Town supplied the amidase for the project.

DL-lactamide (97%) was ordered from Sigma Aldrich SA for use as substrate.

A ceramic, asymmetric, mono-channel, capillary membrane with nominal cut-off of 8 kDa on the lumen side was purchased from Tami-Industries, France. The support matrix of the membrane consists of titanium oxide and the active membrane layer consists of zirconium oxide.

The MBR, connectors and sample stopcocks were constructed by Glasschem (Stellenbosch) and were made from borosilicate glass. Valves were purchased from Jachris (Stellenbosch). The peristaltic pump was purchased from Sigma Aldrich SA.

A list of all chemicals that was required for the project as well as the preparation of the potassium phosphate buffer used in all experiments can be seen in Appendix I.

3.2 Analyses

3.2.1 Amidase

3.2.1.1 Activity assays

The activity of the amidase was determined based on the release of ammonia from the conversion of lactamide to lactic acid and ammonia. The activity was expressed in units where 1 unit was defined as the amount of amidase which catalysed the release of 1 μmol of ammonia per minute at standard assay conditions. The standard assay conditions were a temperature of 50ºC, pH of 8.0 and a lactamide concentration of 80 mM (unless stated otherwise in the text). The specific activity of the amidase was expressed in units per mg of amidase.

A slightly modified version of the phenol-hypochlorite ammonia detection method [Pereira *et al.,* 1998] was used to assay the amount of ammonia released during a reaction. Larger volumes of Reagents A and B were added to the samples to cause a deeper blue colour to develop. This ensured easier distinction between samples when the absorbance was measured. The reagents (A and B) were made up as described by Weatherburn [1967]. The method used was as follows:

1. Preparation of Reagent A: 5 g of phenol and 25 mg of nitroprusside were added to 500 mL of distilled water. The reagent was covered in foil to protect it from light and was stored at 4 °C.

2. Preparation of Reagent B: 2.5 g of sodium hydroxide and 6 mL of household bleach (3.5% available chlorine) was added to 500 mL of distilled water. The reagent was covered in foil and was stored at 4 °C.

3. 1400 μL of Reagent A was added to 350 μL of the reaction mixture that was to be analysed for amidase activity.

4. To this mixture, 1400 μL of Reagent B was added next.

5. The activity was measured spectrophotometrically at 600 nm after 15 minutes' incubation at room temperature.

6. Activity standards were prepared using ammonium chloride and were used to plot a standard curve for relating the absorbance of a sample to the ammonia concentration (Appendix I, Figure A.1).

3.2.1.2 *Enzyme protein concentration assay (50 – 1000 μg/mL)*

If the concentration of enzyme protein in a solution was expected to be in the range 50 – 1000 μg/mL the standard Bradford Coomassie Brilliant Blue dyebinding assay [Bradford Reagent, Product information, Sigma Aldrich] was used.

1. Bradford solution (3 mL) was added to a 100 μL enzyme protein sample.

2. The enzyme protein concentration was then determined spectrophotometically at 595 nm after 8 minutes of incubation at room temperature.

3. Protein standards were prepared with bovine serum albumin and were used to plot a standard curve for relating the absorbance of a sample to the enzyme protein concentration (Appendix I, Figure A.2).

3.2.1.3 Enzyme protein concentration assay (1 – 5 µg/mL)

If the concentration of enzyme protein in a solution was expected to be in the range 1 – 5 µg/mL the micro Bradford Coomassie Brilliant Blue dyebinding assay [Bradford Reagent, Product information, Sigma Aldrich] was used.

1. Bradford solution (1 mL) was added to 1 mL enzyme protein sample.

2. The enzyme protein concentration was then determined spectrophotometrically at 595 nm after 8 minutes of incubation at room temperature.

3. Protein standards were prepared with bovine serum albumin and were used to plot a standard curve for relating the absorbance of a sample to the enzyme protein concentration (Appendix I, Figure A.3).

3.2.2 **Lactic acid**

The phenol-hypochlorite ammonia detection method (Section 3.2.1.1) was used to determine the ammonia concentration in a sample after the amidase catalysed reaction took place. The lactic acid concentration in the sample was the same as the ammonia concentration in the sample since one mole of lactamide lead to the formation of one mole each of lactic acid and ammonia (Figure 3.1).
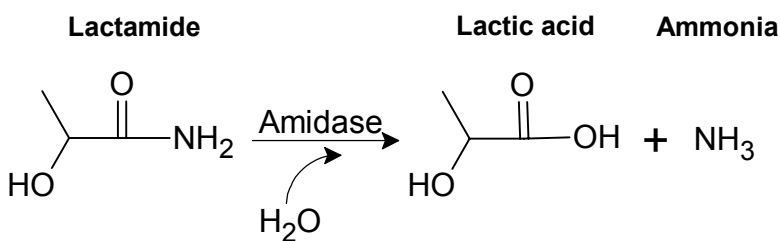
Figure 3.1: Amidase catalysed reaction of lactamide to produce lactic acid and ammonia

3.3 **Methodology: characterisation of free amidase**

3.3.1 **Determination of optimum pH and temperature**

The free amidase was characterised in terms of its optimum temperature and pH by investigating the influence of these two parameters on the activity of the amidase. A temperature range of 30 - 70ºC and a pH range of 6.0 – 8.5 were used. The experiments were designed as a two-by-two factorial design which would enable the development of an

empirical model for the system and the quantification of pH and temperature interaction if any. A constant pH was confirmed throughout the incubation. The following method was employed:

1. Eppendorf tubes (3 replicates) were each filled with 10 µL of an enzyme solution (3mg/mL in phosphate buffer of pH 7.0) and 1250 µL of phosphate buffer at the desired pH. 2 Eppendorf tubes were each filled with 1260 µL of phosphate buffer at the desired pH and no enzyme (blank experiments). A vortex mixer was used to ensure that the solutions were mixed well.

2. The 5 Eppendorf tubes were pre-incubated for 10 minutes at the desired temperature to achieve thermal equilibrium in a Labcon incubator [Purich, 1983].

3. 140 µL of substrate (0.25 mol/L lactamide made up with buffer at the desired pH) was added to the reaction mixture. The final substrate concentration was 25 mmol/L in each Eppendorf tube. A vortex mixer was used to mix the solutions.

4. The reaction mixtures were then incubated for 15 minutes [Almatahwah *et al.*, 1999] at the desired temperature.

5. After incubation the reaction mixtures were mixed.

6. The activity of the enzyme in each Eppendorf tube was measured using the phenol hypochlorite ammonia detection method (Section 3.2.1.1).

7. The procedure above was repeated at the different pHs and temperatures.

3.3.2 <u>Determination of amidase initial rate of reaction at different substrate concentrations</u>

In order to determine the kinetic parameters (K_m and v_{max}) of the free amidase, initial rate assays were performed in duplicate for substrate concentrations of 15 mM, 25 mM, 40 mM, 60 mM, 80 mM, 100 mM and 150 mM. The procedure was as follows:

1. A 5 mL screw-cap glass tube was filled with 250 µL amidase (1mg/mL in phosphate buffer of pH 8). 1150 µL of phosphate buffer (pH 8) was added to the amidase. Another 5 mL screw-cap glass tube was filled with 1150 µL buffer only and used as a blank experiment.

2. Both glass tubes were pre-incubated in a Labcon incubator at 50°C for 10 minutes.

3. Lactamide solutions with concentrations that were double those that needed to be tested (30 mM, 50 mM, 80 mM, 120 mM, 160 mM, 200 mM and 300 mM) were made up by dissolving the required amount of lactamide in phosphate buffer of pH 8.0. This ensured that the final reaction mixture had the lactamide concentration that needed to be evaluated.

4. 1400 µL of the required lactamide solution (for example 30 mM) was added to the two glass tubes after they were pre-incubated to achieve the required final substrate concentration (for example 15 mM) in both tubes (the reaction mixture now had a total volume of 2800 µL).

5. The glass tubes were then incubated at 50°C for 6 minutes.

6. Samples (of 350 µL) were withdrawn every minute and analysed for ammonia with the phenol hypochlorite ammonia detection method (Section 3.2.1.1).

3.3.3 Determination of amidase functional stability

The stability of the free amidase was determined in duplicate at a temperature of 50ºC and substrate (lactamide) concentrations of 40 mM and 80 mM. The method was as follows:

1. A 5 mL aliquot of amidase (1mg/mL) in phosphate buffer (pH 8.0) was prepared. The aliquot was incubated in a Labcon incubator for 18 hours at 50ºC.

2. Two 125 µL enzyme samples were withdrawn from the amidase solution in the incubator after 0.5 hours of incubation. Further sampling took place in intervals of 0.5 to 1.5 hours.

3. Phosphate buffer (pH 8.0) was added to the two enzyme samples (Figure 3.2) and the samples were then pre-incubated at 50ºC for 10 minutes.

4. The required amount of a 100 mM lactamide stock-solution (Figure 3.2) was then added to the samples to obtain final lactamide concentrations of 40 mM and 80 mM and final volumes of 1400 µL.

5. The mixtures were incubated for 15 minutes whereafter the activity was measured with the phenol hypochlorite ammonia detection method (Section 3.2.1.1).

6. The method was repeated for all subsequent samples.
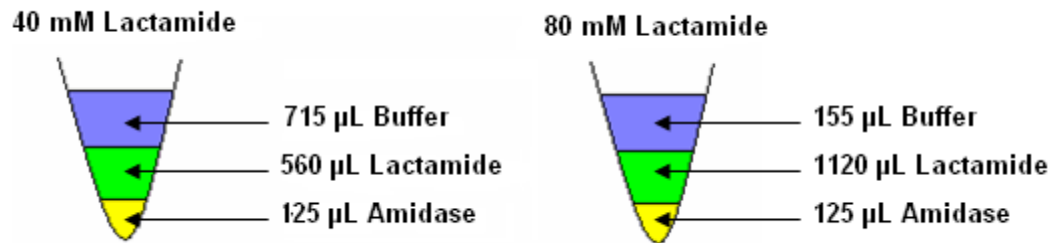
Figure 3.2: Composition of the 40mM and 80mM lactamide reaction solutions to test amidase stability

3.3.4 Effect of different reducing agents and a metal chelating agent on amidase activity and stability

The effect of the reducing agents dithiothreitol (DTT), L-cysteine and N-acetylcysteine (NAC) and the metal chelating agent ethylene diamine tetra-acetic acid (EDTA) on the activity of the amidase was tested in duplicates. The reducing agents and metal chelating agent were dissolved in phosphate buffer (pH 8.0). The effect of L-cysteine, NAC and EDTA was evaluated at a concentration of 0.1 mM and DTT was evaluated at concentrations of 0 mM, 0.1 mM, 1 mM, 5 mM, 10 mM, 15 mM and 20 mM. The procedure was as follows:

1. Seven 5 mL screw-cap glass tubes were each filled with 125 µL of an amidase solution (1mg/mL in phosphate buffer of pH 8.0).

2. Reducing agents and metal chelating agent solutions with concentrations double those that needed to be tested were made up. This ensured that the final reaction mixture had the reagent concentration that needed to be evaluated.

3. 700 µL of the required reducing agent or metal chelating agent solution were added to the enzyme samples.

4. The samples were then incubated in a Labcon incubator for 10 minutes at 50ºC.

5. 575 µL of a 195 mM lactamide stock-solution was then added to the samples to obtain a final lactamide concentration of 80 mM and a final volume of 1400 µL.

6. The mixtures were incubated for 15 minutes whereafter the activity was measured with the phenol hypochlorite ammonia detection method (Section 3.2.1.1).

7. Blank experiments contained no amidase.

The effect of 0.1 mM DTT, L-cysteine, N-acetylcysteine and EDTA on the stability of the amidase was tested (in duplicate) by using the same procedure used to determine the free amidase stability (Section 3.3.3) with the only difference being the addition of the reducing agents and metal chelating agent after sampling.

1. A 5 mL aliquot of amidase (1mg/mL) in phosphate buffer (pH 8.0) was prepared and incubated at 50ºC.

2. Five 125 µL enzyme samples were withdrawn after 0.5 hours of incubation. Three samples were used to test the effect of each of the reducing agents, one sample was used for the metal chelating agent and one sample for no addition of reagents. Further sampling took place in intervals of 0.5 to 1.5 hours.

3. 700 µL of a 0.2 mM solution of the required reducing agent or metal chelating agent in phosphate buffer (pH 8.0) was added to the enzyme samples in order to obtain final reagent concentrations of 0.1 mM.

4. The samples were then pre-incubated at 50ºC for 10 minutes.

5. 575 µL of a 195 mM lactamide stock-solution was then added to the samples to obtain a final lactamide concentration of 80 mM and a final volume of 1400 µL.

6. The mixtures were incubated for 15 minutes whereafter the activity was measured with the phenol hypochlorite ammonia detection method (Section 3.2.1.1).

7. Blank experiments contained no amidase.

3.4 Methodology: development of the experimental MBR system

3.4.1 Construction and set-up

A borosilicate glass bioreactor into which the capillary membrane could be inserted was designed. The set-up is a typical set-up for a shell-to-lumen operation (which implies that the substrate is sent through the shell side of the reactor and the permeate is collected from the lumen side). Giorno *et al.* [2001] used a bioreactor with capillary membranes for the production of malic acid catalysed by fumarase. The experimental set-up they used proved to be successful and it was decided to use a similar construction in this project.

A photo and a schematic diagram of the experimental set-up are shown in Figure 3.3 and Figure 3.4 respectively.
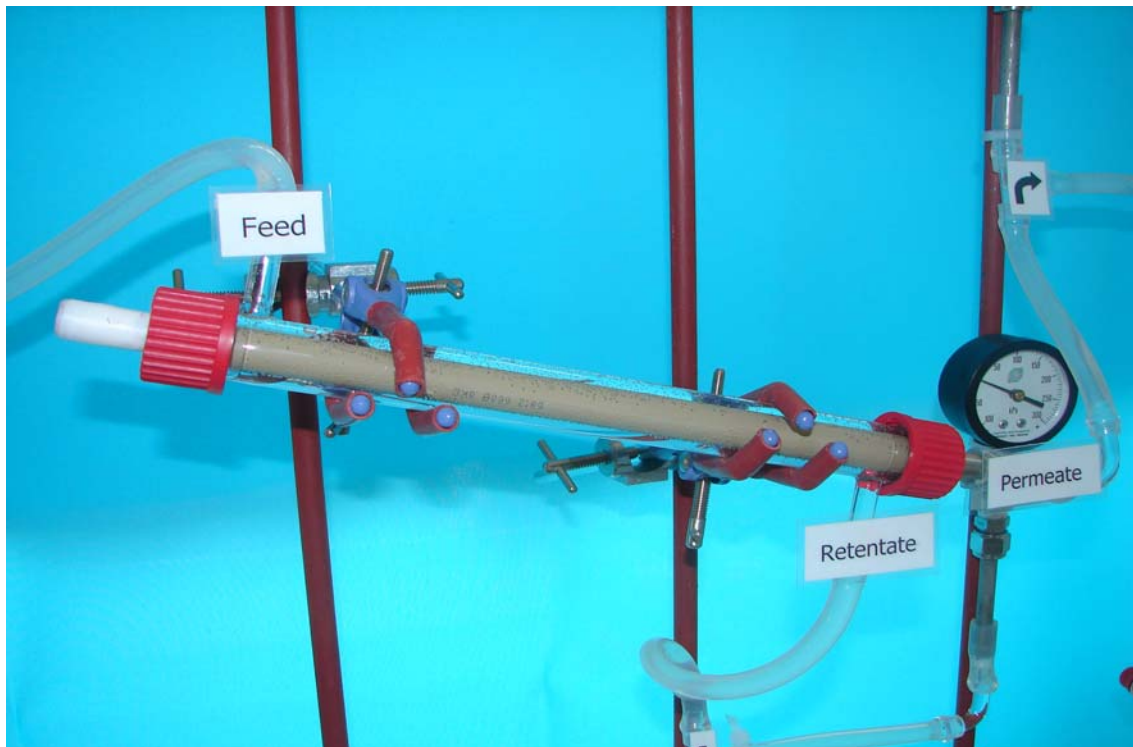
Figure 3.3: Experimental set-up of the membrane bioreactor
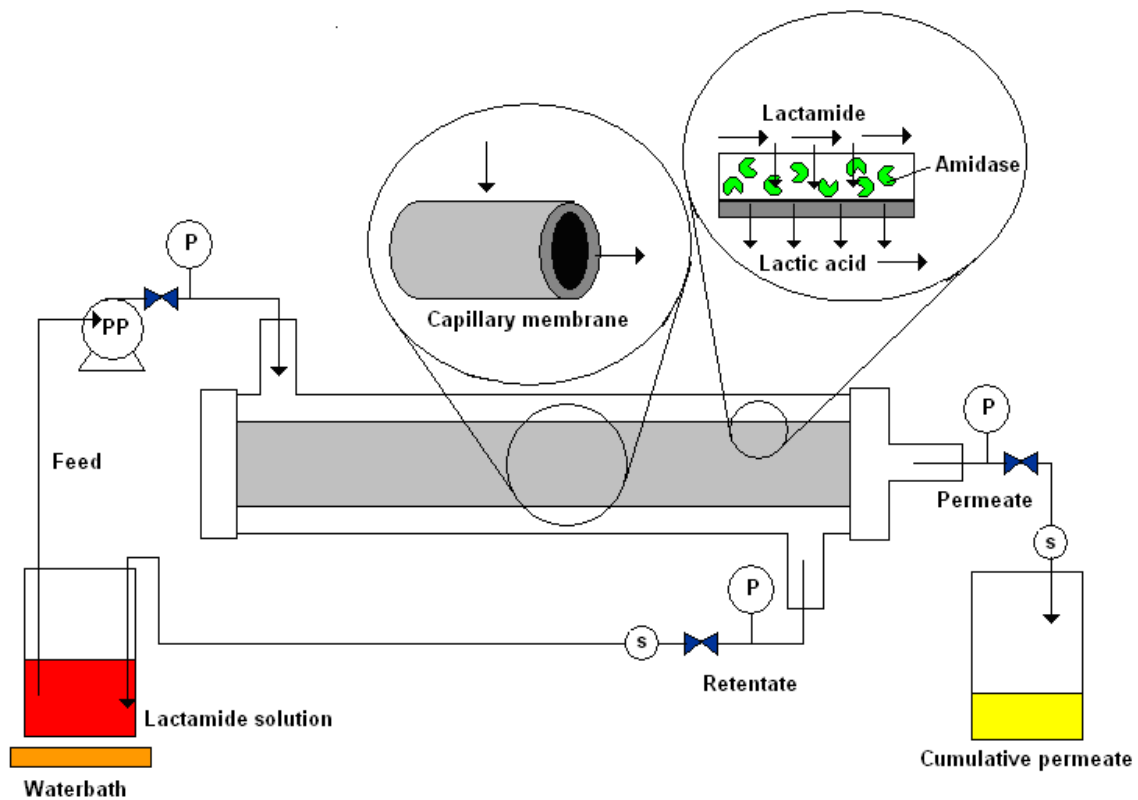
Figure 3.4: Schematic diagram of the membrane bioreactor system (PP = peristaltic pump, P = pressure gauge, s = sample point)

3.4.2 **Membrane cleaning procedure**

The membrane had to be cleaned before and after experiments in order to remove all fouling and enzyme protein that may still have been in the membrane pores. If the MBR wasn't used for more than 24 hours, it had to be filled with jik water (1 mL jik per L distilled water) in order to preserve the membrane. After storage in jik water the membrane also had to be cleaned before resuming experiments. The cleaning procedure for the MBR was as follows:

1. *Alkaline cleaning*: A NaOH solution (30 g/L) was circulated through the reactor for 40 minutes. The temperature was kept at approximately 85°C.

2. *Rinsing*: Distilled water was circulated through the reactor until the pH of the retentate and permeate (which was determined with a pH strip) was 7.0.

3. *Acid cleaning*: Phosphoric acid (75%) was used to make up a diluted phosphoric acid solution (2mL acid per liter of distilled water). This solution was then circulated through the reactor for 20 minutes. The temperature was kept at approximately 50°C.

4. *Rinsing*: Distilled water was circulated through the reactor until the pH of the retentate and permeate (which was determined with a pH strip) was 7.0 [Tami Industries, Technical Directions].

3.4.3 **Characterisation of the membrane module**

The membrane module was characterised by measuring the pure water permeability (distilled water), phosphate buffer permeability and 80 mM lactamide solution (in buffer) permeability. After an experimental run the membrane was cleaned and then the water or buffer permeability was measured again. If the water or buffer permeability remained the same as before the experimental run no permanent fouling occurred. If, however, the water or buffer permeability was lower than before an experimental run, permanent fouling occurred. If permanent fouling of the membrane occurred, the membrane could not be used for further experiments since the fouling affected the accuracy of the results. The procedure used for determining the permeability of the three solutions was as follows:

The permeate flux (J) was measured as a function of time for various transmembrane pressures (TMP's) in the range 0 to 2.2 bar. The steady-state values of J at the different TMP's were then plotted against TMP. The slope of the graph obtained was the pure

water/buffer/lactamide solution permeability (L_p) of the membrane. The following equation shows the relationship between J, TMP and L_p:

$$J = L_p.TMP$$

Equation 3.1

An important part of characterising the membrane was to determine the critical flux since working above the critical flux may result in permanent fouling of the membrane. The critical flux is the lowest flux for which an increase in TMP does not cause a significant increase in the flux. The permeability data obtained from the lactamide solution was used to determine the critical flux since the same lactamide solution was used in experiments. Figure 3.5 shows how to determine the critical flux from a typical permeability curve.
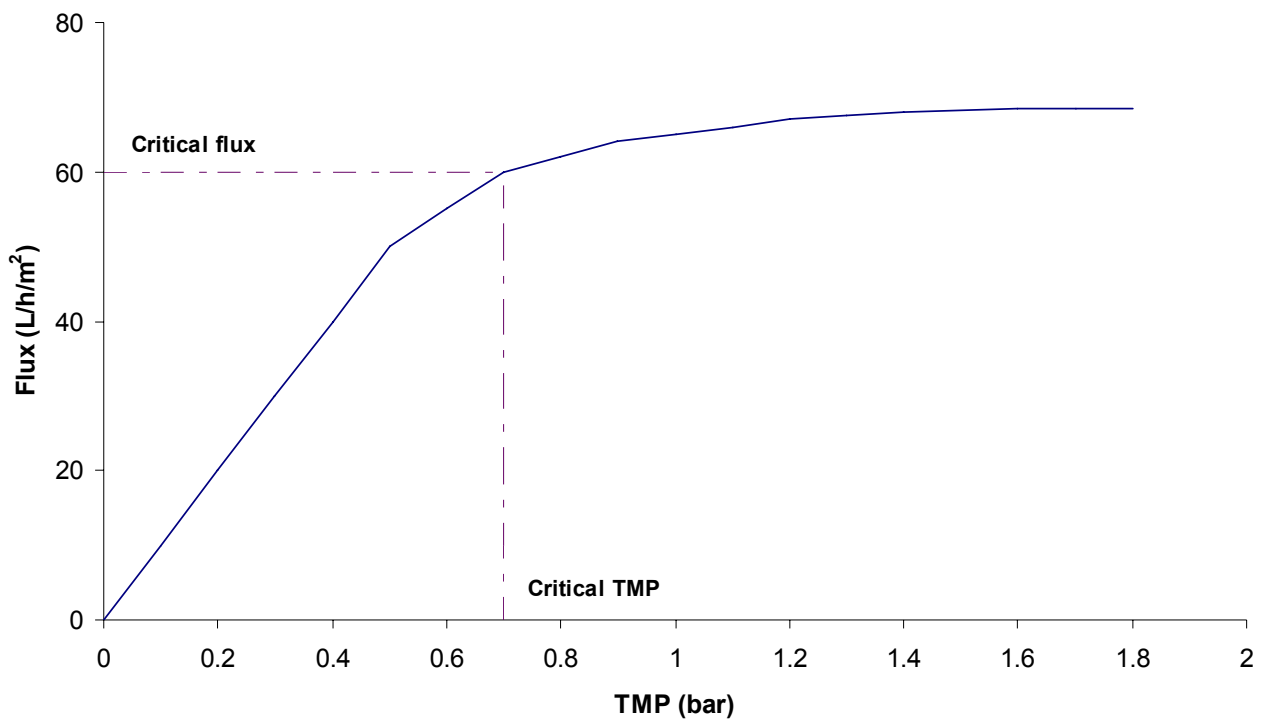
Figure 3.5: Determination of the critical flux for a specific solution in a membrane

3.5 Methodology: quantification of the membrane immobilised amidase process

3.5.1 Immobilisation through physical adsorption in the membrane pores

Three experiments were conducted in which different amounts of amidase were immobilised in the pores of the ceramic membrane through physical adsorption. A similar immobilisation method has previously been used by Giorno *et al.* [2001] to successfully immobilise fumarase in the pores of an asymmetric polysulfone capillary membrane. The procedure was as follows:

1. An amidase solution was prepared by dissolving freeze-dry amidase in potassium phosphate buffer (pH 8.0). The enzyme protein concentration of the solution was 0.27 mg/mL, 0.315 mg/mL and 16.05 mg/mL for experiments one, two and three respectively. The enzyme protein concentrations were determined with the Bradford Coomassie Brilliant Blue dyebinding assay (Section 3.2.1.2).

2. 280 mL of phosphate buffer (pH 8.0) was added to 20 mL of the amidase solution. The enzyme protein concentration of the solution after addition of the phosphate buffer was 0.018 mg/mL, 0.021 mg/mL and 1.07 mg/mL for experiments one, two and three respectively.

3. The enzyme solution was kept on ice and circulated along the shell side of the bioreactor for approximately 2 hours. A TMP of 0.5 bar was applied to force the enzyme into the pores of the membrane. This TMP is below the critical flux of the membrane thereby preventing permanent fouling of the membrane. A low TMP was also chosen to prevent the enzyme from forming a gel layer on the surface of the pores during immobilisation.

4. During the immobilisation procedure all the permeate and retentate were recycled.

5. After two hours the circulation through the reactor was stopped.

6. The system was washed with distilled water in order to remove all the enzyme that did not enter the pores. Samples were taken at intervals of 10 minutes from both the retentate and permeate washing streams and were analysed for enzyme protein with the Bradford Coomassie Brilliant Blue dyebinding assay (Section 3.2.1.3). When no more enzyme protein was detected in the retentate or permeate, the washing was stopped.

7. All the washings (retentate and permeate) were collected in a flask. The concentration of enzyme protein in the flask was determined with the Bradford Coomassie Brilliant Blue dyebinding assay (Sections 3.2.1.2 and 3.2.1.3). The total volume of the washings was also determined.

8. The concentration of enzyme protein and the volume of the residual feed solution were also determined.

9. A mass balance over the reactor quantified the amount of amidase immobilised (Figure 3.6). In order to convert the enzyme protein concentrations of the washing solutions and residual feed to mass, the following formula was used:

$$m_{enzyme} = c_{enzyme}V$$ **Equation 3.2**

The total amount of immobilised amidase was determined from the following equation:

$$m_{enzyme,imm} = m_{enzyme,feed} - m_{enzyme,res.feed} - m_{enzyme,permeate\&retentate}$$ **Equation 3.3**
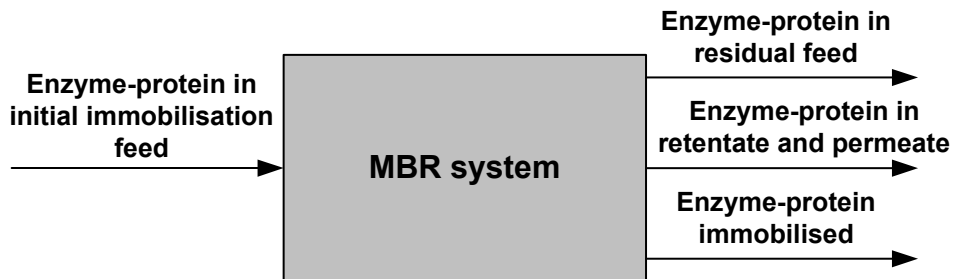
Figure 3.6: Block flow diagram showing the mass balance over the reactor system to determine the amount of amidase immobilised.

3.5.2 Determination of immobilised amidase specific activity and initial rate of reaction

The amidase specific activity at a specific time was determined by measuring the product concentration (*Ca*) in the permeate stream and the permeate flux (*v$_p$*) at that time and relating it to the specific activity with the following equation:

$$Specific\ activity = \frac{v_p Ca}{m_{enzyme,imm}} [mmol/\min.mg]$$ **Equation 3.4**

A product (NH_3) mass balance was done over the membrane in order to derive the following equation for the rate of reaction of the immobilised amidase:

$$In - out + gen. = 0$$
$$0 - v_p Ca + v_r V_{membrane} = 0 \qquad \qquad \textbf{Equation 3.5}$$
$$v_r = \frac{v_p Ca}{V_{membrane}} [mM / \min]$$

In order to determine the rate of reaction at a specific time the product concentration in the permeate stream and the permeate flux at that time were measured and inserted into Equation 3.5.

3.5.3 Determination of immobilised amidase functional stability

The functional stability of the immobilised amidase was determined in duplicate (once during both experiment two and experiment three) by measuring the product concentration in the permeate stream over time. The product concentration was then related to the specific activity of the immobilised amidase by using Equation 3.4.

The amidase specific activity was plotted as a function of time and non-linear regression was used to fit a decay model to the data. The half-life and the deactivation constant of the immobilised amidase was determined from the model.

3.5.4 Determination of instantaneous conversion and instantaneous productivity

It was assumed that the MBR operated like a CSTR since the recycle stream was sufficiently large [Carvalho *et al.*, 2001]. Unsteady state was also assumed since enzyme deactivation took place continuously thereby preventing the system from reaching steady state. The general definition of conversion (which is ratio between the amount of product formed and the amount of substrate fed) and productivity (which is the amount of product formed per unit of time) of a CSTR does not apply in the case of unsteady state because the exact amount of product that is formed cannot be determined due to the accumulation of product in the reactor. The instantaneous conversion and instantaneous productivity were therefore used to measure the reactor performance. The following reaction took place within the MBR:
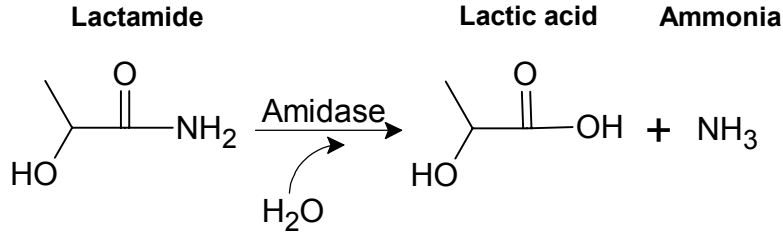
Figure 3.7: Amidase catalysed reaction that took place in the membrane bioreactor

The instantaneous conversion at a specific time during the production of lactic acid was defined as the ratio between the concentration of product in the permeate (ammonia) at that time and the initial substrate concentration in the feed (lactamide) (Figure 3.7). The following equation applied:

$$X = \frac{[Ammonia]_{\text{Permeate,t}}}{[Lactamide]_{\text{Feed,0}}} \times 100\%$$

Equation 3.6

The instantaneous productivity at a specific time during the production of lactic acid was determined by measuring the concentration of product in the permeate stream and the permeate flux at that time and inserting it into Equation 3.7:

$$F_p = \frac{v_p Ca}{V_{membrane}} [mmol/L.\min]$$

Equation 3.7

Note that the instantaneous productivity is the same as the reaction rate at that specific time.

4   Reactor modeling methodology

4.1   Computational fluid dynamic modeling of the reactor

Computational fluid dynamic (CFD) modeling involves the use of numerical methods to yield "discrete" solutions of the fundamental equations for flowing fluids that resemble possible analytical solutions as closely as possible. Before CFD can be used to determine these solutions, however, a model, with the accurate dimensions of the system under investigation, has to be drawn in a typical computer aided design (CAD) program. The CAD program, *Gambit*, was used to draw a model of the MBR used in this research (Figure 4.1).
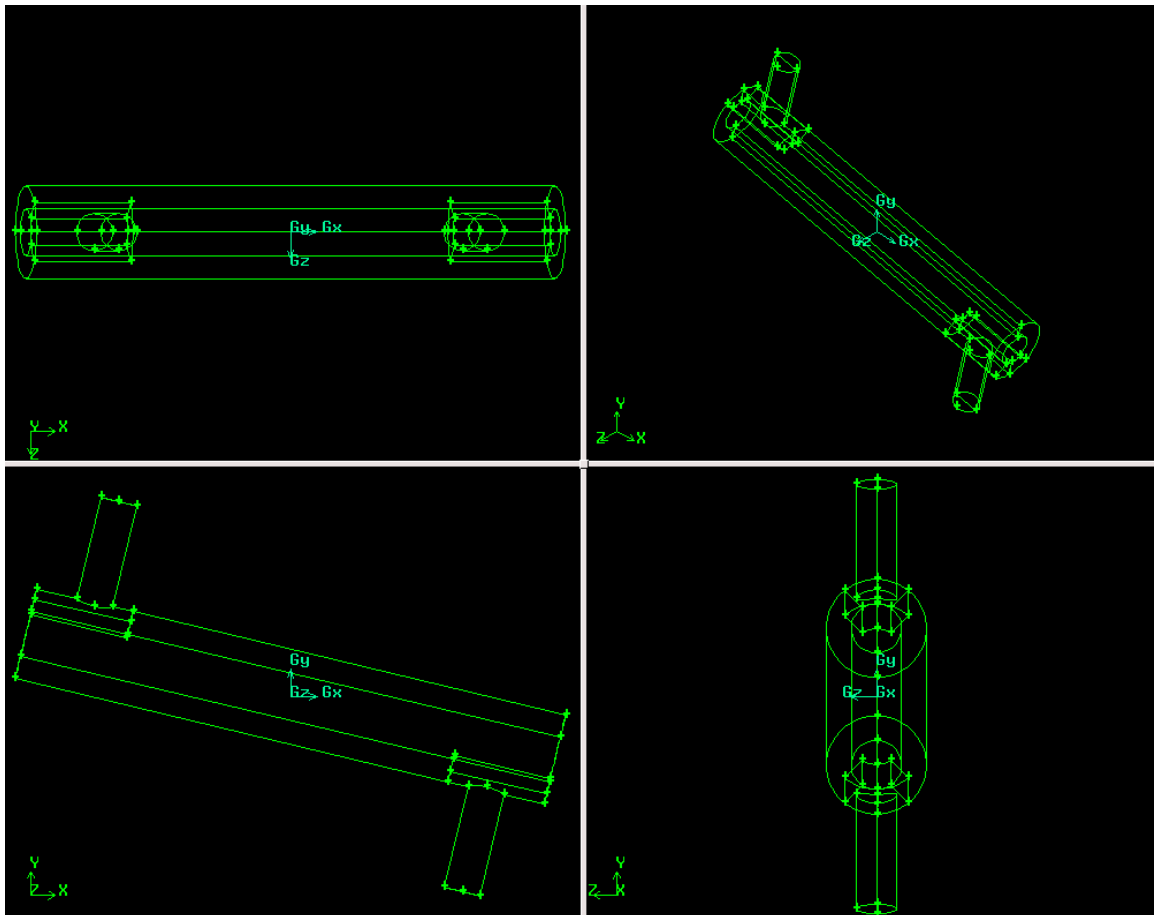
Figure 4.1: Model of the membrane bioreactor as drawn in the CAD program *Gambit*

The model of the reactor was covered with a mesh (Figure 4.2). The purpose of the mesh was to divide the model into thousands of small pieces, each for which the fundamental equations for flowing liquids could be solved by the CFD program, *Fluent*. The model was exported from *Gambit* to *Fluent*.
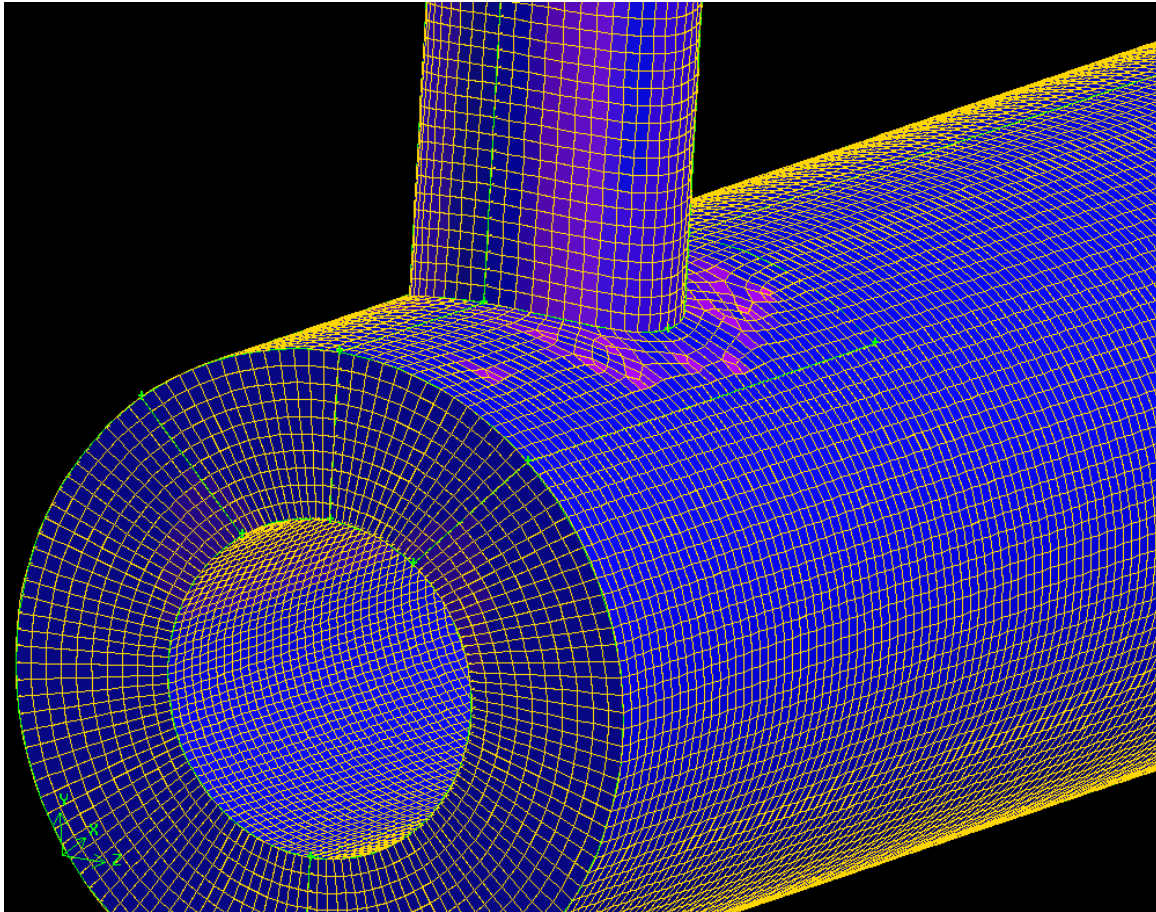
Figure 4.2: The reactor as a meshed computational domain to be solved by the CFD program *Fluent*

Variables such as entry flow rates, feed entry points, entry temperature and pressure, orientation of the reactor, materials from which the reactor is constructed and heat transfer coefficients of these materials were entered into *Fluent.* The following assumptions were made regarding some of these variables:

- The permeate flux through the membrane wall was negligible when compared with the retentate flow rate. Flow through the membrane wall was therefore not modeled.

- The active membrane layer (composed of zirconium oxide) was very thin when compared with the titanium oxide membrane support layer. The heat transfer characteristics of the entire membrane were therefore taken as that of titanium oxide (the support layer).

Fluent then solved the fundamental equations for flowing liquids for each piece of the model by iteration until the best possible analytical solution was found that could explain each piece individually and the model as a whole. The temperature-, pressure- and velocity

profiles in the reactor were determined for three different reactor orientations (13.4º, 30º, and 90º) and two different feed entry points (top or bottom).

4.2 <u>**Mathematical modeling of the reactor**</u>

A mathematical model of the MBR was developed from first principles in order to predict the performance of the reactor under different operating conditions. The performance of the reactor was measured in terms of instantaneous conversion and instantaneous productivity since the reactor was assumed to behave like a CSTR at unsteady state and the general definitions of conversion and productivity were therefore not valid. The model played a critical part in optimisation of the process since it reduced the number of experiments required for optimisation significantly.

The four basic modeling principles (Section 2.6.3) which are: definition of the problem, formulation of the model from first principles, estimation of the parameters and validation of the model, were used as a guideline to develop the model. All the model equations were then inserted into an ordinary differential equation (ODE) solver package, Polymath, to be solved simultaneously.

Step 1: Definition of the problem

It was assumed that the reactor operated like a CSTR at unsteady state (or start-up). According to Carvalho *et al.* [2001] a MBR can be accurately approximated as a CSTR when the recycle ratio between the retentate and the permeate is larger than 100. The recycle ratios used in this research all fell in the range 400 to 2000. The CSTR was assumed to be at unsteady state since the reaction rate was never constant due to amidase deactivation.

Step 2: Formulation of the model from first principles

Mass balances were done in order to determine the concentration of product (*Ca*) and substrate (*Cs*) in the reactor for a deferential element of time. The following two equations were derived:

$$\frac{d(Ca)}{dt} = \frac{v_p}{V_{membrane}}(Ca_0 - Ca) + v_r \qquad\qquad \textbf{Equation 4.1}$$

$$\frac{d(Cs)}{dt} = \frac{v_p}{V_{membrane}}(Cs_0 - Cs) - v_r \qquad\qquad \textbf{Equation 4.2}$$

By assuming Michaelis-Menten kinetics for the immobilised amidase the reaction rate (v_r) was expressed as follows:

$$v_r = \frac{v_{max}Cs}{K_m + Cs}$$

Equation 4.3

An assumption was made that the enzyme operated at its maximum reaction rate (v_{max} is therefore equal to v_r). The maximum reaction rate, however, was directly related to the amount of active enzyme present and therefore changed continuously since the amount of active enzyme was decreasing continuously. Since v_{max} is directly related to the amount of active enzyme (e_a) present, v_{max} could be expressed as:

$$v_{max} = v_r = k_2 e_a$$

Equation 4.4

It was assumed that the immobilised amidase followed a typical one-phase exponential decay model. The amount of active enzyme present in the membrane at a specific time could therefore be expressed as a function of the initial amount of active enzyme (e_{a0}), the deactivation coefficient (k_d) and time (t):

$$e_a = e_{a0}e^{-k_d t}$$

Equation 4.5

By substituting Equations 4.4 and 4.5 into the Michaelis-Menten model (Equation 4.3), the following definition of the reaction rate was found:

$$v_r = \frac{k_2 e_{a0} e^{-k_d t} Cs}{K_m + Cs}$$

Equation 4.6

Step 3: Estimation of the parameters K_m, k_2, k_d and $V_{membrane}$

It was assumed that the Michaelis-Menten constant, K_m, was the same for both the immobilised and the free amidase. This constant was determined from initial rate studies of the free amidase (Section 3.3.2).

The reaction rate was determined during both experiment two and three (Section 3.5.1) by using Equation 4.7.

$$v_r = \frac{v_p Ca}{V_{membrane}}$$

Equation 4.7

The amount of active enzyme present in the reactor for those two times was determined from Equation 4.5 and the permeate flux at the specific time was measured. A value for k_2 was then determined for both experiments by using Equation 4.8.

$$k_2 = \frac{v_r}{e_a}$$

<div align="right">**Equation 4.8**</div>

Due to the difference between the activities of the free amidase used in the two experiments, the activity of the immobilised amidase was also different and therefore the value of k_2 was different for the two experiments. Values of 0.0228 mM/min.mg and 0.00228 mM/min.mg were determined for experiments two and three respectively.

Since the free amidase activity was not always the same, the immobilised activity would also be different for different experiments although the immobilisation procedure was the same. A mathematical prediction of the immobilised amidase activity (and therefore the value of k_2) could therefore not be made since it depended on the free amidase activity. To overcome this problem the model had to be given the initial values of the permeate flux and the product concentration in the permeate stream which was then related to the reaction rate by using Equation 4.7. The reaction rate was then used in Equation 4.8 to determine a value for k_2.

The deactivation constant (k_d) for the immobilised amidase was determined with non-linear regression of the stability curve obtained from experiments two and three (Section 3.5.3) to be 0.0016 min^{-1}.

The volume of the reactor ($V_{membrane}$) was taken as the volume of the membrane (0.01186 L) thereby assuming the support structure's volume to be negligible and the volume of the pores to be equal to the volume of the membrane.

The parameters K_m, k_2 and k_d were all inserted into Equation 4.6 and the parameter $V_{membrane}$ was inserted into Equations 4.1 and 4.2.

Step 4: Validation of the model

The model was validated by evaluating the goodness of fit between the instantaneous conversion and instantaneous productivity predicted by the model and the instantaneous conversion and productivity obtained in experiments two and three (Section 3.5.1) over time. Different operating conditions were used for the two experimental runs in order to determine the validity of the model over a range of operating conditions. The conditions were as follow:

- **Experiment two**: T=50ºC, pH=8.0, s0=80 mM, e0=6.38 mg, v=0.0005 L/min, $a0_{free}$=1.4 U/mg

- **Experiment three:** T=50ºC, pH=8.0, s0=40 mM, e0=20.09 mg, v_p=0.0001 L/min, $a0_{free}$=0.357 U/mg

5 <u>Results and discussion</u>

The results will be discussed under the three main headings that have been used throughout the thesis which are: the characterisation of free amidase, development of the MBR system and quantification of the membrane immobilised amidase process. During the discussion of the results reference will be made to the three immobilisation experiments as experiment 1, 2 and 3. A summary of the conditions used in each experiment can be found in Table 5.1.

Table 5.1: Operating conditions for three immobilisation experiments

	Experiment 1	Experiment 2	Experiment 3
Free enzyme activity			
Activity (U/mg)	1.23	1.40	0.36
Enzyme immobilisation			
Amount of enzyme protein in feed (mg)	18.38	21.04	426.10
Immobilisation time (hours)	2	2	2
Immobilisation TMP (bar)	0.5	0.5	0.5
% of enzyme protein immobilised	38.71	30.35	4.71
Amount of enzyme protein immobilised (mg)	7.11	6.38	20.09
Operational conditions			
Temperature (ºC) and pH	50 and 8.0	50 and 8.0	50 and 8.0
Substrate concentration (mM)	80	80	40
Permeate flux (L/min)	0.0015	0.0005	0.0001
Initial immobilised enzyme activity (U/mg)	0.18	0.15	0.01
Operating time (hours)	3	22.5	22

Programming scripts and reports, any additional figures referred to and statistical validation of some of the results can be found in Appendix II, III and IV respectively.

5.1 Characterisation of free amidase

5.1.1 Determination of the optimum temperature and pH and development of a model predicting the specific activity of the amidase

A two-by-two factorial design was done in order to determine the effect of the temperature and pH and the significance of the interaction of these two parameters on the specific activity of the amidase. An empirical model, containing all possible combinations of pH and temperature that may affect the specific activity of the amidase, was developed in a statistical program, *R*, and an analysis of variance was done on it (Appendix II). From the analysis of variance all factors that affected the specific activity with a certainty of more than 95% were identified. These factors were the following:

- Temperature

- pH

- (Temperature)^2

- (pH)^2

The analysis of variance showed the interaction between pH and temperature cannot be said to be significant at any confidence level (Appendix II). The empirical model was then refined to contain only these four significant factors as variables (Equation 5.1).

$$Specific\ activity = 0.191(T) + 1.71(pH) - 0.00183(T)^2 - 0.109(pH)^2 - 10.39$$ **Equation 5.1**

Two important assumptions were made during the development of the empirical model:

- The residuals between the actual concentrations and the predicted concentrations have homogeneous variances.

- The residuals come from a normal distribution.

When determining the accuracy of a model it is important to first look at the goodness of fit (the correlation coefficient between the two sets of data). A comparison between the predicted amidase specific activity and the experimental amidase specific activity as a function of pH at a temperature of 50ºC (Figure 5.1) and as a function of temperature at a pH of 8.0 (Figure 5.2) was made. Similar graphs comparing the predicted and experimental

amidase specific activity as a function of pH at different temperatures and as a function of temperature at different pHs can be found in Appendix III.
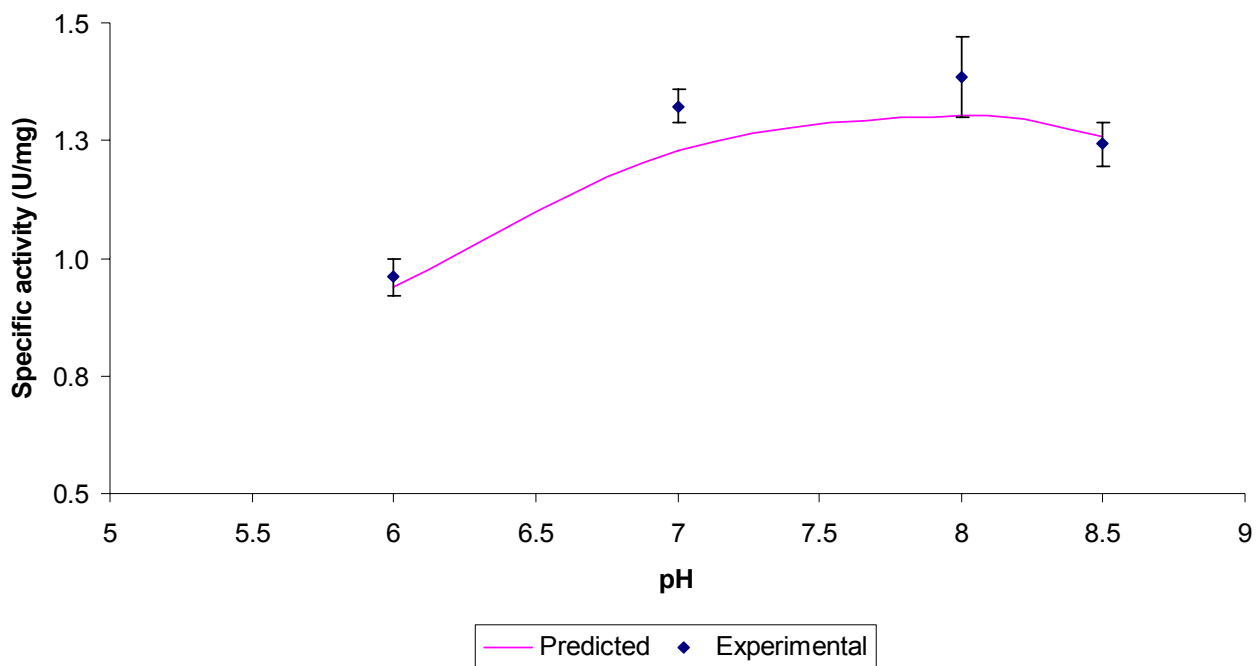
Figure 5.1: Experimental and predicted specific activity of amidase at a temperature of 50ºC
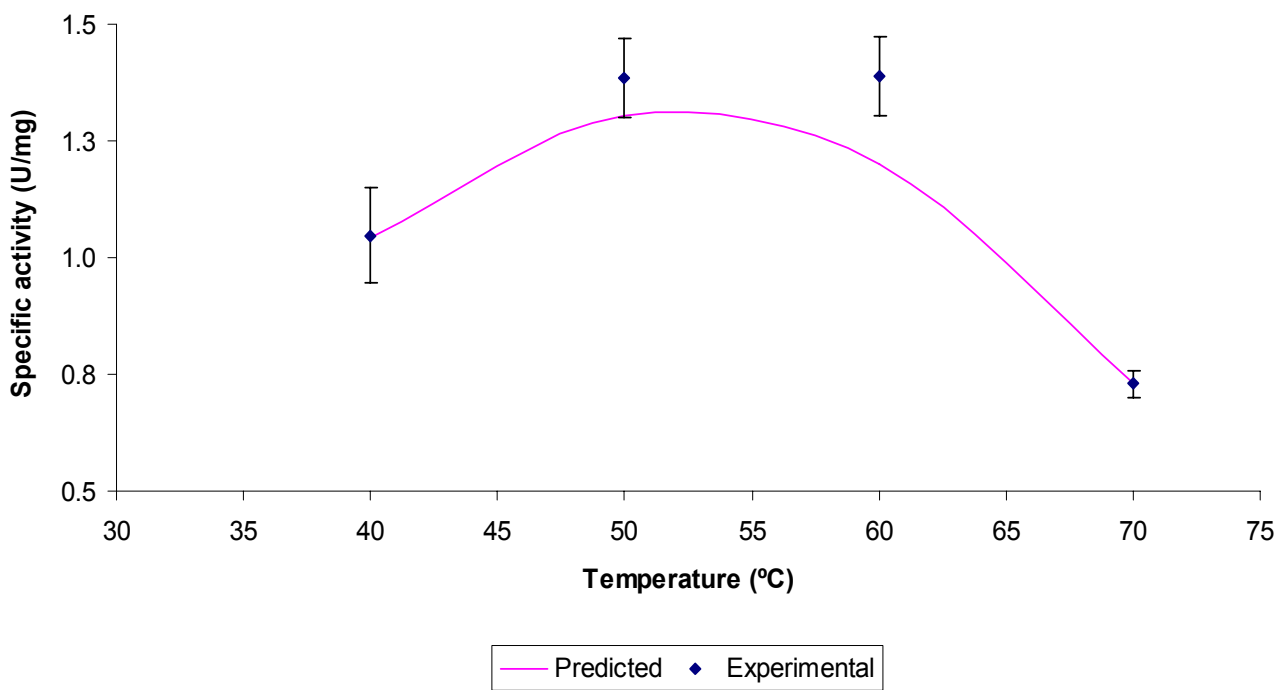
Figure 5.2: Experimental and predicted specific activity of amidase at a pH of 8.0

The correlation coefficient for both Figure 5.1 and Figure 5.2 was calculated as approximately 0.97 which indicates that the model fits the experimental data very well.

The next step in determining whether the model is accurate is to investigate the residuals in order to ensure that the assumptions made during the development of the model have not been violated.

The validity of the assumption of homogeneous variances of the residuals was evaluated by plotting the data predicted by the model against the residuals (Figure 5.3). The random distribution of the residuals in Figure 5.3 is an indication that the residuals do have homogeneous variances. The assumption is therefore valid.

In order to determine if the residuals came from a normal distribution, a plot of the residuals against their index numbers were drawn (Figure 5.4). In Figure 5.4 the residuals follow the pattern of a normal distribution around the zero point. This is an indication that the assumption of normality of the residuals is valid.
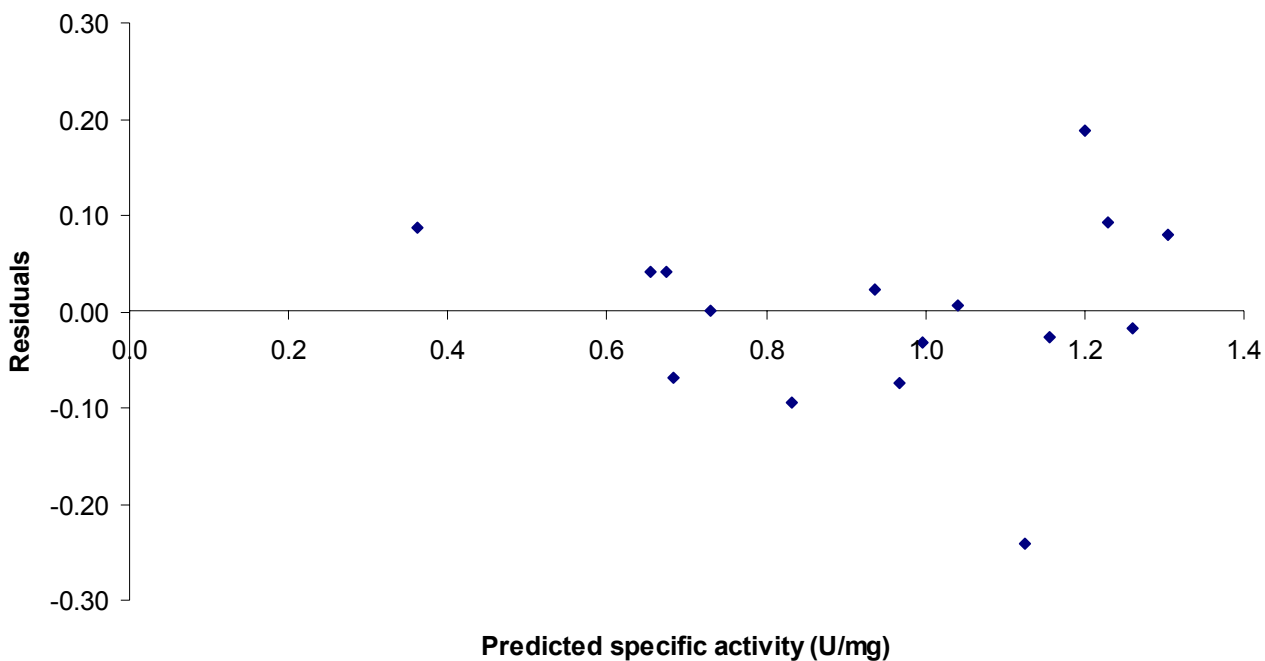
Figure 5.3: Validation of the assumption of homogeneous variances of the residuals
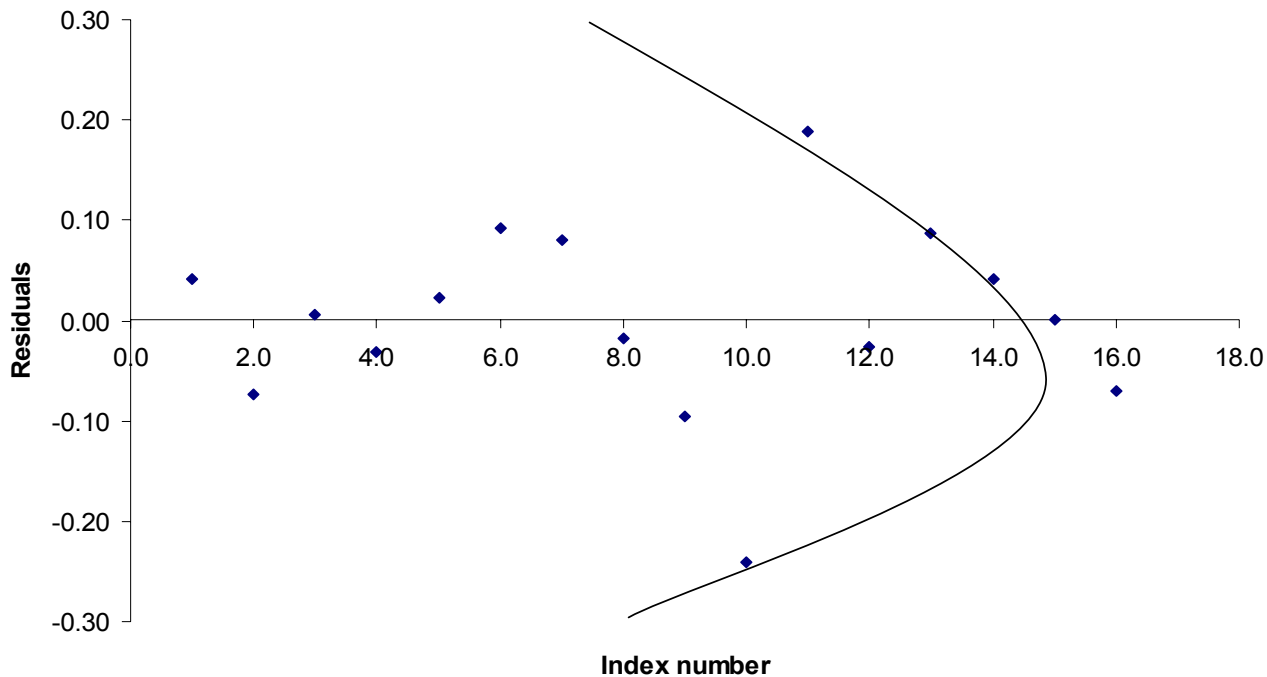
Figure 5.4: Validation of the assumption of normality of the residuals

Since the correlation coefficient proved that the model fits the experimental data very well and the basic assumptions made during the development of the model have not been violated, the model was found to be valid.

The model was then used to predict at what temperature and pH the amidase exhibits the highest specific activity. A 3D graphical representation of the model (Figure 5.5) and a contour graph of the model (Figure 5.6) were drawn. Figure 5.5 and Figure 5.6 show the optimum temperature and pH to be approximately 50ºC and 8.0 respectively (dark red areas). These conditions were therefore maintained during the rest of the experiments.
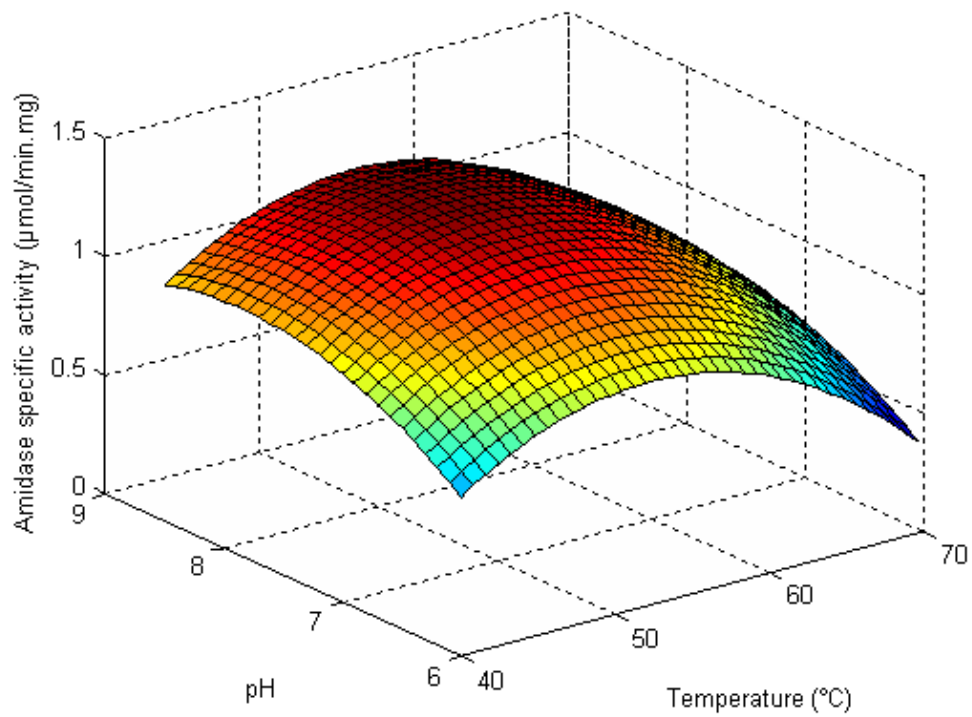
Figure 5.5: Cumulative effect of pH and temperature on the amidase specific activity as predicted by the model
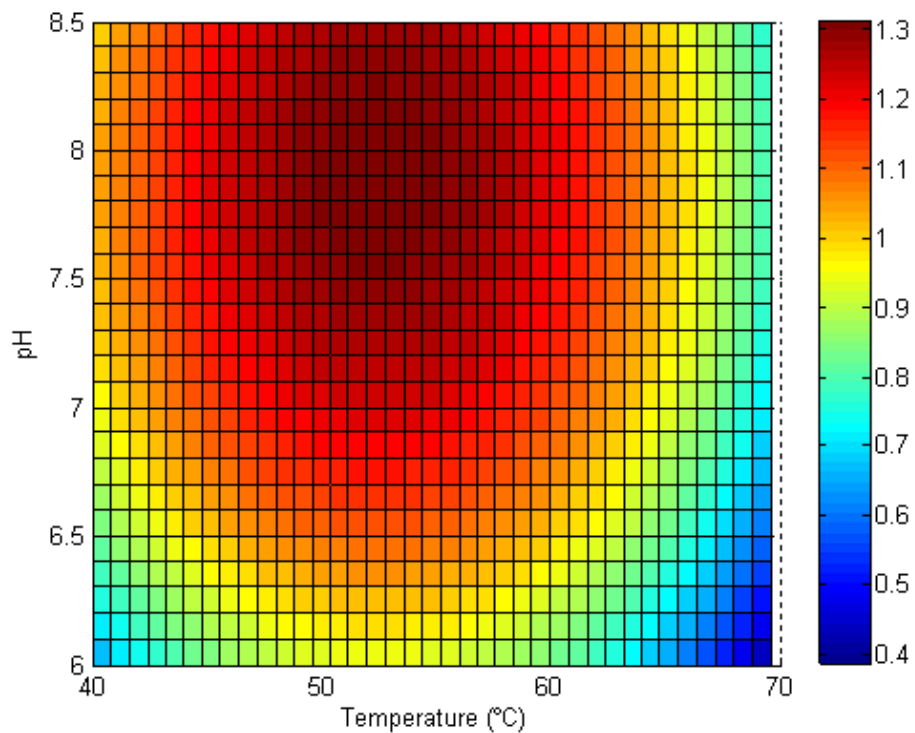
Figure 5.6: Contour graph of predicted amidase activity as a function of pH and temperature

5.1.2 <u>Determination of functional stability</u>

The specific activity of the free amidase was measured over time at a temperature of 50ºC and substrate (lactamide) concentrations of 40 mM and 80 mM (the pH was kept at 8.0 for all experiments). For both substrate concentrations the activity seemed to follow a typical one-phase exponential decay pattern.

A one-phase exponential decay model (Equation 2.6) was fitted onto the experimental data through non-linear regression. The resulting curves showing amidase activity decay at a temperature of 50ºC and substrate concentrations of 40mM and 80mM can be seen in Figure 5.7. The dotted lines represent the 95% confidence interval of the model.
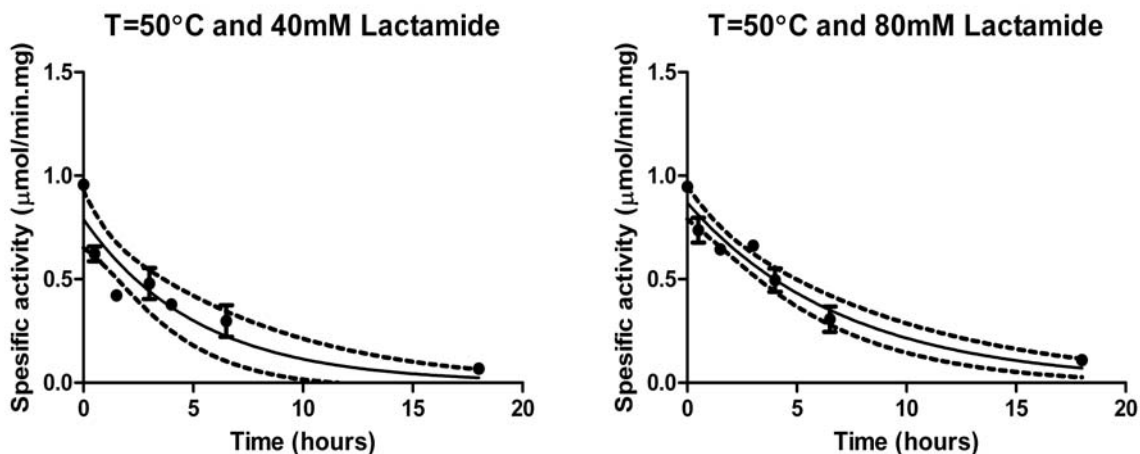
Figure 5.7: One-phase exponential decay of amidase at 50ºC, pH 8.0 and lactamide concentrations of 40mM and 80mM (95% confidence intervals indicated by dashed lines)

The functional stability of enzymes is typically measured in terms of half-life (Section 2.2.5) where the half-life is defined as the time at which the remaining enzyme activity is half the value of the initial enzyme activity. The half-life of the amidase at 40 mM and 80 mM substrate was calculated using Equation 2.8 and can be seen in Table 5.2.

Table 5.2: Half-life of the amidase at 50ºC, pH 8.0 and substrate concentrations of 40mM and 80mM

	T=50ºC	
	40mM	**80mM**
Half-life (hours)	3.6	4.9

Table 5.2 shows that the half-life of the amidase at 80 mM lactamide is 4.9 hours. The 95% confidence interval includes probable half-lives in the range 3.9 to 6.8 hours. For a substrate concentration of 40 mM the half-life has been determined as 3.6 hours with half-lives between 2.4 and 7.1 hours falling in the 95% confidence interval. Since the range of probable half-lives (given with a 95% accuracy) for 40 mM and 80 mM lactamide overlap, statistical tests were used to determine if there is a significant difference between the amidase functional stability at the two different lactamide concentrations. A statistical F-test was used first in order to test the hypothesis of equal variances between the two sets of data. Next a statistical z-test was performed to test the hypothesis of equal means between the two sets of data (Appendix IV).

For the F-test the null hypothesis was that the data comes from two populations with the same variances. Since an F value close to 1 (1.058) was found, the null hypothesis cannot be rejected (with a confidence of 95%).

The null hypothesis for the z-test was that the data comes from two populations with the same means. Since the "z Critical two-tail" value was found to be larger than the absolute value of z, it can be stated with a 95% accuracy that the null hypothesis cannot be rejected. It can therefore be concluded that the amidase functional stability is not dependent on the substrate concentration.

5.1.3   Closeness of the fit of the Michaelis-Menten model to the amidase initial reaction rates and determination of kinetic parameters

Determination of the closeness of fit of the Michaelis-Menten model to the amidase initial reaction rates and calculating the kinetic parameters of the amidase was done in three steps. The first part was to determine the initial rate of reaction experimentally at various substrate concentrations and an enzyme concentration of 1 mg/mL. Next the data gathered in step one was plotted to determine whether or not the amidase follows Michaelis-Menten kinetics. The third part involved fitting the Michaelis-Menten curve to the data and determining the kinetic parameters K_m and v_{max} for the amidase-lactamide system. These parameters were required in order to be able to model the system mathematically.

5.1.3.1 Determination of the initial rate of reaction at various substrate concentrations

The amount of product formed by the amidase over the first few minutes of reaction was determined for various substrate concentrations at a temperature of 50ºC, a pH of 8.0 and an amidase concentration of 1 mg/mL. The amount of product formed over the first 6

minutes of the reaction when the substrate concentration was 60 mM of lactamide for two independent experiments can be seen in Figure 5.8.

The slopes of the straight lines in Figure 5.8 are the initial rates of the amidase catalysed reaction at a substrate concentration of 60 mM for the two independent experiments. The average of the two slopes was taken as the initial rate for the specific substrate concentration. Similar graphs used to determine the amidase initial rate of reaction at substrate concentrations of 15 mM, 25 mM, 40 mM, 80 mM, 100 mM and 150 mM can be found in Appendix III.
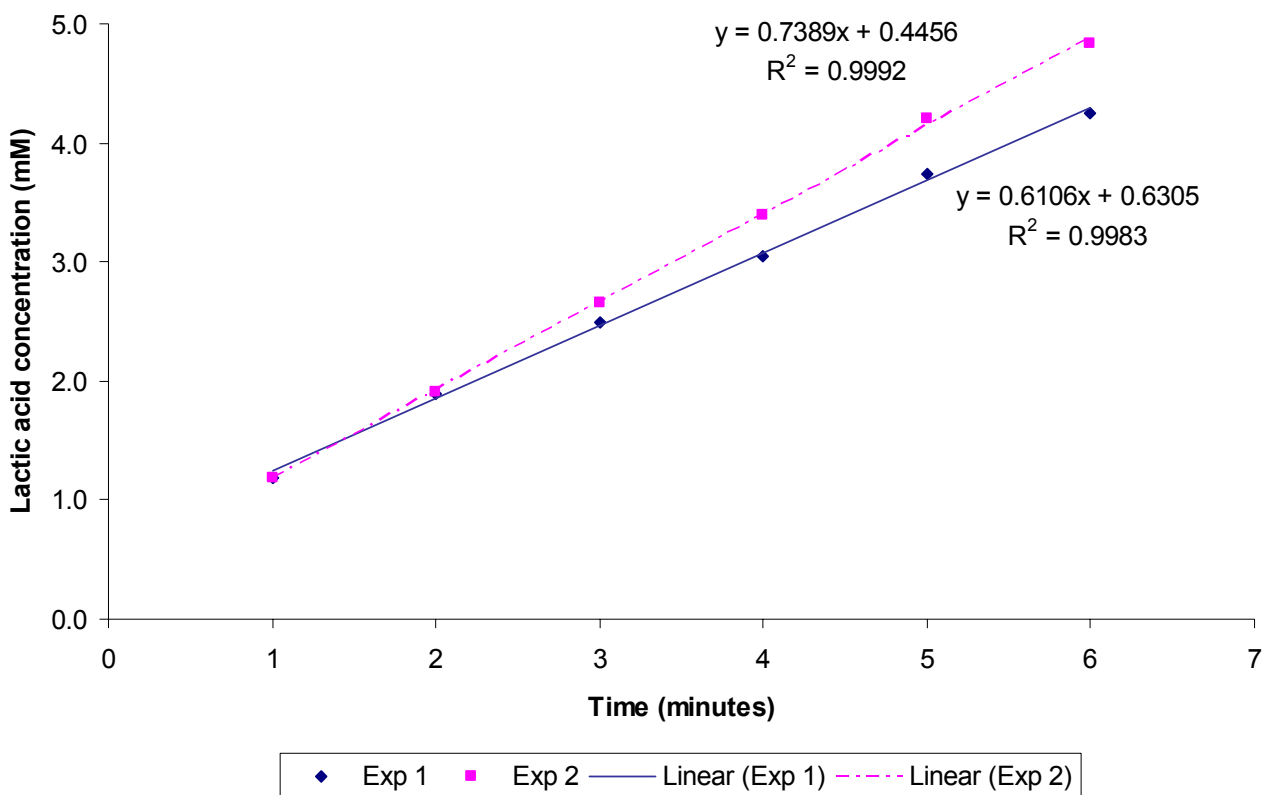
Figure 5.8: Determination of the initial rate of reaction from the average of the two slopes of the graph at a substrate concentration of 60 mM lactamide

Table 5.3 provides a summary of the average initial rate of reaction at the various substrate concentrations.

Table 5.3: Initial rate of reaction at different substrate (lactamide) concentrations

[Lactamide] (mM)	Initial rate (mM/min)
15	0.244
25	0.403
40	0.577
60	0.675
80	0.837
100	0.852
150	0.976

5.1.3.2 Applicability of Michaelis-Menten kinetics

A plot of the initial rates obtained at the different substrate concentrations against the substrate concentrations (Table 5.3) was created (Figure 5.9).
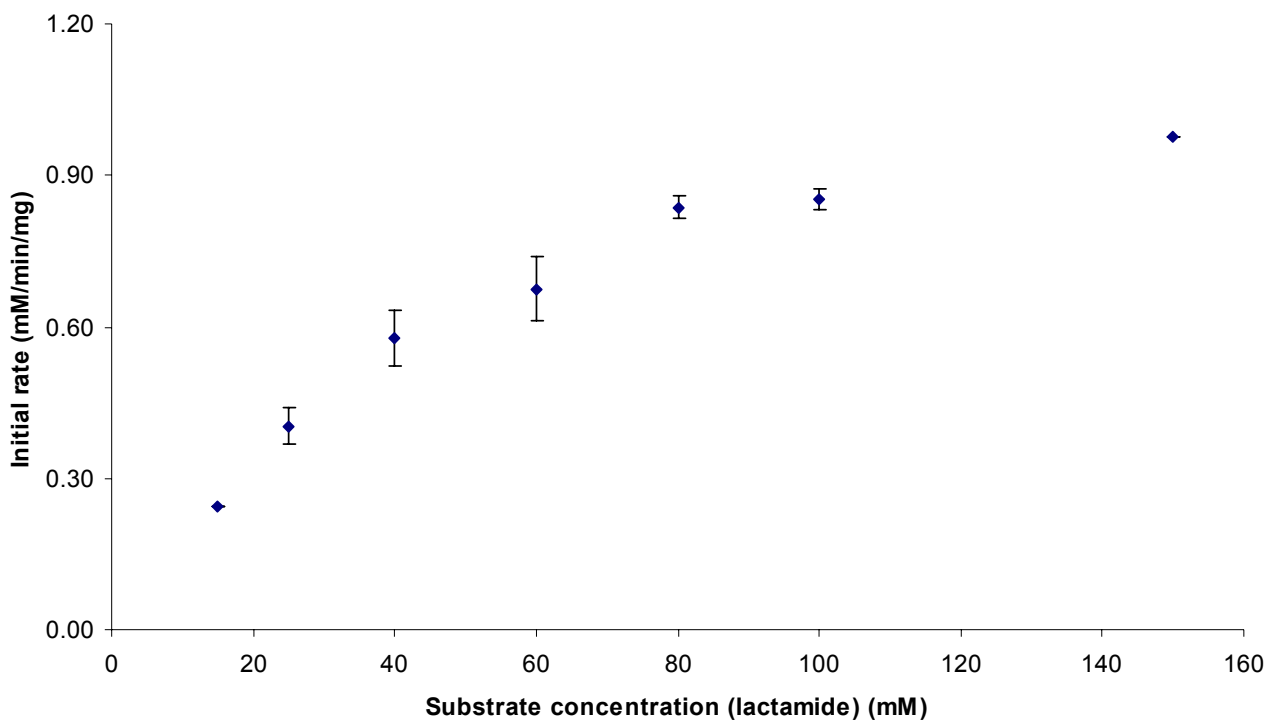
Figure 5.9: Curve used for determining if the amidase reaction rate follows Michaelis-Menten kinetics

In Figure 5.9 the straight line at low substrate concentrations indicates that the amidase rate of reaction was first order in concentration of substrate at lower substrate concentrations. As the substrate concentration was increased, however, the reaction order in substrate concentration tended to zero (the curve tends towards an asymptote). This behaviour is typical of enzymes following Michaelis-Menten kinetics. The amidase reaction rate is therefore consistent with Michaelis-Menten kinetics.

5.1.3.3 Determination of the kinetic parameters K_m and v_{max}

The kinetic parameters of the amidase (K_m and v_{max}) were determined with the Lineweaver-Burk plot, the Hanes-Woolf plot and non-linear regression (Section 2.2.3). A comparison between the values obtained with the three different methods was then made.

Figure 5.10, Figure 5.11 and Figure 5.12 show the Lineweaver-Burk plot, the Hanes-Woolf plot and the plot obtained from non-linear regression respectively.
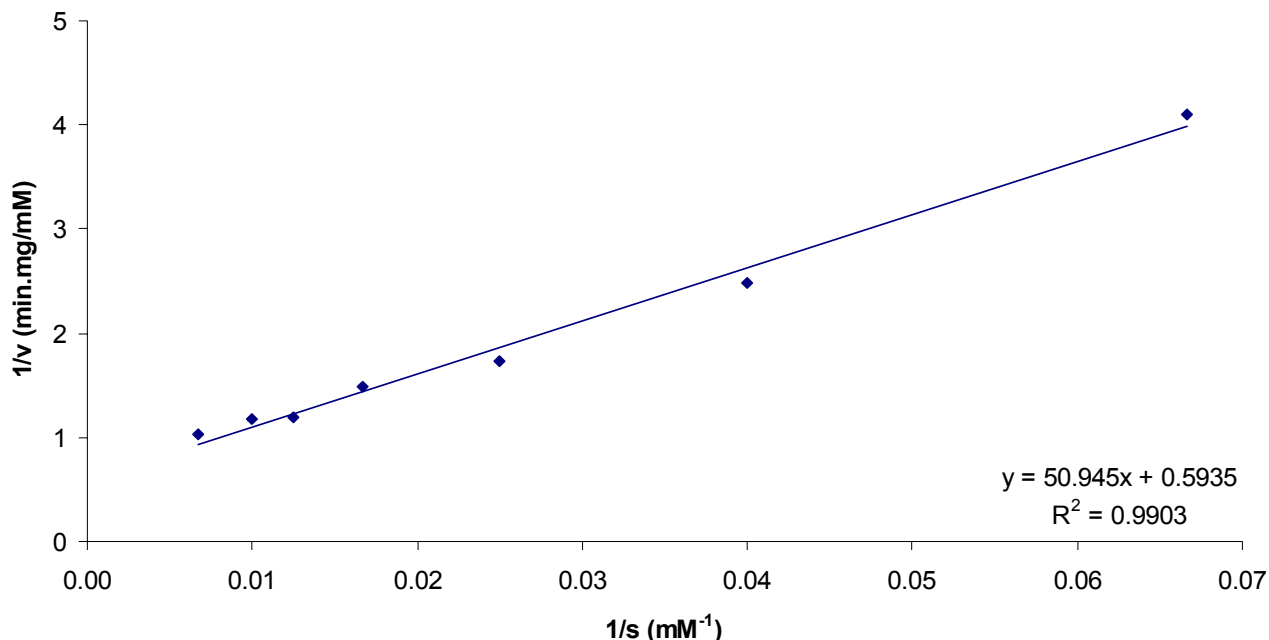
Figure 5.10: Determination of kinetic parameters K_m and v_{max} using the Lineweaver-Burk plot
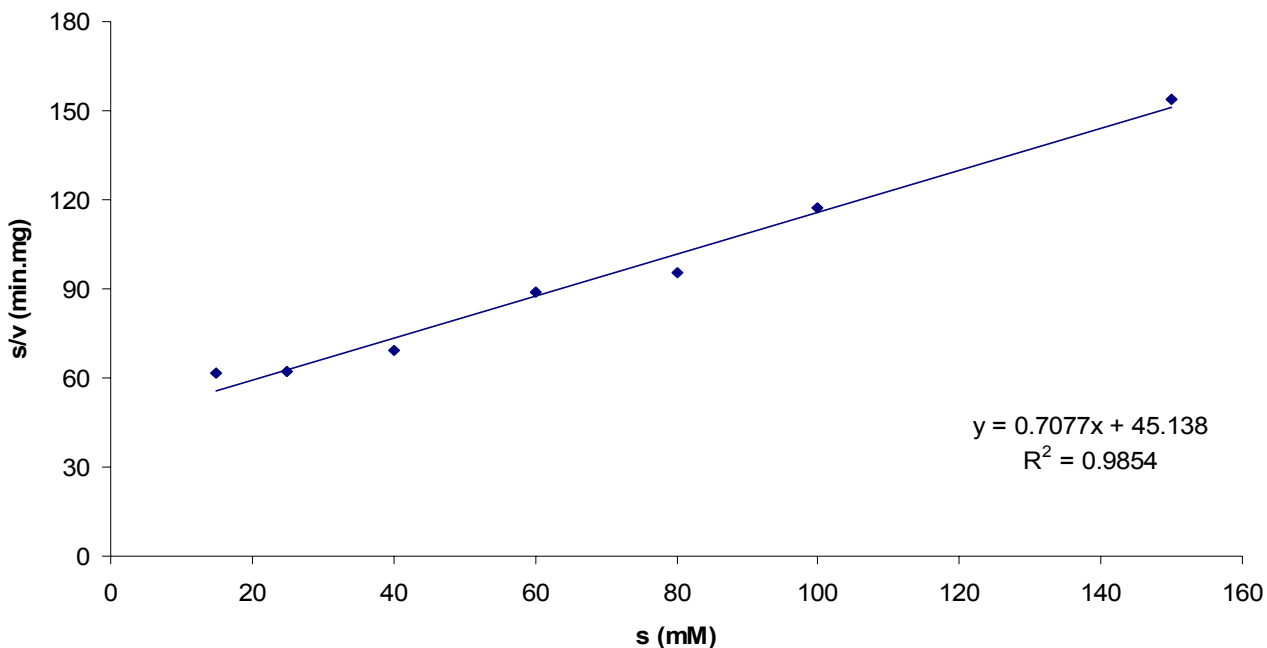
Figure 5.11: Determination of kinetic parameters K_m and v_{max} using the Hanes-Woolf plot
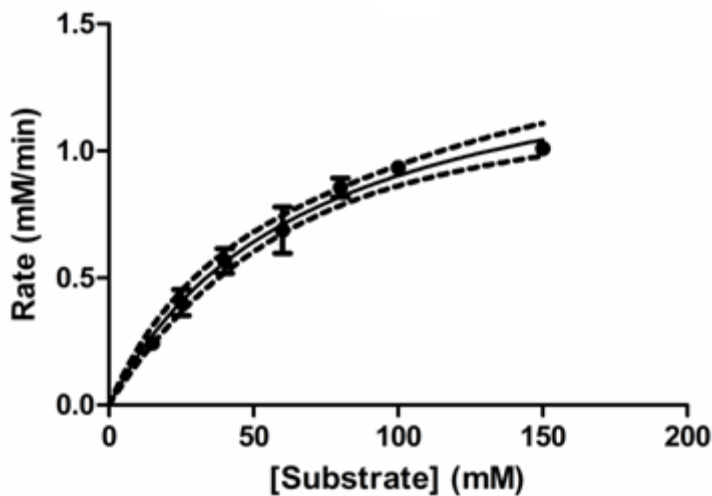
Figure 5.12: Determination of kinetic parameters K_m and v_{max} using non-linear regression

Note that the Michaelis-Menten model (fitted with non-linear regression) fits the data very well (within a 95% confidence interval). It can therefore be concluded that the amidase follows Michaelis-Menten kinetics.

Table 5.4 shows the different values of K_m and v_{max} obtained from the three plots and the correlation coefficient for each plot.

Table 5.4: Comparison of K_m and v_{max} values obtained from the different plots

	Lineweaver-Burk	Hanes-Woolf	Non-linear regression
K_m (mM)	85.84	63.78	68
v_{max} (mM/min)	1.68	1.41	1.48
R^2	0.9903	0.9854	0.9898

Non-linear regression is the most accurate way to predict the values of K_m and v_{max} (Section 2.2.3.3). Although this is a well-known fact, some authors prefer to use linearised methods like the Lineweaver-Burk plot [Belhocine at al., 2000; Giorno *et al.*; 2000]. Note that although the regression coefficient of the Lineweaver-Burk plot shows that the straight line is almost a perfect fit to the data; the values of K_m and v_{max} are significantly higher than that predicted by the Hanes-Woolf plot and the non-linear regression analysis (Table 5.4). The difference between the kinetic constants determined from the Hanes-Woolf plot and that determined with non-linear regression is trivial. Should a linearised model be required for determination of the kinetic parameters, the Hanes-Woolf plot would therefore be a better option to use than the Lineweaver-Burk plot.

The value of K_m determined for the amidase with lactamide as substrate is very high when compared with K_m values of other amidases. Apparent K_m values for an amidase from *Rhodococcus rhodochrous* J1 were determined as 0.48 mM and 0.15 mM for propionamide and benzamide as substrates respectively [Kobayashi *et al*., 1993] and an amidase from Rhodococcus erythropolis MP50 had apparent K_m values of 0.069 mM and 0.067 mM for phenylacetamide and ketoprofen amide as substrates respectively [Hirrlinger *et al*., 1996]. The high K_m value of the amidase implies a low affinity for the lactamide as substrate since a high concentration of lactamide is required for the amidase to operate at its optimum reaction rate.

5.1.4 Determination of the effect of different reducing agents and a metal chelating agent of the amidase activity and functional stability

Enzymes with sulfhydryl groups in their catalytic centers may loose activity or functional stability when exposed to oxygen due to the oxidation of these sulfhydryl groups. The addition of reducing agents, which will reduce the disulfide groups, may restore the activity or functional stability of the enzyme [Makhongela, 2005].

Since the amidase contains sulfhydryl groups in its catalytic centers, the effect of different reducing agents on the activity and functional stability were evaluated. The reducing agents DTT, L-cysteine and NAC (in concentrations of 0.1 mM) had no effect on the amidase specific activity. For higher DTT concentrations, a reduction in the amidase specific activity was found (Figure 5.13).
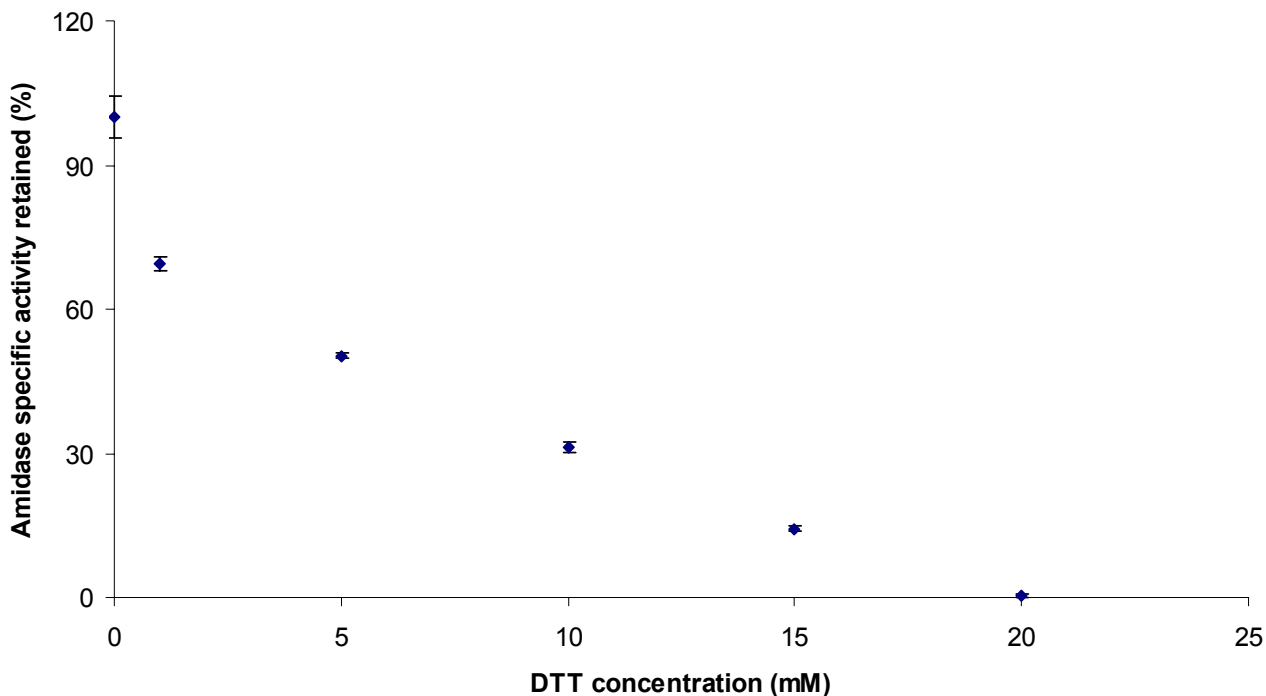
Figure 5.13: Effect of different concentrations of the reducing agent DTT on the amidase specific activity

Piotrowski *et al.* [2001] found that a nitrilase and nitrile hydratase from an *Arabidopsis thaliana* were both inhibited at DTT concentrations higher than 1 mM with only 50% of their activity remaining at a DTT concentration of 10 mM. According to these authors this inhibition proved the importance of a cysteine residue in the catalytic centers of the enzymes. The DTT inhibited these residues which resulted in decreased enzyme activities. Makhongela *et al*. [2005] reported that the addition of certain reducing agents resulted in a decrease in this specific amidase's activity which is consistent with the presence of important cysteine residues in its catalytic centers. The effect of the DTT on the amidase activity (Figure 5.13) confirms the presence of the catalytically active cysteine residue in the catalytic center of the amidase.

The effect of DTT, L-cysteine and NAC on the functional stability of the amidase was investigated in order to determine if oxidation of the sulfhydryl groups occurred during the

18 hour experiments. The reducing agents had no effect on the functional stability of the amidase. No oxidation of the sulfhydryl groups in the catalytic centers therefore occurred during the experiments.

Makhongela [2005] found the amidase to be inhibited by certain metal ions. In order to determine if traces of metal ions may have influenced the amidase activity or stability, a metal chelating agent (EDTA) was added to the reaction mixtures. A metal chelating agent will bond with any traces of metal in the mixture thereby preventing their interference with the amidase active sites [http://scifun.chem.wisc.edu]. EDTA had no effect on either the activity or the functional stability of the amidase thereby proving that either no traces of metal were present in the reaction mixtures or that the amidase is not sensitive to very small amounts of metals.

5.2 Development of the experimental MBR system

After construction of the experimental MBR system, the effect of the reactor orientation on the velocity profile in the reactor was determined in order to establish if an optimum orientation, at which dead volume is minimised, exists. The temperature and pressure profiles were also investigated in order to ensure whether the assumptions of constant temperature and pressure through the reactor are valid. The temperature and pressure at the entry and exit points in the reactor were measured and compared with the values obtained by *Fluent* in order to validate the program for this particular system.

With an orientation decided on, the critical flux, above which permanent fouling of the membrane may occur, was determined and the significance of mass transfer limitations was investigated.

5.2.1 Effect of reactor orientation of the temperature, pressure and velocity profiles

The CFD flow patterns for the temperature-, pressure- and velocity profile in the reactor for different orientations (13.4º, 30º and 90º) and feed entry points (bottom or top) were simulated in the CFD program, *Fluent*.

The temperature-, pressure- and velocity profiles for all three orientations and both feed entry points simulated were the same. The orientation of the reactor therefore did not have any effect on the profiles in the reactor. This was expected since the reactor is very small and the flow rate through the reactor is relatively high (200 mL/min). The changes in gravity occurring with a change in the reactor orientation (which may affect the velocity profiles at very low flow rates) will be negligible at high flow rates. Since the profiles for the different

reactor orientations were the same only the contour drawing for each profile at a reactor orientation of 30º and a top feed entry point will be discussed.

The temperature contours in the reactor (Figure 5.14) show the temperature changes throughout the reactor to be negligible. Temperature measurements were taken at the entrance to the system (the feed temperature) and at the exit of the system (the retentate before it rejoins the feed). Both measurements were in the range 50º ± 2º when the water bath was at a temperature of 50ºC which validates the assumption of constant temperature throughout the reactor.
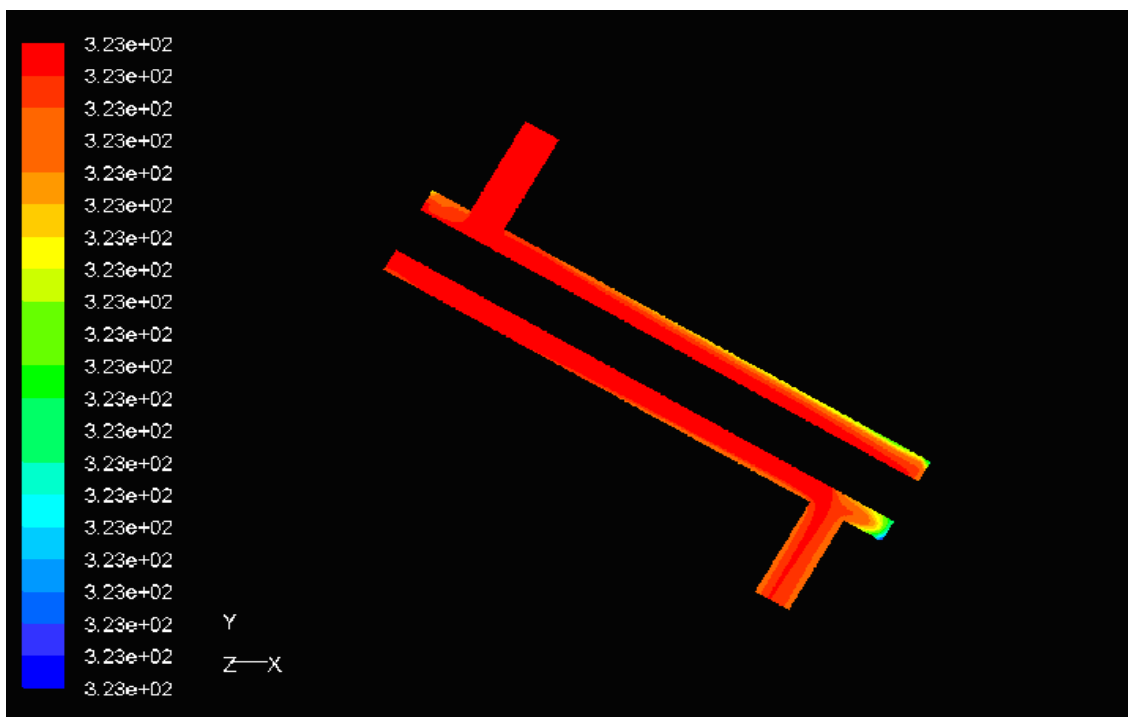
Figure 5.14: Temperature profile in the reactor at an orientation of 30º with top feed entry (temperature in Kelvin)

The pressure contours in the reactor can be seen in Figure 5.15. Although a slight increase in pressure can be seen at the feed entry point, the legend shows the increase to be insignificant. Pressure readings were taken from the pressure gauges at the feed entry and retentate exit points in the reactor. These readings were always exactly the same. The assumption of constant pressure throughout the reactor is therefore accurate.

When looking at the velocity profile in the reactor (Figure 5.16) dead volume can be seen in the corners (dark blue areas). Dead volume causes the loss of part of the membrane which in turn leads to a lower system productivity. By decreasing the dead volume (and therefore

increasing the volume of membrane that is used) the productivity of the reactor could be increased.
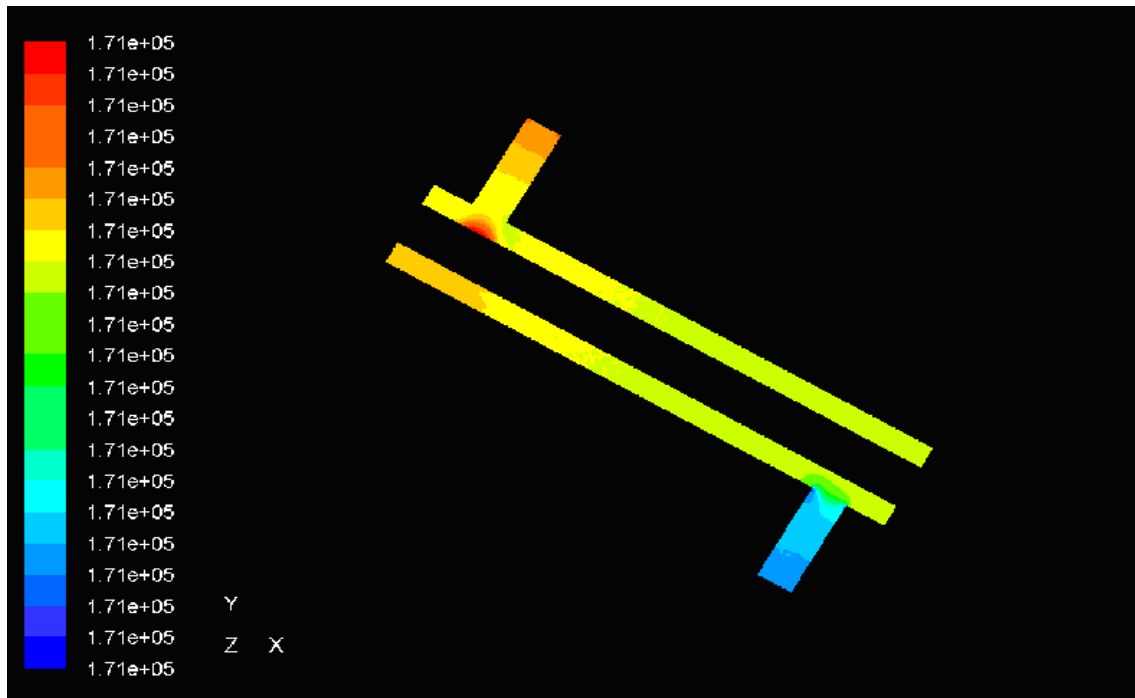
Figure 5.15: Pressure profile in the reactor at an orientation of 30º with top feed entry (pressure in Pascal)
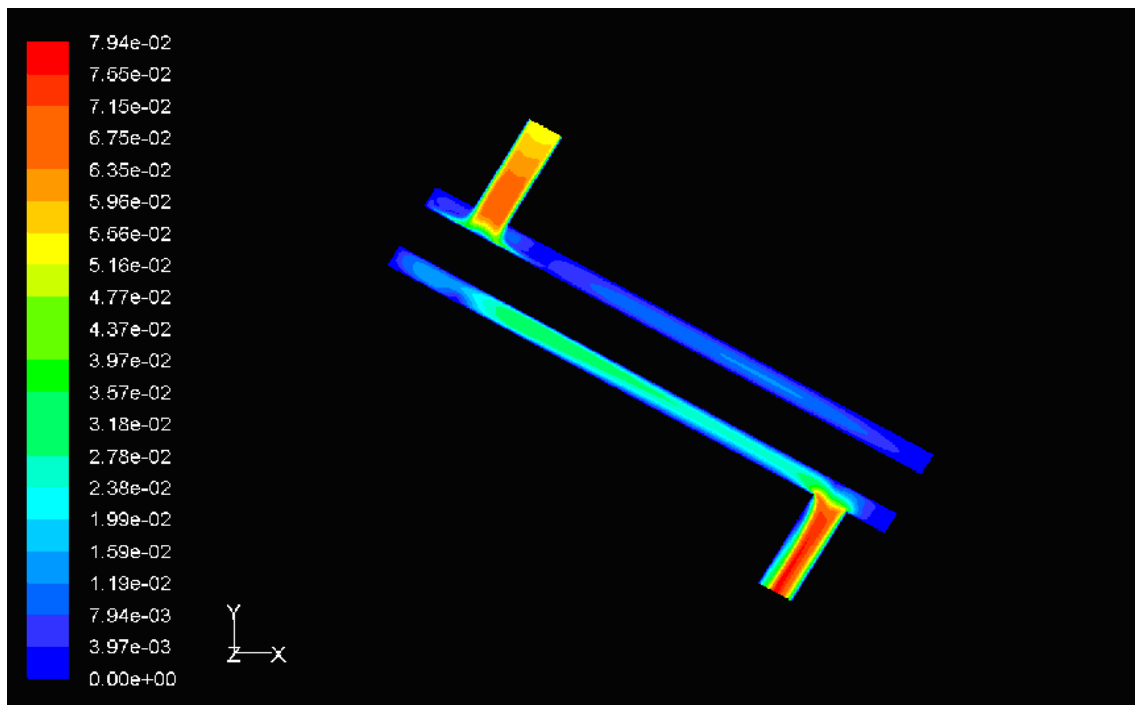
Figure 5.16: Velocity profile in the reactor at an orientation of 30º with top feed entry (flow rates in m/s)

One way of reducing the dead volume in the reactor could be to move the feed entry and exit openings farther apart. It was not possible, however, to eliminate the dead volume by moving the openings since screw caps were used to seal the ends of the reactor and these screw caps ended where the openings began.

5.2.2 <u>Determination of the critical flux through the membrane module</u>

The membrane was characterised with pure water, phosphate buffer (pH=8.0) and a solution of 80 mM lactamide in buffer with a pH of 8.0. The flux of each solution at different transmembrane pressures (TMP's) was determined. The slope of the curve obtained when the flux is plotted against the TMP (Figure 5.17), is the permeability of that specific solution through the membrane.
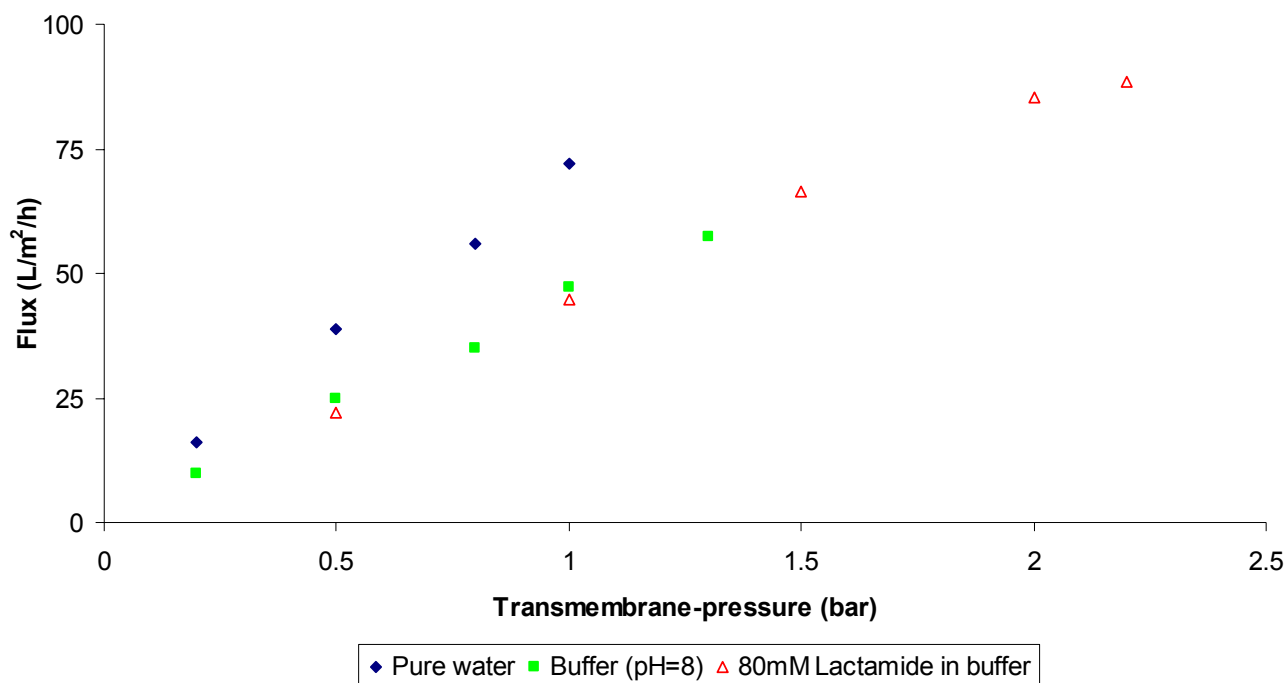
Figure 5.17: Determination of the permeability of pure water, buffer and a solution of 80mM lactamide in buffer through the 8 kDa membrane

Table 5.5 lists the permeabilities obtained for the three different solutions through the 8 kDa membrane. Should the membrane become permanently fouled, the permeability of these solutions will decrease. After each experiment the permeability of either water or buffer was tested. During the course of the experiments the permeability of the membrane remained unchanged and therefore no permanent fouling occurred.

Table 5.5: Permeability of pure water, buffer and a solution of 80mM lactamide in buffer through an 8kDa membrane

	Distilled water	Buffer	80mM Lactamide in buffer
Permeability [L/m^2.h.bar]	68.16	43.66	42.33

The critical flux for the membrane was determined from 80 mM lactamide-buffer solution permeability curve (Figure 5.17) since this was the type of substrate solution that was used in experiments. The critical flux is the lowest flux for which an increase in the TMP will not result in a significant increase in the flux. In Figure 5.17 the permeability curve of the 80 mM lactamide-buffer solution is linear until it reaches a TMP of 2.2 bar. The critical flux therefore occurred at a TMP of 2.2 bar and has a value of 88.5 L/m^2.h. Care was taken to ensure that the operating pressure never exceeded 2.2 bar in order to prevent permanent fouling of the membrane.

5.2.3 Determination of the significance of internal mass transfer limitations

It is desirable to operate an immobilised enzyme bioreactor in a reaction limited rather than mass transfer limited regime since severe mass transfer limitations may affect the productivity (and therefore the economic feasibility) of the process. An estimate of the degree of internal mass transfer limitation, if any, in the amidase immobilised MBR was made.

The values for the diffusivity coefficient of the substrate solution through the membrane (D_A), the effective diffusivity of the solution through the membrane (D_{eff}) and the Thiele modulus (Φ) were determined using Equations 2.10, 2.11 and 2.12.

Table 5.6 is a summary of the parameters used in these equations. Parameters used in the determination of D_A were determined from correlations given in the references whereas parameters used in the determination of D_{eff} were estimated values given by the references.

Table 5.6: Parameters used to determine the Thiele modulus for predicting the effect of mass transfer limitations in the reactor

	Symbol	Description	Value	Units	Reference
Determination of D_A	Φ_{ass}	Association factor for solvent	2.6	m^2/s	Sinnott, 2004
	M	Molecular weight of solvent	18	g/mol	Sinnott, 2004
	T	Temperature	323	K	n.a.
	μ	Viscosity of solvent	0.547	mN.s/m^2	Crowe *et al.*, 2001
	V_m	Molar volume of solute at boiling point	0.0956	m^3/kmol	Sinnott, 2004
Determination of D_{eff}	φ	Membrane porosity	0.4		Fogler, 1999
	σ	Constriction factor	0.8		Fogler, 1999
	τ_t	Tortuosity	3		Fogler, 1999
Determination of Φ	L	Membrane thickness	0.002	m	From suppliers
	v_{max}^*	Amidase maximum reaction rate	0.00187	mM/s	As determined
	K_m^*	Amidase Michaelis constant	68	mM	As determined

The Thiele modulus was calculated as 0.73. Since this value is larger than 0.3 it implies that mass transfer limitations are not negligible. In order to determine the ratio between the actual rate of reaction and the rate of reaction that would result if the mass transfer limitations were negligible, the effectiveness factor was determined. The effectiveness factor was determined from Figure A.30 (Appendix V) as a function of the Thiele modulus and a substrate-to-K_m ratio (beta) for immobilised enzyme catalysts with Michaelis-Menten intrinsic kinetics. An effectiveness factor of 0.7 was found. According to the effectiveness factor calculated, the observed reaction rate is approximately 70% of the reaction rate that would result if there were no internal mass transfer limitations.

An estimation of the effectiveness factor from experimental results was made by assuming the reaction rate that would be obtained without mass transfer limitations would be equal to the reaction rate of the free amidase. The effectiveness factor was calculated for the three immobilisation experiments (Table 5.1). The amidase used in each of the three experiments exhibited a different free and immobilised reaction rate. The following equation was used to determine the effectiveness factor for each of the experiments:

---

[*] As determined for the free amidase at a temperature of 50ºC and a pH of 8.0

$$\eta = \frac{\textit{Observed reaction rate of immobilised amidase}}{\textit{Observed reaction rate of free amidase}}$$

Equation 5.2

The experimental effectiveness factors obtained were 0.146, 0.107 and 0.028 for the three experiments respectively. This means that the observed reaction rate of the immobilised amidase is only 14.6%, 10.7% and 2.8% of the observed reaction rate of the free amidase used in the three experiments. Also note that the experimental effectiveness factors are significantly smaller than the effectiveness factor estimated theoretically.

Various reasons can account for the difference between the theoretical and experimental estimates:

- The theoretical estimate is a very crude estimate of the effectiveness factor since various parameters (for example the membrane porosity, membrane constriction factor and membrane tortuosity) were unknown. References were therefore used to get general estimates for these parameters. From a sensitivity analysis it was seen that an increase in the pellet porosity or constriction factor may lead to a significant decrease in the effectiveness factor whereas an increase in the tortuosity may result in an increase in the effectiveness factor.

- The kinetic parameters K_m and v_{max} were assumed to be the same for both the free and immobilised amidase. In reality, there may be differences between the kinetic parameters of the free and immobilised amidase. The Thiele modulus is sensitive for changes in the kinetic parameters. For example, if the kinetic parameter K_m were to increase and v_{max} were to decrease (which sometimes occurs in immobilised enzyme systems where mass-transfer limitations are significant) the Thiele modulus would increase thereby resulting in a decreased effectiveness factor.

- The observed reaction rate of immobilised amidase was calculated from Equation 3.5. From this equation it can be seen that the reaction rate is sensitive for changes in the permeate flux and product concentration in the permeate stream. Unfortunately the permeate flux cannot be determined very accurately and since the values of the permeate flux are very low, small errors in measurement lead to large errors in the permeate flux value (for example: if the permeate flux is measured as 0.6 mL/min and it is actually 0.7 mL/min the error looks small but in reality it leads to a permeate flux which is 17% less than the actual permeate flux). The observed reaction rate of the immobilised amidase may therefore be inaccurate in which case the effectiveness factor obtained from the experimental results may be inaccurate.

- The reaction rate for the free amidase (1.48 mM/min) has been determined from non-linear regression of experimental data. Statistics show that although this reaction rate ensures the best fit of the Michaelis-Menten curve to the data, the reaction rate can be anywhere between 1.29 and 1.76 mM/min and still be in the 95% confidence range.

- When the theoretical effectiveness factor was determined from the Thiele modulus, the figure used (Figure A.30 in Appendix V) was for immobilised enzymes following intrinsic Michaelis-Menten kinetics. It was assumed that the amidase follows Michaelis-Menten kinetics when immobilised. This may not be the case. Different correlations to relate the Thiele modulus to the effectiveness factor would then be applicable.

- The assumption that the immobilised amidase should have the same specific activity as the free amidase if no mass transfer limitations were present may also be inaccurate. Due to the low stability of the free amidase, the amidase would already have lost a significant amount of its activity during the immobilisation procedure. Immobilisation may also have affected the activity of the amidase which will mean that even without mass transfer limitations a lower amidase specific activity will be observed.

Although the theoretically estimated effectiveness factor differs significantly from the effectiveness factor determined from the experimental data, both factors show that mass transport limitations are not negligible.

In the future, mass transport limitations in the reactor may be reduced by replacing the one membrane (which has a relatively thick wall or support structure) with multiple smaller membranes with thin walls. When looking at Equation 2.10 which is used to calculate the Thiele modulus, it can be seen that a reduction in the membrane wall-thickness will lead to a reduction in the Thiele modulus. Immobilisation of the enzyme in a large number of thin-walled membranes in a single reactor will also reduce the mass transfer limitations resulting from a large amount of enzyme immobilised in one membrane.

5.3 <u>Quantification of the membrane immobilised amidase process</u>

Quantification of the membrane immobilised amidase process was done in three parts. The first part consisted of determining the effectiveness of the immobilisation method by looking at the amount of amidase immobilised, whether it was physically retained and the effect of immobilisation on the amidase activity and functional stability.

Validation of the theoretical model developed from first principles in Section 4.2 was done next. This was achieved by statistically comparing the results from Experiments 2 and 3 (Table 5.1) to results predicted by the model.

The last part in the quantification of the process consisted of using the model to predict the effect of amidase activity, amidase functional stability, permeate flux, amount of enzyme protein immobilised and substrate concentration on the reactor performance. The reactor performance was measured in terms of instantaneous conversion, instantaneous productivity (refer to Section 3.5.4 for explanation) and cumulative amount of lactic acid produced. The cumulative amount of lactic acid produced was determined in order to evaluate the industrial viability of the process for changes in the operating parameters. The cumulative amount of lactic acid produced was calculated as follows:

1. The instantaneous productivity curves were divided into two sections. The first section was the linear part (up until the peak) and the second section was the polynomial part (after the peak).

2. A program, written in Visual Basic for use in Excel, was used to determine the equations for each of the two sections on the instantaneous productivity curve.

3. The equations were then integrated with respect to time in order to obtain equations expressing the amount of product formed per liter of membrane as a function of time.

4. The amount of product formed per liter of membrane after 500, 1000, 1500, 2000, 2500 and 3000 minutes was then determined. These results were multiplied with the membrane volume in order to determine the amount of product formed at each of the time intervals mentioned above.

A summary of the ranges used to predict the effect of changes in the parameters on the reactor performance can be seen in Table 5.7.

Table 5.7: Summary of parameter ranges used in model predictions

Parameter	Level				
	1	**2**	**3**	**4**	**5**
Amidase activity (U/mg)	0.05	0.15	0.5	1	2
Amidase functional stability (h)	1.8	3.6	7.3	14.5	115.5
Permeate flux (L/min)	0.00001	0.0001	0.0005	0.001	0.005
Amount of enzyme protein immobilised (mg)	2	6.38	20	50	100
Substrate concentration (mM)	20	40	80	120	160

At the end of this section the changes and improvements required for optimisation of the system were considered to formulate a definite plan containing steps that should be followed to optimise the process.

5.3.1 Membrane immobilisation of amidase

The amidase was immobilised in the membrane pores through physical adsorption (Section 3.5.1). In order to determine how effective adsorption in the membrane pores is as an immobilisation method, the amount of enzyme protein that is adsorbed and thereafter physically retained and the effect of immobilisation on the amidase activity and functional stability was determined. Three experimental runs have been conducted to evaluate the effectiveness of immobilising the amidase in the membrane pores.

5.3.1.1 *Amount of amidase immobilised*

Wenten and Widiasa [2002] proved that the initial enzyme protein concentration in the solution that is recycled during immobilisation (initial feed stream) has an effect on the amount of enzyme protein adsorbed in the membrane pores in a microfiltration membrane. An optimum enzyme protein concentration existed whereafter an increase in the enzyme protein concentration of the initial feed resulted in a decrease in the percentage of enzyme protein immobilised. In this research, although only 3 data points were generated, the effect of enzyme protein concentration in the immobilisation feed on the amount of enzyme protein immobilised using an ultrafiltration membrane (with 8 kDa cut-off) indicated an exponential relationship (Figure 5.18). An increase of 0.0026 mg/L (from 0.0184 mg/L to 0.021 mg/L) in the enzyme protein concentration of the initial immobilisation feed caused the amount of initial enzyme protein immobilised to decrease from 38.7% to 30.4%. At an

initial enzyme protein concentration of 1.07 mg/L the amount of enzyme protein immobilised was only 4.7%.

The plot shows the curve with the fitted equation $y = 4.8521x^{-0.498}$ and $R^2 = 0.9942$. The y-axis is labelled "Amount of intial protein immobilised (%)" and the x-axis is labelled "Protein concentration (mg/mL)".
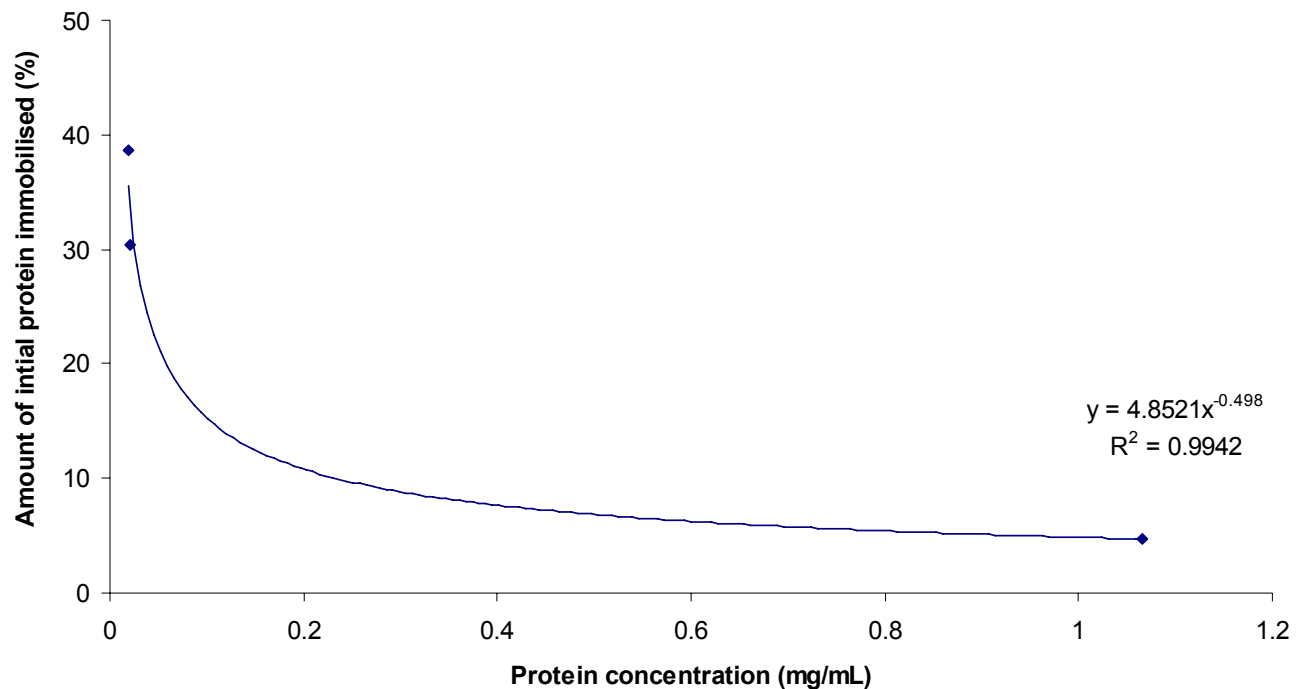
Figure 5.18: Effect of enzyme protein concentration in the initial immobilisation feed on the amount of enzyme protein immobilised

A possible explanation for this phenomenon is that an increase in the enzyme protein concentration in the initial feed will result in more molecules competing for the same number of membrane pores. The competition may lead to the formation of an enzyme protein gel layer on the surface of the membrane. This layer effectively prevents enzyme protein molecules from entering the pores. During washing of the membrane after immobilisation (Section 3.5.1) the layer is washed off and very little enzyme protein remains in the membrane.

The transmembrane pressure (TMP) could also have an effect on the amount of enzyme protein immobilised. If the TMP is too high the enzyme protein entering the reactor in the initial immobilisation feed may not diffuse into the membrane pores – instead the pressure will force the enzyme protein molecules against the membrane surface where they will block the entrance to the pores and form a gel layer on the membrane surface. This may especially be the case with high enzyme protein concentrations. If, on the other hand, the TMP is too low, the enzyme protein molecules may not have a sufficient driving force for entering the pores which will lead to a decrease in the amount of enzyme protein immobilised. Lower enzyme protein concentrations in the initial feed will be affected more

than higher enzyme protein concentrations if the TMP is too low since at lower concentrations the statistical probability of enzyme protein entering the pores is lower. A TMP of 0.5 bar was decided on for immobilisation purposes in this research since it was below the critical flux. It was also assumed that a TMP of 0.5 bar is low enough to prevent an enzyme protein gel layer from forming.

5.3.1.2 Physical retention of enzyme protein during operation

After immobilisation the membrane was washed with distilled water in order to remove all enzyme protein that did not adsorb in the membrane pores. The amount of enzyme protein immobilised was determined with a mass balance (Section 3.5.1).

Three experimental runs (Table 5.1) were conducted during which the permeate and retentate streams were monitored to detect any loss of enzyme protein from the system. The running time for the three experiments was 3 hours, 20.5 hours and 21 hours respectively. During all three experiments no enzyme protein losses occurred for the full time of operation. Since no enzyme protein passed through the membrane, the cut-off size of the membrane (8 kDa) is adequate to retain the amidase.

5.3.1.3 Effect of immobilisation on amidase activity

Ideally the immobilisation of an enzyme should not affect its specific activity. In reality activity losses do occur and can be caused by among others solvents, chemicals, harsh immobilisation conditions or the loss of some enzyme activity centers due to binding to the matrix [www.kochmembrane.com]. Physical adsorption as an immobilisation method usually doesn't affect the activity of the enzyme as much as chemical immobilisation methods would since harsh conditions are absent during immobilisation. For instance, Giorno *et al.* [2001] used fumarase adsorbed in the pores of a MBR to produce L-malic acid. The activity of the free and immobilised fumarase was found to be almost identical.

In this research, however, significant differences were seen between the free and immobilised amidase activities for the same immobilisation procedure used by Giorno *et al.* [2001]. The difference between the free and immobilised amidase activities for the three different experiments (Table 5.1) can be seen in Figure 5.19.
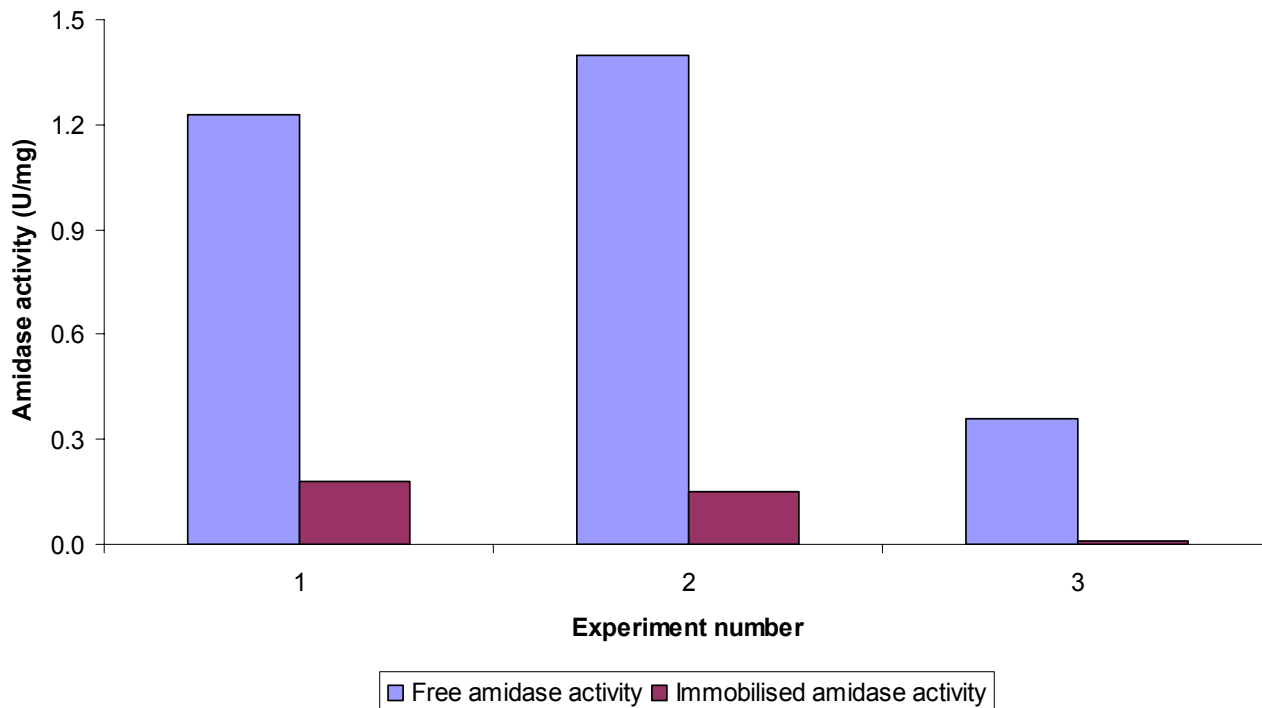
Figure 5.19: Effect of immobilisation on amidase activity in three experimental runs

An interesting observation is that the activity of the immobilised amidase was approximately 7, 10 and 35 times lower than that of the free amidase for each of the three experiments respectively.

In Section 5.2.3 the effect of mass transfer limitations on the system were estimated. It can be assumed that a part of the difference between the free and immobilised amidase activities are as a result of mass transfer limitations since it has been found to be the limiting step in the system. The amidase activity measured is therefore not necessarily the true amidase activity since it is disguised by mass transfer effects.

Another reason for the difference that is seen between the free and immobilised amidase activities is the low functional stability of the amidase. During immobilisation and washing (which typically lasts for approximately 2 to 3 hours) the free amidase (with a half-life of approximately 5 hours) that is circulated through the MBR will have lost almost a ¼ of its activity.

A comparison of the ratio of free to immobilised amidase activity with the initial enzyme protein concentration in the immobilisation feed (Figure 5.20), show that an increase in the initial enzyme protein concentration resulted in an increased ratio which indicates a larger discrepancy between the free and immobilised amidase activities. The amidase therefore

lost more activity during immobilisation at higher concentrations of enzyme protein in the immobilisation feed than at lower concentrations.
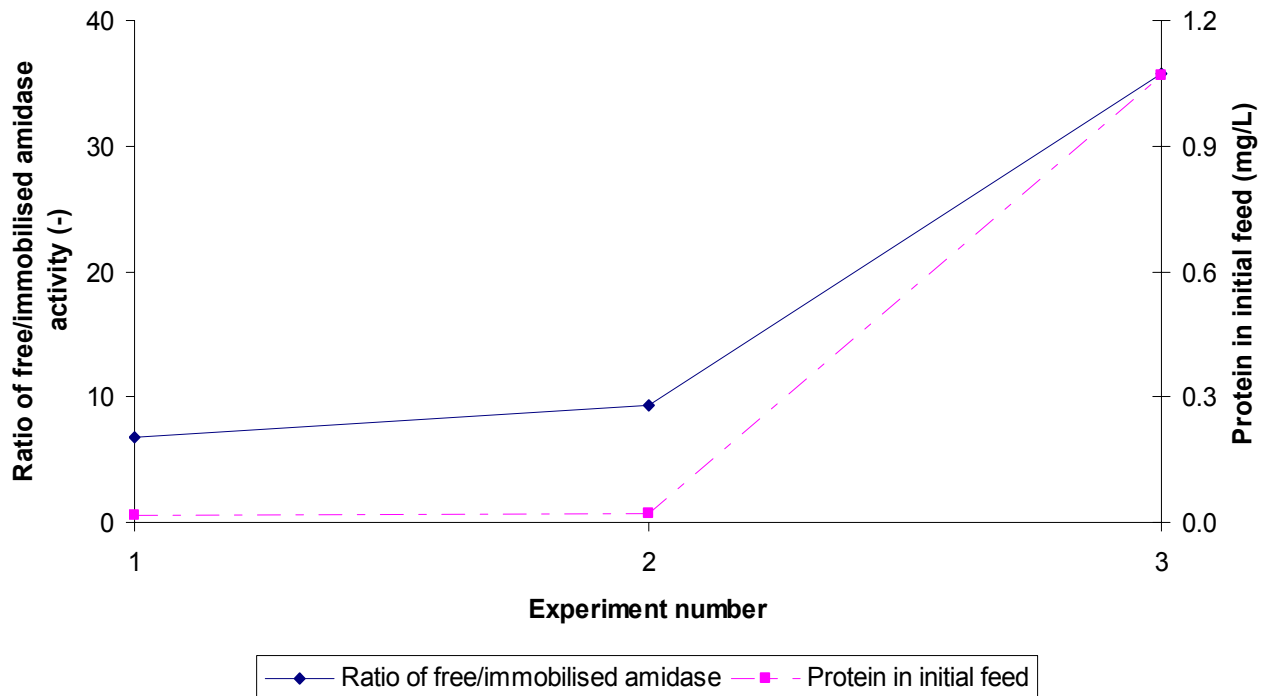
Figure 5.20: Effect of amount of enzyme protein in initial feed on immobilised amidase activity

Wenten and Widiasa [2002] found a similar relationship between the initial enzyme protein concentration in the immobilisation feed and the specific activity of the enzyme (penicillin acylase) after immobilisation by adsorption in the pores of a microfiltration membrane. After a certain optimum concentration of enzyme protein in the immobilisation feed any further increase in the concentration resulted in a decrease in the enzyme specific activity. The decrease in specific activity was attributed to the increase in competition for pores between the enzyme protein molecules.

In order to see an improvement in the immobilised amidase activity the following three steps can be considered:

- Mass transfer effects need to be eliminated. This can be done by rather using a few smaller membranes than one large membrane. The same surface area required for immobilisation can be obtained but mass transfer through the thinner, smaller membranes will be much better than through one thick, large membrane.

- The functional stability of the free amidase should be improved in order to efficiently immobilise it. Shorter periods of immobilisation can also be considered but it is doubtful whether it will prove to be sufficient for effective immobilisation.

- A larger range of enzyme protein concentrations in the immobilisation feed could be investigated in order to determine whether an optimum concentration exists.

5.3.1.4 Effect of immobilisation on amidase functional stability

The functional stability of enzymes has been found to improve with immobilisation. Various reasons have been given for this behaviour, the main reason being that when immobilised, enzymes are in a microenvironment. Changes or fluctuations in the macro environment are not felt as strongly by the immobilised enzymes since the microenvironment serves as a type of buffer against the macro environment. Denaturation of the immobilised enzymes therefore does not occur at the same rate as denaturation of free enzymes in the same environment [Zhang *et al.*, 2005; Giorno and Drioli, 2000; Ye *et al.*, 2006; Tramper, 1996]. Enzyme molecules immobilised in a matrix are also prevented from interaction with each other, thereby ensuring additional stabilisation [http://www.lsbu.co.uk/biology/enztech].

The functional stability of the immobilised amidase was determined at a temperature of 50ºC and a substrate concentration of 80 mM. This was done by measuring the product concentration in the permeate stream and relating the concentration to amidase specific activity with Equation 3.4. Fitting a plateau plus one-phase exponential decay model to the data with non-linear regression resulted in the curve shown in

Figure 5.21. This specific model was chosen since the amidase remained stable for the first three hours of operation (the plateau part of the model) whereafter it followed typical one-phase exponential decay. With non-linear regression the half-life of the immobilised amidase during the one-phase exponential decay part of the graph was determined as 6.4 hours. The 95% confidence interval includes probable half-lives in the range 5.5 to 7.6 hours.
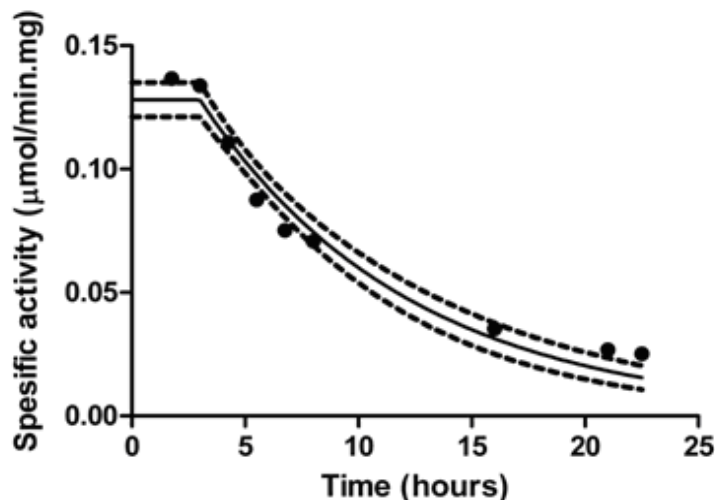
Figure 5.21: Plateau plus one-phase exponential decay of immobilised amidase at 50ºC and a lactamide concentrations of 80mM

By combining the plateau phase and the half-life obtained during the one-phase exponential decay the actual half-life of the immobilised amidase was determined as 9.4 hours. This is a significant improvement on the half-life of 4.9 hours exhibited by the free amidase. Immobilisation has therefore increased the stability of the amidase significantly.

5.3.2 Experimental validation of the immobilised amidase model

The CSTR model developed in Section 4.2 to predict the behaviour of the MBR was validated by comparing the predicted data to results obtained in two experimental runs at different conditions. To determine the goodness of fit between the predicted and experimental data the correlation coefficients were determined. The residuals were then investigated to ensure that the statistical assumptions made during development of the model had not been violated. These plots (for the instantaneous conversion and productivity for both experiments) can be found in Appendix IV.

Since the MBR was assumed to operate as a CSTR at unsteady state (Section 4.2), the validation of the model had to be carried out by calculating the instantaneous conversion and instantaneous productivity achieved in the reactor (see explanation in Section 3.5.4).

The correlation coefficients (95.4% for the first experiment and 80% for the second experiment) established the goodness of fit (Figure 5.22). Error bars are not shown due to the fact that errors between measurements were less than 0.2%. Although the residual plots (Appendix IV) have a low number of data points, it didn't indicate that assumptions of

normality and homoscedacity of the residuals, which were made during the development of the model, have been violated.

Figure 5.22: Instantaneous conversion profiles in the reactor. Conditions: □ (T=50ºC, pH=8.0, s0=80 mM, e0=6.38 mg, v=0.0005 L/min, a0$_{free}$=1.4 U/mg) and ■ (T=50ºC, pH=8.0, s0=40 mM, e0=20.09 mg, v$_p$=0.0001 L/min, a0$_{free}$=0.357 U/mg)

The model does, however, seem to under predict the instantaneous conversion in the region around the peak and over predict it at the initial decline after the peak. The discrepancies between the predicted and experimental values may be a result of a difference between the permeate flux used in the model and that used in the experiment. The permeate flux cannot be measured accurately since it is very low (typically in the range 0.0001 – 0.0005 L/min) and the error can therefore be out with as much as 500%.

Although the same over- and under predictions that were seen in Figure 5.22 can also be seen for the instantaneous productivity in Figure 5.23, the correlation coefficients of 95.4% and 80.2% for experiments 1 and 2 respectively confirm a good fit of the model to the experimental results. The residual plots (Appendix IV) didn't indicate that the assumptions of normality and homoscedacity of the residuals that were made during the development of the model were violated.
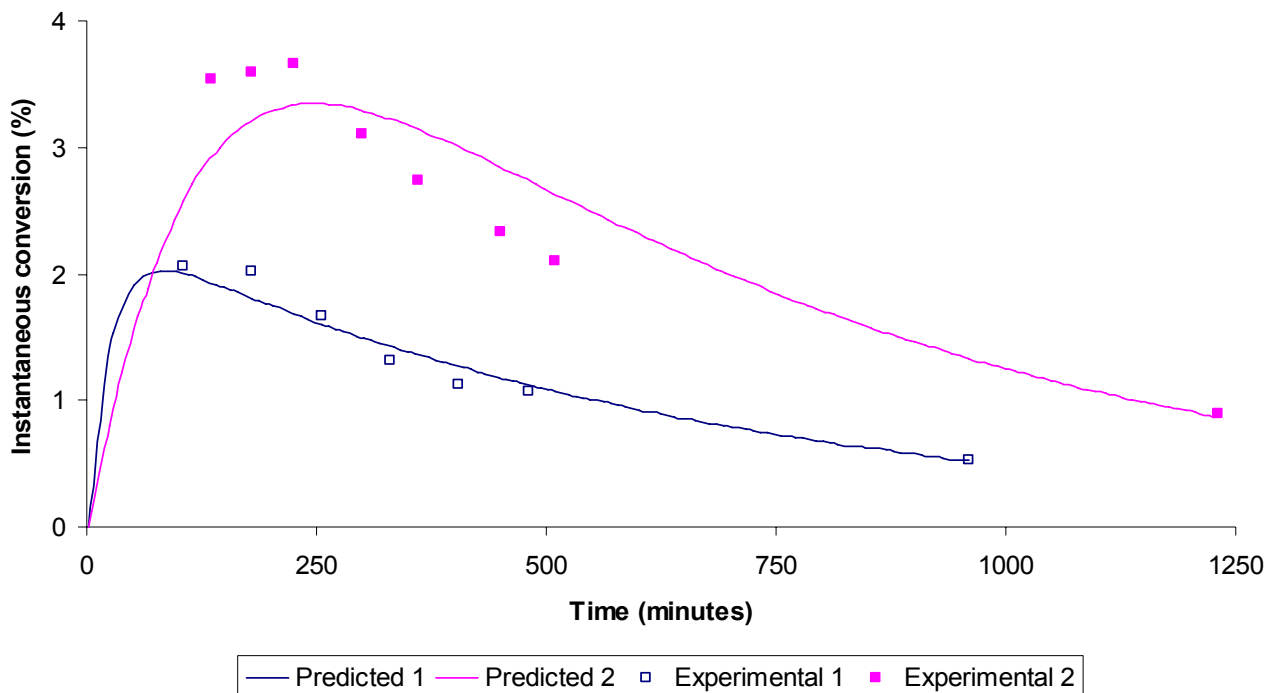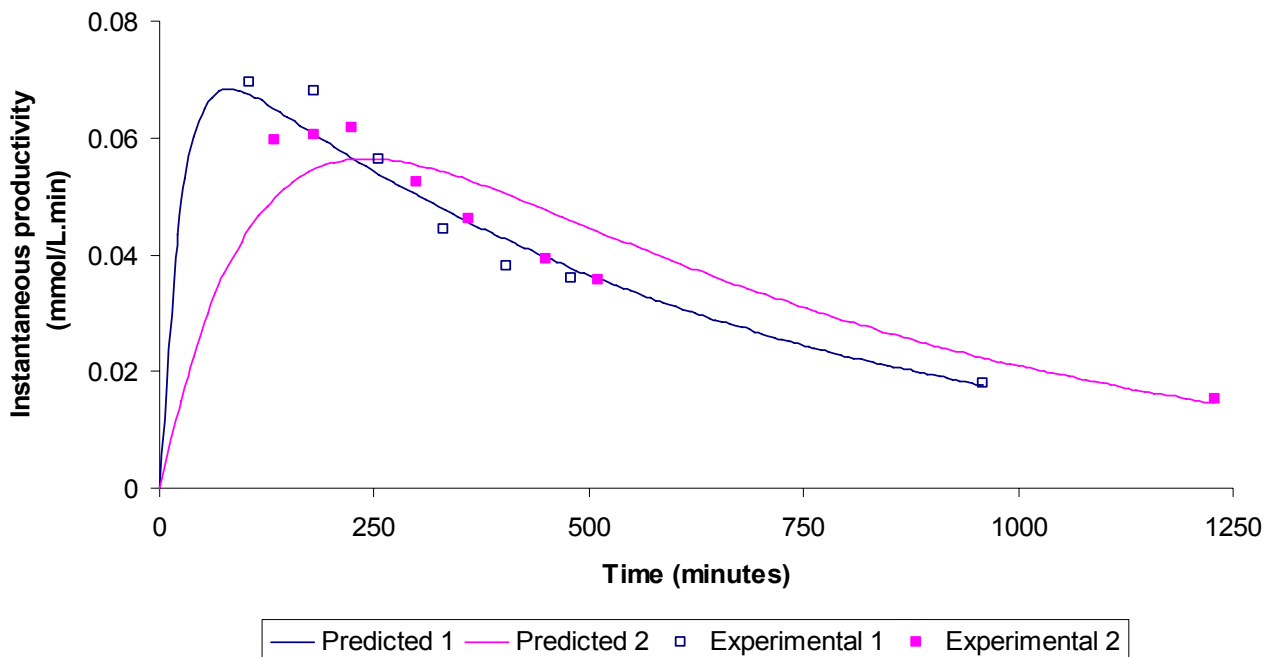
Figure 5.23: Instantaneous productivity profiles in the reactor. Conditions: □ **(T=50ºC, pH=8.0, s0=80 mM, e0=6.38 mg, v=0.0005 L/min, a0$_{free}$=1.4 U/mg) and** ■ **(T=50ºC, pH=8.0, s0=40 mM, e0=20.09 mg, v$_p$=0.0001 L/min, a0$_{free}$=0.357 U/mg)**

Since the model has been validated by the experimental results, the model can now be used to make certain predictions regarding the sensitivity of the reactor performance to various operating parameters. It should be mentioned that although the model has technically only been validated for a specific range in the operating parameters (due to process constraints for example permeate flux measurement), values outside of this range will also be used in the model predictions in order to emphasize the sensitivity of the reactor performance to changes in these operating parameters. It is advisable that future work should include the validation of the model over a wider range of values for the different operating variables.

5.3.3 <u>Model predictions</u>

The CSTR model of the MBR (derived in Section 4.2 and validated in Section 5.3.2) was developed specifically to evaluate the effect of the amidase stability, amidase activity, permeate flux, amount of immobilised enzyme protein and substrate concentration on the instantaneous conversion, instantaneous productivity and cumulative amount of lactic acid produced. Refer to Section 5.3 for a summary of the parameter ranges used in the model predictions.

5.3.3.1 Effect of amidase stability on conversion and productivity

During the three experimental runs very low amounts of product left the system. After approximately 22 hours only 0.75 millimoles of lactic acid was collected for the first experiment. During the second experiment only 0.12 millimoles was collected after 22 hours. One of the causes for these low amounts of product collected could be the relatively low amidase stability since the immobilised form had a half-life of approximately 9 hours. According to Schoemaker *et al.* [2003] one of the main reasons for the limited amount of industrial biocatalytic processes is the uneconomic operational stability of enzymes. The effect of different half-lives on the reactor performance was therefore investigated. A range of half-lives (between 1.8 hours and 115.5 hours) was investigated in order to determine the sensitivity of the reactor performance to half-lives longer and shorter than that of the amidase (9 hours). Predictions were made over a time of 3500 minutes (58 hours).

For all half-lives an initial rise in the instantaneous conversion was predicted (Figure 5.24) and a peak occurred after approximately 100 minutes. The peak indicates the time at which the first product leaves the bioreactor. The peak occurred at the same time for all the half-lives since the time at which the first product leaves the bioreactor will only depend on the permeate flux and the permeate flux was kept constant. After the peak a decrease in the instantaneous conversion for all the half-lives can be observed. However, a less rapid decrease in instantaneous conversion occurs with an increase in the half-life of the amidase.

This type of trend was expected since a longer half-life would mean that the amidase activity decay will be slower. This, in turn, will result in higher product concentrations in the permeate stream over the same time than that achieved at lower half-lives.
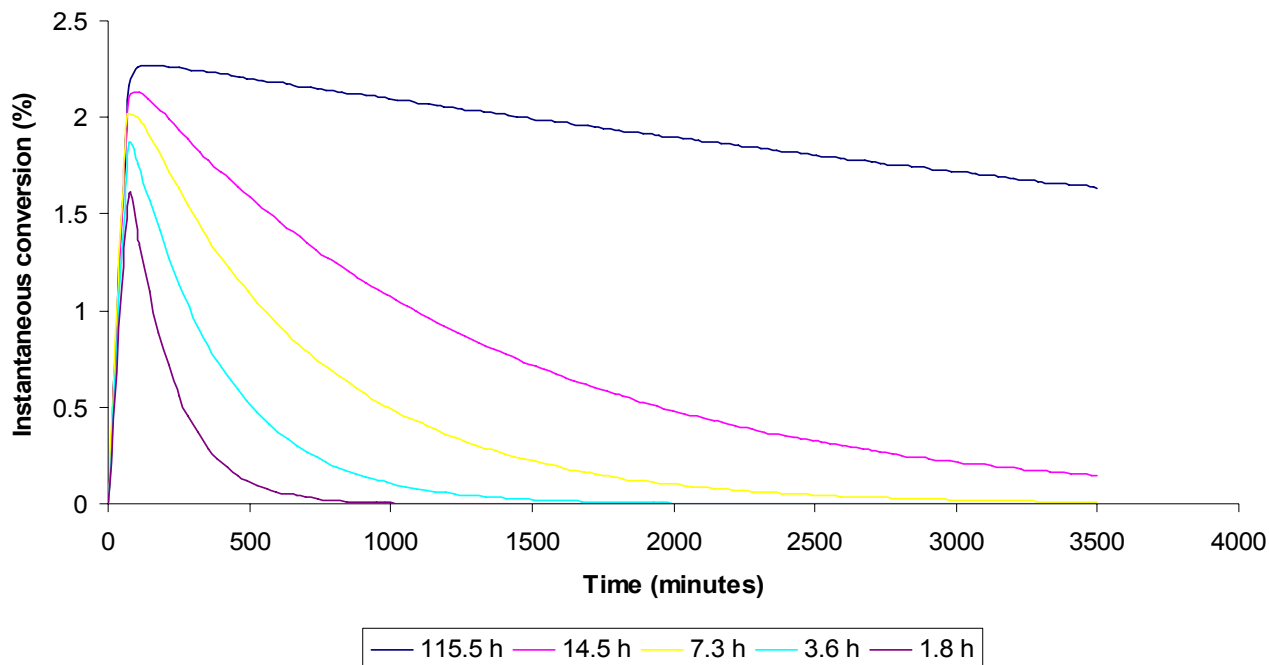
Figure 5.24: Effect of amidase stability in terms of half-life on the instantaneous conversion (T=50ºC, pH=8.0, s0=80 mM, e0=6.38 mg, v_p=0.0005 L/min, $a0_{imm}$=0.15 U/mg)

The instantaneous productivity followed a similar trend as that of the instantaneous conversion. An initial increase is observed up until a peak is reached at approximately 100 minutes whereafter a decline in the instantaneous productivity over time occurs. As the amidase half-life was increased, a less pronounced decrease in the instantaneous productivity was observed (Figure 5.25).

Since the activity of the amidase is decreased at a slower rate (due to the increased stability), the product concentration in the permeate stream is also decreasing at a slower rate, thereby ensuring higher instantaneous productivities.

Considering the maximum instantaneous conversion and productivity achieved for each half-life (Figure 5.24 and Figure 5.25) it can be seen that in general it is very low (2.2% and 0.08 mmol/L.min) and above a half-life of 14.5 hours, an increase in the half-life of the amidase will not result in a significant increase in the maximum instantaneous conversion and productivity achieved (Figure 5.26).

Figure 5.25: Effect of amidase stability in terms of half-life on the productivity (T=50ºC, pH=8.0, s0=80 mM, e0=6.38 mg, v_p=0.0005 L/min, $a0_{imm}$=0.15 U/mg)
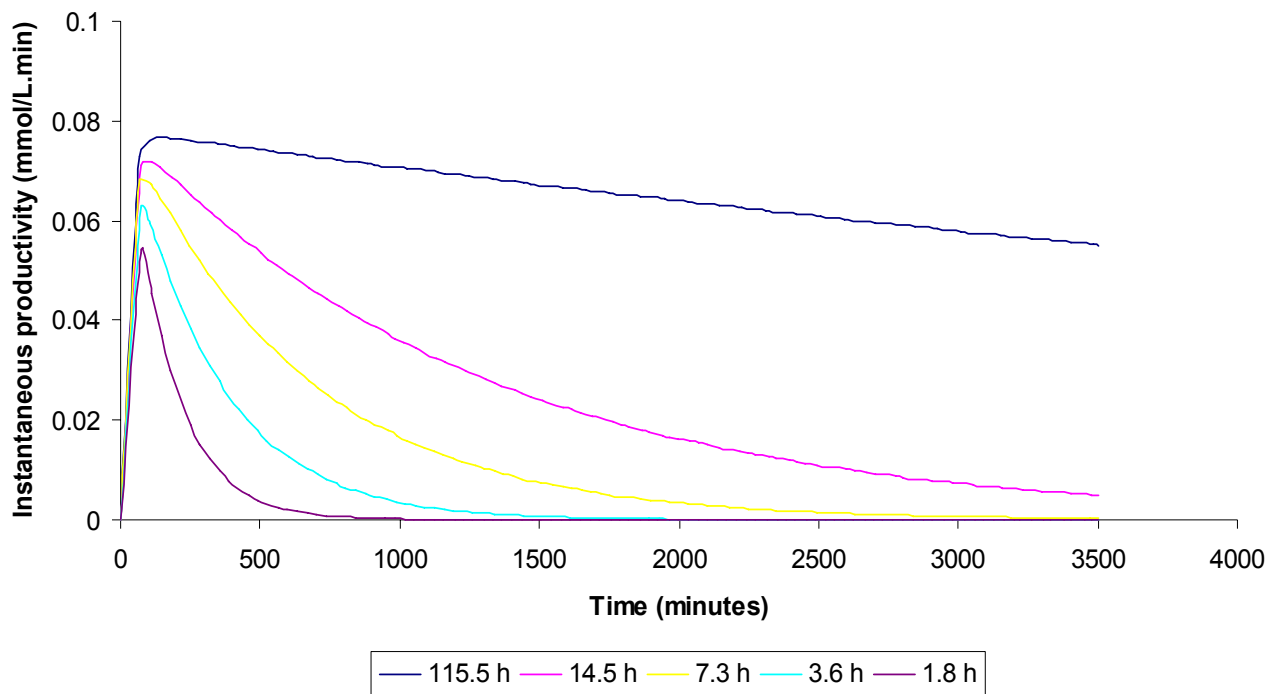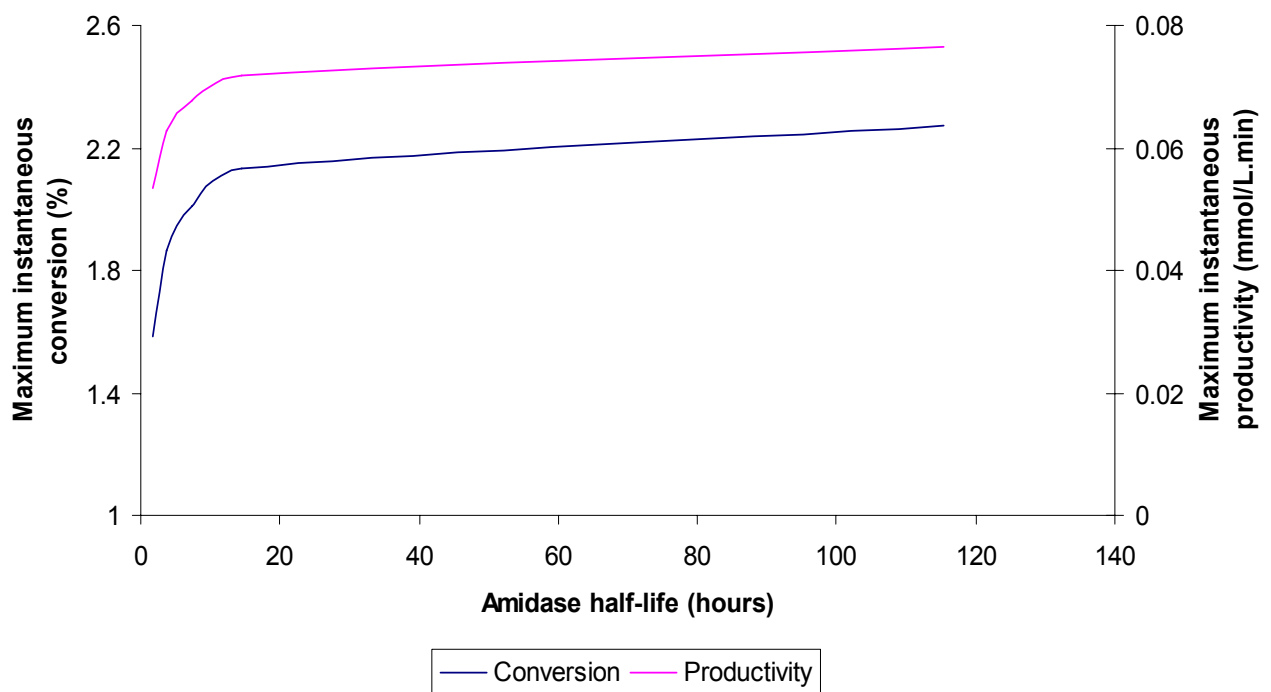

Figure 5.26: Effect of amidase stability in terms of half-life on the maximum instantaneous conversion and maximum productivity (T=50ºC, pH=8.0, s0=80 mM, e0=6.38 mg, v_p=0.0005 L/min, $a0_{imm}$=0.15 U/mg)

The maximum instantaneous conversion and productivity for all the half-lives are achieved after approximately 100 minutes. An amidase with a short half-life (for example 1.8 hours) will already have lost almost a half of its initial activity after 100 minutes – whereas an amidase with a longer half-life (for example 14.5 hours) will only have lost a small fraction of its activity. As the half-life of the amidase is increased above 14.5 hours less of an effect of half-life on both the instantaneous conversion and instantaneous productivity is observed because the fraction of the initial amidase activity that is lost in 100 minutes becomes insignificantly small in comparison with the Half-lives.

In accordance with the importance of the cumulative amount of lactic acid collected (Section 5.3.1), the amount collected after 3500 minutes was determined for each of the half-lives. According to the predictions, an increase in the half-life of the amidase will result in a direct increase in the amount of lactic acid collected (refer to Figure 5.27 and Figure 5.28). For a half-life of 14.5 hours, the maximum amount of product that can be collected is less than 1.2 millimoles whereas a higher half-life (for example 115.5 hours) could increase that amount considerably.
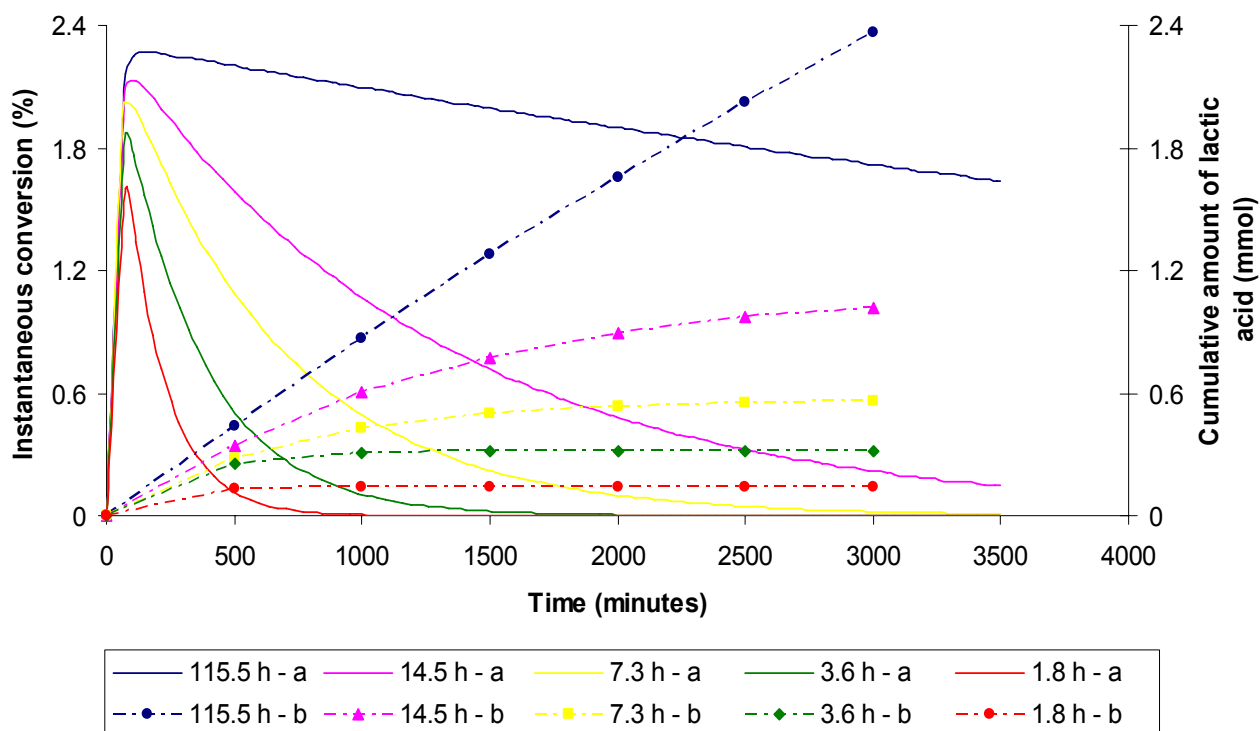
Figure 5.27: Effect of amidase stability on instantaneous conversion and cumulative amount of lactic acid produced (T=50ºC, pH=8.0, s0=80 mM, e0=6.38 mg, v_p=0.0005 L/min, $a0_{imm}$=0.15 U/mg)

Figure 5.27 also shows that for half-lives of 1.8 hours and 3.6 hours no marked difference in the amount of lactic acid collected will be observed after 500 minutes (8.3 hours). This

result is mirrored in the instantaneous conversion and productivity which had by that time decreased to almost zero due to the low stability of the enzyme. For half-lives above 3.6 hours but below 14.5 hours (in which category the amidase currently falls with its 9 hour half-life), no significant increase in the amount of lactic acid collected will be seen after 2000 minutes (33.3 hours) due to low remaining enzyme activity and therefore low instantaneous conversions and productivities. Since the cumulative amount of lactic acid produced tends toward a constant value over time if the enzyme is close to total deactivation, the model can be used to predict for how long the reactor should be run to collect the maximum amount of product for an enzyme with a specific half-life,
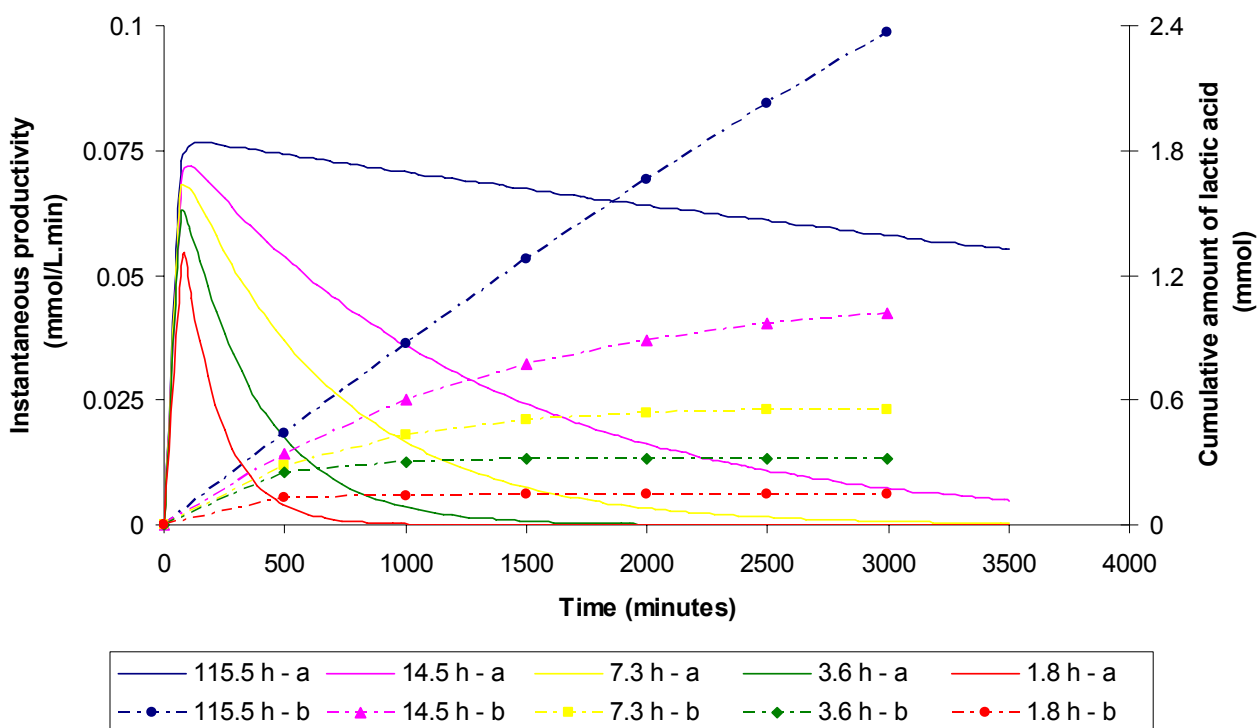
Figure 5.28: Effect of amidase stability on instantaneous productivity and cumulative amount of lactic acid produced (T=50ºC, pH=8.0, s0=80 mM, e0=6.38 mg, v_p=0.0005 L/min, $a0_{imm}$=0.15 U/mg)

The stability of the amidase has been found to have a significant impact on the reactor performance. For this process to become viable, the stability of the amidase would have to be improved. Investigation of the effect of a variety of stabilising agents on the amidase stability has been done (Section 5.1.4) but no improvement was observed.

5.3.3.2 *Effect of amidase activity on conversion and productivity*

The immobilised activity of an enzyme also plays a significant role when determining whether a specific process may be viable for industrial application. An immobilised enzyme

may be very stable but if its activity is too low, the conversion and productivity of the system may be too low for an economic process. The effect of different immobilised amidase activities on the instantaneous conversion and productivity was evaluated for the range 0.05 U/mg to 2 U/mg with the actual immobilised amidase activity being 0.15 U/mg.

The instantaneous conversion (Figure 5.29) and instantaneous productivity (Figure 5.30) both showed an initial increase up until a peak value whereafter a decrease could be observed. The decrease in the instantaneous conversion and instantaneous productivity at different amidase activities occur at the same rate since the amidase stability, which is the only parameter influencing the rate of activity decay, was kept constant.
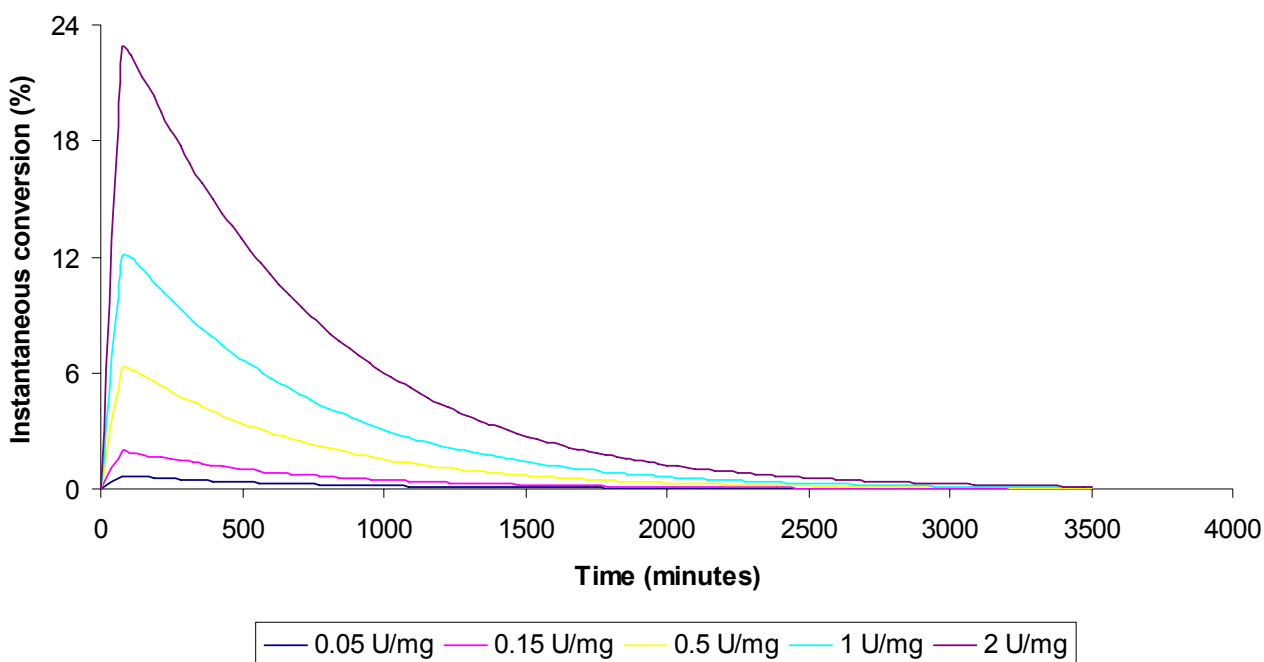
Figure 5.29: Effect of amidase specific activity on the instantaneous conversion (T=50°C, pH=8.0, s0=80 mM, e0=6.38 mg, v$_{p}$=0.0005 L/min, t$_{h}$=7.3 h)

An increase in the immobilised amidase activity was seen to result in a proportional increase in the maximum instantaneous conversion and maximum instantaneous productivity achieved (Figure 5.31). This could be expected since doubling the amidase activity from 1 U/mg to 2 U/mg would result in double the amount of substrate being converted at a specific time.
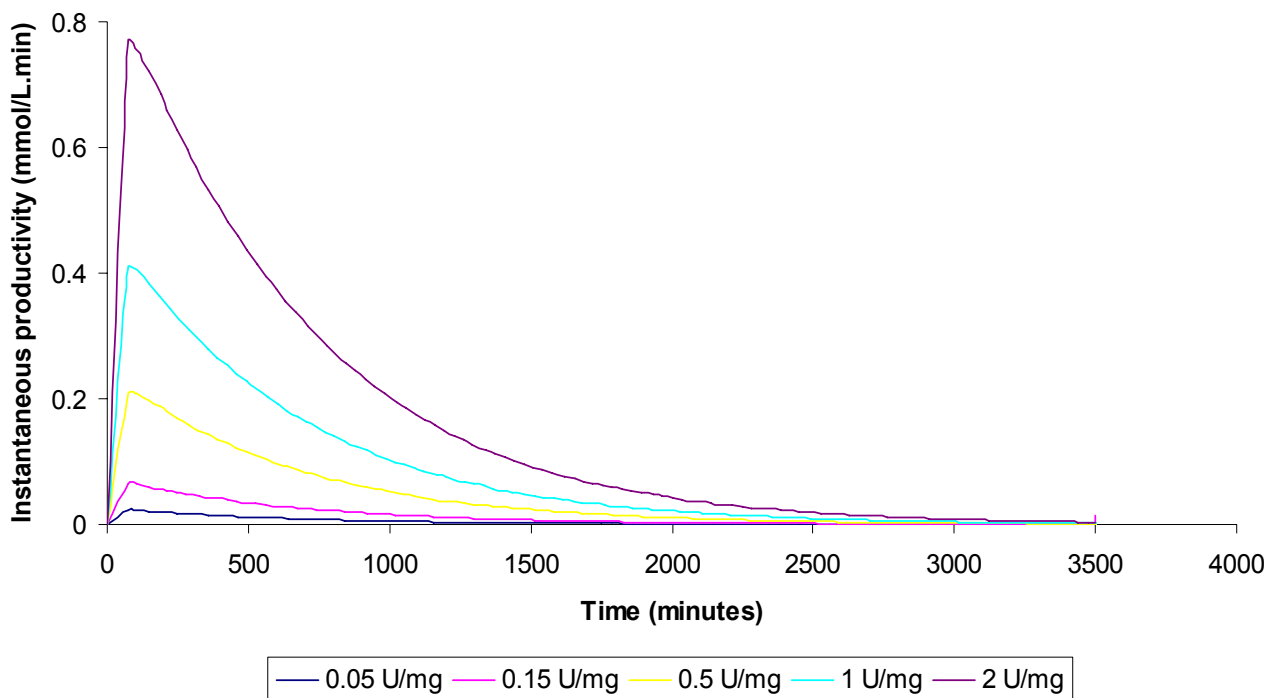
Figure 5.30: Effect of amidase specific activity on the productivity (T=50ºC, pH=8.0, s0=80 mM, e0=6.38 mg, v_p=0.0005 L/min, t_h=7.3 h)
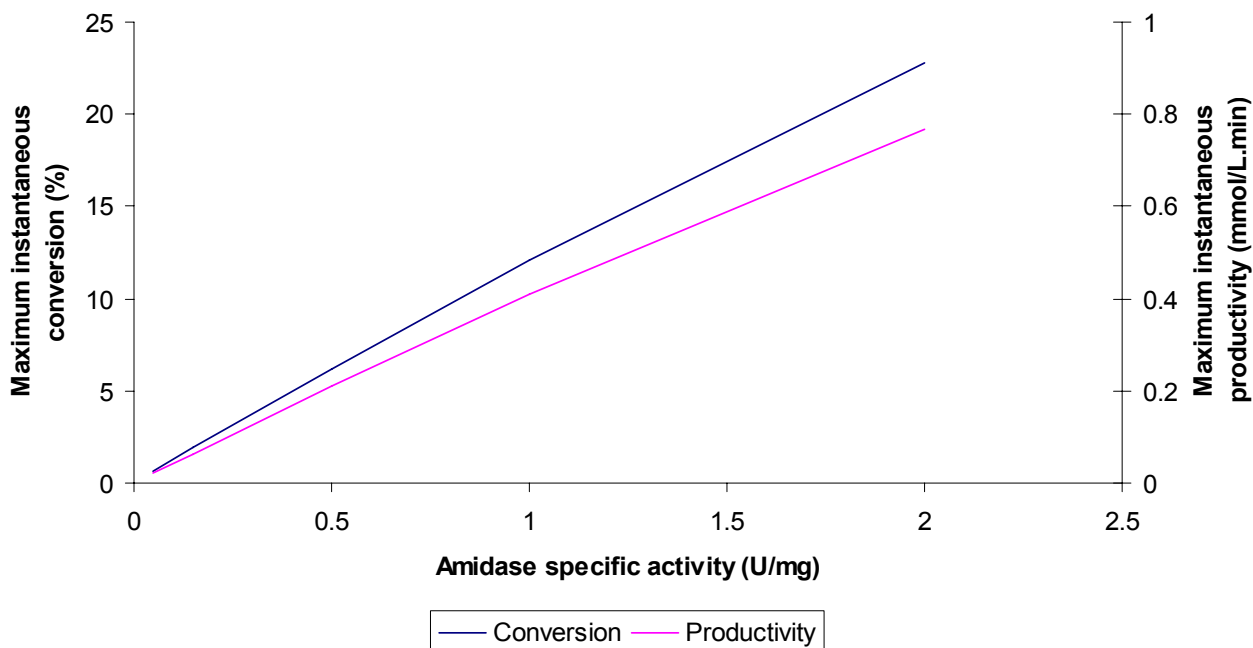
Figure 5.31: Effect of amidase activity in terms of U/mg on the maximum instantaneous conversion and maximum productivity (T=50ºC, pH=8.0, s0=80 mM, e0=6.38 mg, v_p=0.0005 L/min, t_h=7.3 h)

When considering the cumulative amount of lactic acid collected over time for different enzyme activities it can be seen that for immobilised amidase activity of 2 U/mg the maximum amount of product collected is predicted to be just over 6.5 milimoles after 3000 minutes (50 hours) of production time and no significant increase will be seen after that time since a plateau has been reached (Figure 5.32).
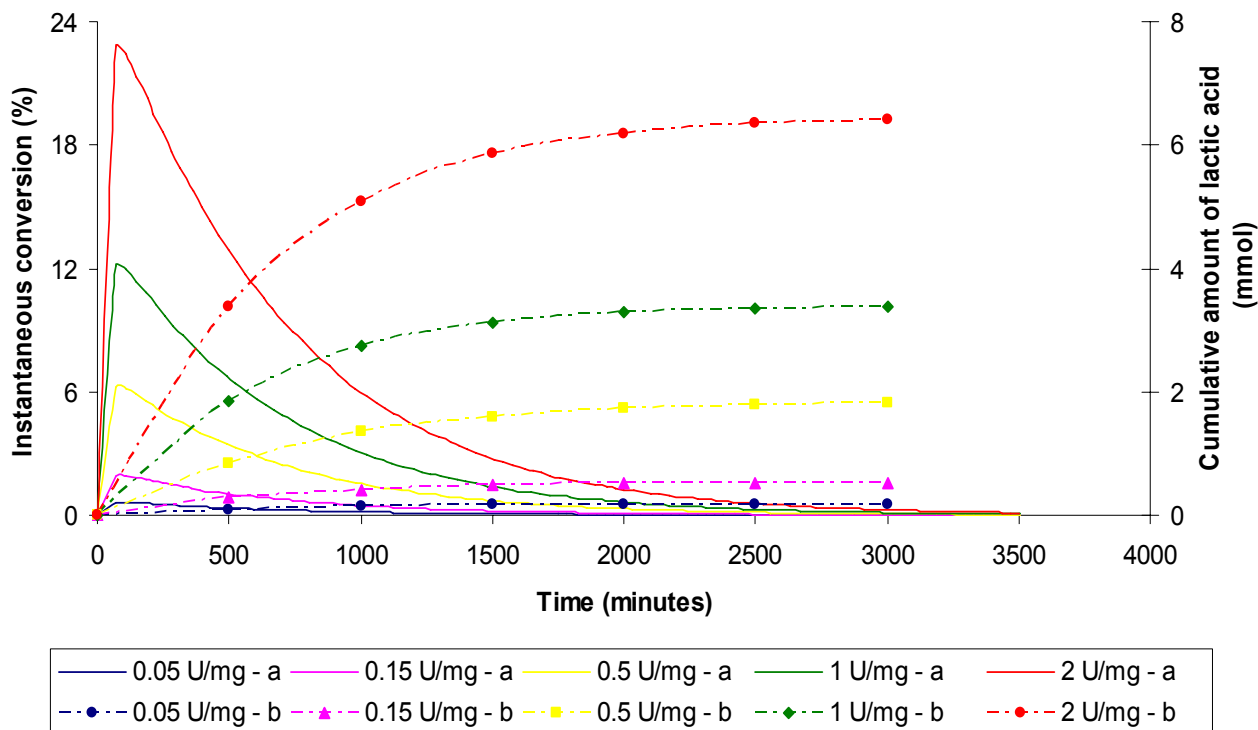
Figure 5.32: Effect of amidase specific activity on instantaneous conversion and cumulative amount of lactic acid produced (T=50ºC, pH=8.0, s0=80 mM, e0=6.38 mg, v_p=0.0005 L/min, t_h=7.3 h)

For amidase activities of 0.15 U/mg and below no significant increase in the amount of lactic acid collected can be seen after 1500 minutes (25 hours) whereas activities of more than 0.5 U/mg still showed a slight increase in amount of lactic acid collected after 2000 minutes (33.3 hours). The reaction time for which the maximum amount of product can be collected is therefore dependent on the activity of the amidase. For lower activities shorter reaction times are required than for higher activities.

The curves representing the cumulative amount of lactic acid can be seen to reach a plateau as the instantaneous conversion (Figure 5.32) and instantaneous productivity (Figure 5.33) decreases. The maximum amount of lactic acid that can be collected from the system therefore relies strongly on both the stability and the activity of the amidase.
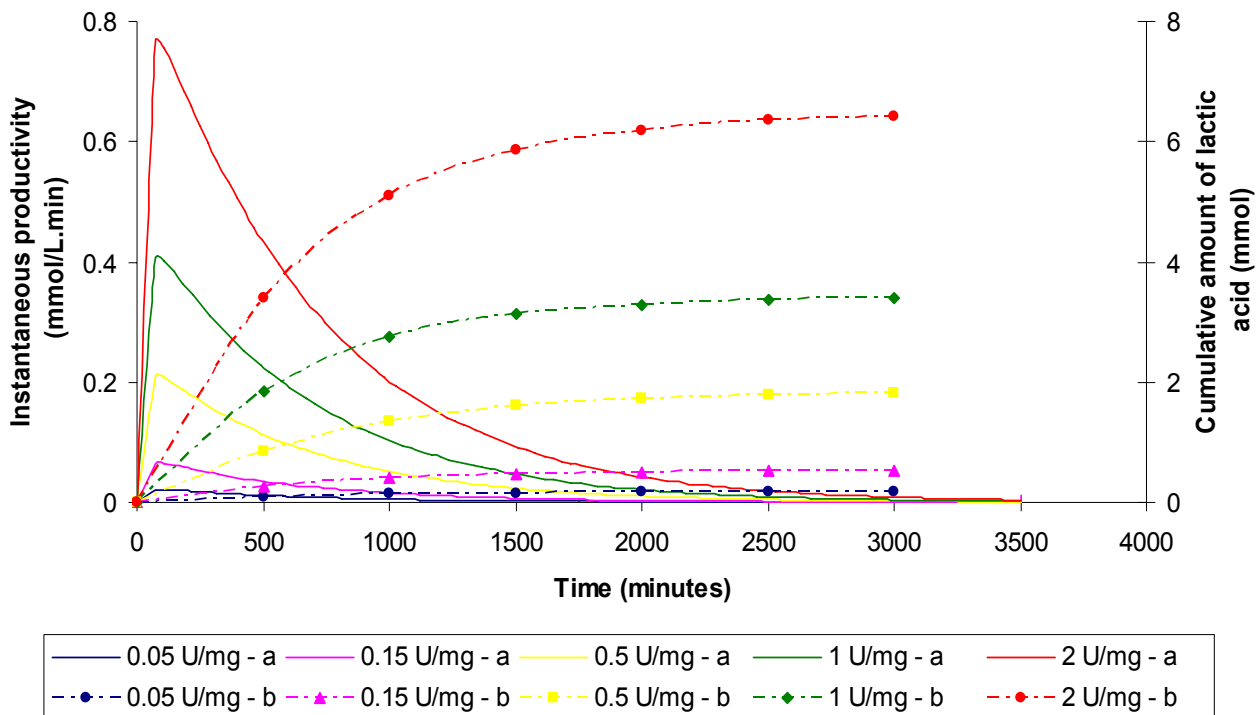
Figure 5.33: Effect of amidase specific activity on instantaneous productivity and cumulative amount of lactic acid produced (T=50ºC, pH=8.0, s0=80 mM, e0=6.38 mg, v_p=0.0005 L/min, t_h=7.3 h)

An increase in the amidase specific activity, however, has a greater effect on the maximum instantaneous conversion (Figure 5.34) and maximum instantaneous productivity (Figure 5.35) than an increase in the amidase stability would have. For instance, at a specific activity of 2 U/mg an increase in the half-life of the amidase from 1.8 hours to 115.5 hours only increases the maximum instantaneous conversion from approximately 17% to 25% and the maximum instantaneous productivity from approximately 0.6 to 0.85 mmol/L.min. On the other hand, at a half-life of 115.5 hours the maximum instantaneous conversion and productivity is increased from 1% to 25% and 1 to 0.85 mmol/L.min respectively for an increase in amidase specific activity from 0.05 U/mg to 2 U/mg.

Hence, an increase in the amidase specific activity (especially if combined with an increase in the amidase stability) is likely to have a significant effect on the process economics.
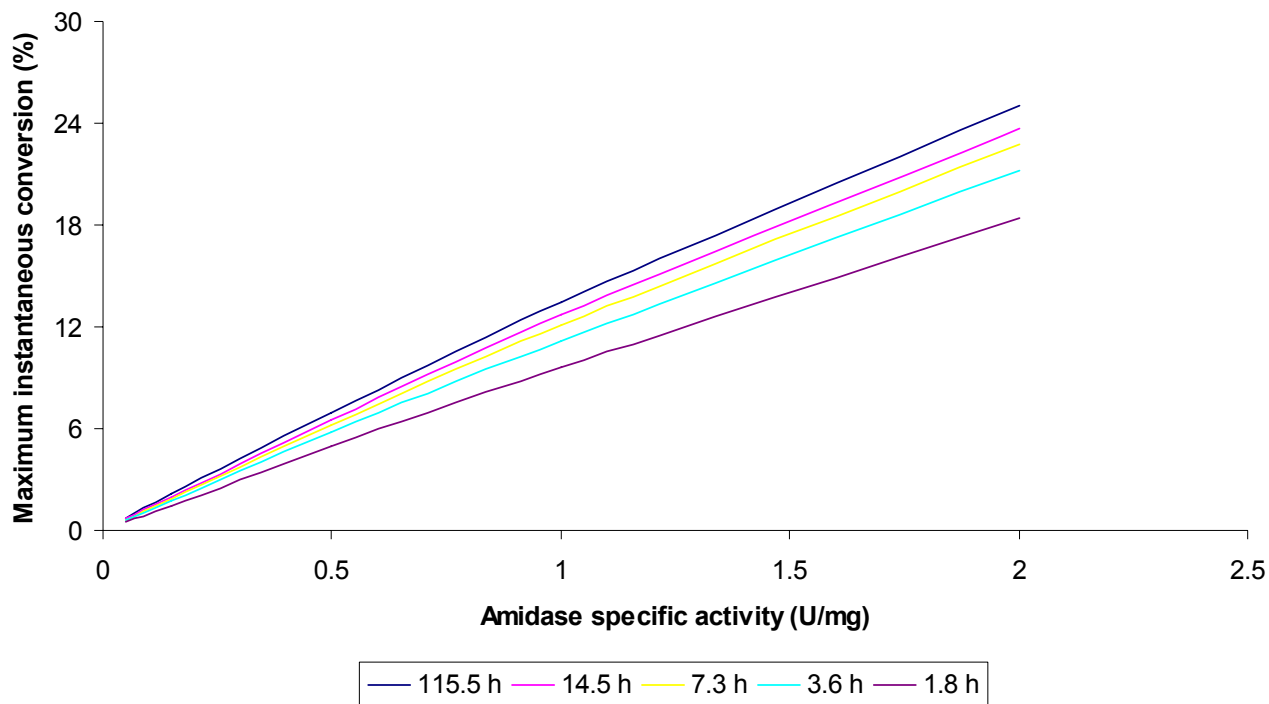
Figure 5.34: Comparison of significance of amidase stability and specific activity on maximum instantaneous conversion (T=50ºC, pH=8.0, s0=80 mM, e0=6.38 mg, v_p=0.0005 L/min)
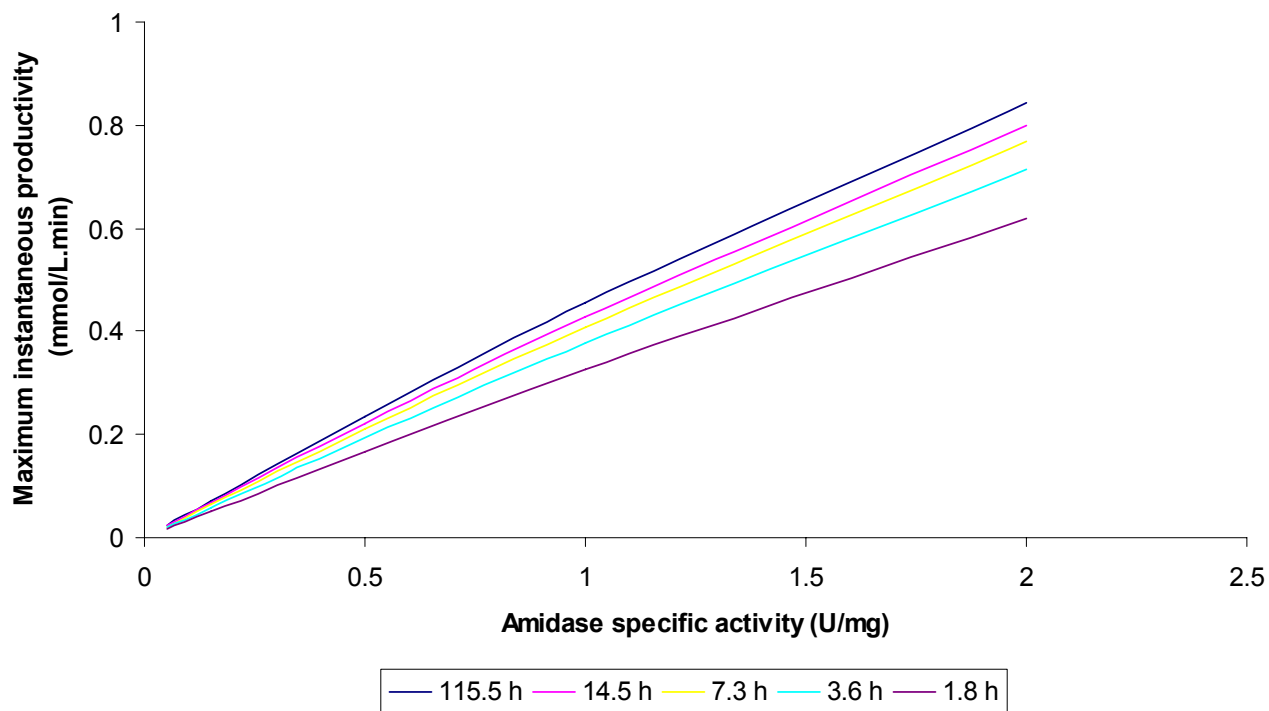
Figure 5.35: Comparison of significance of amidase stability and specific activity on maximum instantaneous productivity (T=50ºC, pH=8.0, s0=80 mM, e0=6.38 mg, v_p=0.0005 L/min)

A higher amidase specific activity may be obtained in a number of different ways. An unpurified amidase was used in these experiments. The specific activity of the purified amidase may be higher than that of the unpurified amidase. A compromise should, however, be made between the cost of purifying the amidase and the increase in activity that may be obtained. Further, the amidase exhibits a greater substrate specificity towards acrylamide, propionamide and acetamide than toward lactamide. The specific activity of the amidase was more than 8 times higher for acrylamide and acetamide and more than 6 times higher for propionamide [Makhongela, 2005]. The process may therefore be more economic if other substrates were used. A chelating agent (other than EDTA and DTT which proved to have no effect on the activity in Section 5.1.4) may also prove beneficial to the amidase activity.

5.3.3.3 Effect of permeate flux on conversion and productivity

The permeate flux has been found by various authors to have a significant impact on both the conversion and productivity of immobilised enzyme MBRs. Wenten and Widiasa [2002] immobilised a penicillin acylase in the pores of a microfiltration membrane for the hydrolisation of penicillin G. They found that increased permeate flux rates resulted in an exponential decrease in the conversion of penicillin G. Similar results were reported by Carvalho *et al.* [2000] for a recombinant cutinase immobilised in a membrane. A permeate flux of 0.025 mL/min resulted in a substrate conversion of 79.3% whereas for a permeate flux of 0.4 mL/min a substrate conversion of only 35.6% was achieved. The reactor productivity for the two separate permeate flux rates, however, increased from 41 $g_{product}$/day.$g_{cutinase}$ to 294 $g_{product}$/day.$g_{cutinase}$ respectively.

These results are predictable since the permeate flux is indirectly proportional to the residence time of substrate in the membrane. Low permeate fluxes therefore allow the substrate to remain in contact with the enzyme in the membrane for a longer time. Longer contact with the enzyme will result in higher conversions of the substrate but will also result in lower productivities since the product leaves the reactor at lower rates if the permeate flux is low. In industrial applications both conversion and productivity is important. A compromise will therefore have to be made between the conversion and the productivity and depending on the situation this compromise will not be the same for different industrial applications.

The range of permeate fluxes investigated in this research ranged from 0.00001 L/min to 0.005 L/min. The lowest permeate flux (0.00001 L/min), as expected, resulted in the highest instantaneous conversion which was almost 28% (Figure 5.36). As the permeate

flux was increased, the conversion decreased to almost zero for a permeate flux of 0.005 L/min.
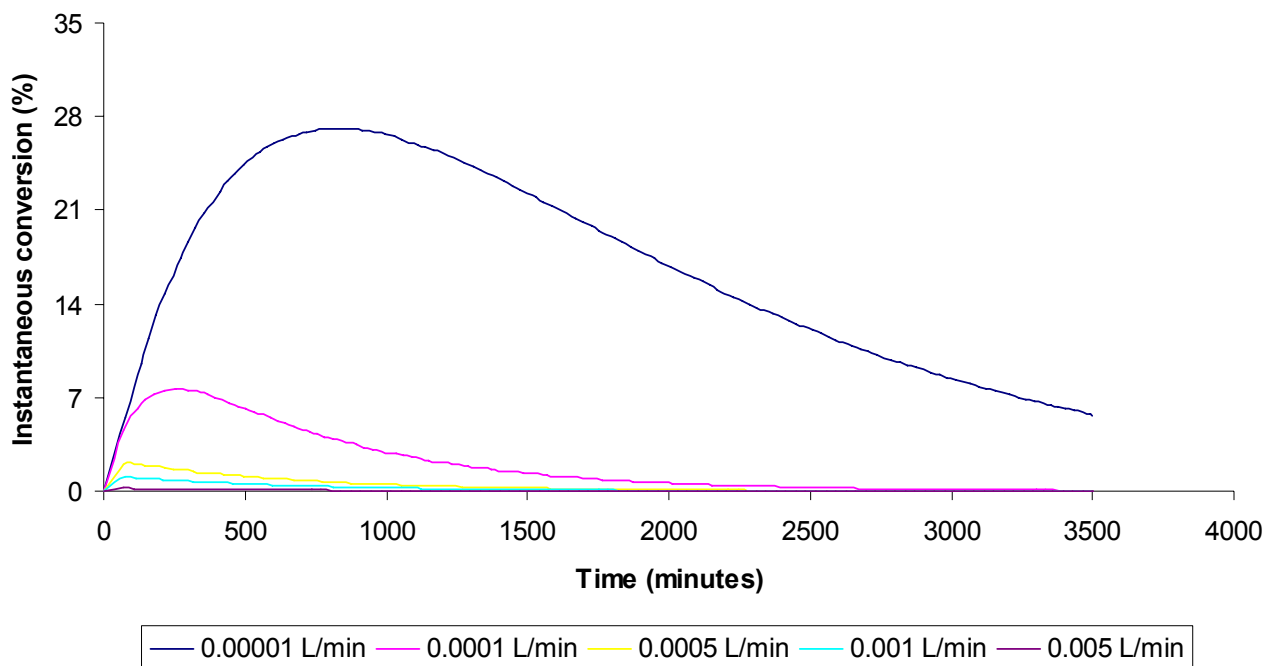
Figure 5.36: Effect of permeate flux on the instantaneous conversion (T=50ºC, pH=8.0, s0=80 mM, e0=6.38 mg, $a0_{imm}$=0.15 U/mg, t_h=7.3 h)

The instantaneous productivity showed the opposite – as the permeate flux was increased, the productivity also increased (Figure 5.37). For a permeate flux of 0.00001 L/min, where the highest instantaneous conversion was achieved, the productivity was the lowest (approximately 0.02 mmol/L.min) and for a permeate flux of 0.005 L/min (where the instantaneous conversion was almost zero) the highest instantaneous productivity was achieved (approximately 0.07 mmol/L.min).
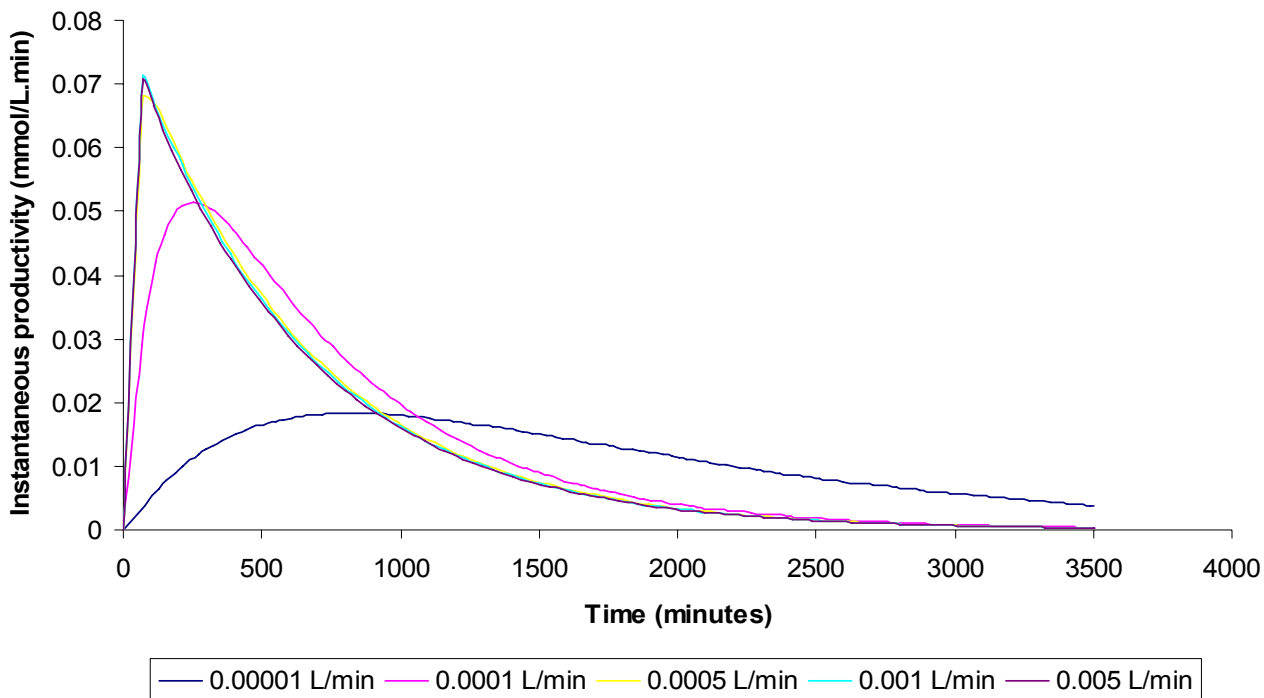
Figure 5.37: Effect of permeate flux on the productivity (T=50ºC, pH=8.0, s0=80 mM, e0=6.38 mg, a0$_{imm}$=0.15 U/mg, t$_h$=7.3 h)

As the permeate flux was decreased the difference between the maximum instantaneous conversions became less pronounced (Figure 5.36) whereas the difference between the maximum instantaneous productivities became less pronounced with an increase in the permeate flux (Figure 5.37). This indicated possible exponential trends for both the maximum instantaneous conversion and productivity. By plotting the maximum instantaneous conversions and productivities as a function of the permeate flux, two opposite exponential trends could be seen (Figure 5.38). The reason for these types of curves can be understood when remembering that the permeate flux is indirectly proportional to the residence time of substrate in the membrane. An increase in the permeate flux from 0.00001 L/min to 0.0001 L/min will result in a sharp decrease in the maximum instantaneous conversion since the residence time of the substrate has been decreased from 1186 minutes to 118.6 minutes. Another significant decrease in the maximum instantaneous conversion is seen when the permeate flux is increased from 0.0001 L/min to 0.001 L/min since the residence time has been decreased from 118.6 minutes to 11.9 minutes. For an increase in the permeate flux above 0.001 L/min no significant decrease in the maximum instantaneous conversion is seen since the residence times are all so low that the substrate essentially just passes through the membrane (without 'residing' in the membrane to be converted). Some substrate molecules are still converted since they come into contact with enzyme molecules when passing through the

membrane. The effect of the rate at which the substrate passes through (the permeate flux) is not significant anymore because the only factor playing a role in how much substrate is converted is whether the substrate encounters an enzyme molecule as it passes through the membrane.
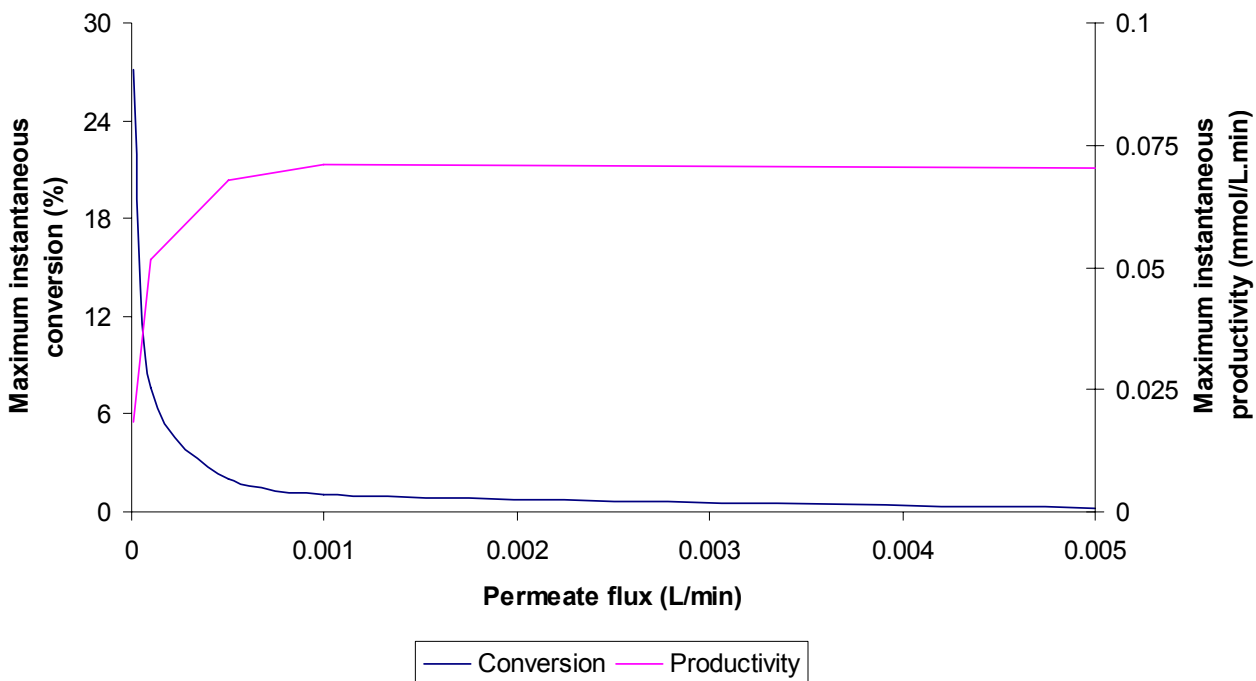
Figure 5.38: Effect of permeate flux on the maximum instantaneous conversion and maximum productivity (T=50ºC, pH=8.0, s0=80 mM, e0=6.38 mg, a0$_{imm}$=0.15 U/mg, t$_h$=7.3 h)

The maximum instantaneous productivity, on the other hand, shows a sharp increase when the permeate flux is increases initially from 0.00001 L/min to 0.0001 L/min. Since the residence time has been decreased significantly (as mentioned above) the product removal from the membrane is much faster. Increasing the permeate flux above 0.001 L/min can be seen to have no significant effect on the maximum instantaneous productivity since there is no significant change in the amount of product formed.

When considering the effect of a variation in permeate flux on the cumulative amount of lactic acid produced, the explanation above may be expressed more clearly. For permeate fluxes below 0.001 L/min an increase in the permeate flux results in a increase in the cumulative amount of lactic acid produced (Figure 5.39). For example, when the permeate flux is increased from 0.00001 L/min to 0.0001 L/min the cumulative amount of lactic acid collected is increased from approximately 0.45 mmol to 0.55 mmol. However, for permeate fluxes higher than 0.001 L/min no increase in the amount of lactic acid collected can be seen. Also note that although the instantaneous conversion is its highest for a permeate

flux of 0.00001 L/min (approximately 28%); the cumulative amount of lactic acid collected is the lowest (0.45 mmol).
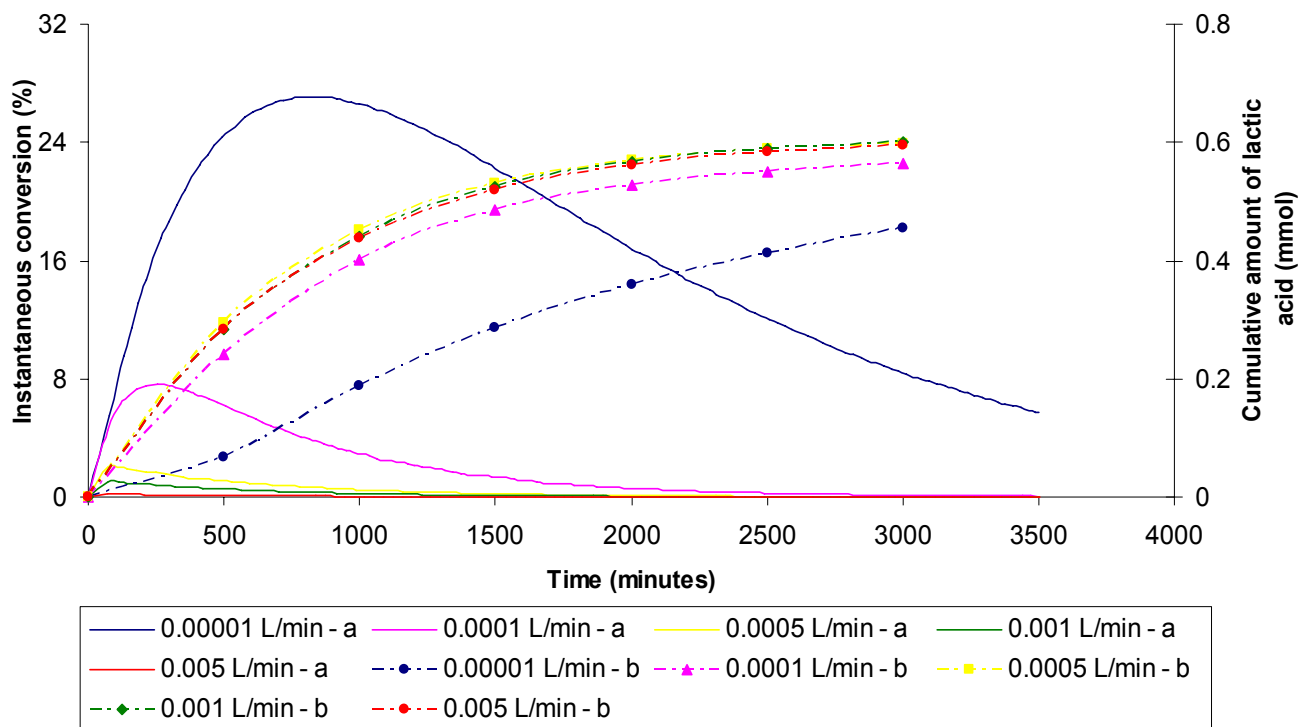
Figure 5.39: Effect of permeate flux on instantaneous conversion and cumulative amount of lactic acid produced (T=50ºC, pH=8.0, s0=80 mM, e0=6.38 mg, a0$_{imm}$=0.15 U/mg, t$_h$=7.3 h)

An increase in the instantaneous productivity coincides with an increase in the cumulative amount of lactic acid collected from the reactor. As can be seen in Figure 5.40, this increase only occurs if the permeate flux is lower than 0.001 L/min. For an increase in the permeate flux above 0.001 L/min no increase is seen in the cumulative amount of lactic acid collected. Also note that for permeate fluxes above 0.0005 L/min the reaction time required to collect the maximum amount of lactic acid from the system is the same whereas below 0.0005 L/min the reaction times will be different depending on the permeate flux. The model can therefore be used to determine what reaction time would be the most efficient for a specific permeate flux.
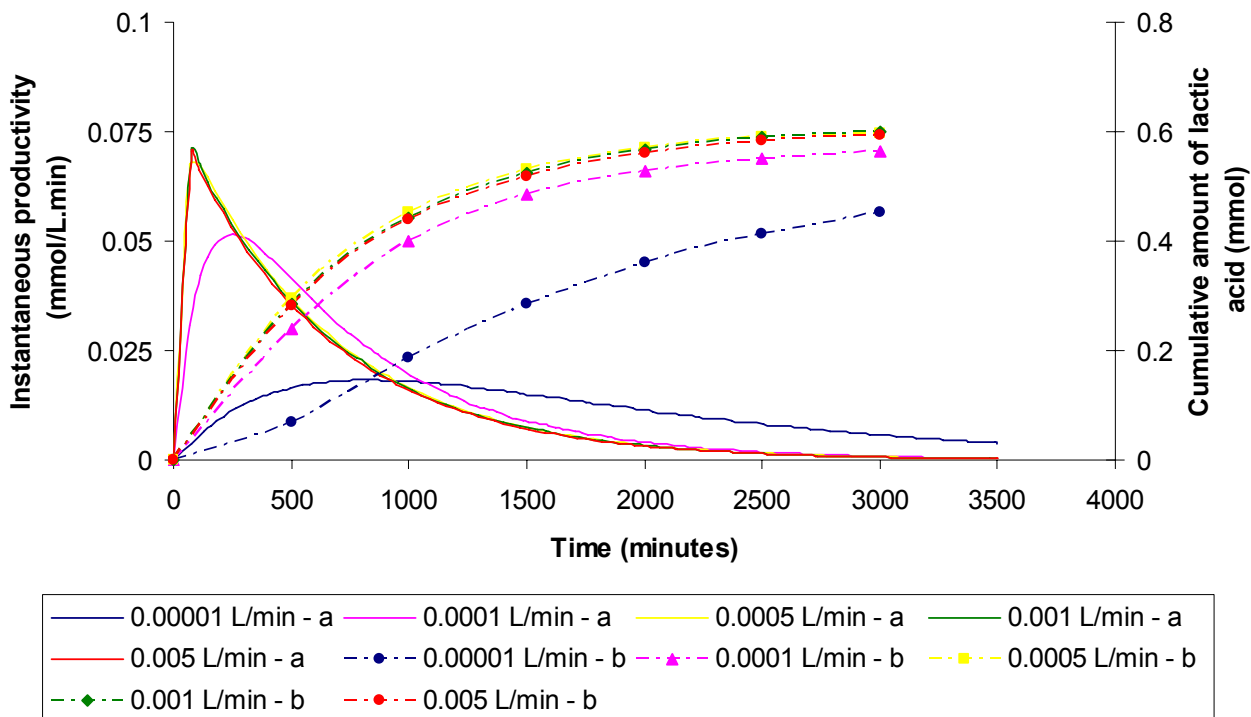
Figure 5.40: Effect of permeate flux on instantaneous productivity and cumulative amount of lactic acid produced (T=50ºC, pH=8.0, s0=80 mM, e0=6.38 mg, a0$_{imm}$=0.15 U/mg, t$_h$=7.3 h)

For this system a permeate flux above 0.001 L/min is not recommended since no significant effect can be seen on either the instantaneous conversion or productivity for permeate fluxes of more than 0.001 L/min and further, higher permeate fluxes may result in enzyme denaturation, as has been found by Belhocine *et al.* [2000] in their study on the enzymatic hydrolysis of haemoglobin immobilised in a MBR.

The critical membrane flux of 88 L/h.m^2 (at a transmembrane pressure of 2.2 bar) corresponded to a permeate flux of approximately 0.0055 L/min. If the reactor were to be operated at or above this permeate flux, permanent membrane fouling may also become a significant problem. For permeate fluxes below 0.001 L/min a play-off will have to be made between the instantaneous conversion and productivity. In order to achieve high conversions, the permeate flux should be very low. As mentioned before, a maximum instantaneous conversion of 28% can be achieved if the permeate flux is 0.00001 L/min. If, however, productivity is more important the permeate flux should be closer to 0.001 L/min. A maximum instantaneous productivity of approximately 0.07 mmol/L.min can be achieved. This will be at the cost of a high conversion since the conversion will only be approximately 2%.

5.3.3.4 Effect of amount of immobilised enzyme protein on conversion and productivity

Evidence in the literature suggests that enzymes are more active in dilute solutions and when immobilised that this characteristic becomes even more pronounced. This is so because when too much enzyme protein is immobilised in a support the enzyme is no longer distributed in a monolayer but instead may form a gel layer on the support. The mass transfer resistance of the support therefore becomes significantly higher. An increase in the mass transfer resistance will result in poor transfer of substrate to and product away from the reaction sites and many reaction sites may not even be reached by substrate. A decrease in the conversion and productivity of the reactor will then be observed [Giorno *et al.*, 2001; Long *et al.*, 2005].

Giorno *et al.* [2001] studied the effect of the immobilised enzyme concentration on the conversion achieved in a MBR with fumarase immobilised in the pores. An increase in the amount of immobilised fumarase resulted in an increase in the conversion until an optimum conversion was reached at an immobilised fumarase concentration of 1.2 mg/cm^3 of membrane. Up until this point, although mass transfer resistance increased with and increase in the amount of immobilised amidase, the reaction rate remained the limiting factor. For fumarase concentrations of more than 1.2 mg/cm^3 a decrease in conversion could be seen due to mass transfer resistance (caused by a gel layer of fumarase that formed on the membrane) became the limiting factor.

It is therefore important to determine the effect of the amount of immobilised enzyme protein on the conversion and productivity of a reactor in order to determine if and at what amount of enzyme an optimum reactor performance can be achieved.

Considering the predicted instantaneous conversion achieved as a function of the amount of immobilised enzyme protein, the characteristic peak can be seen with a decrease in the instantaneous conversion shortly after. Also not that as the amount of enzyme protein is increased the instantaneous conversion is also increased (Figure 5.41).

More enzyme protein in the reactor will be able to convert more product thereby resulting in an increase in the instantaneous conversion achieved. The model predicts that for a 100 mg of immobilised enzyme protein, a maximum instantaneous conversion of approximately 28% can be achieved.

The same trends can be seen when studying the effect of the amount of immobilised enzyme protein on the instantaneous productivity (Figure 5.42) since more enzyme protein will be able to convert more product in a shorter period of time.
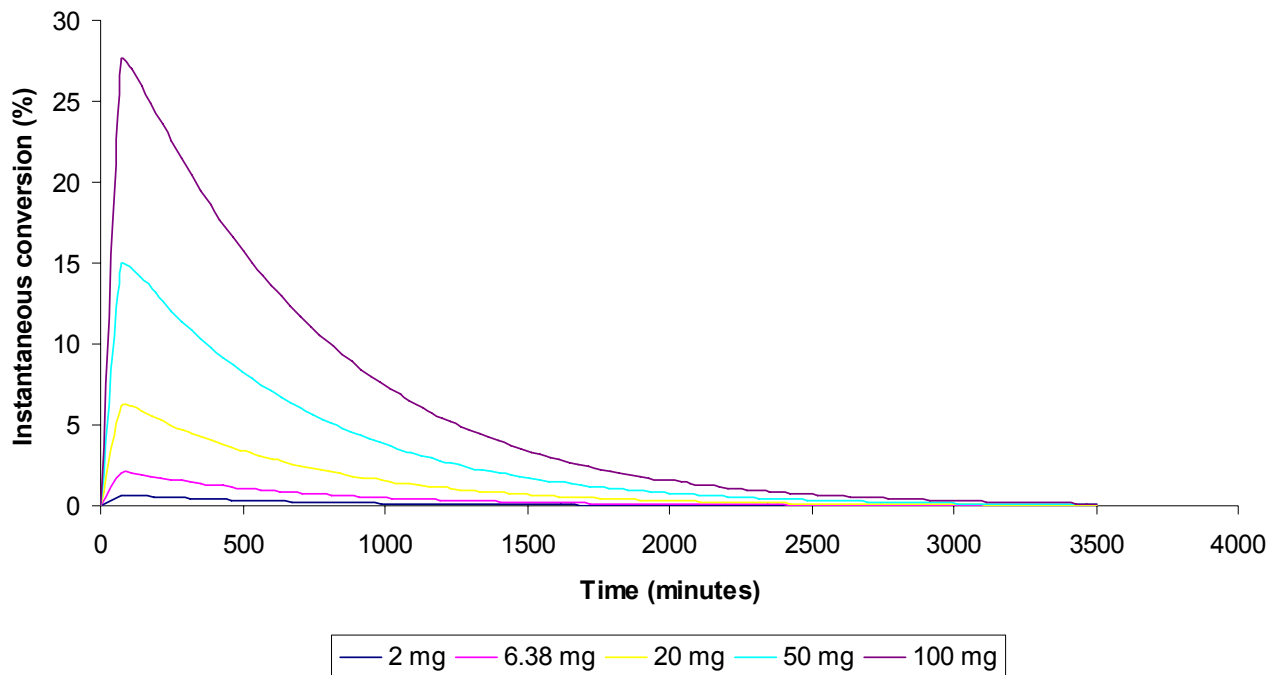
Figure 5.41: Effect of initial enzyme concentration on the instantaneous conversion (T=50ºC, pH=8.0, s0=80 mM, v_p=0.0005 L/min, $a0_{imm}$=0.15 U/mg, t_h=7.3 h)
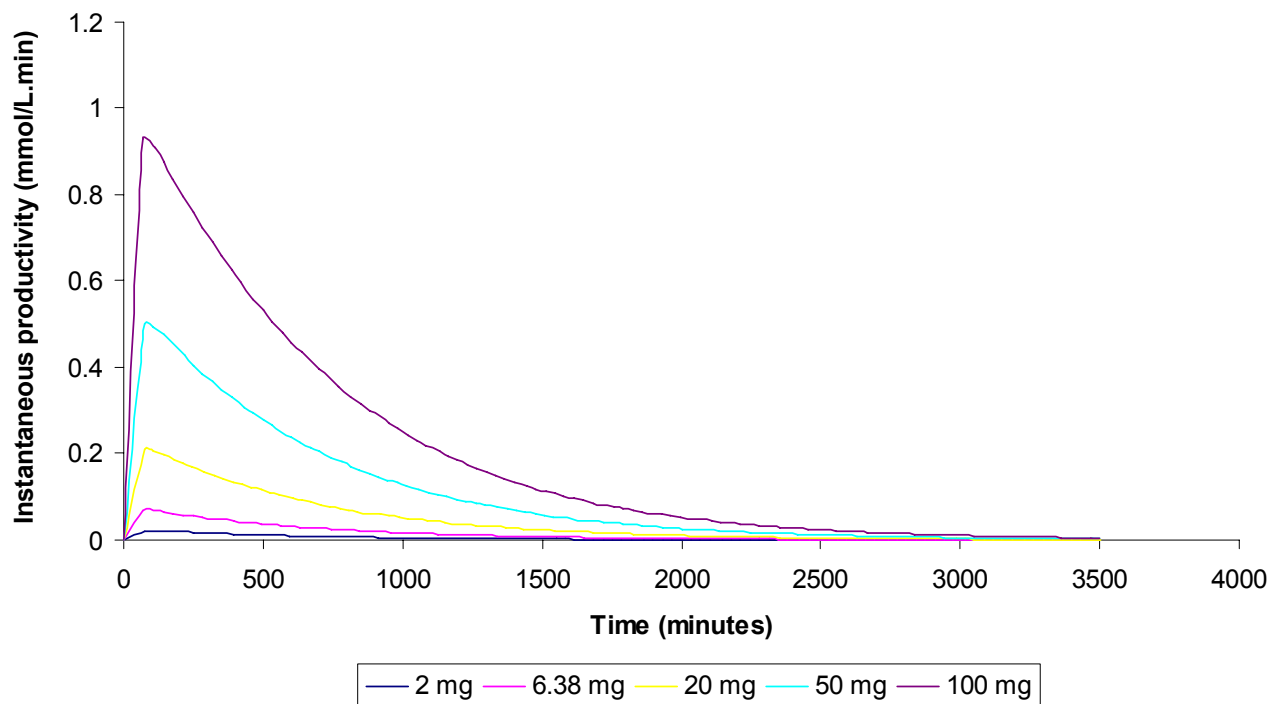
Figure 5.42: Effect of initial enzyme concentration on the productivity (T=50ºC, pH=8.0, s0=80 mM, v_p=0.0005 L/min, $a0_{imm}$=0.15 U/mg, t_h=7.3 h)

104

According to the model a 100 mg of immobilised enzyme protein will result in a maximum instantaneous productivity of approximately 0.95 mmol/L.min. When comparing the effect of the amount of immobilised enzyme protein on the instantaneous productivity with the effects of amidase stability (Figure 5.25), activity (Figure 5.30) and permeate flux (Figure 5.37) on the instantaneous productivity it can be seen that the effect of the amount of immobilised enzyme protein is the most significant. The maximum instantaneous productivities achieved for changes in the amidase stability, activity and the permeate flux were only 0.08, 0.8 and 0.07 mmol/L.min respectively. The instantaneous productivities that can be achieved by increasing the amount of immobilised enzyme protein is considerably higher than that achieved by changing the amidase activity, stability or permeate flux.

As mentioned, an initial increase in the conversion and productivity of a reactor is expected for an increase in the amount of immobilised enzyme protein. An optimum enzyme protein concentration is expected to be reached whereafter a decrease in the reactor performance is anticipated. According to the predicted results, however, an indefinite linear increase in the maximum instantaneous conversion and productivity occurs with an increase in the amount of immobilised enzyme protein (Figure 5.43).
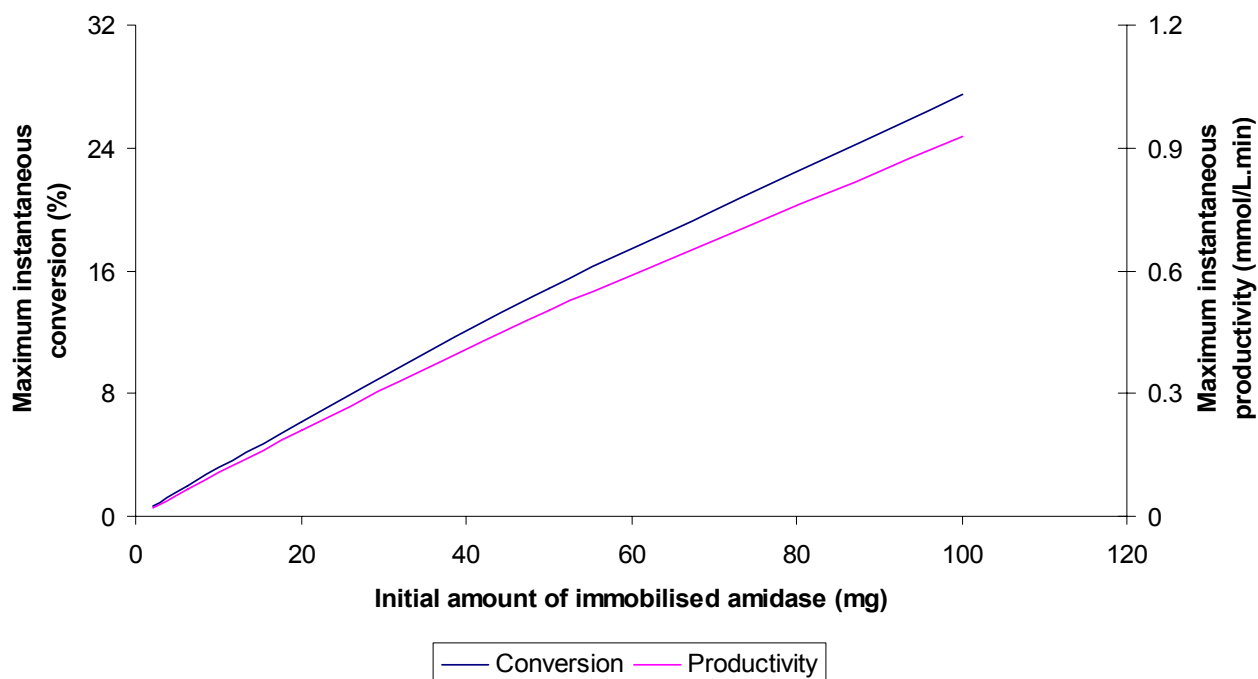
Figure 5.43: Effect of initial enzyme concentration on the maximum instantaneous conversion and maximum productivity (T=50°C, pH=8.0, s0=80 mM, v_p=0.0005 L/min, a0$_{imm}$=0.15 U/mg, t_h=7.3 h)

This behaviour of the model is due to a significant limitation in the model. The reaction rate observed experimentally for a specific amount of enzyme protein immobilised was used in the model but no the mass transfer resistance (as a function of the amount of immobilised amidase) was not accounted for. According to Bhatia *et al.* [2004] and Long *et al.* [2005] the effective diffusion coefficient of the substrate and product through the membrane should be determined experimentally for different amounts of immobilised enzyme protein. The effective diffusion coefficient can then be used to develop an empirical correlation between the amount of enzyme protein immobilised and the Thiele modulus for the system (Equation 2.10). Despite the limitations of the model, the predictions nevertheless highlight the importance of optimising the amount of enzyme protein immobilised.

If a small amount of enzyme protein is immobilised the instantaneous conversion and productivity is low and therefore the cumulative amount of lactic acid collected from the system is low (Figure 5.44 and Figure 5.45).
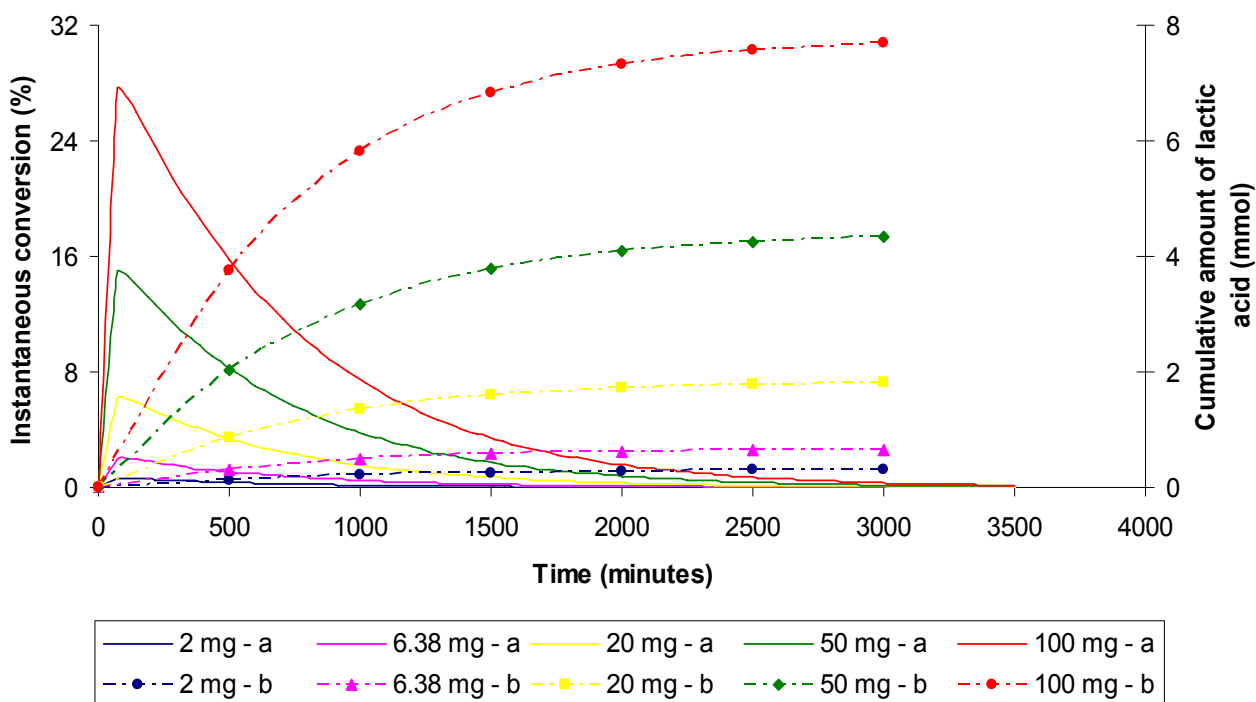
Figure 5.44: Effect of initial enzyme concentration on the instantaneous conversion and cumulative amount of lactic acid produced (T=50ºC, pH=8.0, s0=80 mM, v_p=0.0005 L/min, $a0_{imm}$=0.15 U/mg, t_h=7.3 h)

For example, at an amount of 6.38 mg immobilised enzyme protein (identical to that used in Experiment 2) the maximum amount of lactic acid collected from the system is approximately 0.7 millimoles. This maximum is attained after just 1500 minutes (25 hours) whereafter no more product was collected. For an amount of 100 mg of immobilised

enzyme protein the instantaneous conversion and productivity is 28% and 0.95 mmol/L.min respectively (which is considerably higher than the 3% and 0.08 mmol/L.min achieved with 6.38 of immobilised enzyme protein) and almost 8 millimoles of lactic acid is collected after 3000 minutes (50 hours). This amount is still increasing slowly over time. The model can therefore be used to predict what reaction time is required to collect the optimum amount of lactic acid for a specific amount of amidase immobilised.
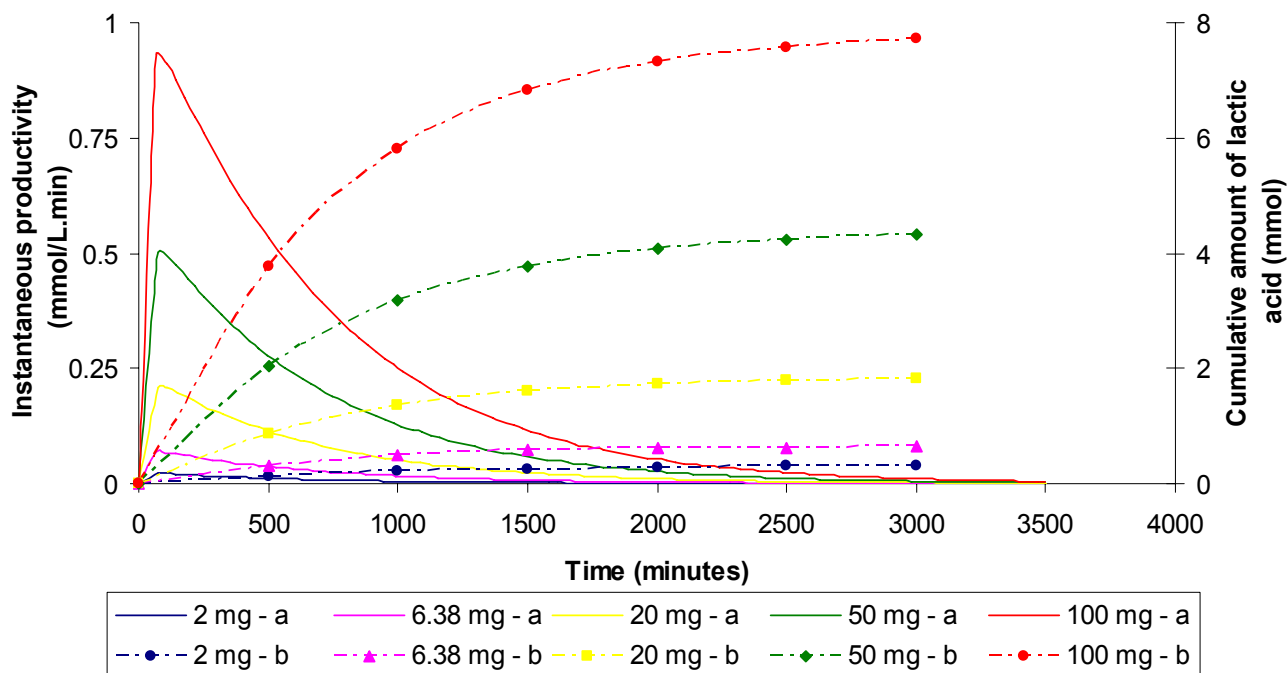
Figure 5.45: Effect of initial enzyme concentration on instantaneous productivity and cumulative amount of lactic acid produced (T=50ºC, pH=8.0, s0=80 mM, v_p=0.0005 L/min, $a0_{imm}$=0.15 U/mg, t_h=7.3 h)

As much enzyme protein as possible, without allowing diffusional limitations to become controlling, should therefore be immobilised in order to optimise the instantaneous conversion and productivity and, as a result, the cumulative amount of lactic acid collected. Since one membrane can only accommodate a specific amount of enzyme before diffusional limitations become controlling, the use of a few membranes in the reactor should be considered. If more membranes are used the total amount of immobilised enzyme protein can be increased without increasing the mass transfer limitations.

5.3.3.5 *Effect of initial substrate concentration on conversion and productivity*

As with free enzymes, the kinetics of immobilised enzymes is also a function of the substrate concentration. The kinetics of an immobilised enzyme may, however, differ

107

substantially from that of the free enzyme since it may be affected, amongst others, by the properties of the immobilisation support, conformational changes in the enzyme structure during immobilisation and mass transfer limitations. The apparent kinetic constants of the immobilised enzyme (determined with initial rate studies) may also differ from the kinetic constants determined for the free enzyme due to mass transfer limitations. The intrinsic kinetic constants of the immobilised enzyme may again be different from the apparent kinetic constants due to differences between the bulk solution properties and the properties of the solution in the immediate vicinity of the enzyme [http://www.lsbu.co.uk/biology/ enztech]. Immobilised enzyme kinetics is not always different from the free enzyme kinetics. Giorno *et al.* [2001] physically immobilised fumarase in the pores of a capillary membrane using the same immobilisation method employed in this research. Under kinetically controlled reaction conditions the kinetic parameters of the immobilised fumarase was found to be the same as that of the free fumarase.

The free amidase used in this research was found to exhibit Michaelis-Menten kinetics (refer to Section 5.1.3.2). Although the apparent kinetics of the immobilised amidase was different from that of the free amidase (the reaction rate of the free and immobilised amidase was shown to differ substantially by the effectiveness factor calculations in Section 5.2.3) the intrinsic kinetics of the immobilised amidase was assumed to be the same as the kinetics of the free amidase. By making this assumption two other assumptions were made indirectly, namely the substrate concentration in the bulk solution and that in the microenvironment around the immobilised amidase is essentially the same and no significant internal conformational changes occurred in the amidase during immobilisation. Since the model fitted the experimental data relatively well (Section 5.3.2) these assumptions appear to be validated. A reaction controlled environment should, however, be created in order to test these assumptions. As mentioned in Section 5.3.3.4, this can be achieved by using a few smaller membranes instead of one large membrane.

The maximum instantaneous conversion was seen to increase with a decrease in the initial substrate concentration (Figure 5.46). This tendency can be explained by referring to the definition of the instantaneous conversion. Instantaneous conversion is defined as the ratio between the concentration of lactic acid in the permeate stream and the initial substrate concentration. An increase in the substrate concentration will lead to an increase in the rate of reaction (Section 2.2.3) consequently resulting in an increase in the lactic acid concentration in the permeate stream. The instantaneous conversion, however, will decrease since the increase in the lactic acid concentration is not large enough to offset the significant increase in the initial substrate concentration.
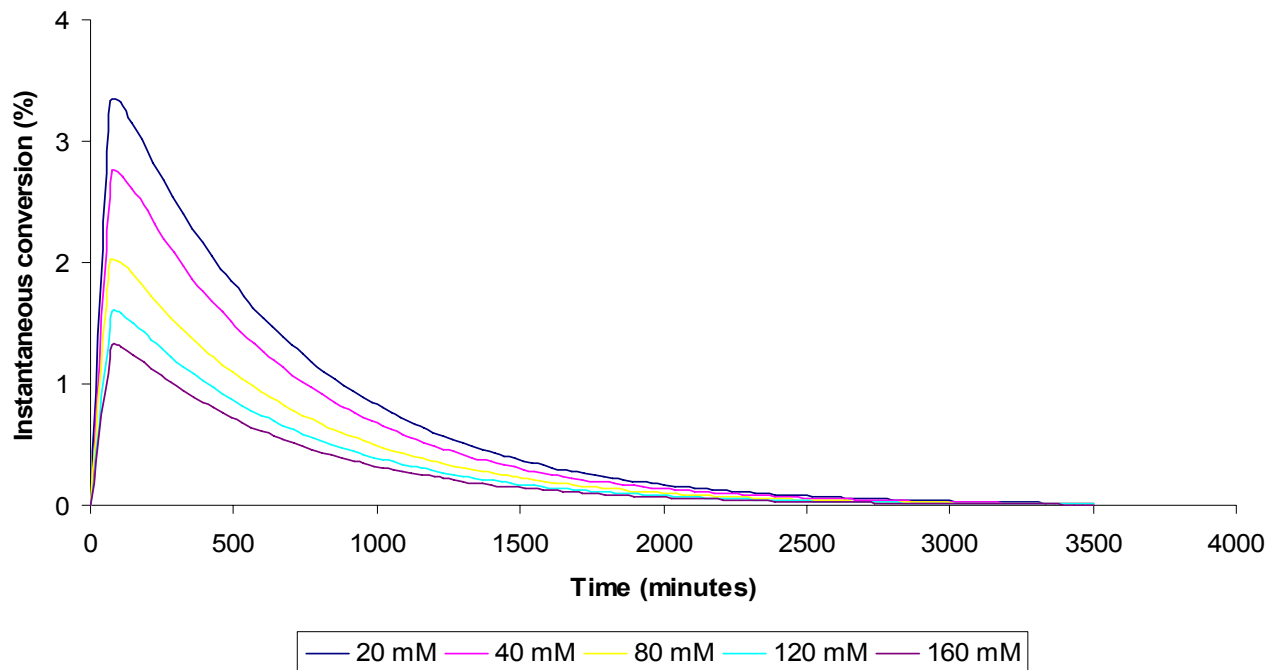
Figure 5.46: Effect of initial substrate concentration on the instantaneous conversion (T=50ºC, pH=8.0, e0=6.38 mg, v_p=0.0005 L/min, $a0_{imm}$=0.15 U/mg, t_h=7.3 h)

The instantaneous productivity, on the other hand, will increase with an increase in the substrate concentration since a higher reaction rate will result in more product being produced faster (Figure 5.47).

For a substrate concentration of 20 mM a maximum instantaneous conversion (Figure 5.46) and maximum instantaneous productivity (Figure 5.47) of approximately 3.3% and 0.028 mmol/L.min is achieved respectively. A substrate concentration of 160 mM can be seen to lead to a maximum instantaneous conversion and productivity of 1.3% and 0.09 mmol/L.min respectively. Once again, as was seen with the permeate flux in Section 5.3.3.3; a compromise would therefore have to be reached between the instantaneous conversion and productivity.
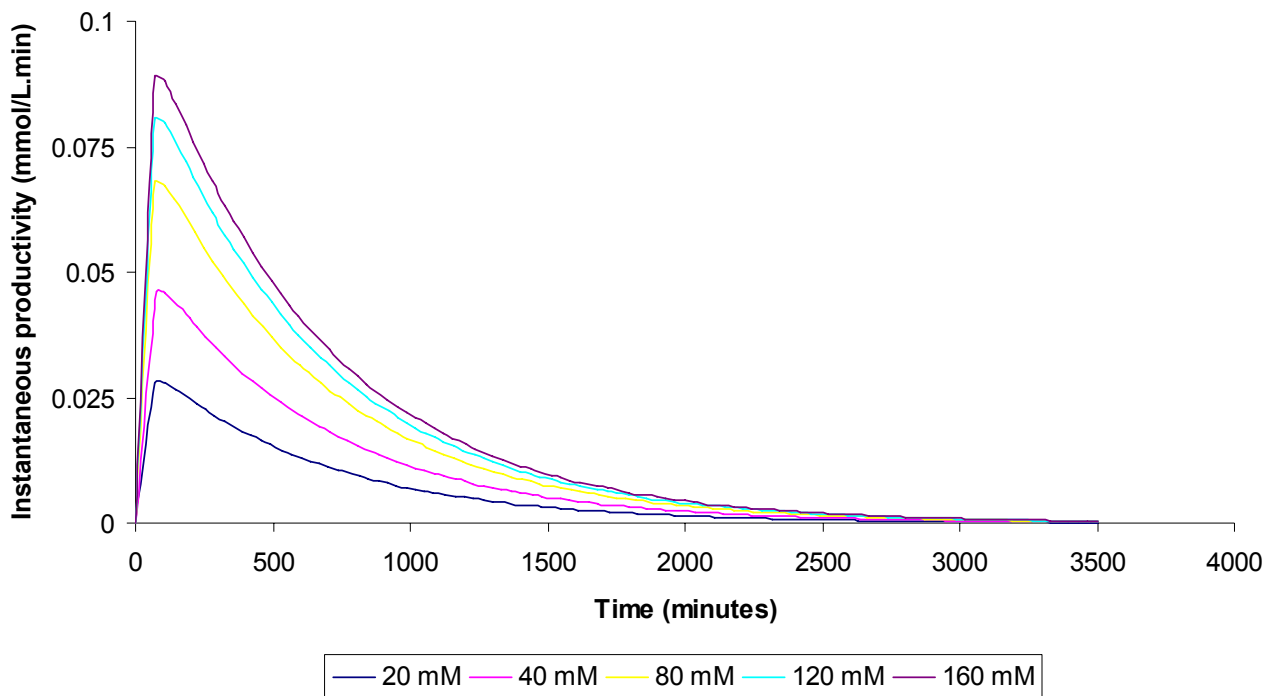
Figure 5.47: Effect of initial substrate concentration on the productivity (T=50ºC, pH=8.0, e0=6.38 mg, v$_p$=0.0005 L/min, a0$_{imm}$=0.15 U/mg, t$_h$=7.3 h)

By plotting the maximum instantaneous conversions and productivities achieved at different substrate concentrations together, the range of possible substrate concentrations that would be the most efficient (in terms of instantaneous conversion and productivity) may be determined. The plot shows the decrease in the maximum instantaneous conversion that occurs with an increase in the substrate concentration (Figure 5.48). Also note that the curve tends to a plateau at higher substrate concentrations.

This tendency is in accordance with Michaelis-Menten kinetics (Section 2.2.3). At higher substrate concentrations a further increase in the substrate concentration will not result in a significant increase in the reaction rate (and therefore in the concentration of product in the permeate stream) since the active sites of the enzyme molecules are already saturated. The increase in the maximum instantaneous productivity between different substrate concentrations also becomes less significant at high substrate concentrations due to the smaller increase in the rate of reaction. When comparing the two trend lines the range of substrate concentrations for which the reactor performance would be the most efficient seem to be between approximately 50 mM and 70 mM. For substrate concentrations below and above this range the difference between the maximum instantaneous conversion and productivity becomes significant. If conversion is more important than productivity lower

substrate concentrations should be used whereas higher substrate concentrations should be used if the productivity is the important factor.
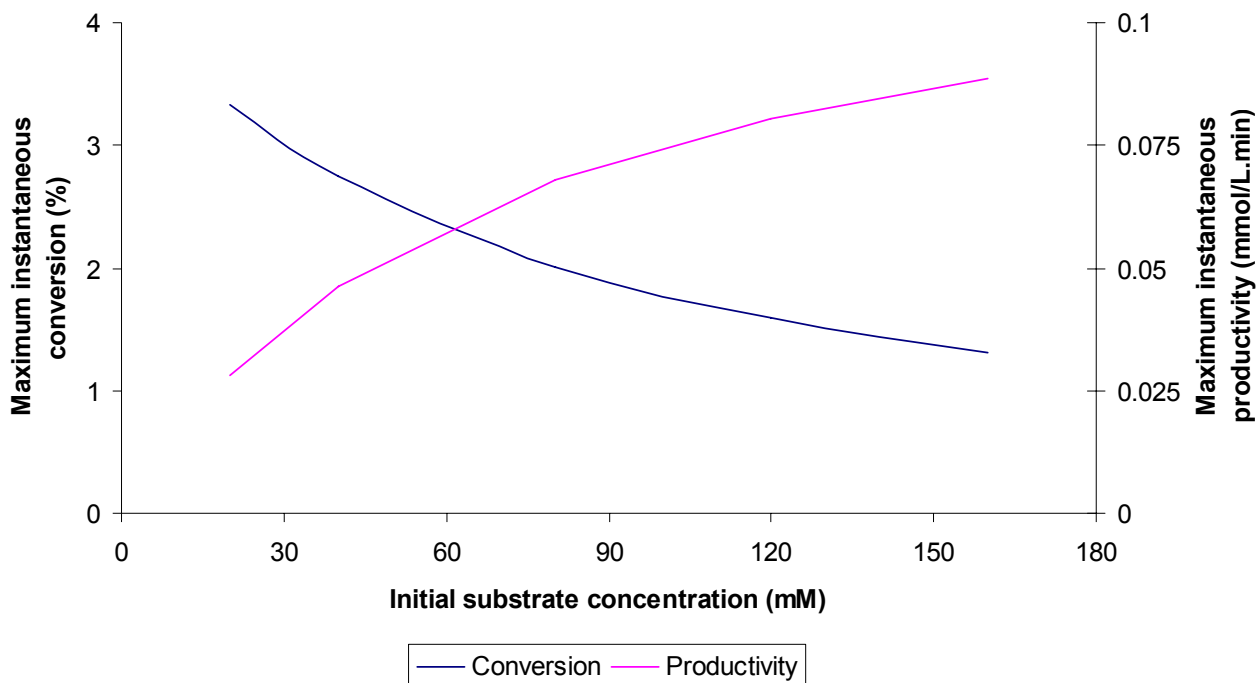
Figure 5.48: Effect of initial substrate concentration on the maximum instantaneous conversion and maximum productivity (T=50ºC, pH=8.0, e0=6.38 mg, v_p=0.0005 L/min, $a0_{imm}$=0.15 U/mg, t_h=7.3 h)

The cumulative amount of lactic acid collected from the reactor can be seen to increase with an increase in the substrate concentration due to the faster reaction rates achieved at higher substrate concentrations (refer to Figures Figure 5.49 and Figure 5.50).

For a substrate concentration of 20 mM (with maximum instantaneous conversion and productivity of 3.3% and 0.028 mmol/L.min respectively) the maximum amount of lactic acid collected from the reactor is approximately 0.25 mmol after 2500 minutes (42 hours). For a substrate concentration of 160 mM, on the other hand, the maximum amount of lactic acid collected (with maximum instantaneous conversion and productivity of 1.3% and 0.09 mmol/L.min respectively) is approximately 0.8 mmol and is achieved after 3000 minutes (50 hours). Depending on the substrate concentration fed to the reactor, the operation time required for the maximum amount of lactic acid collected can therefore be determined.
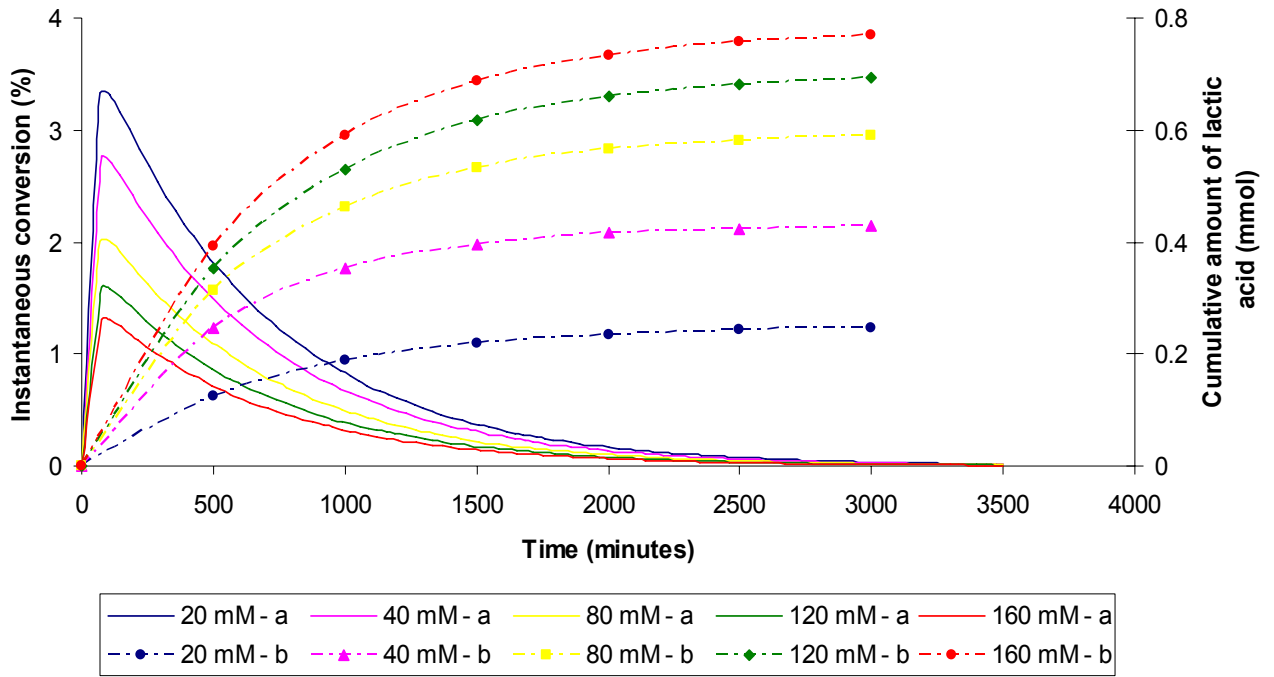
Figure 5.49: Effect of initial substrate concentration on instantaneous conversion and cumulative amount of lactic acid produced (T=50ºC, pH=8.0, e0=6.38 mg, v_p=0.0005 L/min, $a0_{imm}$=0.15 U/mg, t_h=7.3 h)
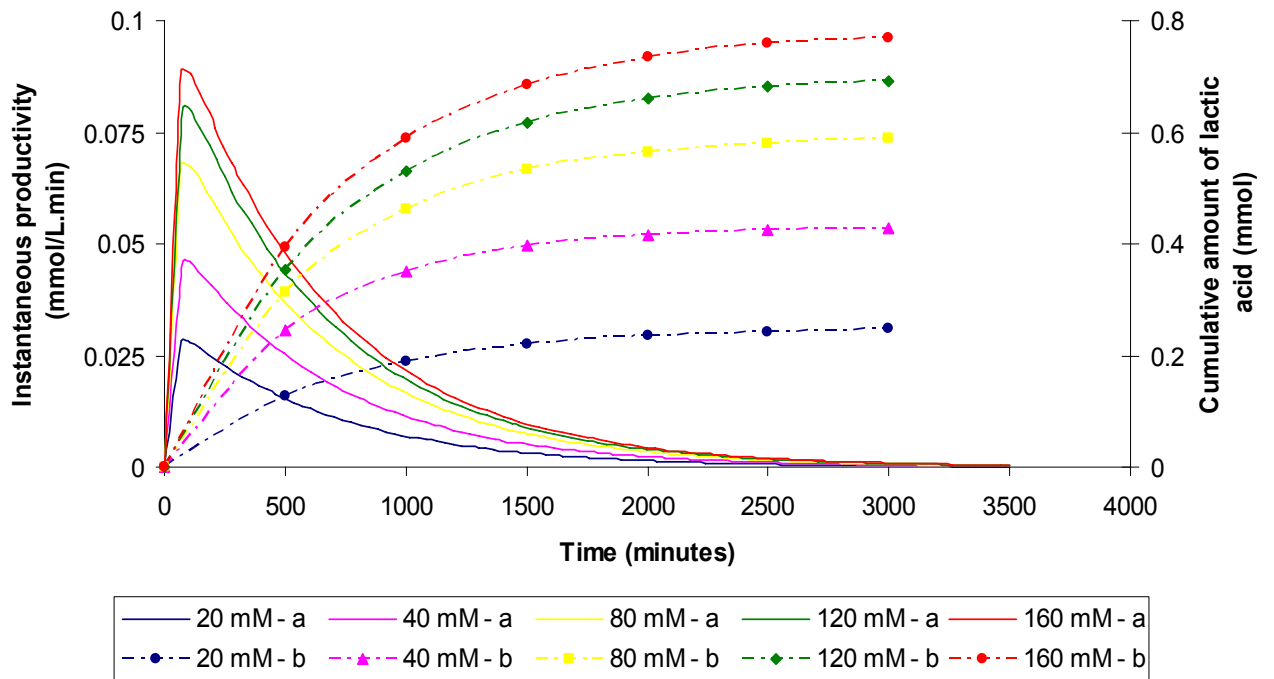
Figure 5.50: Effect of initial substrate concentration on instantaneous productivity and cumulative amount of lactic acid produced (T=50ºC, pH=8.0, e0=6.38 mg, v_p=0.0005 L/min, $a0_{imm}$=0.15 U/mg, t_h=7.3 h)

Although the impact of the substrate concentration on the instantaneous conversion and productivity and cumulative amount of lactic acid collected does not seem as significant as some of the other factors investigated, in conjunction with the optimisation of the other factors the substrate concentration could lead to a considerable improvement in the reactor performance.

5.3.4 <u>Requirements for process optimisation</u>

The effectiveness of immobilisation and validation of the model was discussed in Sections 5.3.1 and 5.3.2. The effect of amidase stability, amidase activity, permeate flux, amount of amidase immobilised and the initial substrate concentration on the reactor performance has been investigated in Section 5.3.3. Improvements in reactor performance with respect to these parameters have been discussed in these sections. In this section these discussions will be used to form a definite plan towards process optimisation in addition to discussing the process conditions at which the reactor should be operated for optimum performance.

1. ***Improve of the activity and functional stability of the amidase.***

    A purified amidase could be used in order to obtain higher activities. The effect of temperature on the stability should be studied to determine if a lower temperature may not lead to a significant improvement in stability (the improvement should be considerable in order to make up for the loss in activity at lower temperatures). The activity of the amidase on other substrates should be determined in order to see if another substrate may not prove to be more economical than lactamide. The effect of chelating agents (other than EDTA and DTT) and stabilising agents on the amidase activity and stability should also be tested.

2. ***Increase the membrane surface area and reduce the wall-thickness.***

    At this stage the system is operating in a mass transfer limited regime which makes the accurate determination of the kinetic constants impossible. It is also responsible for the low immobilised amidase activities compared with the free amidase activities. By using a few smaller membranes instead of one large membrane the membrane surface area will be increased (therefore more enzyme protein can be immobilised without affecting the mass transfer) and the thinner walls of the membranes will reduce the mass transfer limitations.

3. ***Optimise the immobilisation method.***

The immobilisation method can be optimised by doing a factorial design with the enzyme protein concentration in the immobilisation feed and the transmembrane pressure as the input variables and the amount of enzyme protein that is immobilised as the response variable. An empirical model predicting the amount of enzyme protein that will be immobilised for a specific enzyme protein concentration in the feed and transmembrane pressure can be developed from the factorial design. The optimum concentration of enzyme protein in the immobilisation feed and transmebrane pressure required to obtain a certain amount of immobilised enzyme protein can then be predicted from the model.

4. ***Determine the effective diffusion coefficient of the substrate through the membrane for various amounts of immobilised enzyme protein.***

If the effective diffusion coefficient of the substrate through the membrane is known for different amount of immobilised enzyme protein, an empirical correlation can be developed and incorporated into the reaction rate in the model to predict the effect of the amount of immobilised enzyme protein on the reactor performance. The optimum amount of immobilised enzyme protein can then be determined.

5. ***The operating permeate flux should not exceed the threshold value.***

For this system permeate fluxes higher than 0.001 L/min (the threshold value) resulted in no significant increase in either the instantaneous conversion or productivity. In addition operation at high permeate fluxes may result in amidase denaturation or permanent membrane fouling (if the critical flux of 0.055 L/min is exceeded). This system should therefore be operated at permeate fluxes below 0.001 L/min.

6. ***The initial substrate concentration should be in the range 50 mM to 70 mM.***

For substrate concentrations below 50 mM the low reaction rates resulted in a significant decrease in the instantaneous productivity whereas substrate concentrations above 70 mM resulted in low instantaneous conversions. For optimum reactor performance the substrate concentration for this system should therefore be between 50 mM and 70 mM.

6 <u>Conclusions</u>

The conclusions to this thesis will be discussed under the same headings and in the same order as the hypotheses for ease of comparison between these two sections. The main sections are: characterisation of free amidase, development of the MBR system and quantification of the membrane immobilised amidase process. The results and discussion led to the following conclusions regarding this research:

6.1 <u>Characterisation of free amidase</u>

1. ***The pH and temperature of the reaction mixture has a significant influence on the activity of the amidase. The interaction between the pH and the temperature, however, are insignificant. Experimental data showing the amidase activity at different pH's and temperatures could be used to predict the amidase activity at a specific pH and temperature.***

    The pH and temperature at which the amidase exhibited optimum activity was determined as 8.0 and 50ºC respectively by using a factorial design with the input variables pH (6.0 to 8.5) and temperature (40ºC to 70ºC) and response variable amidase specific activity. A statistical empirical model containing both pH and temperature, their squared values and all possible interactions was developed. An analysis of variance was carried out on the model. The factors having the most significant effect on the amidase specific activity was found to be pH, temperature, $(pH)^2$ and $(temperature)^2$. The interaction between the pH and temperature was found to be insignificant.

2. ***Neither the activity nor the stability of the amidase can be improved by the addition of the metal chelating agent ethylene diamine tetra-acetic acid (EDTA) or the reducing agents dithiolthreitol (DTT), L-cysteine or N-acetylcysteine (NAC).***

    The metal chelating agent EDTA was added to ensure that any trace of metal that might be present in the substrate did not decrease amidase activity and stability. Since no increase in activity or stability was seen after the addition of EDTA to the reaction mixture it could be concluded that either there were no trace metals in the mixture that could affect the amidase activity and stability or the amidase was not sensitive to the presence of trace metals. Reducing agents DTT, L-cysteine and NAC were used to determine if oxidation of the amidase's sulfhydryl groups, which are essential for catalysis, may be occurring. Since the

reducing agents had no effect on the activity or stability of the amidase it could be concluded that either these reducing agents did not work or oxidation of the catalytic groups of the amidase was not the reason for the low activity and stability.

3.   ***The rate of reaction catalysed by amidase can be predicted using Michaelis-Menten kinetics.***

It was determined that the amidase rate of reaction follows the general Michaelis-Menten plot. The rate of reaction was first order in concentration of substrate at lower substrate concentrations but as the substrate concentration was increased the reaction order in substrate concentration tended to zero. The kinetic parameters of the amidase were determined by using the Lineweaver-Burke plot, Hanes-Woolf plot and non-linear regression. The K_m and v_{max} values determined with the Lineweaver-Burke plot (85.84 mM and 1.68 mM/min respectively) was significantly higher than those determined with non-linear regression (68 mM and 1.48 mM/min) and the Hanes-Woolf plot (63.78 mM and 1.41 mM/min). Non-linear regression is generally accepted to be the most accurate method for determining K_m and v_{max}. The difference between the kinetic constants obtained from non-linear regression and those obtained from the Hanes-Woolf plot was insignificant. If a linearised method needs to be used for determining the kinetic constants of an enzyme, an accurate estimation can be obtained from the Hanes-Woolf plot.

6.2 Development of the experimental membrane bioreactor system

1.   ***Constant temperature and pressure are maintained over the whole length of the reactor system, irrespective of reaction orientation.***

The inlet and outlet temperature and pressure were measured directly. Differences of ± 2ºC were measured between the inlet and outlet temperature and no differences were found between the inlet and outlet pressure. Computational fluid dynamics was used to predict the distribution of temperature and pressure for different orientations (13.4º, 30º and 90º) inside the reactor. The pressure and temperature profiles showed no variation over the length of the reactor for any orientation. The temperature and pressure were therefore assumed to be constant throughout the reactor, irrespective of the orientation, and no temperature and pressure profiles were incorporated in the model.

2.   ***The velocity profile in the MBR is the same for all reactor orientations.***

Computational fluid dynamics was used to predict the type of flow patterns that would occur in the reactor for a flow rate of 200 mL/min and different reactor orientations (13.4º, 30º and 90º). Each of the reactor orientations resulted in the same amount of dead volume in the corners of the reactor. The reactor orientation therefore has no effect on the size of the stagnant zones in the reactor. The reactor was operated in a laminar flow region.

3.   ***Internal mass transfer limitations in the MBR are significant.***

The Thiele modulus was calculated to determine if the reactor was operating in a reaction limited or mass transfer limited regime. Since the Thiele modulus was 0.73 (which is larger than 0.3) the reactor could possibly be operating in an internal mass transfer limited regime. It was, however, still possible that the process was reaction limited. The effectiveness factor, which is a ratio between the actual rate of reaction and the rate of reaction that would be achieved without mass transfer limitations, was found to be 0.7 which means that the reaction rate in the reactor was 70% of the reaction rate that it would have been without internal mass transfer limitations. Experimental effectiveness factors of 0.146, 0.107 and 0.028 were calculated for the three different experiments respectively. The observed reaction rate was therefore only 14.6%, 10.7% and 2.8% of the reaction rate it would have been without mass transfer limitations. The significant difference between the theoretical and experimental estimations of the effectiveness factors can be ascribed to assumptions made during the calculations of the effectiveness factors. Although the exact extent of the internal mass transfer limitations could therefore not be determined, it can be concluded that mass transfer limitations do exist.

6.3 <u>Quantification of the membrane immobilised amidase process</u>

1.   ***The amidase can be effectively immobilised through physical adsorption in the pores of ceramic asymmetric, capillary membranes in a MBR.***

Three experiments were conducted to evaluate the effectiveness of the immobilisation method. It was determined that the enzyme protein concentration in the immobilisation feed has a definite effect on the amount of enzyme protein immobilised. An increase of 0.0026 mg/L (from 0.0184 mg/L to 0.021 mg/L) in the enzyme protein concentration of the initial feed caused the amount of initial enzyme protein immobilised to decrease from 38.7% to 30.4%. At an enzyme

protein concentration of 1.07 mg/L in the initial feed the amount of enzyme protein immobilised was only 4.7%. These results showed an exponential trend between the amount of enzyme protein immobilised and the enzyme protein concentration in the immobilisation feed. Immobilisation procedures with each of the three different enzyme protein immobilisation feed concentrations were conducted. The three experiments where conducted for 3 hours, 20.5 hours and 21 hours respectively. During all three experiments no physical loss of enzyme protein occurred. The 8 kDa membrane was therefore sufficient to retain the amidase.

The difference between the free and immobilised amidase activity was found to be considerable (with the immobilised amidase activity being 7, 9 and 35 times lower than the free amidase activity for the three experiments respectively). This could not only be attributable to mass transfer limitations but also to the low functional stability of the amidase. During immobilisation and washing (which lasted between 2 and 3 hours) the amidase would have lost a ¼ of its activity. Immobilisation in the pores may also have resulted in a decrease in the amidase activity.

An interesting trend was also found between the concentration of enzyme protein in the immobilisation feed and the amount of activity retained by the immobilised amidase (compared with that of the free amidase). Higher enzyme protein concentrations in the feed resulted in higher losses of amidase activity.

2.   ***The stability of the amidase will be increased by immobilisation.***

The stability of the immobilised amidase was determined by measuring the product concentration in the permeate over time. A plateau plus one-phase exponential decay model was fitted to the data with non-linear regression. From the regression the half-life of the immobilised amidase during the one-phase exponential decay was determined as 6.4 hours. By combining the plateau phase (of 3 hours) and the half-life obtained during the one-phase exponential decay period the actual immobilised amidase half-life was found to be 9.4 hours. The half-life of the immobilised amidase is therefore 4.5 hours more than the 4.9 hours exhibited by the free amidase. Immobilisation therefore increased the functional stability of the amidase significantly.

3. ***The MBR can be modeled theoretically and the percentage conversion of lactamide and the reactor productivity can be predicted by using an ordinary differential equation (ODE) solver software package.***

Four basic modeling principles were followed in order to develop a model of the MBR. The MBR was assumed to operate as a CSTR since the recycle ratios between the retentate and the permeate were larger than 100 for all experiments. The CSTR was also assumed to be at unsteady state since the reaction rate was never constant due to the amidase deactivation. The necessary differential equations for a CSTR were formulated. Two experiments were conducted at different conditions and the instantaneous conversion and instantaneous productivity for both experiments were determined.

An ODE solver software package (*Polymath*) was used to solve the CSTR differential equations simultaneously (for the two different experimental conditions) in order to predict the instantaneous conversion and instantaneous productivity of the reactor over time.

The experimental results and the predicted results were compared statistically and it was found that the model fitted the experimental data very well. Regression coefficients of 95.4% (experiment 1) and 80% (experiment 2) were determined for the fit between the experimental and predicted instantaneous conversion and productivities. The model could therefore be used to predict the performance of the reactor for changes in different operating parameters. These predictions formed the technological platform on which the optimisation of the reactor performance could be based. Specifically the sensitivity analysis predicted improved reactor performance providing the amidase activity and functional stability can be improved, the permeate flux is operated below its threshold value of 0.001 L/min, the amount of immobilised enzyme protein resulting in an optimum reactor conversion is determined empirically and the substrate concentrations is kept in the range 50 mM to 70 mM.

7 <u>Recommendations</u>

The following recommendations are made to guide in future work:

1. ***The first priority should be to optimise the amidase activity and functional stability with regards to lactamide as substrate.***

   If the activity and functional stability of the amidase cannot be improved, this process is unlikely to be feasible for commercial use. A more purified amidase extract should be used in the process to determine whether higher activities and stabilities can be obtained. The effect of other reducing agents and metal chelating agents on the activity and stability should also be evaluated. In order to improve the immobilised amidase activity and stability the immobilisation procedure should be optimised as discussed in Section 5.3.4.

2. ***The reactor design should be improved in order to reduce dead volume and mass transfer limitations.***

   Dead volume in the reactor results in a reduced active membrane area. The dead volume in the reactor can be decreased by inserting baffles in the reactor wall to increase the turbulence. If the mass transfer limitations could be reduced the reactor might operate in the reaction limited rather than mass transfer limited regime. The immobilised amidase activity might then be higher which will result in higher instantaneous conversions and productivities. The effect of mass transfer limitations could be reduced by using a few, thin-walled membranes instead of one thick-walled membrane.

3. ***The model should be refined to contain a correlation that relates the amount of immobilised enzyme protein to the mass transfer in order to determine the optimum amount of immobilised enzyme protein for the system.***

   The effective diffusion coefficient of the substrate through the membrane for different amounts of immobilised enzyme protein should be determined. The results obtained can be used to develop an empirical correlation between the Thiele modulus and the amount of enzyme protein immobilised. The correlation can then be incorporated into the reaction rate in the model to predict the effect of the amount of immobilised amidase on the reactor performance. The correlation is critical to the accurate determination of the optimum amount of immobilised enzyme protein for the system.

8 <u>References</u>

1. Almatawah Q.A., Cramp R. and Cowan D.A., 1999, 'Characterization of an inducible nitrilase from a thermophilic bacillus', *Extremophiles*, vol. 3, 283-291.

2. Baily J.E. and Ollis D.F., 1977, 'Biochemical Engineering Fundamentals', McGraw-Hill Inc., New York.

3. Baily J.E. and Ollis D.F., 1986, 'Biochemical Engineering Fundamentals', McGraw-Hill Inc., New York.

4. Banerjee A., Sharma R. and Banerjee U.C., 2002, 'The nitrile degrading enzymes: current status and future prospects', *Applied Microbiology and Biotechnology*, vol. 60, 33-44.

5. Bas, D. and Boyaci, I.H., 2007, 'Modeling and optimization II: Comparison of estimation capabilities of response surface methodology with artificial neural networks in a biochemical reaction', *Journal of Food Engineering*, vol. 78, pp. 846-854.

6. Belfort G., 1989, 'Membranes and bioreactors: A technical challenge in biotechnology', *Biotechnology and Bioengineering*, vol. 33, no. 8, pp. 1047-1066.

7. Belhocine D., Mokrane H., Grib H., Lounici H., Pauss A. and Mameri N., 2000, 'Optimization of enzymatic hydrolysis of haemoglobin in a continuous membrane bioreactor', *Chemical Engineering Journal*, vol. 76, 189–196.

8. Bhatia S., Long W.S. and Kamaruddin A.H., 2004, 'Enzymatic membrane reactor for the kinetic resolution of racemic ibuprofen ester: modeling and experimental studies', Chemical Engineering Science, vol. 59, 5061-5068.

9. Bickerstaff G.F., 1997, 'Immobilisation of enzymes and cells', *Methods in Biotechnology*, Humana press, New Jersey, pp.1-10.

10. Bisset, H. and Krieg, H., 2006, 'New developments in composite ceramic membranes', *Journal of Chemical Technology*, March 2006, pp.4-7.

11. Boshoff A., Edwards W., Leukes W.D., Rose P.D. and Burton S.G., 1998, 'Immobilisation of polyphenol oxidase on nylon and polyethersulphone membranes: Effect on product formation', *Desalination*, vol. 115, pp.307-312.

12. Brady D., Beeton A., Zeevaart J., Kgaje C., Van Rantwijk F. and Sheldon R.A., 2004, 'Characterisation of nitrilase and nitrile hydratase biocatalytic systems', *Applied Microbiology and Biotechnology*, vol. 64, 76-85.

13. Breuer M., Ditrich K., Habicher T., Hauer B., Kesseler M., Sturmer R. and Zelinski T., 2004, 'Industrial methods for the production of optically active intermediates', *Aangewandte Chemie International Addition*, vol. 43, 788-824.

14. Burton, S.G., 2001, 'Development of bioreactors for application of biocatalysts in biotransformations and bioremediation', *Pure and Applied Chemistry*, Vol. 73, No. 1, pp.77-83.

15. Carvalho C. M. L., Aires-Barros M. R., Cabral J. M. S., 2001, 'A Continuous membrane bioreactor for ester synthesis in organic media: I. Operational characterization and stability', *Biotechnology and Bioengineering*, vol. 72, 127-135.

16. Cheryan M., 1998, *Ultrafiltration and Microfiltration Handbook*, Technomic Publishing Company, Pennsylvania.

17. Cleland W.W., 1963, *Diothiothreitol, a new protective reagent for SH groups*, Journal of Biochemistry, vol. 3, 480-482.

18. Cowan D., Cramp R., Pereira R., Graham D. and Almatawah Q., 1998, 'Biochemistry and biotechnology of mesophilic and thermophilic nitrile metabolizing enzymes', *Extrermophiles*, vol. 2, 207-216.

19. Crowe C.T., Elger D.F. and Roberson J.A., 2001, 'Engineering fluid mechanics', 7th edition, John Wiley and Sons, Inc., New York.

20. D'Souza S.F., 1999, 'Immobilized enzymes in bioprocess', *Current Science*, vol. 77, 69-79.

21. Doran, P.M., 2004, *Bioprocess Engineering Principles*, Elsevier Ltd., United Kingdom, pp. 268-275.

22. Edward V.A., Pillay V.L., Swart P., Jacobs E. and Singh S., 2005, 'Degradation of synthetic xylan effluent using a membrane bioreactor', *Journal of Chemical Technology*, February 2005, pp.26-28.

23. Egorova K., Trauthwein H., Verseck S. and Antranikian G., 2004, 'Purification and properties of an enantioselective and thermoactive amidase from the thermophilic

actinomycete Pseudonocardia thermophila', *Applied Microbiology and Biotechnology*, vol. 65, 38-45.

24. Ferreira J.S., Straathof A.J.J., Franco T.T. and Van der Wielen L.A.M., 2004, 'Activity and stability of immobilized penicillin amidase at low pH values', Journal of Molecular Catalysis B: Enzymatic, vol. 27, 29-35.

25. Flaschel E. and Wandrey C., 1979, 'Membrane reactors'. In: Buchholz K. (ed), *Characterization of immobilised biocatalysts*, Schön & Wetzel GmbH, Frankfurt, pp. 337-343.

26. Fluent 6.3.26 (2006).

27. Fogler H.S., 1999, 'Elements of chemical reaction engineering', 3rd edition, Prentice-Hall, Inc., New Jersey.

28. Fournand D. and Arnaud A., 2001, 'Aliphatic and enantioselective amidases: from hydrolysis to acyl transfer activity', *Journal of Applied Microbiology*, vol. 91, 381-393.

29. Gambit 2.4.6 (2006).

30. Gavagan J.E., DiCosimo R., Eisenberg A., Fager S.K., Folsom P.W., Hann E.C., Schneider K.J. and Fallon R.D., 1999, 'A gram-negative bacterium producing a heat-stable nitrilase highly active on aliphatic dinitriles', *Applied Microbiology and Biotechnology*, vol. 52, 654-659.

31. Gemeiner P., 1992, 'Materials for enzyme engineering', *Enzyme engineering*, Ellis Horwood, New York, pp.13-119.

32. Giorno L. and Drioli E., 2000, 'Biocatalytic membrane reactors: applications and perspectives', *TIBTECH*, vol. 18, 339-349.

33. Giorno L., Drioli E., Carvoli G., Cassano A. and Donato L., 2000, 'Study of an enzyme membrane reactor with immobilised fumarase for production of L-malic acid', *Biotechnology and Bioengineering*, vol. 72, no.1, pp.77-84.

34. Graham D., Pereira R., Barfield D. and Cowan D., 2000, 'Nitrile biotransformations using free and immobilised cells of a thermophilic Bacillus spp.', *Enzyme and Microbial Technology*, vol. 26, 368-373.

35. Grzeoekowiak-Przywecka A. and Slominska L., 2005, 'Continuous potato starch hydrolysis process in a membrane reactor with tubular and hollow-fiber membranes', *Desalination*, vol. 184, 105-112.

36. Guit R. P. M., Kloosterman M., Meindersma G. W., Mayer M. and Meijer E. M., 1991, 'Lipase kinetics: Hydrolysis of triacetin by lipase from *Candida cylindruceu* in a hollow fiber membrane reactor', *Biotechnology and Bioengineering*, vol. 38, 727-732.

37. Hirrlinger B., Stolz A. and Knackmuss H., 1996, 'Purification and properties of an amidase from *Rhodococcus erythropolis* MP50 which enantioselectively hydrolyzes 2-arylpropionamides', *Journal of Bacteriology*, vol. 178, 3501-3507.

38. http://academic.brooklyn.cuny.edu/biology/bio4fv/page/enz_act.htm

39. http://scifun.chem.wisc.edu/CHEMWEEK/Chelates/Chelates.html

40. http://users.rcn.com/jkimball.ma.ultranet/BiologyPages/E/EnzymeKinetics.html

41. http://www.cheresources.com

42. http://www.kochmembrane.com

43. http://www.novasep.com

44. http://www.rpi.edu/dept/chem-eng/Biotech-Environ.htm

45. Kalayanpur M., 1999, 'Membrane separations'. In: Flickinger M.C., Drew S.W. (eds), *Encyclopedia of bioprocess technology: fermentation, biocatalysis and bioseparation*, John Wiley & Sons, Inc., New York, 1695-1705.

46. Kato Y., Tsuda T. and Asano Y., 1999, 'Nitrile hydratase involved in aldoxime metabolism from *Rhodococcus* sp. strain YH3-3: purification and characterization', *European Journal of Biochemistry*, vol. 263, 662-670.

47. Kobayashi M. and Shimizu S., 2000, 'Nitrile hydrolases', *Current Opinion in Chemical Biology*, vol. 4, 95-102.

48. Kobayashi M., Komeda H., Nagasawa T., Nishiyama M., Horinouchi S., Beppu T., Yamada H. and Shimizu S., 1993, 'Amidase coupled with low-molecular-mass nitrile hydratase from *Rhodococcus rhodocrous* J1', *European Journal of Biochemistry*, vol. 217, 327-336.

49. Kobayashi M., Nagasawa T. and Yamada H., 1989, 'Nitrilase of *Rhodococcus rhodochrous* J1: purification and characterization', *European Journal of Biochemistry*, vol. 182, 349-356.

50. Komeda H. and Asano Y., 2000, 'Gene cloning, nucleotide sequencing and purification and characterization of the D-stereospecific amino-acid amidase from Ochrobacturm anthropi SV3', *European Journal of Biochemistry*, vol. 267, 2028-2035.

51. Konar A.F. and Oysal Y., 2003, 'Generalized modeling principles of a nonlinear system with dynamic fuzzy network', *Journal of Electrical and Electronic Engineering*, vol. 3, 727-734.

52. Kotlova E.K., Chestukhina G.G., Astaurova O.B., Leonava T.E., Yanenko A.S. and Debabov V.G., 1999, 'Isolation and primary characterization of an amidase from *Rodococcus rodochrous*', *Biochemistry (Moscow)*, vol. 64, 459-565.

53. Kragl U., Greiner L. and Wandrey C., 1999, 'Enzymes, immobilised, reactors'. In: Flickinger M.C., Drew S.W. (eds), *Encyclopedia of bioprocess technology: fermentation, biocatalysis and bioseparation*, John Wiley & Sons, Inc., New York, 1064-1065.

54. Long W.S., Bhatia S. and Kamaruddin A., 2003, 'Modeling and simulation of enzymatic membrane reactor for kinetic resolution of ibuprofen ester', *Journal of Membrane Science*, vol. 219, 69.

55. Long W.S., Kamaruddin A. and Bhatia S., 2005, 'Chiral resolution of racemic ibuprofen ester in an enzymatic membrane reactor', *Journal of Membrane Science*, vol. 247, 185–200.

56. Lopez-Ulibarri R. and Hall G.M., 1997, 'Saccharification of cassava flour starch in a hollow-fiber membrane reactor', *Enzyme and Microbial Technology*, vol. 21, 398-404.

57. Makhongela H.S., 2005, 'Characterization of a thermostable amidase and development of a bioreactor process for lactic acid production', MSc. Thesis, University of Cape Town.

58. Malcata F. X., Reyes H. R., Garcia H. S., Hill C. G. and Amundson C. H., 1992, 'Kinetics and mechanisms of reactions catalyzed by immobilized lipases', *Enzyme and Microbial Technology*, vol. 14, 426-446.

59. Martinkova L. and Mylerova V., 2003, 'Synthetic applications of nitrile-converting enzymes', *Current Organic Chemistry*, vol. 7, 1279-1295.

60. Matlab 6.5 (2002).

61. Monsan P. and Combes D., 1988, 'Enzyme stabilization by immobilization', *Methods in Enzymology*, vol. 137, 584-598.

62. Motulsky H. and Christopoulos A., 2003, 'Fitting models to biological data using linear and non-linear regression: a practical guide to curve fitting', *GraphPad Software Inc.*, San Diego CA, 29-30.

63. Motulsky H.J. and Ransnas L.A., 1987, 'Fitting curves to data using nonlinear regression: a practical and nonmathematical review', *FASEB Journal*, vol. 1, 365-374.

64. Mountzouris K. C., Gilmour S. G., Grandison A. S. and Rastall R. A., 1999, 'Modeling of oligodextran production in an ultrafiltration stirred-cell membrane reactor', *Enzyme and Microbial Technology*, vol. 24, 75-85.

65. Nagasawa T. and Yamada H., 1995, 'Microbial production of commodity chemicals', *Pure and Applied Chemistry*, vol. 67, 1241-1256.

66. Nishizawa K., Nakajima M. and Nabetani H., 1999, 'A forced-flow membrane reactor for transfructosylation using ceramic membrane', *Biotechnology and Bioengineering*, vol. 68, 92-97.

67. O'Reilly C. and Turner P.D., 2003, 'The nitrilase family of CN hydrolysing enzymes – a comparative study', *Journal of Applied Microbiology*, vol. 95, 1161-1174.

68. Okada M., Fuji K., Hoshino M., Noguchi T., Tsujimura M., Nagashima S., Honda J., Nagamune T., Sasabe H., Inoue Y. and Endo I., 1997, 'Activity regulation of photoreactive nitrile hydratase by nitric oxide', *Journal of American Chemistry Society*, vol. 119, 3785-3791.

69. Pereira R.A., Graham D., Rainey F.A. and Cowan D.A., 1998, 'A novel thermostable nitrile hydratase', *Extremophiles*, vol. 2, 347-357.

70. Piotrowski M, Schonvelder S. and Weiler E.W., 2001, 'The *Arabidopsis thaliana* isogene *NIT4* and its orthologs in tobacco encode b-Cyano-L-alanine hydratase/nitrilase', *Journal of Biological Chemistry*, vol. 276, 2616-2621.

71. Polymath 5.X, Shacham, M., Cutlip, M.B. and Elly, M., Copyright, 2008.

72. R 2.4.1, A Language and Environment Copyright, 2006.

73. Salmon P.M. and Robertson C.R., 1995, 'Membrane reactors'. In: Asenjo J.A., Merchuk J.C. (eds), *Bioreactor system design*, Marcel Dekker Inc., New York, pp.305-315.

74. Sanchez Marcano J.G. and Tsotsis T.T., 2003, 'Design of immobilised biocatalyst reactors'. In: Elvers B., Hawkins S., Schulz G. (eds), *Ullman's Encyclopedia of Industrial Chemistry*, Electronic version, Wiley-VCH Verlag GmbH & Co. KGaA.

75. Sato T. and Tosa T., 1999, 'Enzymes, immobilisation methods'. In: Flickinger M.C., Drew S.W. (eds), *Encyclopedia of bioprocess technology: fermentation, biocatalysis and bioseparation*, John Wiley & Sons, Inc., New York, 1062-1063.

76. Schmid A., Dordick J.S., Hauer B., Kieners A., Wubbolts M. and Witholt B., 2001, 'Industrial biocatalysis today and tomorrow', *Nature*, vol. 409, 258-268.

77. Schoemaker H.E., Mink D. and Wubbolts M.G., 2003, 'Dispelling the myths – biocatalysis in industrial synthesis', Science, vol. 299, 1694-1697.

78. Setti L., Lanzarini G. and Pifferi P.G., 1997, 'Whole cell biocatalysis for an oil desulfurization process', *Fuel Processing Technology*, vol. 52, 145-153.

79. Sinnott R.K., 2004, 'Chemical engineering design'. In: Coulson, J.M. and Richardson, J.F. (eds), *Coulson and Richardson's Chemical Engineering Volume 6*, 3rd edition, Elsevier Butterworth-Heinemann, London, 332 -334.

80. Sousa H.A., Rodrigues C., Klein E., Afonso C.A.M. and Crespo J.G., 2001, 'Immobilisation of pig liver esterase in hollow fiber membranes', *Enzyme and Microbial Technology*, vol. 29, pp.625-634.

81. Thomas S.M., DiCosimo R. and Nagarajan V., 2002, 'Biocatalysis: applications and potentials for the chemical industry', *Trends in Biotechnology*, vol. 20, 238-242.

82. Tischer W. and Kasche V., 1999, 'Immobilized enzymes: crystals or carriers', *TIBTECH*, vol. 17, 326-335.

83. Tramper J., 1996, 'Chemical versus biochemical conversion: when and how to use biocatalysts', *Biotechnology and Bioengineering*, vol. 52, 290-295.

84. Walas S.M., 1998, 'Chemical reactors'. In: Perry, R.H. and Green, D.W. (eds), *Perry's Chemical Engineers' Handbook*, 7th edition, McGraw-Hill International, Singapore, 23-4-23-5.

85. Wang M., 2005, 'Enantioselective biotransformations of nitriles in organic synthesis', *Topics in Catalysis*, vol. 35, 117-130.

86. Wenten I.G. and Widiasa I.N., 2002, 'Enzymatic hollow fiber membrane bioreactor for penicillin hydrolysis', *Desalination*, vol. 149, 279-285.

87. Wimpenny J.W.T., 1997, 'The validity of models', *Advances in Dental Research*, vol. 11, 150-159.

88. Yamada H. and Kobayashi M., 1996, 'Nitrile hydratase and its application to industrial production of acrylamide', *Bioscience, Biotechnology and Biochemistry*, vol. 60, 1291-1400.

89. Yamaki T., Oikawa T., Ito K. and Nakamura T., 1997, 'Cloning and sequencing of a nitrile hydratase gene from *Pseudonocardia Thermophila* JCM 3095', *Journal of Fermentation and Bioengineering*, vol. 83, 474-477.

90. Ye P., Xu Z., Wu J., Innocent C. and Seta P., 2006, 'Entrusting poly(acrylonitirle-co-maleic acid) ultrafiltration hollow fiber membranes with biomimetric surfaces or lipase immobilization', *Journal of Molecular Catalysts B: Enzymatic,* vol. 40, pp. 30-37.

91. Yildirim S., 2005, 'Selective dihydroxylation of aromatic nitriles with tailored Escherichia coli', PhD Thesis, Technical University of Hamburg – Harburg.

92. Zhang X., Guan R., Wu D. and Chan K., 2005, 'Enzyme immobilization on amino-functionalized mesostructured cellular foam surfaces, characterization and catalytic properties', *Journal of Molecular Catalysis B: Enzymatic*, vol. 33, 43–50.

Appendix I: Preparation of buffers and standards

Preparation of NH$_4$Cl standard solutions and standard curve

The ammonia chloride standard curve was prepared by using the following method:

0.10698 g of NH$_4$Cl was dissolved in 1 L of distilled water to make up a 2.0 mM solution which served as the stock solution and was used to prepare various concentrations of NH$_4$Cl as shown in Table A.1:

Table A. 1: Preparation of the ammonium chloride standard solutions

NH$_4$Cl Standard Concentration (mM)	Volume of stock solution (µL)	Volume of distilled water (µL)
0	0	1000
0.2	100	900
0.4	200	800
0.6	300	700
0.8	400	600
1.0	500	500
1.5	750	250
2.0	1000	0

1400 µL of reagent A of the ammonia detection assay were added to 350 µL of each standard and 1400 µL of reagent B of the ammonia detection assay was then added. The mixtures were left for 15 minutes at room temperature and then the absorbance of each mixture was measured with a spectrophotometer at 600 nm. From this data an ammonium chloride standard curve was constructed (Figure A.1).
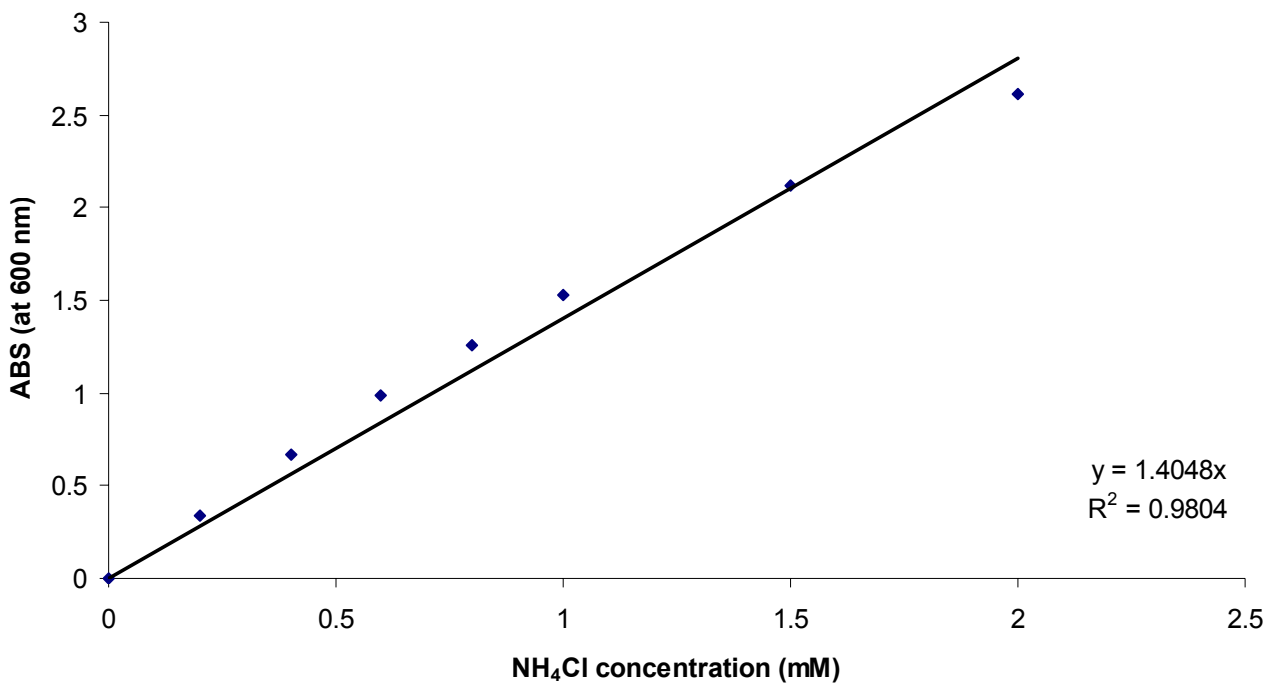
Figure A.1: Ammonia chloride standard curve for determination of product concentration in samples

This curve was used relate the absorbance of a sample at 600 nm to the ammonia concentration in the sample [Pereira *et al.*, 1998].

Preparation of BSA standard solutions and standard curves

Since the method used to measure enzyme protein is slightly different for lower enzyme protein concentrations than for higher enzyme protein concentrations a standard curve for each range of enzyme protein was constructed. The first range was between 50 and 1000 μg/mL and the second range was between 1 and 5 μg/mL.

For enzyme protein concentrations between 50 and 1000 μg/mL

Preparation of the bovine serum albumin (BSA) standards was done according to the following method [Bradford Reagent, Product information, Sigma Aldrich]:

A ready-to-use stock solution of 1 mg/mL BSA was purchased and used to prepare various concentrations of BSA standards as shown in Table A.2.

Table A.2: Preparation of the BSA standard solutions for the standard Bradford assay

BSA Standard Conc. (µg/mL)	Volume of stock solution (µL)	Volume of phosphate buffer (µL)
0	0	200
200	40	160
400	80	120
600	120	80
800	160	40
1000	200	0

Bradford's reagent (3 mL) was added to 100 µL of each BSA standard. The solution was left at room temperature for 8 minutes after which a spectrophotometer was used to measure the absorbance at 595 nm. From this data a protein standard curve (Figure A.2) was drawn from which the enzyme protein concentration could be determined from the absorbance of a sample at 595 nm.

$y = 0.8074x$

$R^2 = 0.9981$
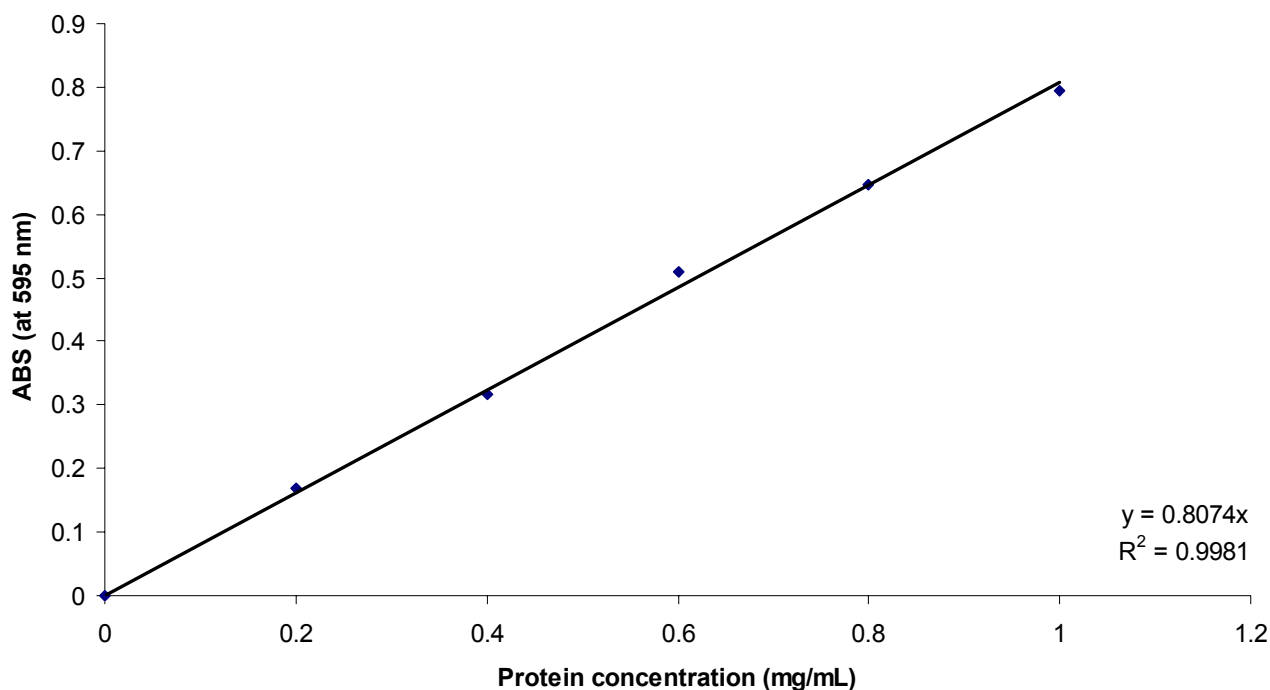
Figure A.2: BSA standard curve for determining protein concentrations in the range 50 – 1000 µg/mL

For enzyme protein concentrations between 1 and 5 µg/mL

Preparation of the bovine serum albumin (BSA) standards was done according to the following method [Bradford Reagent, Product information, Sigma Aldrich]:

A stock solution of 200 µg/mL BSA was made up and used to prepare various concentrations of BSA standards as shown in Table A.3.

Table A.3: Preparation of the BSA standard solutions for the micro Bradford assay

BSA Standard Conc. (µg/mL)	Volume of stock solution (µL)	Volume of phosphate buffer (µL)
0	0	2000
1	10	1990
5	50	1950
10	100	1900
15	150	1850

Bradford's reagent (1 mL) was added to 1 mL of each BSA standard. The solution was left at room temperature for 8 minutes after which a spectrophotometer was used to measure the absorbance at 595 nm. From this data a protein standard curve were drawn from which enzyme protein concentrations in the range 1 – 5 µg/mL could be determined at 595 nm (Figure A.3).
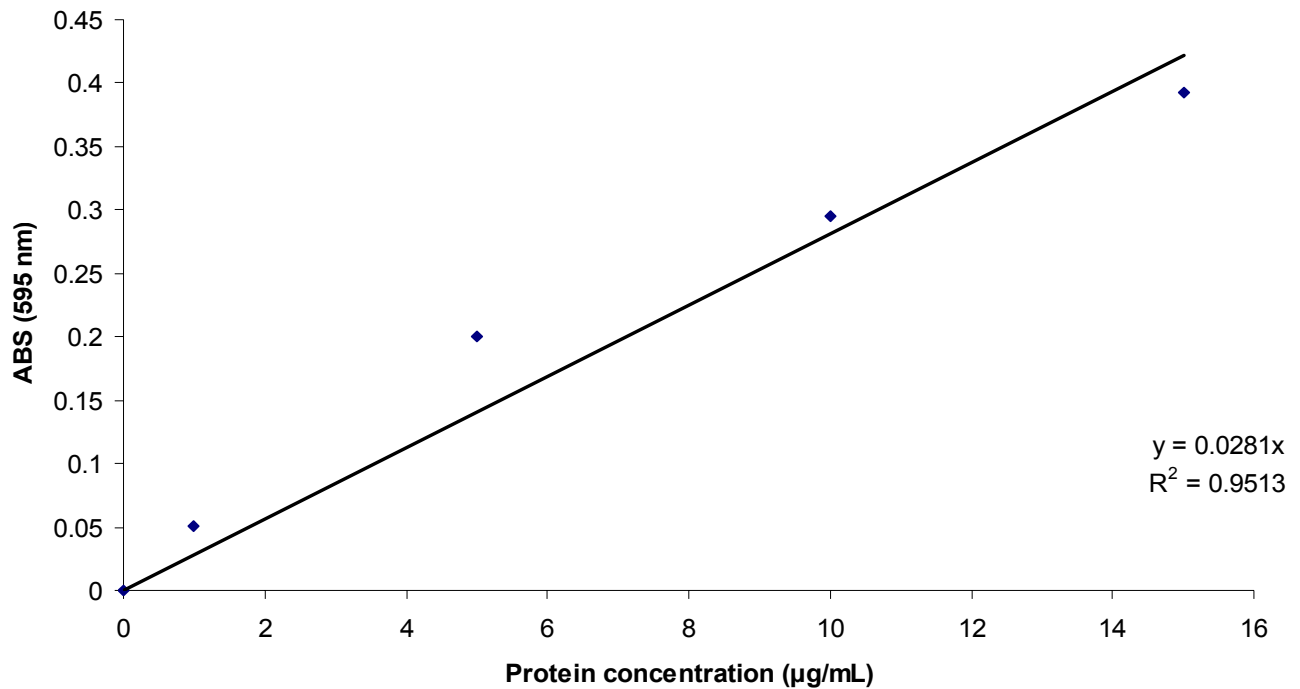
Figure A.3: BSA standard curve for determining protein concentrations in the range 1 – 5 µg/mL

Preparation of potassium phosphate buffer

The 50 mM phosphate buffer that was used in this project was prepared as follows [Makhongela, 2005]:

The following two stock solutions were made up:

- M K_2HPO_4 solution (17.4 g of K_2HPO_4 in 1 L of distilled water)
- M KH_2PO_4 solution (13.6 g of KH_2PO_4 in 1 L of distilled water)

A specific pH was obtained by adding the desired volumes of the two stock solutions together.

Table 0.1: Preparation of the 50 mM phosphate buffer

Desired pH	Volume of K_2HPO_4 (mL)	Volume of KH_2PO_4 (mL)
5.5	6.5	93.5
6.0	12.3	87.7
6.5	31.5	68.5
7.0	61.0	39.0
7.5	84.0	16.0
8.0	94.7	5.3

List of chemicals used

The following chemicals were used throughout the project. The name of the supplier is shown in brackets after each chemical.

- Sodium hydroxide – reagent grade (Kimix)
- Household bleach (Spar)
- Phenol – reagent grade (Merck)
- Nitroprusside – reagent grade (Merck)
- Bradford reagent (Sigma Aldrich)
- Dipotassium hydrogen phosphate – reagent grade (Merck)
- Potassium dihydrogen phosphate – reagent grade (Merck)

Appendix II: Programming scripts and reports

Development of a model predicting the activity of amidase at a specific temperature and pH

'R', which is a free-software statistical program, was used to develop the empirical model for predicting the activity of amidase at a specific temperature and pH. The following script was used:

```
> Freeenzymedata <-
read.csv("C:\\Freeenzymedata.csv",header=T,dec=".",sep=",")
> attach(Freeenzymedata)
> Freeenzymedata
   T.code pH.code       SpA
1      40     6.0   0.7158961
2      40     7.0   0.8930665
3      40     8.0   1.0479651
4      40     8.5   0.9649008
5      50     6.0   0.9592544
6      50     7.0   1.3218764
7      50     8.0   1.3841746
8      50     8.5   1.2419490
9      60     6.0   0.7377287
10     60     7.0   0.8842205
11     60     8.0   1.3885035
12     60     8.5   1.1285826
13     70     6.0   0.4496387
14     70     7.0   0.6960084
15     70     8.0   0.7298238
16     70     8.5   0.6147008
> Freeenzymedata <-
data.frame(T.code=T.code,pH.code=pH.code,SpA=SpA)
> Model=lm(SpA~ T.code*pH.code + I(T.code^2)*I(pH.code^2)-
I(T.code^2):I(pH.code^2), data = Freeenzymedata)
> Model
Call:
lm(formula = SpA ~ T.code * pH.code + I(T.code^2) * I(pH.code^2) -
I(T.code^2):I(pH.code^2), data = Freeenzymedata)
```

```
Coefficients:
   (Intercept)            T.code            pH.code       I(T.code^2)
I(pH.code^2)  T.code:pH.code
    -1.051e+01         1.936e-01         1.729e+00       -1.834e-03
-1.092e-01      -3.106e-04
> anova(Model)
Analysis of Variance Table
Response: SpA
                 Df    Sum Sq    Mean Sq   F value        Pr(>F)
T.code            1    0.21665   0.21665   15.2997   0.0029063 **
pH.code           1    0.25222   0.25222   17.8114   0.0017706 **
I(T.code^2)       1    0.53813   0.53813   38.0021   0.0001063
***
I(pH.code^2)      1    0.08043   0.08043   5.6801    0.0383957 *
T.code:pH.code    1    0.00018   0.00018   0.0126    0.9129681
Residuals        10    0.14161   0.01416
---
Signif. codes:  0 '***' 0.001 '**' 0.01 '*' 0.05 '.' 0.1 ' ' 1
> Model2=lm(SpA~ T.code*pH.code + I(T.code^2)*I(pH.code^2)-
I(T.code^2):I(pH.code^2)-T.code:pH.code, data = Freeenzymedata)
> Model2
Call:
lm(formula = SpA ~ T.code * pH.code + I(T.code^2) * I(pH.code^2) -
I(T.code^2):I(pH.code^2) - T.code:pH.code, data = Freeenzymedata)
Coefficients:
 (Intercept)          T.code             pH.code         I(T.code^2)
I(pH.code^2)
  -10.386495        0.191324         1.712239         -0.001834      -
0.109195
> anova(Model2)
Analysis of Variance Table
Response: SpA
             Df   Sum Sq   Mean Sq    F value     Pr(>F)
T.code        1   0.21665  0.21665    16.8086   0.001760 **
pH.code       1   0.25222  0.25222    19.5680   0.001022 **
I(T.code^2)   1   0.53813  0.53813    41.7498   4.668e-05 ***
I(pH.code^2)  1   0.08043  0.08043    6.2403    0.029609 *
Residuals    11   0.14178  0.01289
---
```

```
Signif. codes:  0 '***' 0.001 '**' 0.01 '*' 0.05 '.' 0.1 ' ' 1
```

CFD modeling report (*Fluent*)

Fluent does not require programming in a command window. It requires you to insert parameters e.g. heat transfer coefficients, wall materials and flow rates for your specific drawing. The Fluent report below was for a top entry and 30º orientation of the reactor. Other reports were identical except for the flow rate specification and orientation specification.

```
FLUENT
Version: 3d, pbns, lam (3d, pressure-based, laminar)
Release: 6.3.26
Title:
Models
------

   Model                         Settings
   -------------------------------------

   Space                         3D
   Time                          Steady
   Viscous                       Laminar
   Heat Transfer                 Enabled
   Solidification and Melting    Disabled
   Radiation                     None
   Species Transport             Disabled
   Coupled Dispersed Phase       Disabled
   Pollutants                    Disabled
   Pollutants                    Disabled
   Soot                          Disabled
Boundary Conditions
-------------------

   Zones


       name              id    type
       ------------------------------------
       fluid             2     fluid
       wall              3     wall
       outlet            4     outflow
       inlet             5     mass-flow-inlet
```

```
     default-interior    7     interior
 Boundary Conditions                                        fluid
 Condition                                                  Value
        ---------------------------------------------------------
-------------------------------------------------------------------
-------------------------------------------------------------------
-----------------------------------
Material Name                                          water-liquid
Specify source terms?                                      no
        Source Terms
((mass) (x-momentum) (y-momentum) (z-momentum))
  Specify fixed values?                                    no
  Local Coordinate System for Fixed Velocities             no
        Fixed Values
((x-velocity (inactive . #f) (constant . 0) (profile  )) (y-
velocity (inactive . #f) (constant . 0) (profile  )) (z-velocity
(inactive . #f) (constant . 0) (profile  )))
   Motion Type                                             0
   X-Velocity Of Zone (m/s)                                0
   Y-Velocity Of Zone (m/s)                                0
   Z-Velocity Of Zone (m/s)                                0
   Rotation speed (rad/s)                                  0
   X-Origin of Rotation-Axis (m)                           0
   Y-Origin of Rotation-Axis (m)                           0
   Z-Origin of Rotation-Axis (m)                           0
   X-Component of Rotation-Axis                            0
   Y-Component of Rotation-Axis                            0
   Z-Component of Rotation-Axis                            1
   Deactivated Thread                                      no
   Porous zone?                                            no
   Conical porous zone?                                    no
   X-Component of Direction-1 Vector                       1
   Y-Component of Direction-1 Vector                       0
   Z-Component of Direction-1 Vector                       0
   X-Component of Direction-2 Vector                       0
   Y-Component of Direction-2 Vector                       1
   Z-Component of Direction-2 Vector                       0
   X-Component of Cone Axis Vector                         1
   Y-Component of Cone Axis Vector                         0
```

```
Z-Component of Cone Axis Vector                          0
X-Coordinate of Point on Cone Axis (m)                   1
Y-Coordinate of Point on Cone Axis (m)                   0
Z-Coordinate of Point on Cone Axis (m)                   0
Half Angle of Cone Relative to its Axis (deg)           0
Relative Velocity Resistance Formulation?              yes
Direction-1 Viscous Resistance (1/m2)                   0
Direction-2 Viscous Resistance (1/m2)                   0
Direction-3 Viscous Resistance (1/m2)                   0
Choose alternative formulation for inertial resistance?   no
Direction-1 Inertial Resistance (1/m)                   0
Direction-2 Inertial Resistance (1/m)                   0
Direction-3 Inertial Resistance (1/m)                   0
C0 Coefficient for Power-Law                            0
C1 Coefficient for Power-Law                            0
Porosity                                                1
Solid Material Name                               aluminum
wall

    Condition                                       Value
    ----------------------------------------------------------
---

    Wall Thickness (m)                                 0
    Heat Generation Rate (w/m3)                        0
    Material Name                           titanium oxide
    Thermal BC Type                                    2
    Temperature (k)                                  300
    Heat Flux (w/m2)                                   0
    Convective Heat Transfer Coefficient (w/m2-k)      4
    Free Stream Temperature (k)                      293
    Enable shell conduction?                          no
    Wall Motion                                        0
    Shear Boundary Condition                           0
    Define wall motion relative to adjacent cell zone?   yes
    Apply a rotational velocity to this wall?         no
    Velocity Magnitude (m/s)                           0
    X-Component of Wall Translation                    1
    Y-Component of Wall Translation                    0
    Z-Component of Wall Translation                    0
```

```
      Define wall velocity components?                    no
      X-Component of Wall Translation (m/s)               0
      Y-Component of Wall Translation (m/s)               0
      Z-Component of Wall Translation (m/s)               0
      External Emissivity                                 1
      External Radiation Temperature (k)                  300
      Rotation Speed (rad/s)                              0
      X-Position of Rotation-Axis Origin (m)              0
      Y-Position of Rotation-Axis Origin (m)              0
      Z-Position of Rotation-Axis Origin (m)              0
      X-Component of Rotation-Axis Direction              0
      Y-Component of Rotation-Axis Direction              0
      Z-Component of Rotation-Axis Direction              1
      X-component of shear stress (pascal)                0
      Y-component of shear stress (pascal)                0
      Z-component of shear stress (pascal)                0
      Surface tension gradient (n/m-k)                    0
      Specularity Coefficient                             0
  outlet

      Condition                Value
      --------------------------
      Flow rate weighting    1
  inlet

      Condition                                   Value
      ----------------------------------------------------
      Mass Flow Specification Method              0
      Mass Flow-Rate (kg/s)                       0.010611
      Mass Flux (kg/m2-s)                         1
      Average Mass Flux (kg/m2-s)                 1
      Upstream Torque Integral (n-m)              1
      Upstream Total Enthalpy Integral (w/m2)     1
      Total Temperature (k)                       323
      Supersonic/Initial Gauge Pressure (pascal)  171325
      Direction Specification Method              1
      Reference Frame                             0
      Coordinate System                           0
      X-Component of Flow Direction               1
```

```
            Y-Component of Flow Direction                    0
            Z-Component of Flow Direction                    0
            X-Component of Axis Direction                    1
            Y-Component of Axis Direction                    0
            Z-Component of Axis Direction                    0
            X-Coordinate of Axis Origin (m)                  0
            Y-Coordinate of Axis Origin (m)                  0
            Z-Coordinate of Axis Origin (m)                  0
            is zone used in mixing-plane model?          no


      Equations


      Equation    Solved
      ----------------
      Flow        yes
      Energy      yes


   Numerics


      Numeric                         Enabled
      ---------------------------------------
      Absolute Velocity Formulation    yes


   Relaxation


      Variable         Relaxation Factor
      -------------------------------
      Pressure        0.30000001
      Density         1
      Body Forces     1
      Momentum        0.69999999
      Energy          1


   Linear Solver


                  Solver      Termination    Residual Reduction
      Variable    Type        Criterion      Tolerance
      -----------------------------------------------------------
      Pressure    V-Cycle     0.1
```

```
    X-Momentum     Flexible    0.1              0.7
    Y-Momentum     Flexible    0.1              0.7
    Z-Momentum     Flexible    0.1              0.7
    Energy         Flexible    0.1              0.7
 Pressure-Velocity Coupling

  Parameter    Value
  -----------------
  Type           SIMPLE
 Discretization Scheme

  Variable    Scheme
  ----------------------------
  Pressure    PRESTO!
  Momentum    First Order Upwind
  Energy      First Order Upwind

 Solution Limits

  Quantity                    Limit
  --------------------------------
  Minimum Absolute Pressure    1
  Maximum Absolute Pressure    5e+10
  Minimum Temperature          1
  Maximum Temperature          5000

Material Properties
-------------------

  Material: water-liquid (fluid)

  Property                        Units      Method    Value(s)
  ----------------------------------------------------------------
-
    Density                       kg/m3      constant    998.2
    Cp (Specific Heat)            j/kg-k     constant    4182
    Thermal Conductivity          w/m-k      constant    0.6
    Viscosity                     kg/m-s     constant    0.001003
    Molecular Weight              kg/kgmol   constant    18.0152
```

```
        L-J Characteristic Length       angstrom    constant    0
        L-J Energy Parameter            k           constant    0
        Thermal Expansion Coefficient   1/k         constant    0
        Degrees of Freedom                          constant    0
        Speed of Sound                  m/s         none        #f
                    Mass Flow Rate                (kg/s)
--------------------------------    --------------------
                        inlet               0.010611
                       outlet             -0.010611001
                --------------- --------------------
                          Net            -1.8626451e-09
```

Polymath scripts for reactor modeling from first principles

The following scripts were used for modeling experiments two and three in Polymath. The predicted results obtained from these two experiments were compared with the experimental results obtained in order to validate the model of the MBR that was developed from first principles.

Script for experiment two

ODE Report (RKF45)

Differential equations as entered by the user
[1] d(Ca)/d(t) = (v/V)*(Ca0-Ca) + rA
[2] d(Cp)/d(t) = (Ca*v - Cp*v)/Vp
[3] d(Cs)/d(t) = (v/V)*(Cs0 - Cs) - rA
Explicit equations as entered by the user
[1] v = 0.0005
[2] V = 0.01186
[3] timek2 = 330
[4] ea0 = 6.38
[5] kd = 0.0016
[6] Km = 68
[7] Ca0 = 0
[8] ea = ea0*exp(-kd*t)
[9] Vp = v*t
[10] Vso = 1.2
[11] Cs0 = 80

[12] Coutk2 = 1.07

[13] X = (Ca/Cs0)*100

[14] eak2 = 6.38*exp(-0.0016*timek2)

[15] Foutk2 = 0.95

[16] ratek2 = (Foutk2*Coutk2/1000)/V

[17] k2 = ratek2/eak2

[18] rA = k2*(ea0*(exp(-kd*t))*(Cs))/(Km + Cs)

[19] Fproduct = Ca*v/V

Comments

[4] v = 0.0005

   Permeate flux (L/min)

[5] V = 0.01186

   Membrane volume (L)

[6] k2 = ratek2/eak2

   Constant (mM/min.mg)

[7] ea0 = 6.38

   Initial amount of active amidase (mg)

[8] kd = 0.0016

   Deactivation constant (min-1)

[9] Km = 68

   MM constant (mM)

[10] Ca0 = 0

   Initial product concentration (mM)

[11] ea = ea0*exp(-kd*t)

   Amount of active amidase at a specific time (mg)

[12] Vp = v*t

   Total volume of permeate formed (L)

[13] Vso = 1.2

   Initial volume of substrate (L)

[14] Cs0 = 80

   Initial substrate concentration (mM)

[15] rA = k2*(ea0*(exp(-kd*t))*(Cs))/(Km + Cs)

   Reaction rate (mmol/L.min)

[16] X = (Ca/Cs0)*100

   Instantaneous conversion (%)

[17] timek2 = 330

   Time at which k2 to is calculated (minutes)

[18] Foutk2 = 0.95

   Permeate flowrate at time at which k2 is calculated (mL/min)

[19] Coutk2 = 1.07
   Product concentration in permeate stream at time at which k2 is calculated (mM)
[20] ratek2 = (Foutk2*Coutk2/1000)/V
   Rate that is used to calculate k2 (mmol/L.min)
[21] eak2 = 6.38*exp(-0.0016*timek2)
   Amount of active enzyme used to calculate k2 (mg)
[22] Fproduct = Ca*v/V
   Instantaneous productivity (mmol/L.min)
Independent variable
variable name : t
initial value : 1
final value : 3000
Precision
Step size guess. h = 0.000001
Truncation error tolerance. eps = 0.000001
General
number of differential equations: 3
number of explicit equations: 20

Script for experiment 3

ODE Report (RKF45)

Differential equations as entered by the user
[1] d(Ca)/d(t) = (v/V)*(Ca0-Ca) + rA
[2] d(Cp)/d(t) = (Ca*v - Cp*v)/Vp
[3] d(Cs)/d(t) = (v/V)*(Cs0 - Cs) - rA
Explicit equations as entered by the user
[1] v = 0.0001
[2] V = 0.01186
[3] timek2 = 135
[4] ea0 = 20.09
[5] kd = 0.0016
[6] Km = 68
[7] Ca0 = 0
[8] ea = ea0*exp(-kd*t)
[9] Vp = v*t
[10] Vso = 1
[11] Cs0 = 40

[12] Coutk2 = 1.46

[13] X = (Ca/Cs0)*100

[14] eak2 = ea0*exp(-kd*timek2)

[15] Foutk2 = 0.3

[16] ratek2 = (Foutk2*Coutk2/1000)/V

[17] k2 = ratek2/eak2

[18] rA = (k2*(ea)*(Cs))/(Km + Cs)

[4] v = 0.0001

Permeate flux (L/min)

[5] V = 0.01186

Membrane volume (L)

[6] k2 = ratek2/eak2

Constant (mM/min.mg)

[7] ea0 = 20.09

Initial amount of active amidase (mg)

[8] kd = 0.0016

Deactivation constant (min-1)

[9] Km = 68

MM constant (mM)

[10] Ca0 = 0

Initial product concentration (mM)

[11] ea = ea0*exp(-kd*t)

Amount of active amidase at a specific time (mg)

[12] Vp = v*t

Total volume of permeate formed (L)

[13] Vso = 1

Initial volume of substrate (L)

[14] Cs0 = 40

Initial substrate concentration (mM)

[15] rA = k2*(ea0*(exp(-kd*t))*(Cs))/(Km + Cs)

Reaction rate (mmol/L.min)

[16] X = (Ca/Cs0)*100

Instantaneous conversion (%)

[17] timek2 = 135

Time at which k2 to is calculated (minutes)

[18] Foutk2 = 0.3

Permeate flowrate at time at which k2 is calculated (mL/min)

[19] Coutk2 = 1.46

Product concentration in permeate stream at time at which k2 is calculated (mM)

[20] ratek2 = (Foutk2*Coutk2/1000)/V

Rate that is used to calculate k2 (mmol/L.min)

[21] eak2 = 6.38*exp(-0.0016*timek2)

Amount of active enzyme used to calculate k2 (mg)

[22] Fproduct = Ca*v/V

Instantaneous productivity (mmol/L.min)

Independent variable

variable name : t

initial value : 1

final value : 5000

Precision

Step size guess. h = 0.000001

Truncation error tolerance. eps = 0.000001

General

number of differential equations: 3

number of explicit equations: 18

Appendix III: Characterisation of the free amidase

Comparison of experimental and predicted amidase specific activity at different temperatures and pHs

The results obtained from the factorial design experiment were used to develop an empirical model predicting the specific amidase activity at different temperatures and pHs. From a comparison of the experimental and predicted results it can be seen that the model fits the experimental results very well.

Effect of temperature on amidase specific activity at a specific pH
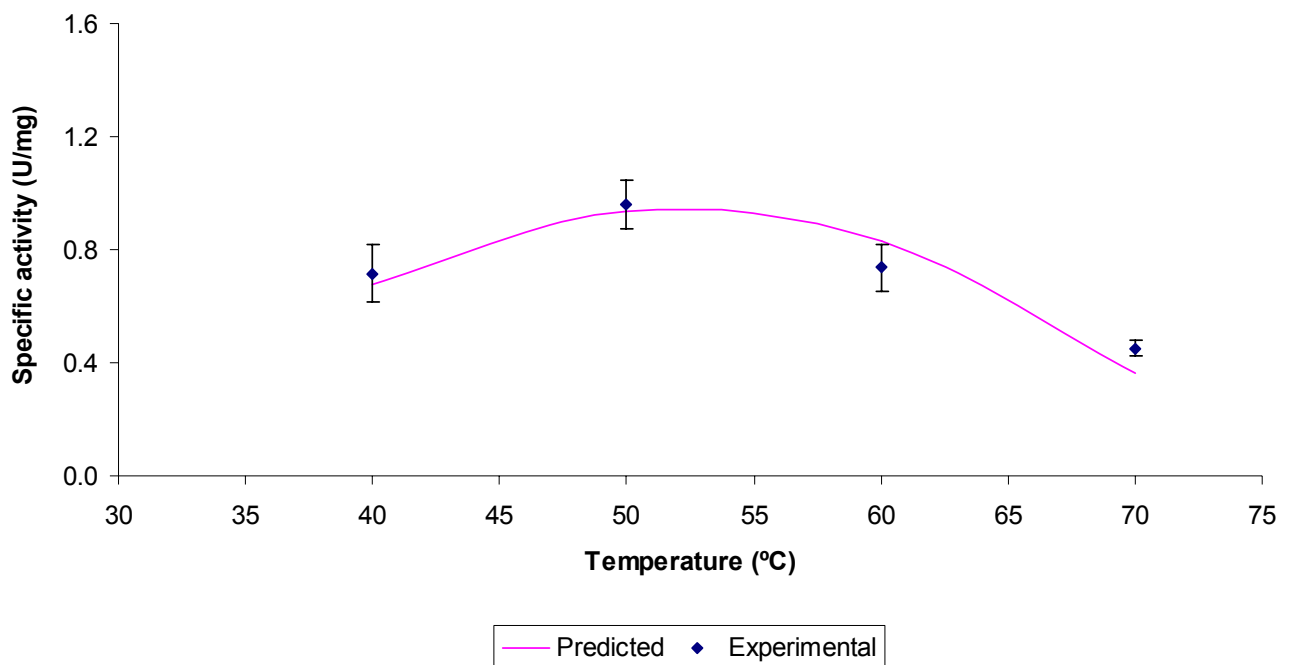
Figure A.4: Experimental and predicted specific activity of amidase at a pH of 6.0
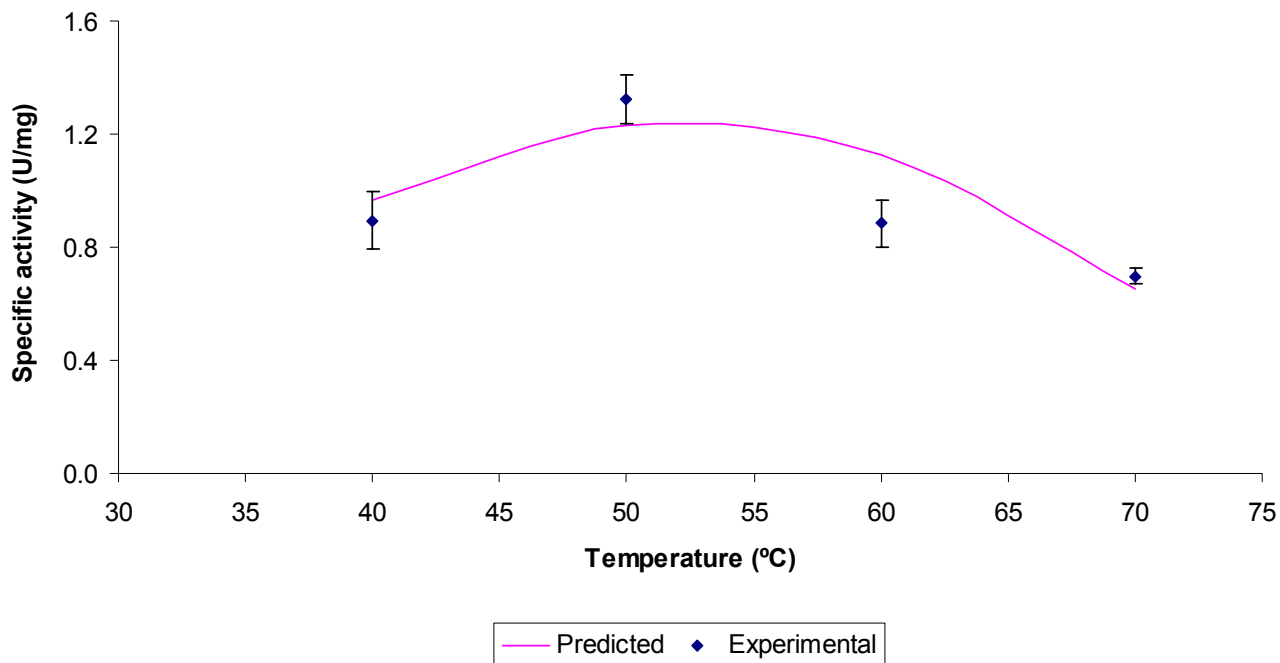
Figure A.5: Experimental and predicted specific activity of amidase at a pH of 7.0
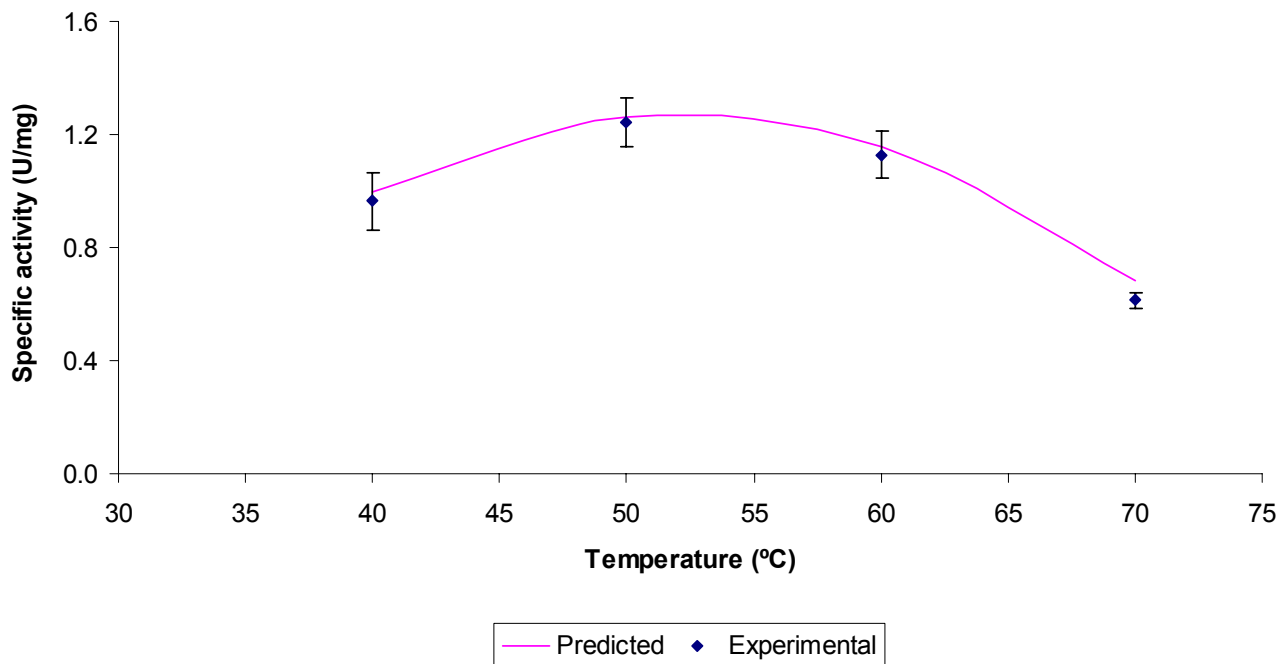
Figure A.6: Experimental and predicted specific activity of amidase at a pH of 8.5

Effect of pH on amidase specific activity at a specific temperature
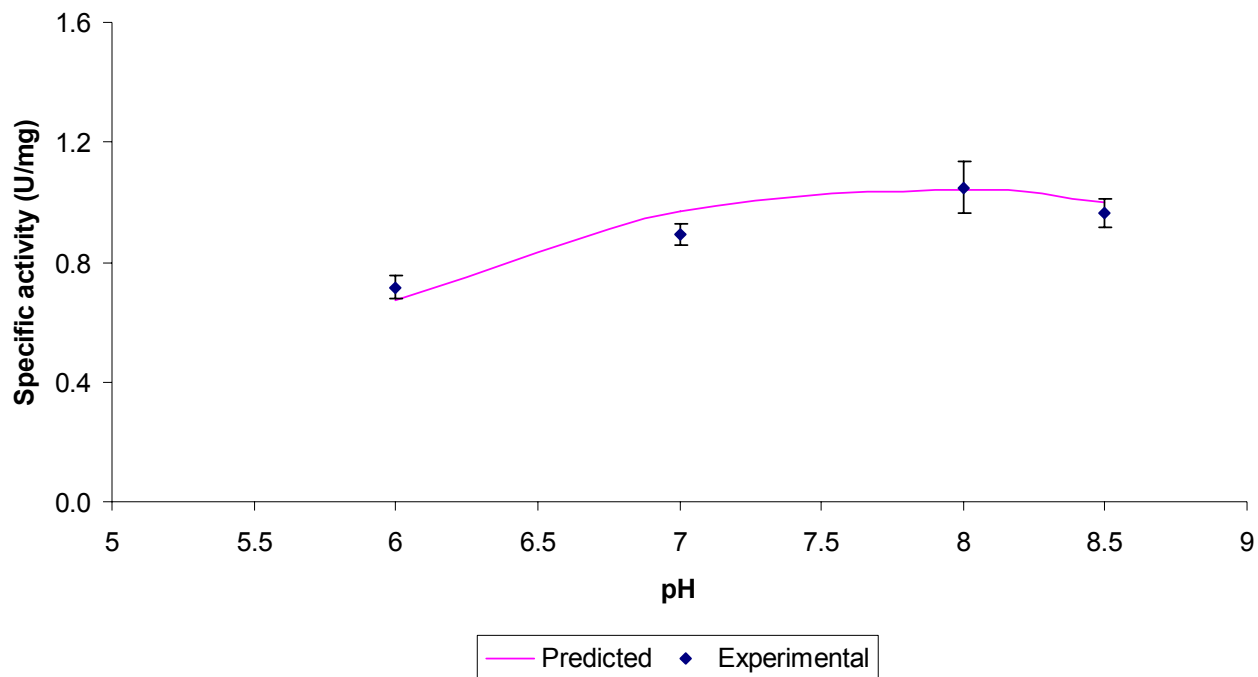
Figure A.7: Experimental and predicted specific activity of amidase at a temperature of 40ºC
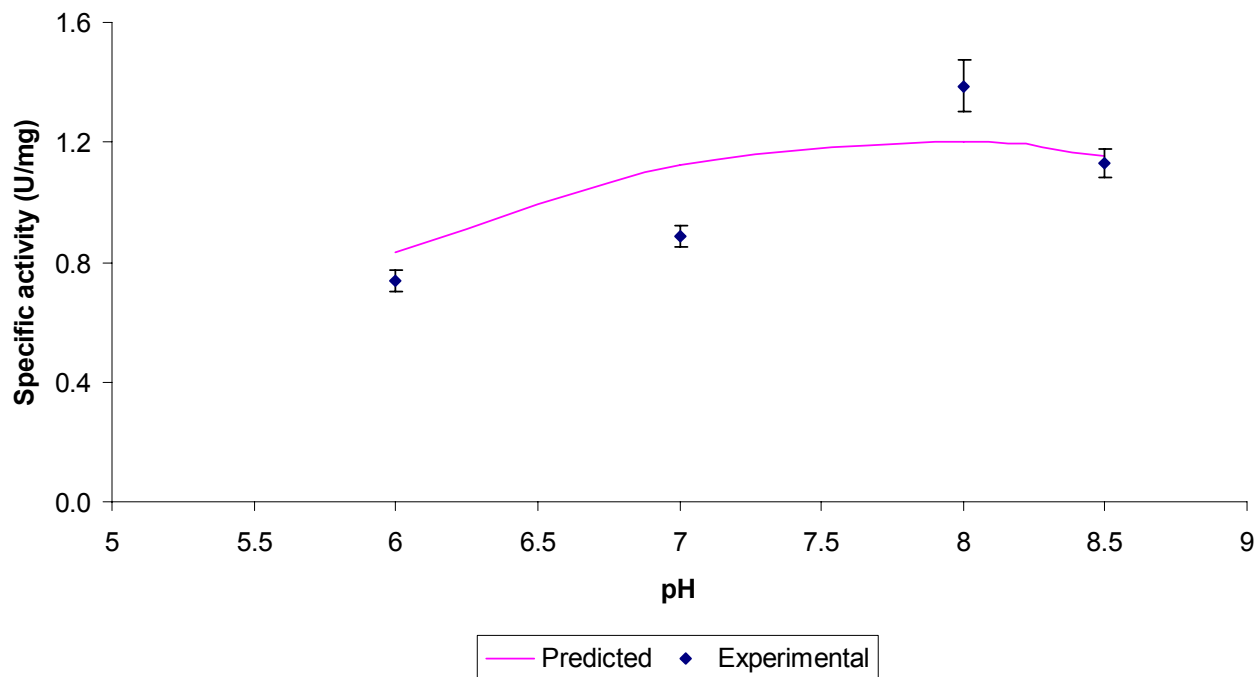
Figure A.8: Experimental and predicted specific activity of amidase at a temperature of 60ºC
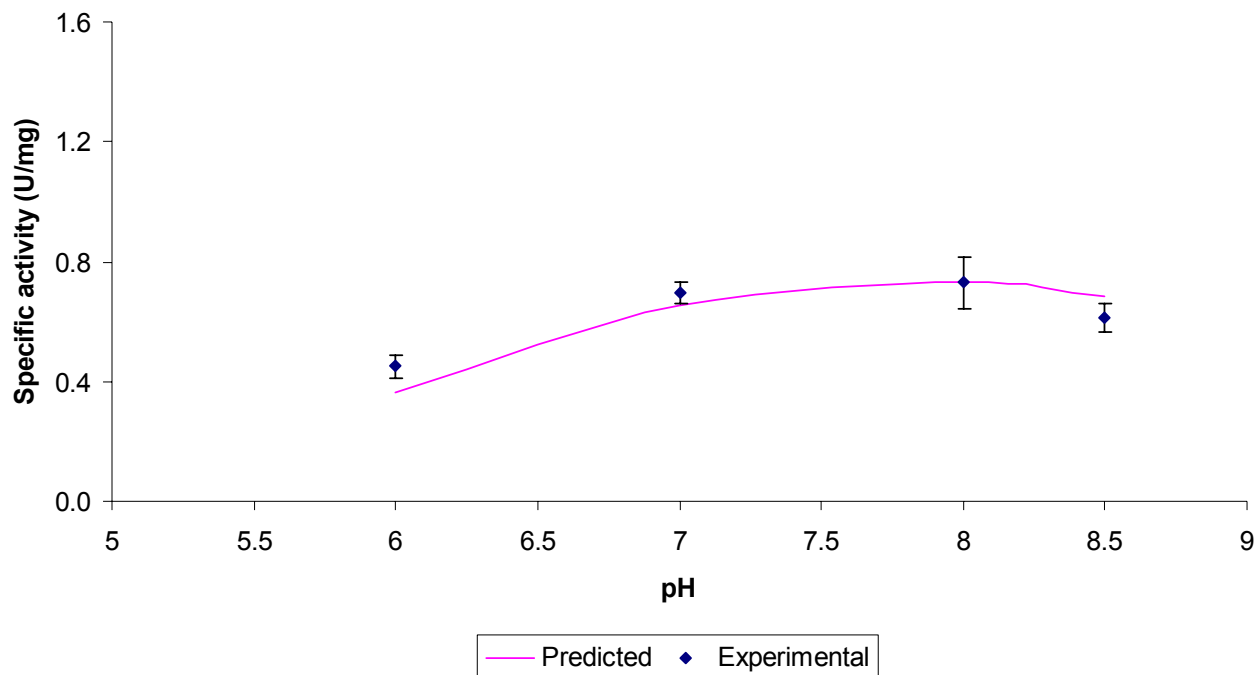
Figure A.9: Experimental and predicted specific activity of amidase at a temperature of 70ºC

Determination of amidase initial rate of reaction at different substrate concentrations

The amount of product formed by the amidase over the first few minutes of reaction were determined and plotted for various substrate concentrations at a temperature of 50ºC, a pH of 8.0 and an amidase concentration of 1mg/mL. Two independent experiments were conducted and plotted on the same curve. The initial rate of the amidase at a specific substrate concentration was the slope of each curve. For a specific substrate concentration the initial rate of reaction was taken as the average initial rate or reaction obtained from the two independent experiments.

$y = 0.2443x + 0.786$
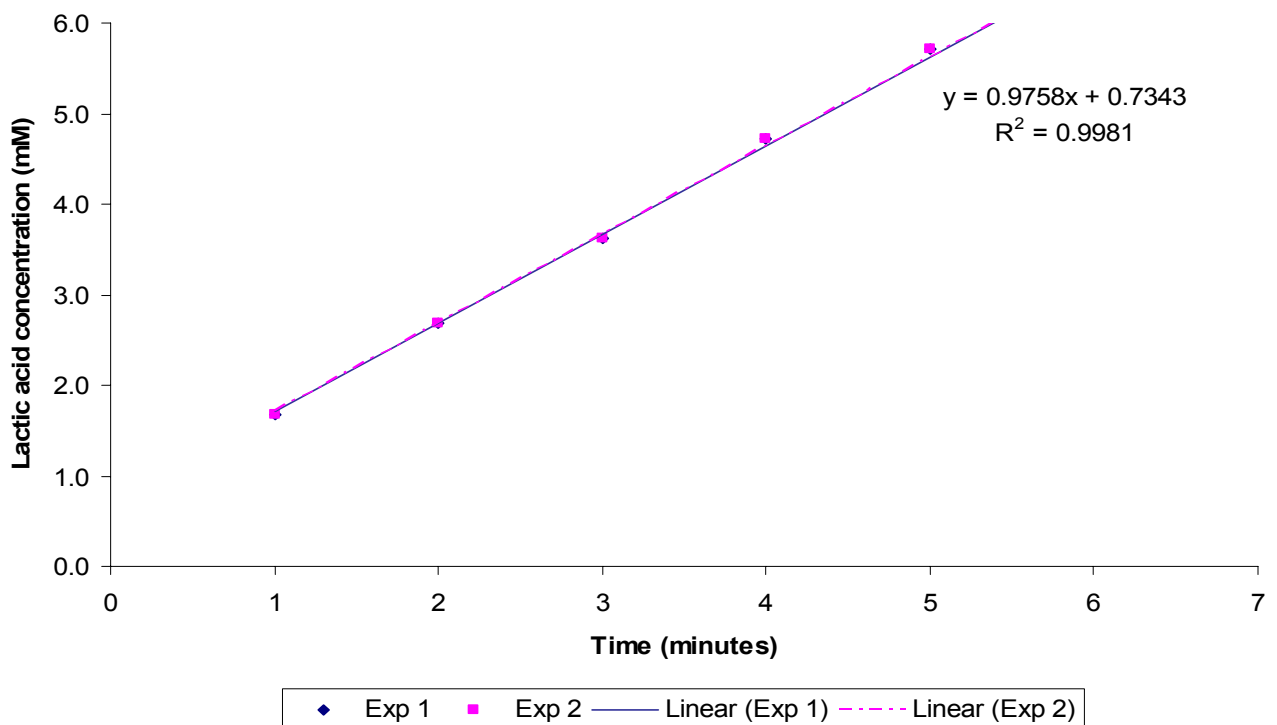$R^2 = 0.9517$

$y = 0.2427x + 0.3163$
$R^2 = 0.9969$
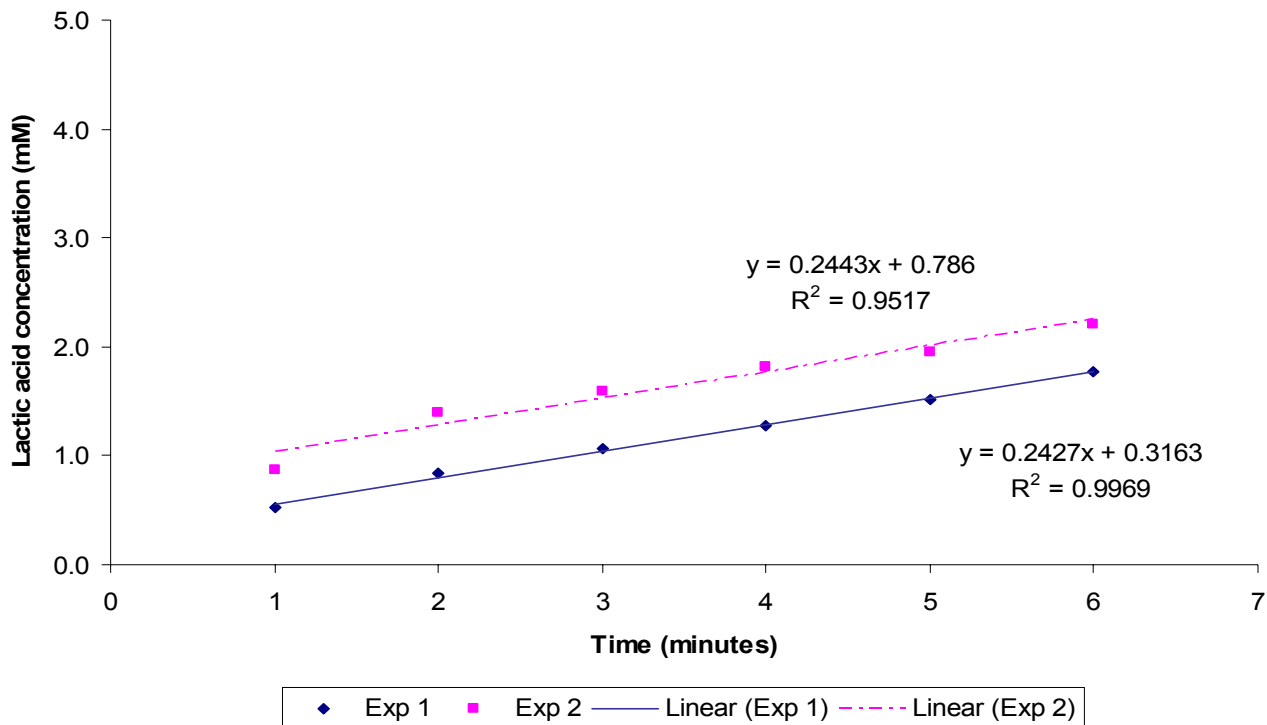
Figure A.10: Determination of the initial rate of reaction from the average of the two slopes of the graph at a substrate concentration of 15mM lactamide

$y = 0.4392x + 0.2718$
$R^2 = 0.9969$

$y = 0.3667x + 0.2483$
$R^2 = 0.9981$
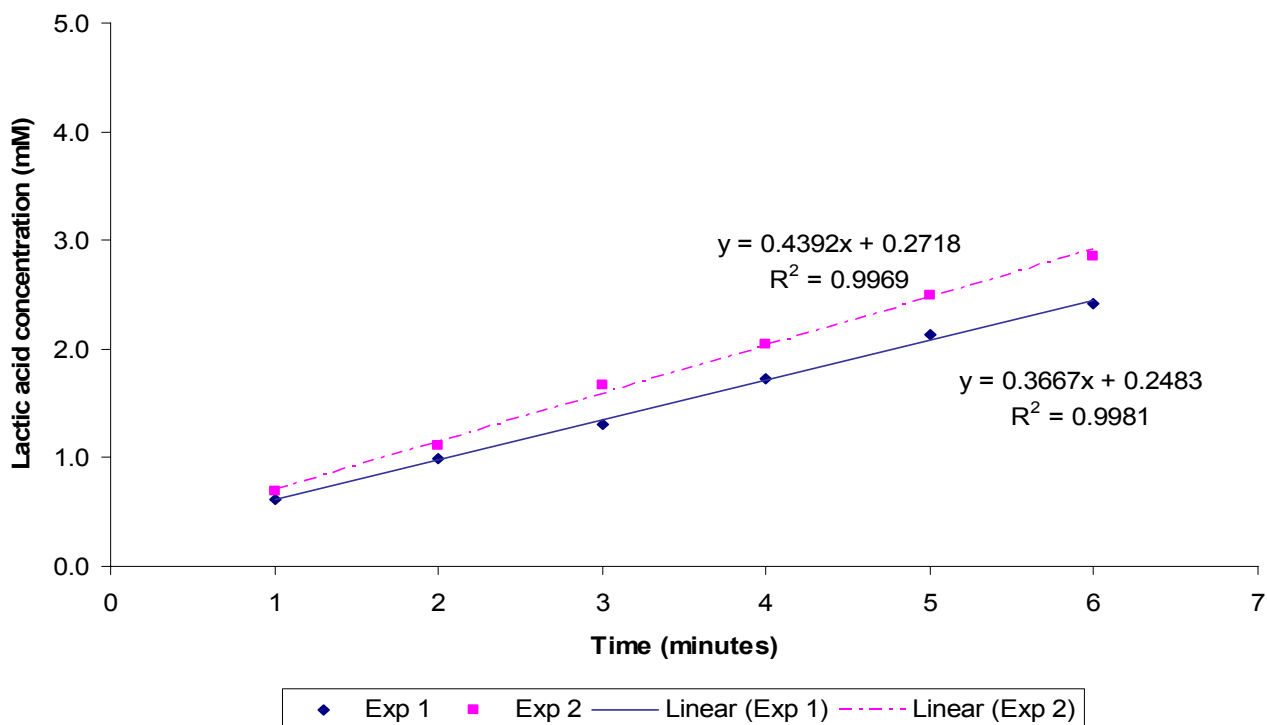
Figure A.11: Determination of the initial rate of reaction from the average of the two slopes of the graph at a substrate concentration of 25mM lactamide

$y = 0.6323x + 0.3761$
$R^2 = 0.9908$

$y = 0.5213x + 0.5189$
$R^2 = 0.9988$
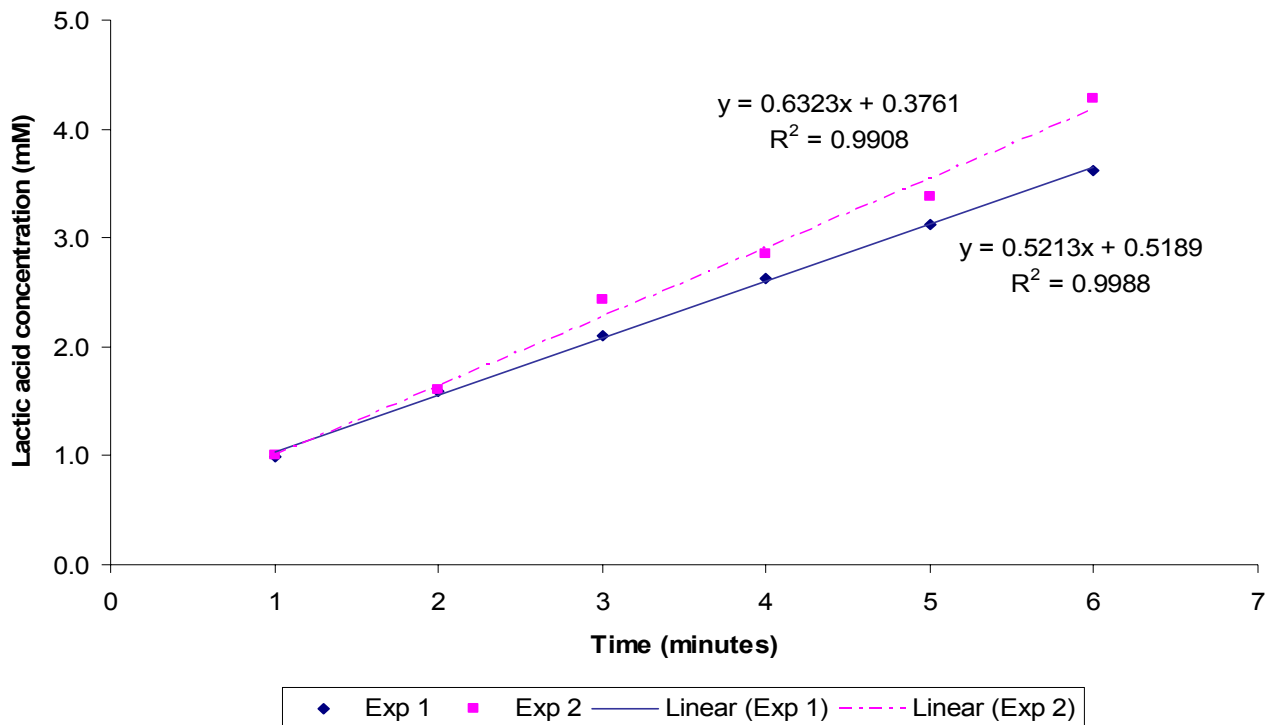
Figure A.12: Determination of the initial rate of reaction from the average of the two slopes of the graph at a substrate concentration of 40mM lactamide

$y = 0.8595x + 0.6546$
$R^2 = 0.998$

$y = 0.8146x + 0.5156$
$R^2 = 0.997$
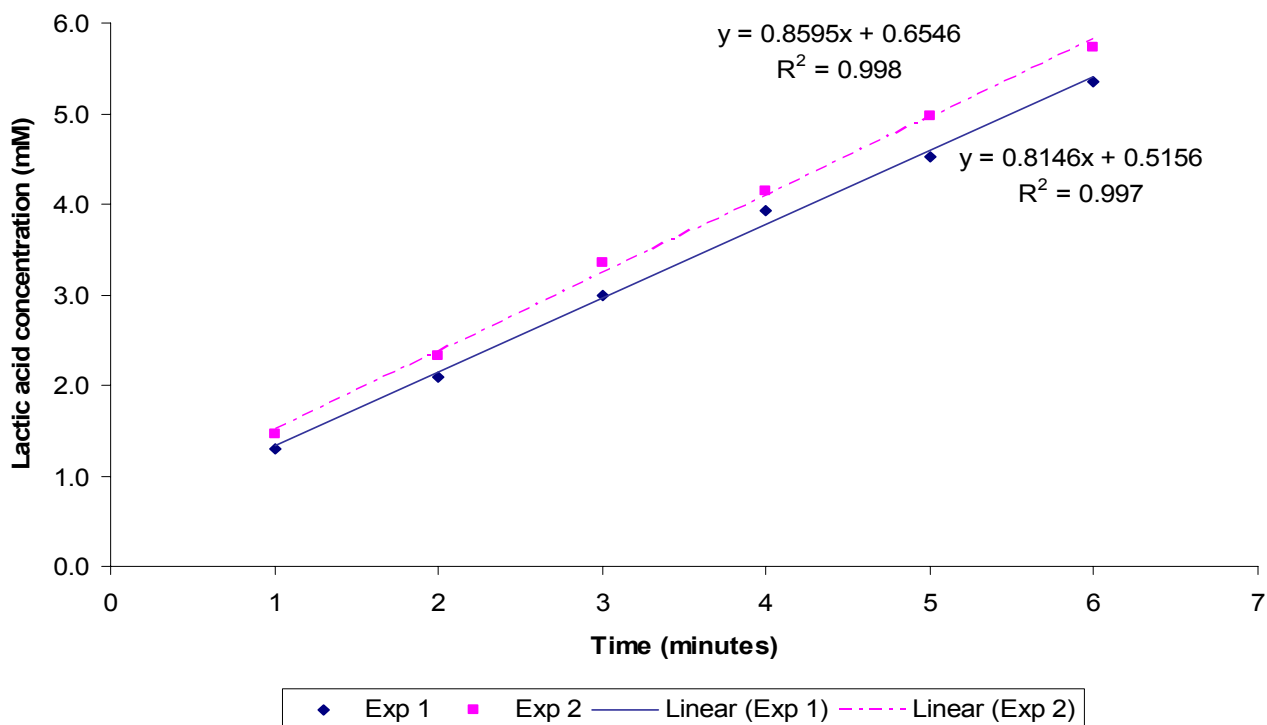
Figure A.13: Determination of the initial rate of reaction from the average of the two slopes of the graph at a substrate concentration of 80mM lactamide

153
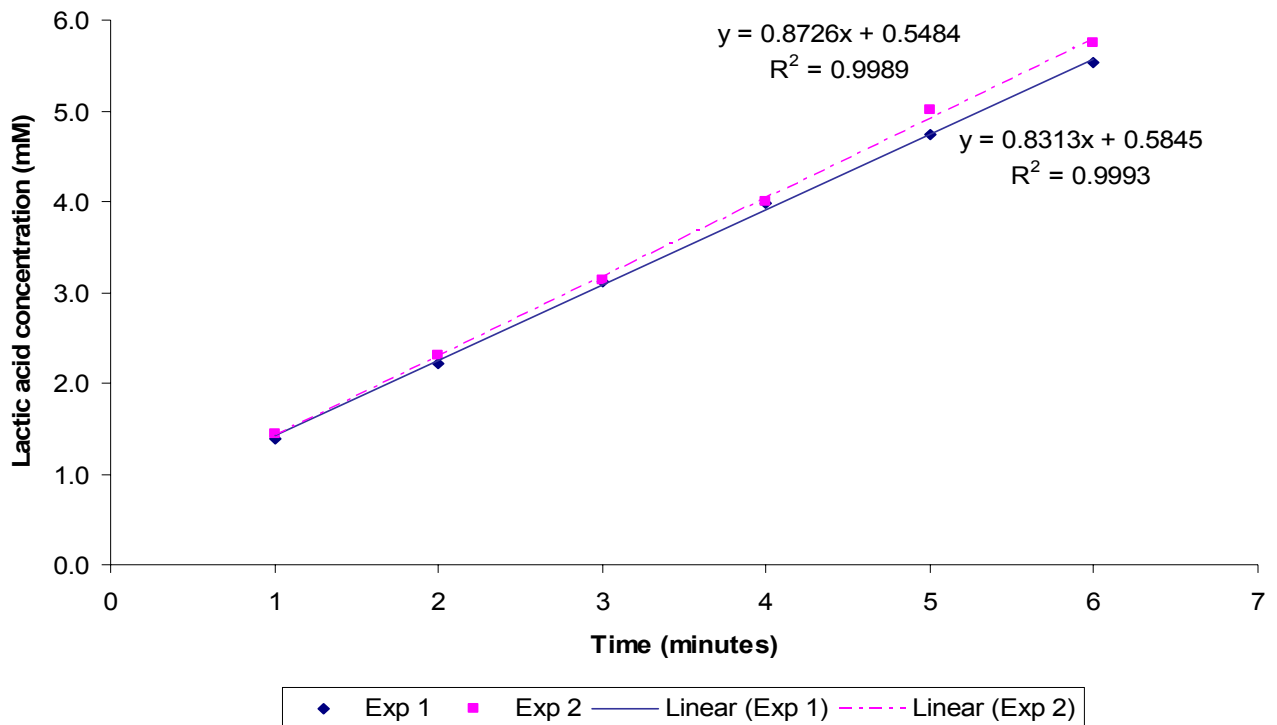
Figure A.14: Determination of the initial rate of reaction from the average of the two slopes of the graph at a substrate concentration of 100mM lactamide

Figure A.15: Determination of the initial rate of reaction from the average of the two slopes of the graph at a substrate concentration of 100mM lactamide

Appendix IV: Statistical validation of results

Residual plots for validation of model for free amidase half-life

The half-life of the free amidase was determined at substrate concentrations of 40 mM and 80 mM. An exponential decay model was fitted to the data with non-linear regression. Residual plots were drawn at both substrate concentrations to ensure the basic model assumptions were not violated.

Residual plots at a substrate concentration of 40 mM
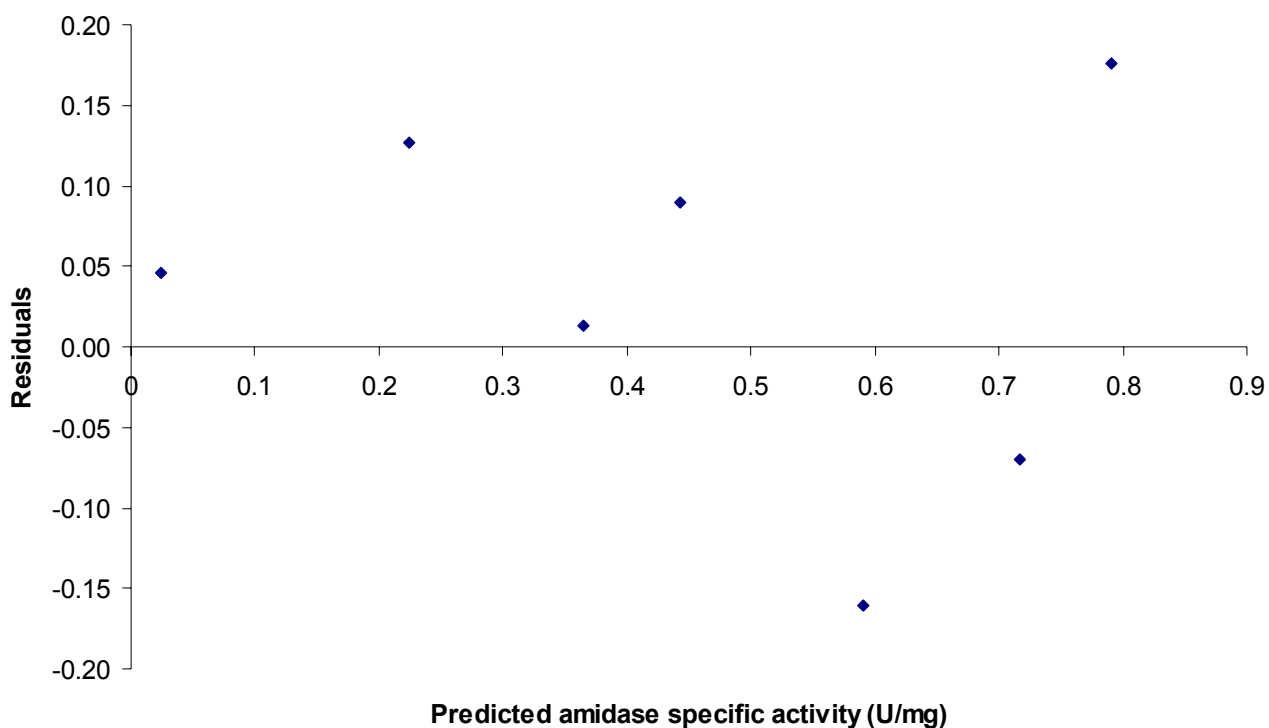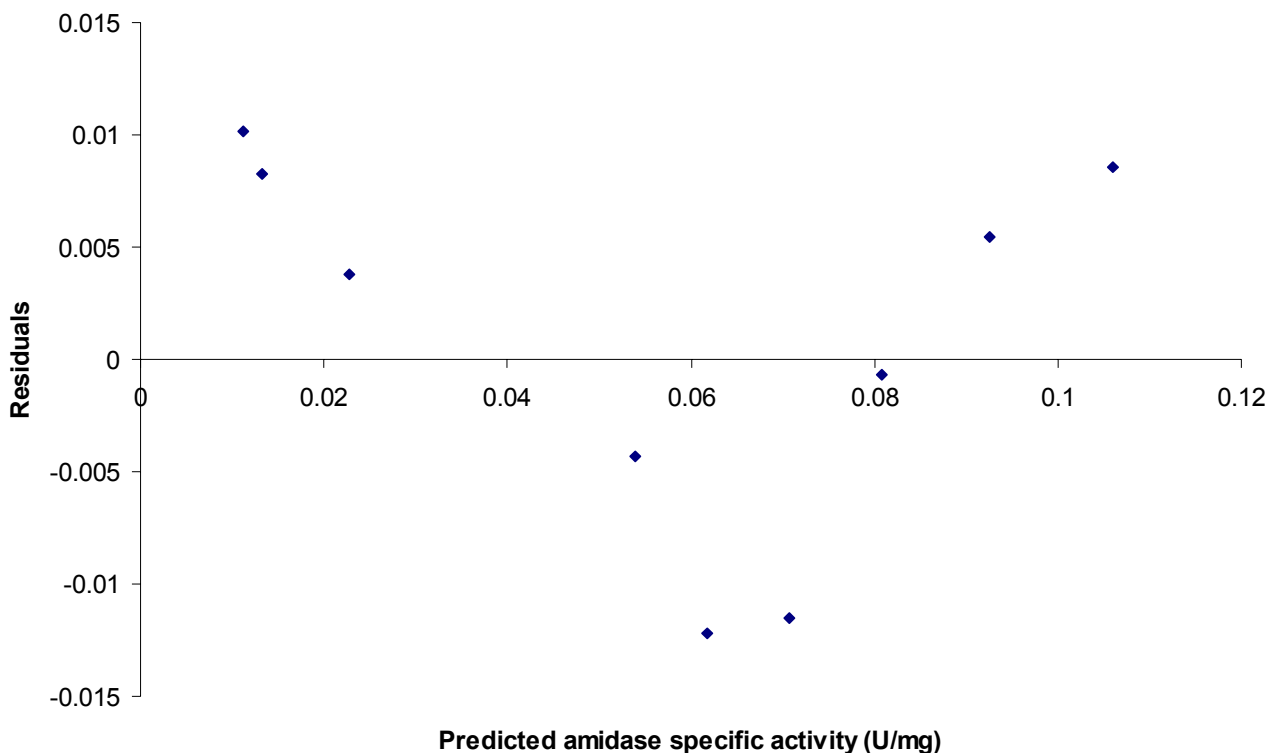

Figure A.16: Validation of the assumption of homogeneous variances of the residuals
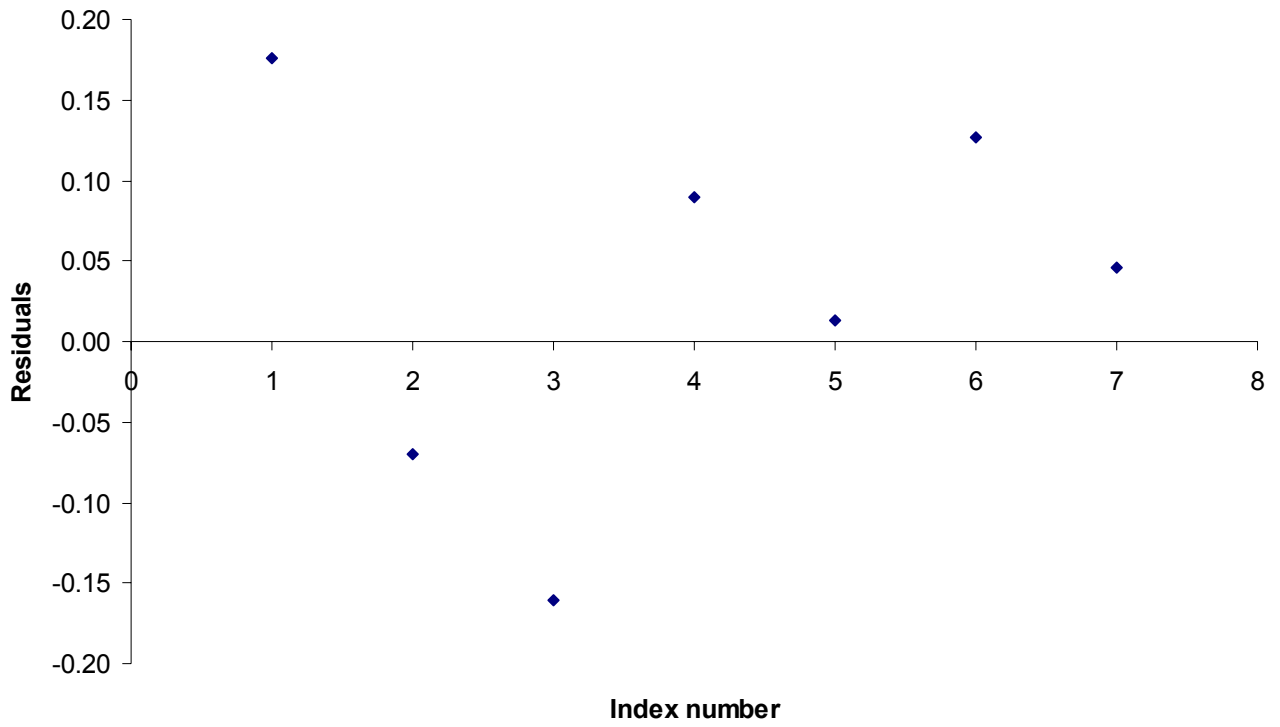
Figure A.17: Validation of the assumption of normality of residuals

Residual plots at a substrate concentration of 80 mM
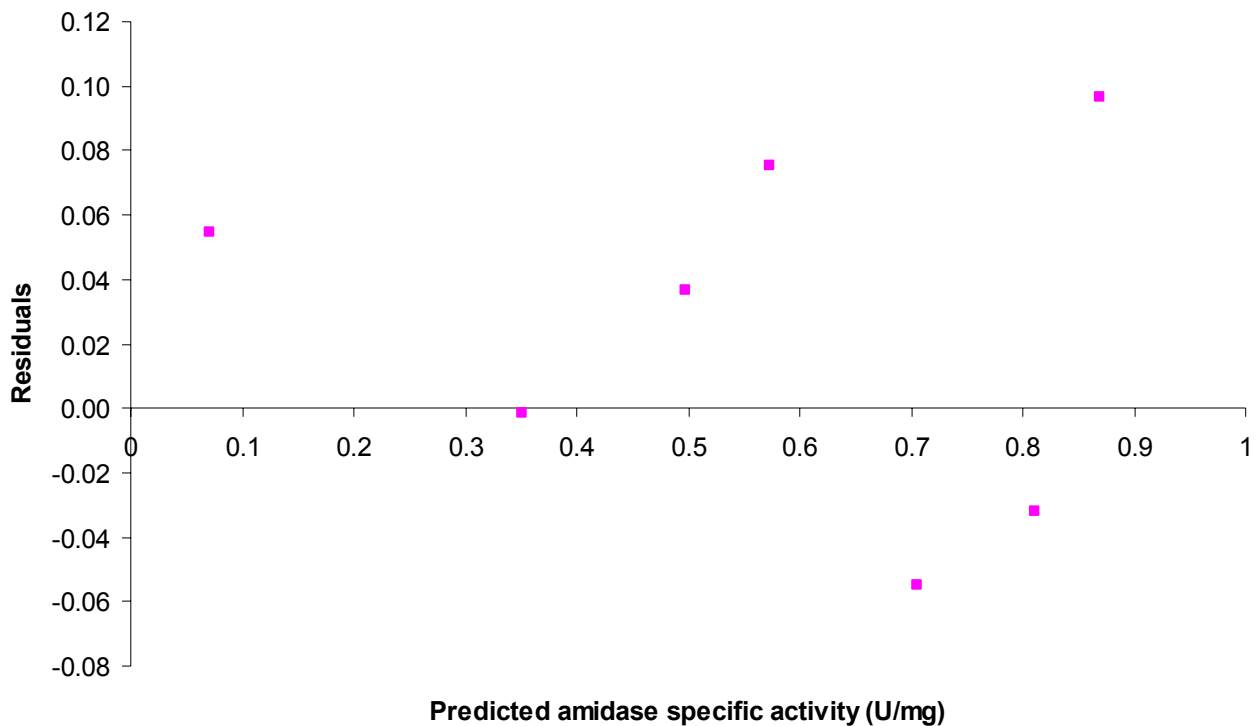
Figure A.18: Validation of the assumption of homogeneous variances of the residuals
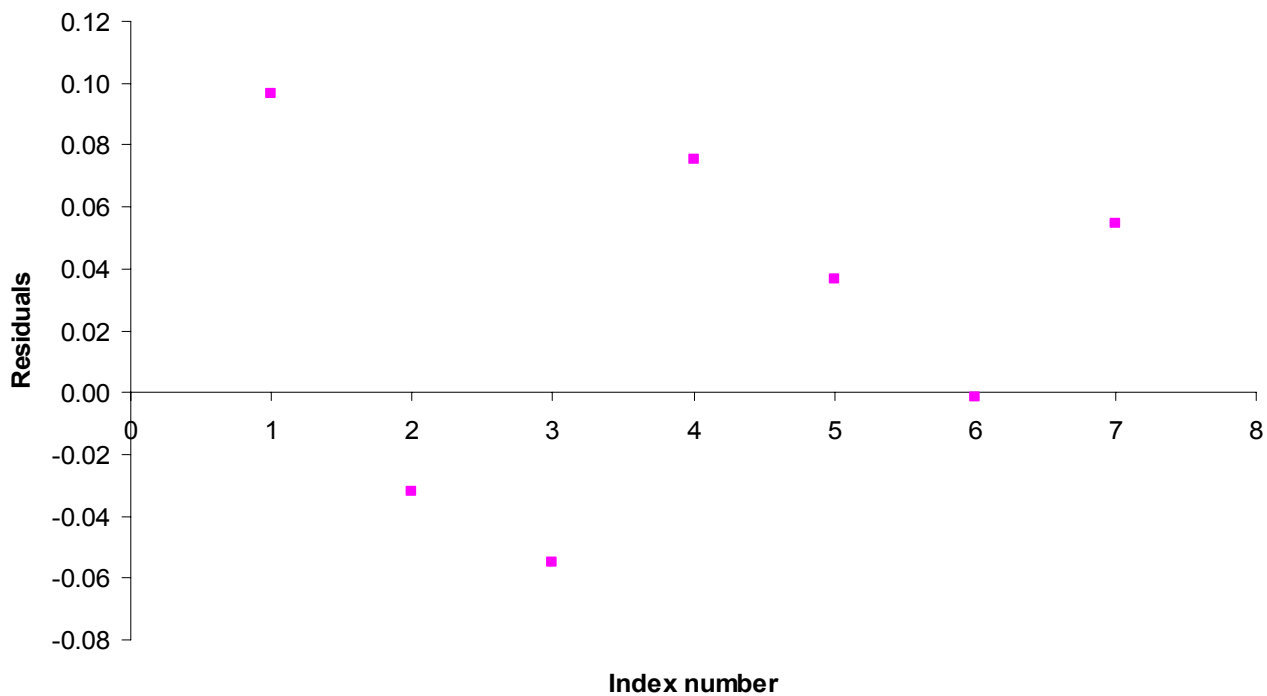
Figure A.19: Validation of the normality of residuals

Determination of significance of the effect of substrate concentration on the free amidase half-life

The significance of the difference between the free amidase specific activity obtained over time at a substrate concentration of 40 mM and at a substrate concentration of 80 mM was determined in order to evaluate the effect of substrate concentration on the stability of the free amidase. A statistical F-test was used first in order to test the hypothesis of equal variances between the two sets of data. Next a statistical z-test was performed to test the hypothesis of equal means between the two sets of data.

Statistical F-test

F-Test Two-Sample for Variances: T=50ºC

	40 mM	*80 mM*
Mean	0.467	0.557
Variance	0.0774	0.0732
Observations	13	14
df	12	13
F	1.058	
P(F<=f) one-tail	0.458	
F Critical one-tail	2.603	

The null hypothesis is that the data comes from two populations with the same variances. Since F is close to 1 (1.058) the null hypothesis cannot be rejected (with a confidence of 95%). The value "P(F<=f) one-tail" gives the probability (45.8%) of seeing a F value greater than 1.058 if the populations have the same variances.

Statistical z-test

z-Test Two Sample for Means: T=50ºC

	40 mM	*80 mM*
Mean	0.467	0.557
Known Variance	0.0775	0.0732
Observations	13	14
Hypothesized Mean Difference	0	
z	-0.853	
P(Z<=z) two-tail	0.394	
z Critical two-tail	1.959	

The null hypothesis for the z-test is that the data comes from two populations with the same means. Since the "z Critical two-tail" value is larger than the absolute value of z, it can be stated with a 95% accuracy that the null hypothesis cannot be rejected. The "P(Z<=z) two tail" value gives the probability of a z value that is farther away from zero than the absolute value of the current z is if the populations have the same means. The probability in this case is 39.4%.

Residual plots for validation of model for immobilised amidase half-life

A one-phase exponential decay model was fitted with non-linear regression to the data obtained from the free amidase stability studies. Residual plots were drawn to ensure the basic model assumptions were not violated.

Figure A.20: Validation of the assumption of homogeneous variances of the residuals
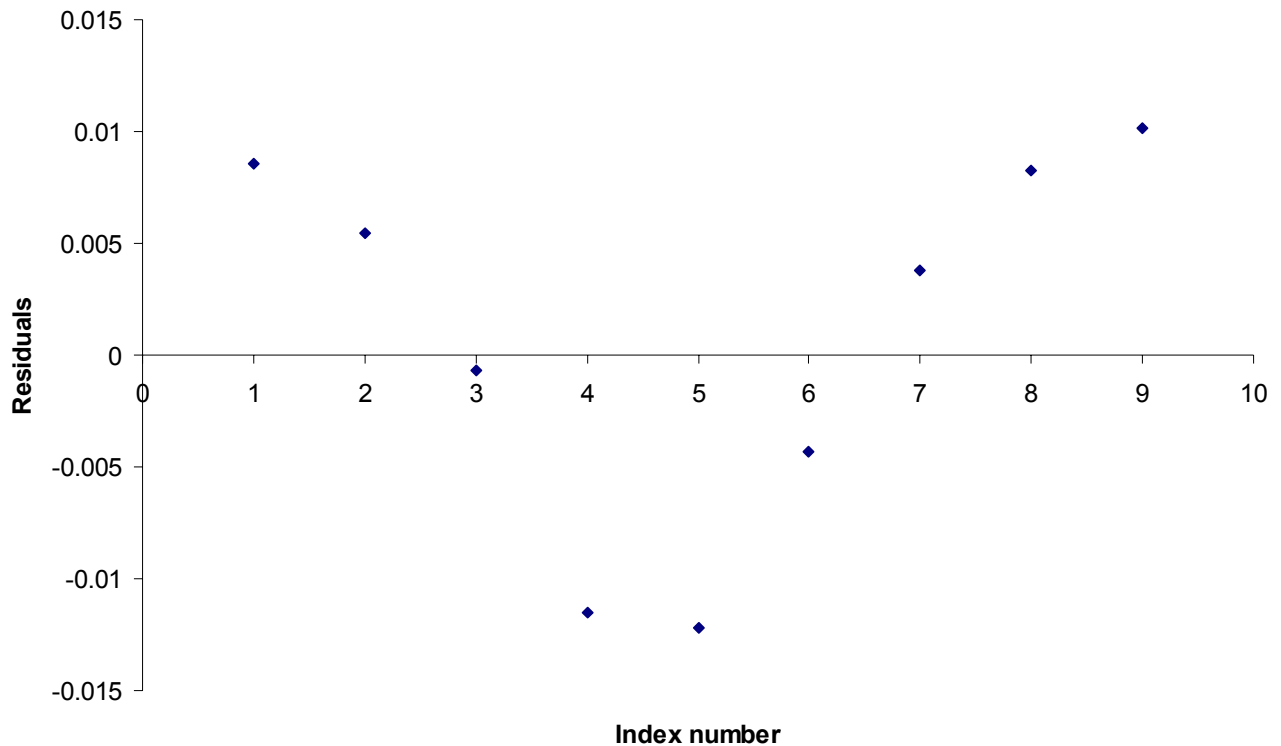
Figure A.21: Validation of the assumption of normality of residuals

Residual plots for validation of the CSTR model

Residual plots for the instantaneous conversion and instantaneous productivity for both experiments were drawn to check whether the assumptions of homoscedacity and normality of residuals made during the development of the model have not been violated.

Residual plots for experiment 1
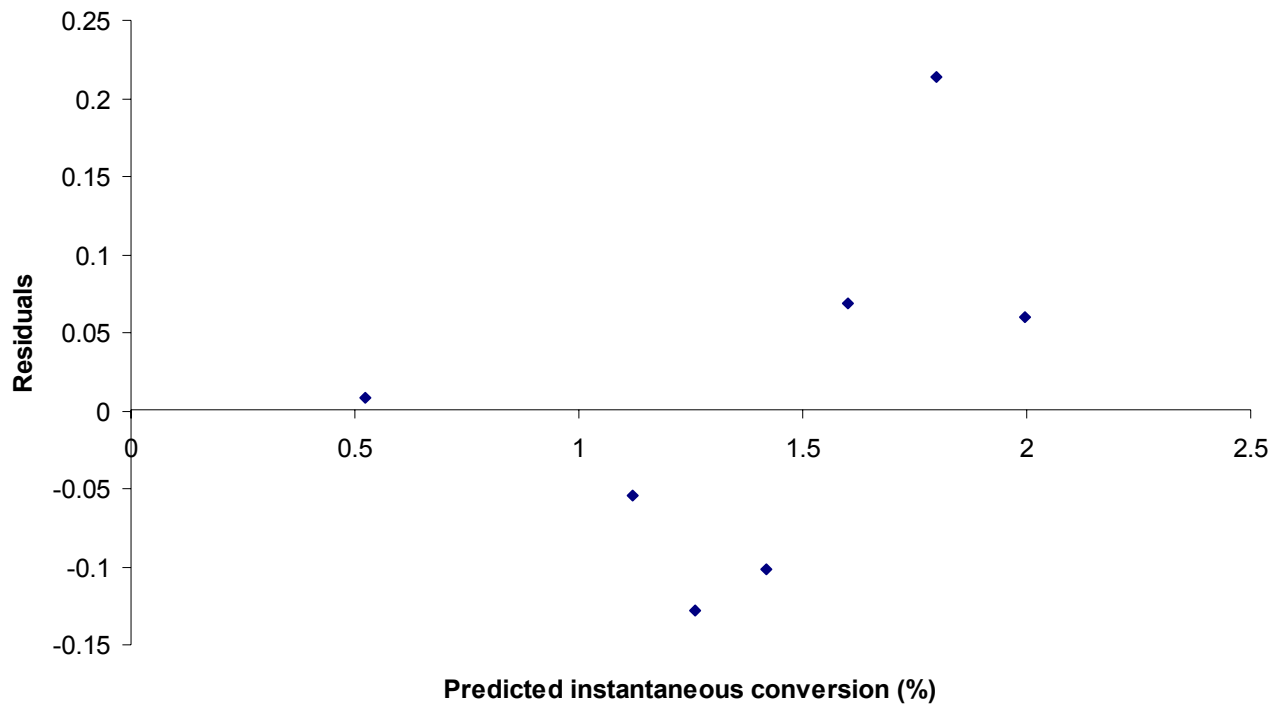
Figure A.22: Validation of the assumption of homogeneous variances of the residuals for the instantaneous conversion
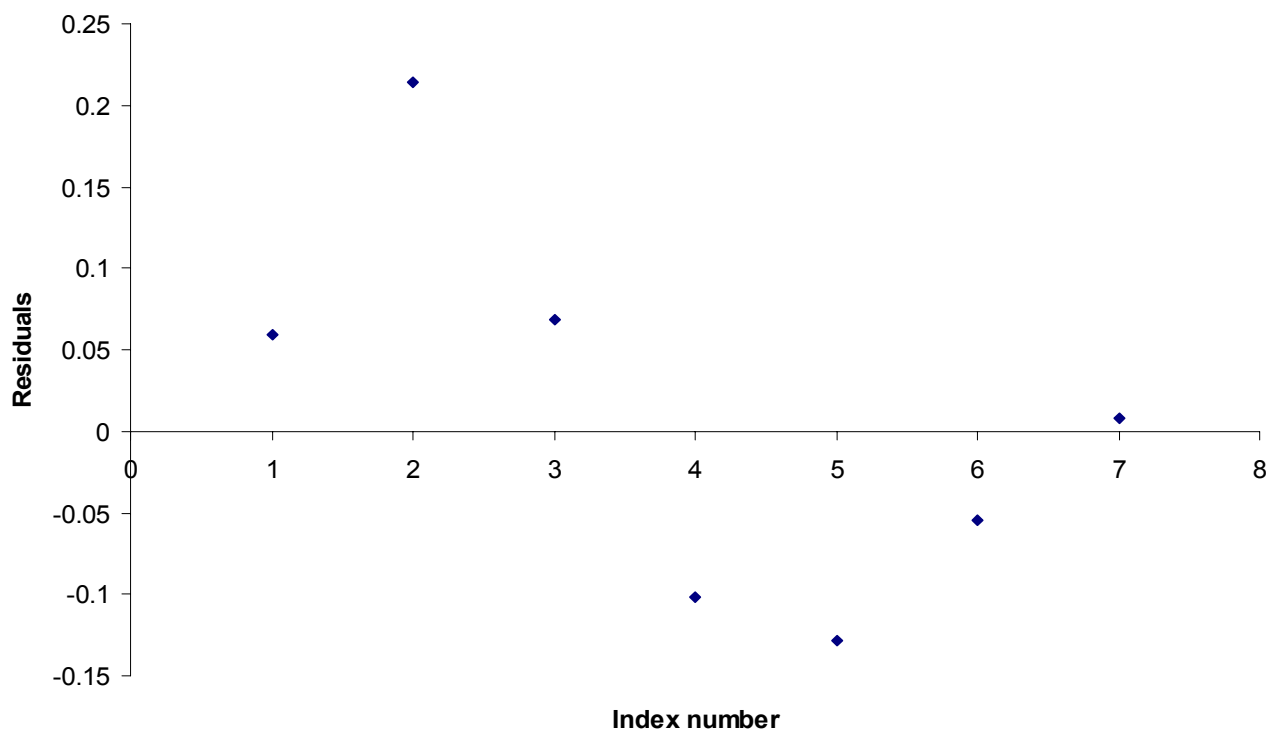
Figure A.23: Validation of the assumption of normality of residuals for the instantaneous conversion
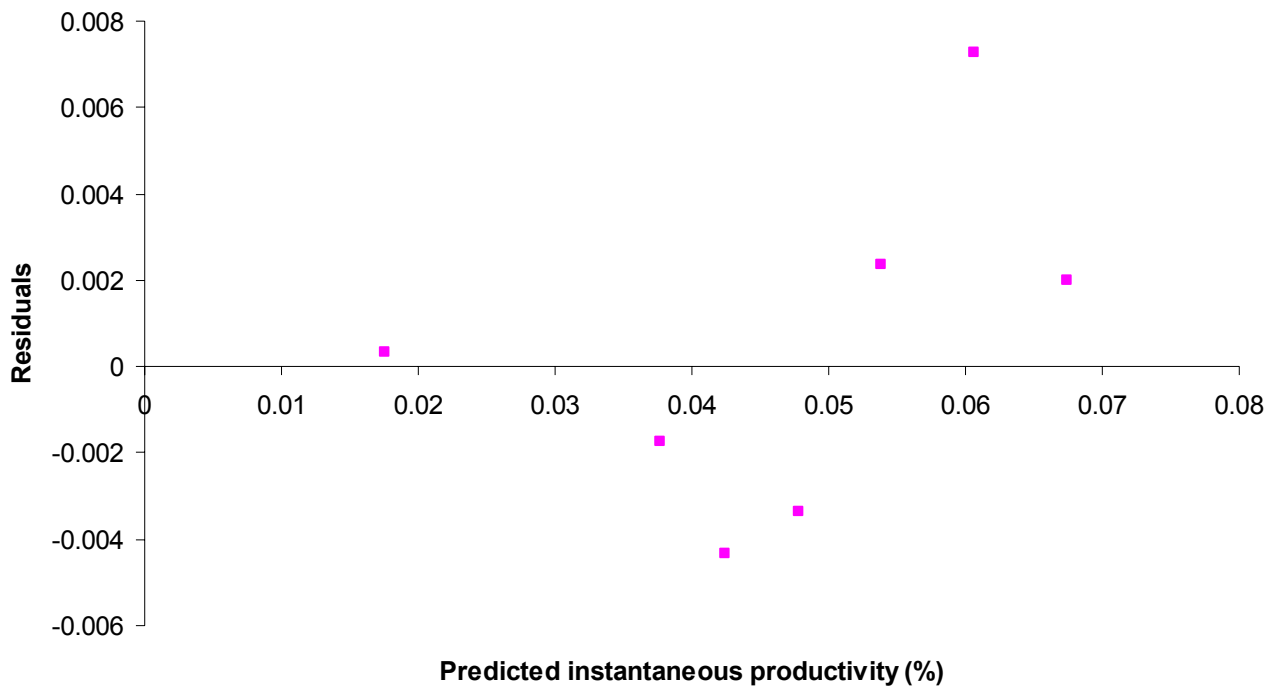
Figure A.24: Validation of the assumption of homogeneous variances of the residuals for the instantaneous productivity
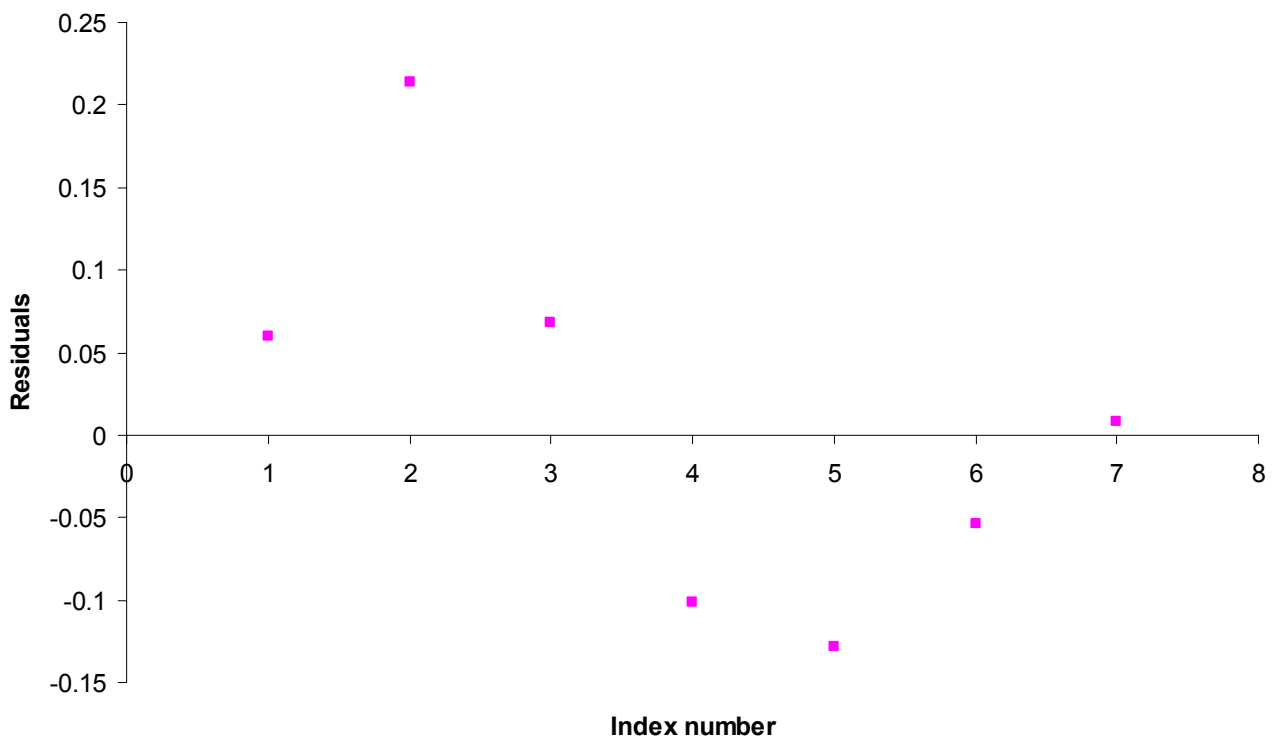
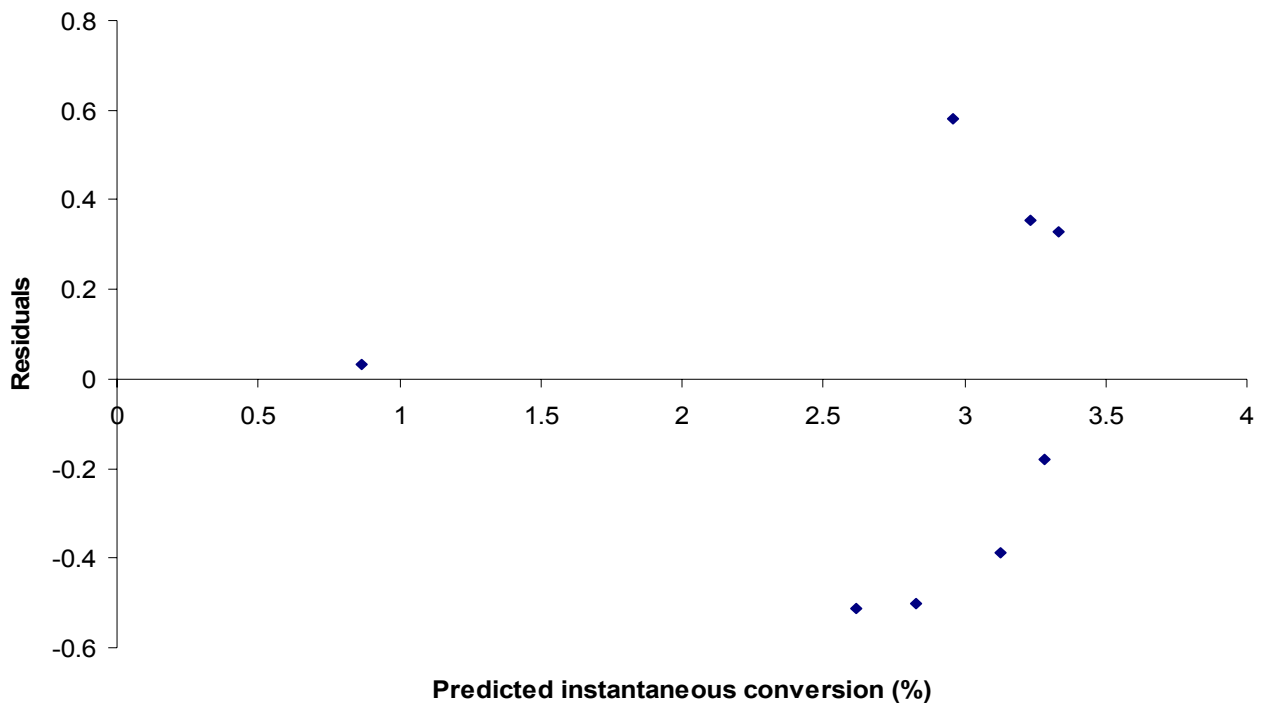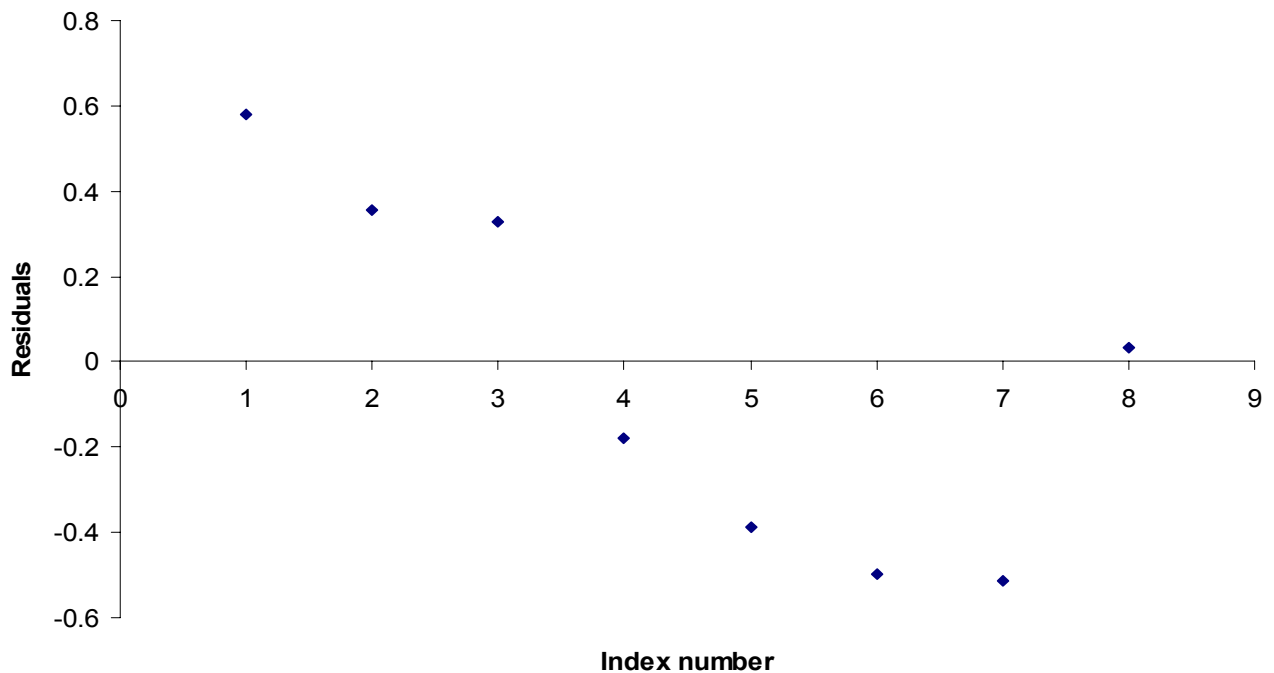**Figure A.25: Validation of the assumption of normality of residuals for the instantaneous productivity**

Residual plots for experiment 2

Figure A.26: Validation of the assumption of homogeneous variances of the residuals for the instantaneous conversion

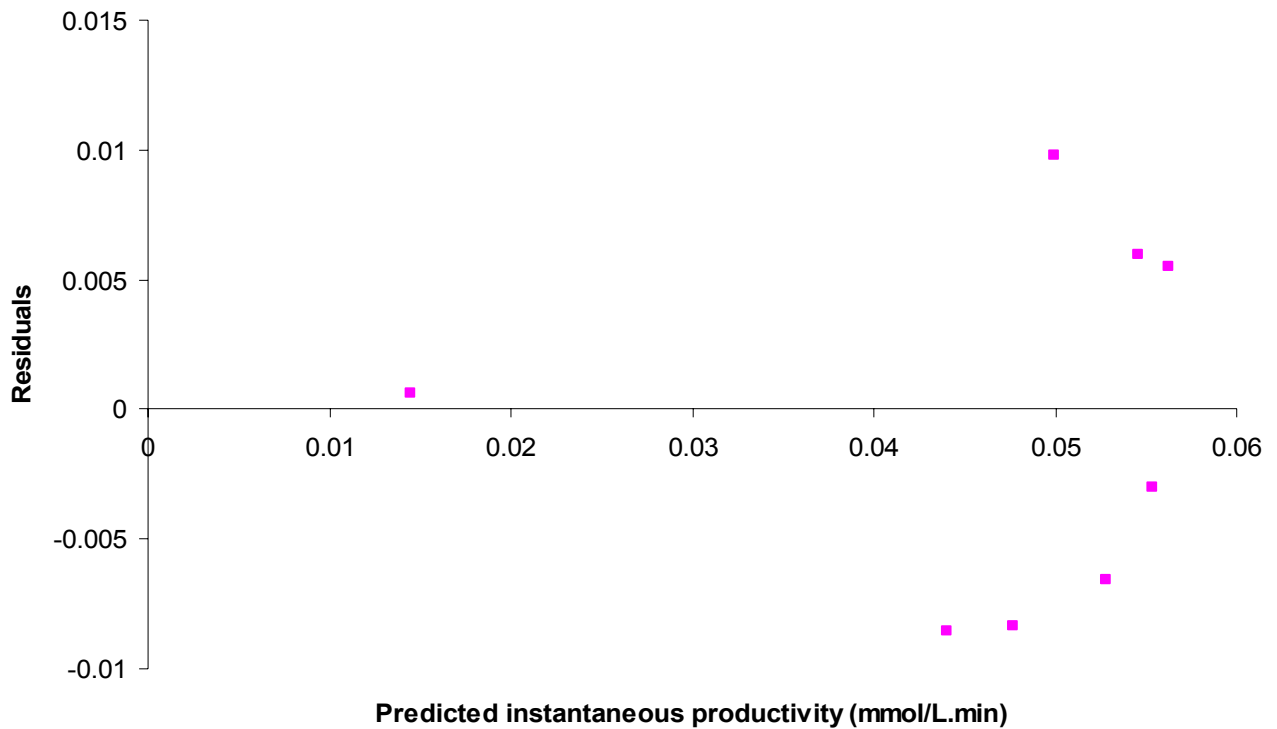**Figure A.27: Validation of the assumption of normality of residuals for the instantaneous conversion**

163

Figure A.28: Validation of the assumption of homogeneous variances of the residuals for the instantaneous productivity
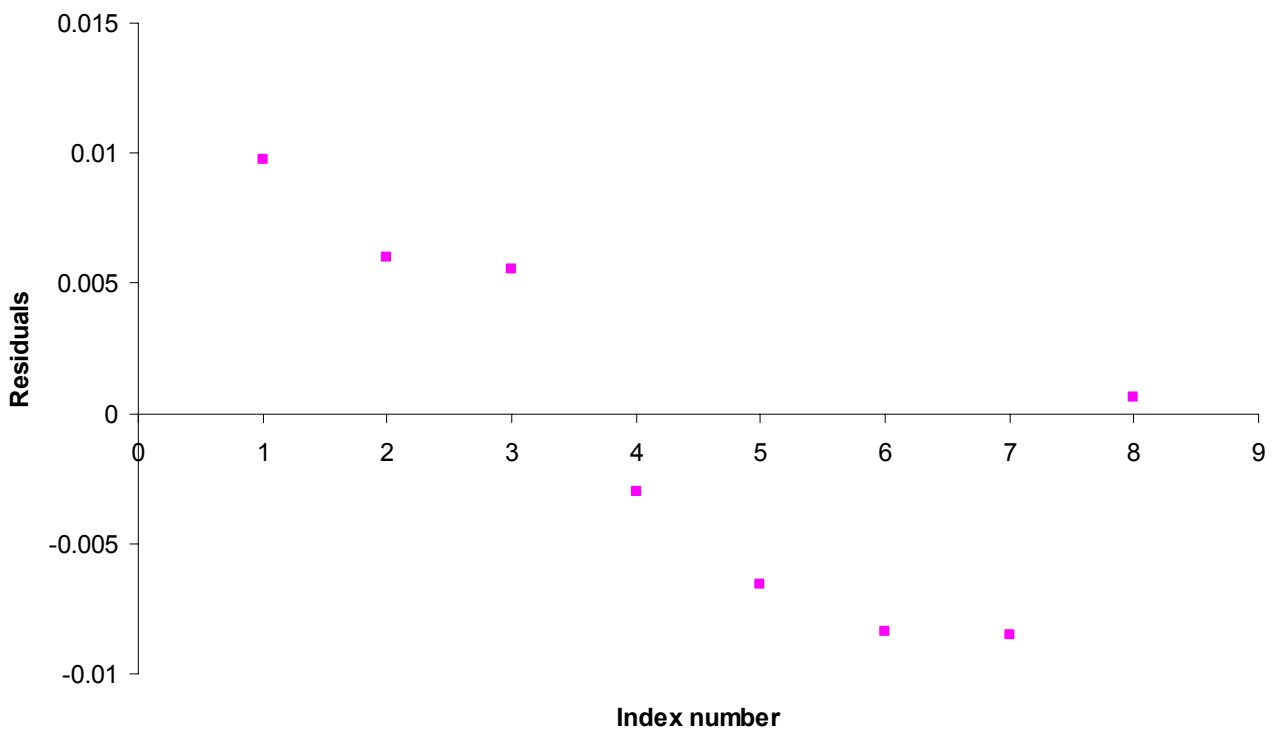

Figure A.29: Validation of the assumption of normality of residuals for the instantaneous productivity

Appendix V: Determining the effectiveness factor

The effectiveness factor for the immobilised amidase reaction was determined from the Thiele modulus (Section 5.2.3) by using Figure A.30. Beta (s_0/K_m) was calculated as 1.18.
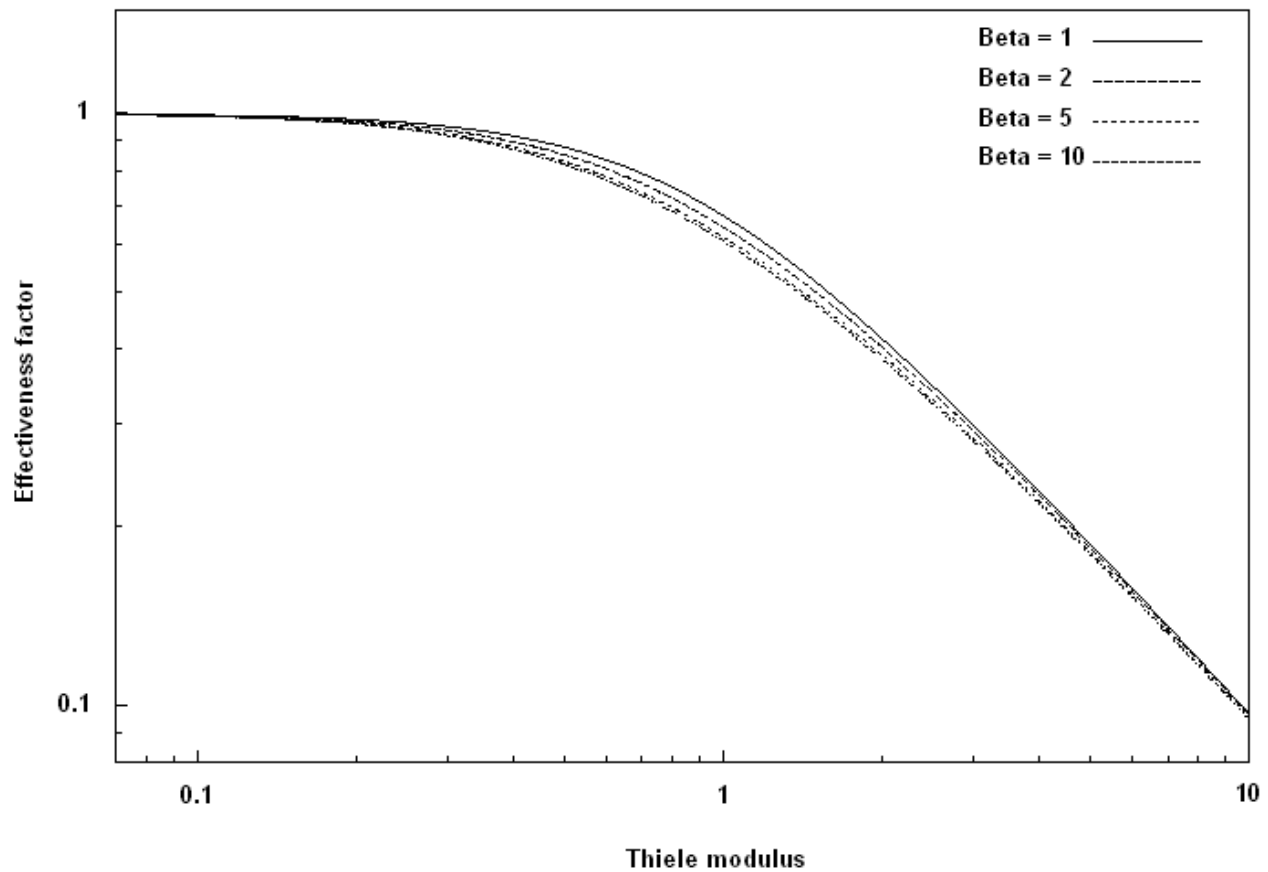

Figure A.30: Effectiveness factors for immobilised enzyme catalysts with Michaelis-Menten intrinsic kinetics with Beta = s_0/K_m (adapted from Bailey and Ollis, 1986).